ULTRASONIC VELOCITY MEASUREMENTS ON LIMESTONES FROM THE PORTLAND GROUP: CORRELATION WITH POROSITY AND OTHER LITHOLOGICAL FACTORS

A thesis submitted in the University of Southampton for the degree of Doctor of Philosophy.

by

Douglas Ingle Cole
B.Sc. (Southampton)

Department of Geology
The University
SOUTHAMPTON.

August 1974

ABSTRACT

FACULTY OF SCIENCE

GEOLOGY

Doctor of Philosophy

ULTRASONIC VELOCITY MEASUREMENTS ON LIMESTONES FROM THE PORTLAND GROUP : CORRELATION WITH POROSITY AND OTHER LITHOLOGICAL FACTORS.

by Douglas Ingle Cole

Laboratory-determinations of velocity and porosity have been made on nearly 900 core-specimens taken from 72 surface-outcrop samples of limestones from the Portland Group of southern England. These limestones have been petrographically classified into four basic types - Sparites, Micrites, Chalks and Microsparites, partly following criteria used by Folk (1962). Simple linear-regression-analysis has been used to establish empirical relationships between velocity and porosity for each of the four limestone-types. Additionally, multiple linear-regression-analysis was employed to determine the extent to which 21 other physical parameters, mainly petrographic, are related to velocity. 245 members of the core-specimen population were used for this aspect of the work.

Representative specimens of the limestone-types have been analysed using reflected-light microscopy and scanning-electron microscopy, in order to provide information on type, size, distribution, morphology and orientation of the pores.

Porosity is shown to be the major cause of velocity-variation in all four limestone-types, with the exception of low-porosity Micrites ($<$ 12% porosity). Propagation of the elastic-waves appears to be confined to the matrix in these low-porosity Micrites, whereas propagation occurs through both matrix and pores in the other types. A limited study of the effect of water-saturation on velocity supports this conclusion.

'Planar fabric-elements', in the form of preferred mineral- and/or

shell-orientation, are significantly related to velocity in all limestone-types excepting Chalks. Preferred pore-orientation, which is limited to some core-specimens of Micrites and Sparites, is associated with these 'planar fabric-elements'. Mineral-variation in Microsparites is believed to have some effect on velocity. Other significant velocity-controlling petrographic parameters also show significant but inverse relationships with porosity.

Correlation of lithostratigraphy with velocity and/or porosity is not possible, because of overlapping ranges in the local bed-sequences, together with an absence of data from several beds in these sequences.

A study of velocity-anisotropy on a lithostratigraphic basis, i.e. in individual beds, shows that 65% of the beds are isotropic. The majority of the remaining beds have a velocity-anisotropy of the transversely-isotropic type, suggesting that primary bedding or lamination is a probable cause.

Comparison of the laboratory-velocities with a limited number of outcrop-velocities, determined on quarry floors using a hammer seismic-refraction system, indicates that the outcrop-velocities are reduced to between 20% and 40% of the magnitude of the laboratory-velocities, probably as a result of fractures.

ACKNOWLEDGEMENTS

I wish to thank all those people who have assisted me in various ways during the course of this research, which was largely financed from a three year research studentship awarded by the Natural Environment Research Council. All other financial assistance, which was received throughout the period of this research is duly acknowledged.

My sincere thanks go to Professor F. Hodson for allowing me the use of facilities at the Geology Department, Southampton University, without which this research would not have been possible.

I am most indebted to Dr. N. Hamilton for his supervision and guidance given throughout this research, and for his critical reading of the manuscript. He also assisted in the sampling-program and, initially, in the seismic-refraction studies described in Appendix 1.

Several other members of the academic staff at the Geology Department, Southampton University, gave me both advice and assistance. In particular, I am very grateful to Mr. I.M. West for his useful discussion on the stratigraphic and petrographic aspects of this research, together with his substantial assistance in the sampling-program.

Also, I much appreciate the help given by Mr. T. Clayton with the data-processing computer programs, and his advice and discussion on some of the statistical methods used in this research.

Finally, I would like to thank all members of the technical staff at the Geology Department, Southampton University, for their invaluable assistance, especially Mr. D. Utton and Mrs. P. Lawrence who rendered considerable time and skill on the photography used in this research.

CONTENTS

		Page
CHAPTER 1	INTRODUCTION	1
CHAPTER 2	HISTORY OF PREVIOUS RESEARCH	3
2.1	Introduction	3
2.2	Effect of Methods of Determination on Elastic-Wave Velocity	3
2.3	Effect of Elastic-Wave Frequency on Velocity	4
2.4	Effect of Bulk Lithology on Elastic-Wave Velocity ...	5
2.5	Effect of Pressure on Elastic-Wave Velocity	6
2.6	Effect of Temperature on Elastic-Wave Velocity	7
2.7	Effect of Depth on Elastic-Wave Velocity	7
2.8	Effect of Saturants on Elastic-Wave Velocity	9
2.9	Effect of Porosity and Density on Elastic-Wave Velocity	12
2.10	Effect of Fabric on Elastic-Wave Velocity	14
2.11	Effect of Discrete Lithological Factors on Elastic-Wave Velocity	18
2.12	Elastic-Wave Velocities in Unconsolidated Marine Sediments	22
2.13	Conclusions	23
CHAPTER 3	GEOLOGICAL BACKGROUND AND SAMPLE LOCALITIES	24
3.1	Introduction	24
3.2	Regional Geology of the Portland Group	25
3.2.1	Stratigraphy	25
3.2.2	Structure	27
3.3	Sampling Localities	28
3.3.1	Introduction	28
3.3.2	Locality 1 - Swanworth Quarry /SY 969784/	30

		Page
3.3.3	Locality 2 - Lulworth Cove Area [SY 8279]	34
3.3.4	Locality 3 - Chalbury Camp [SY 694838]	37
3.3.5	Locality 4 - Road-cutting near Corton Farm [SY 636855]	39
3.3.6	Locality 5 - Portesham Quarry [SY 610859]	41
3.3.7	Locality 6 - Isle of Portland	41
a)	West Weare Cliffs [SY 682724]	41
b)	Freshwater Bay [SY 692702]	46
c)	Perryfield Quarries [SY 694712]	46
3.3.8	Locality 7 - Chilmark Ravine [ST 974313]	49
3.3.9	Locality 8 - Upper Chicksgrove Quarry [ST 962296]	50
CHAPTER 4	EXPERIMENTAL TECHNIQUES	56
4.1	Introduction	56
4.2	Sample Preparation	56
4.3	Velocity Determinations	59
4.3.1	Instrumentation	59
4.3.2	Velocity - Measurement Procedure	62
4.3.3	Errors in Velocity-Determinations	63
4.4	Porosity and Density Determinations	65
4.4.1	Terminology	65
4.4.2	Methods of Determination	66
4.4.3	Errors in Density and Porosity Determinations ...	67
4.5	Petrographic Analysis	69
4.5.1	Introduction	69
4.5.2	Terminology and Classification of Carbonate Rocks (Folk, 1959, 1962)	69
4.5.3	Descriptions and Determinations of Possible Velocity-controlling Parameters	71
4.5.4	Methods of Analysis	78
4.5.4.1	Thin-Section Analysis	78

		Page
4.5.4.2	Errors in Thin-Section Analysis	79
4.5.4.3	X-Ray Diffraction Analysis	82
4.5.4.4	Ultra-Violet Fluorescence	83
4.6	Pore-Structure Analysis	83
4.6.1	Introduction	83
4.6.2	Terminology	84
4.6.3	Methods of Analysis	86
CHAPTER 5	VARIATION OF ELASTIC-WAVE VELOCITY WITH LITHOSTRATIGRAPHY	101
5.1	Introduction	101
5.2	Elastic-Wave Velocity Variation with Lithostratigraphy	102
5.2.1	Introduction	102
5.2.2	Results	102
a)	East Purbeck	102
b)	Lulworth Cove	104
c)	Central Dorset	104
d)	Isle of Portland	104
e)	Vale of Wardour	108
f)	Regional Correlations	108
5.2.3	Conclusions	111
5.3	Velocity Anisotropy in relation to Lithostratigraphy	111
5.3.1	Introduction and Methods	111
5.3.2	Results and Discussions	112
a)	East Purbeck	112
b)	Lulworth Cove	114
c)	Central Dorset	115
d)	Isle of Portland	116
e)	Vale of Wardour	116

		Page
f)	Regional Correlations	119
5.3.3	Conclusions	119
5.4	Analysis of Velocities in Lithostratigraphic Units of the Portland Group, including the Effect of Porosity	120
5.4.1	Introduction	120
5.4.2	Results	120
a)	East Purbeck	122
b)	Lulworth Cove	122
c)	Central Dorset	124
d)	Isle of Portland	126
e)	Vale of Wardour	126
f)	Regional Correlations	129
5.5	Discussion and Conclusions	130
CHAPTER 6	VARIATION OF ELASTIC-WAVE VELOCITY WITH POROSITY..	137
6.1	Introduction	137
6.2	Porosity/Density Relationships	137
6.3	Velocity/Porosity Relationships	144
6.3.1	Methods of Statistical Analysis	144
6.3.2	Simple Linear Regression Analysis between Velocity and Percentage Porosity	149
6.3.3	Analysis of the Effects of Pore-Orientation, Pore-Structure and Pore-Type on Velocity..	159
a)	Introduction	159
b)	Pore-Orientation	160
c)	Pore-Structure and Pore-Type	162
6.4	Conclusions	167
CHAPTER 7	RELATIONSHIPS BETWEEN VELOCITY, POROSITY AND OTHER PHYSICAL PARAMETERS	183
7.1	Introduction	183
7.2	Methods of Statistical Analysis	183
7.3	Results	186

		Page
7.3.1	Basic Statistics and Simple Correlation Coefficients	186
7.3.2	Multiple Regression Analysis	194
a)	Sparites	194
b)	Chalks	203
c)	Micrites	206
d)	Microsparites	212
7.4	Discussion and Conclusions	215
CHAPTER 8	CONCLUSIONS	229
REFERENCES	.....	234
APPENDIX 1	OUTCROP VELOCITIES DETERMINED USING A HAMMER-SEISMIC METHOD FOR SOME LITHOSTRATIGRAPHIC UNITS AT SWANWORTH QUARRY	245
A 1.1	Introduction	245
A 1.2	Methods of Velocity-Determination	245
A 1.3	Results	247
A 1.4	Summary and Conclusions	250
APPENDIX 2	VARIATION IN ULTRASONIC VELOCITY WITH DEGREE OF WATER-SATURATION	253
A 2.1	Introduction	253
A 2.2	Methods of Analysis	253
A 2.3	Discussion and Conclusions	254
APPENDIX 3	LOCATION AND DESCRIPTION OF SAMPLES	259
APPENDIX 4	CORE SPECIMEN ORIENTATION	264
APPENDIX 5	VELOCITY-, POROSITY-, and DENSITY-DETERMINATIONS OF CORE-SPECIMENS	276

		Page
APPENDIX 6	LIMESTONE CLASSIFICATION OF CORE-SPECIMENS	304
APPENDIX 7	PORE CLASSIFICATION, -DIMENSIONS AND -ORIENTATION OF SOME 36 CORE-SPECIMENS	320

LIST OF ILLUSTRATIONS

FIGURE		Page
3.1	Outcrops of the Portland Group in Dorset and the Vale of Wardour, Wiltshire with positions of sampling localities	29
3.2	Section of the Portland Limestone, Portesham Quarry..	42
3.3	Sampled section of the Portland Group, West Weare Cliffs	44
3.4	Section of the Portland Group, Upper Chicksgrove Quarry	53
4.1	Classification of Carbonate Rocks (after Folk, 1962)..	74
4.2	Geologic Classification of Porosity in Carbonate Rocks (after Choquette & Pray, 1970)	85
5.1	Elastic-wave velocities and porosities in some beds of the Portland Group, Swanworth Quarry	123
5.2	Elastic-wave velocities and porosities in some beds of the Portland Group, Central Dorset	125
5.3	Elastic-wave velocities and porosities in some beds of the Portland Group, Isle of Portland	127
5.4	Elastic-wave velocities and porosities in some lithostratigraphic units of the Portland Group, Vale of Wardour	128
6.1	Variation of density with porosity - Sparites (n=460).	139
6.2	Variation of density with porosity - Chalks (n=162)...	140
6.3	Variation of density with porosity - Micrites (n=128).	141

FIGURE		Page
6.4	Variation of density with porosity - Microsparites (n=148)	142
6.5	Plot of calcite, dolomite and quartz contents showing variation in absolute density of the Portland Group limestone-types	143
6.6	Relationship between velocity and porosity - Sparites (n=460)	151
6.7	Relationship between velocity and porosity - Chalks (n=162)	152
6.8	Relationship between velocity and porosity - Micrites (n=128)	153
6.9	Relationship between velocity and porosity - Microsparites (n=148)	154
6.10	Relationship between velocity and porosity - Total data, Portland Group (n=898)	155
6.11	Frequency distributions of velocity and porosity of the Portland Group limestone-types	156
7.1	Relationships between velocity and porosity - Sparites (n=128)	196
7.2	Variation of fabric with velocity - Sparites (n=128)	197
7.3	Variation of pellet content with velocity - Sparites (n=128)	198
7.4	Variation of oolith mean size with velocity - Sparites (n=128)	199
7.5	Variation of sponge spicule content with velocity - Sparites (n=128)	200
7.6	Relationships between velocity and porosity - Chalks (n=31)	204
7.7	Variation of calcite vein mean grain-size with velocity - Chalks (n=31)	205
7.8	Relationship between velocity and porosity - Micrites (n=38)	209
7.9	Variation of fabric with velocity - Micrites (n=38)	210
7.10	Variation of bioclast content with velocity - Micrites (n=38)	211
7.11	Relationships between velocity and porosity - Microsparites (n=48)	220

Page

FIGURE

7.12 Variation of fabric with velocity - Microsparites (n=48) 221

7.13 Variation of calcite mean grain-size with velocity - Microsparites (n=48) 222

7.14 Variation of dolomite mean grain-size with velocity - Microsparites (n=48) 223

7.15 Variation of dolomite content with velocity - Microsparites (n=48) 224

7.16 Variation of calcite vein content with velocity - Microsparites (n=48) 225

7.17 Variation of bioclast content with velocity - Microsparites (n=48) 226

7.18 Variation of bioclast mean size with velocity - Microsparites (n=48) 227

7.19 Variation of detrital grains mean size with velocity - Microsparites (n=48) 228

A1.1 Plan of Swanworth Quarry, August, 1971, showing position of refraction lines 246

A2.1 Relationship between velocity and degree of water-saturation for some Sparites and Micrites from the Portland Group, Swanworth Quarry 256

PLATE

3.1 SAMPLING. Size and shape of a typical sample *in situ* with orientation marks 31

3.2 Exposure of the Portland Group, Swanworth Quarry, looking south 32

3.3 Exposure of the sampled part of the section in the Portland Group, Dungy Head 36

3.4 Exposure of the sampled part of the section in the Portland Limestone, Chalbury Camp 38

3.5 Exposure at top of road-cutting, Corton Farm, showing the sampled part of the section in the Portland Sandstone 40

3.6 Exposure of the section in the Portland Limestone, Portesham Quarry 43

3.7 Exposure of the sampled part of the section in the Portland Group, West Weare Cliffs 45

PLATE		Page
3.8	Exposure of the section in the Portland Group, Freshwater Bay	47
3.9	Exposure of the section in the Portland Limestone, Perryfield Quarries	48
3.10	Exposure of part of the section in the Portland Sandstone, main face, Upper Chicksgrove Quarry	54
3.11	Exposure of the Portland Limestone / Purbeck beds contact, Upper Chicksgrove Quarry	55
4.1	Diamond-tipped rotary drill used for extracting 2.54 cm. diameter cores from the samples	57
4.2	Core-orientation device	58
4.3	Ultrasonic materials tester, with a core-specimen in position between the transducers	60
4.4	Oscilloscope trace of received pulse after travel through core-specimen, transmitted pulse, time-base and time-markers	61
4.5-4.23	.....	90 to 100
	These plates mainly illustrate the petrography	
6.1-6.18	.....	171 to 182
	These plates illustrate pore-types and pore-structure	

LIST OF TABLES

TABLE		Page
3.1	Generalised Stratigraphy of the Portland Group in Dorset and the Vale of Wardour	27
3.2	Lithostratigraphic Section in the Portland Group, Swanworth Quarry	33
3.3	Generalised Section in the Portland Group, Lulworth Cove Area	35
3.4	Section in the Portland Group, Chalbury Camp	37
3.5	Section in the Portland Sandstone at top of road-cutting, Corton Farm	39
3.6	Section in Part of the Portland Group, Freshwater Bay	46
3.7	Section in the Portland Limestone, Perryfield Quarries	49
3.8	Generalised Section in the Portland Group, Chilmark Ravine	50
4.1	Student's t-test Results for Velocity Statistics on two standards	64
4.2	Results of Initial and Repeat Porosity and Density Measurements made on ten Cores	67
4.3	Classification of Calcite Replacement and Recrystallisation Fabrics in Bioclasts (after Wilson, 1967)	75
4.4	Results of Initial and Repeat Thin-Section Analyses of ten Core-Specimens	79
4.5	Pore-Structure Determinations	88
5.1	Comparison of Elastic-Wave Velocities in some beds of the Portland Group, Swanworth Quarry	103
5.2	Comparison of Elastic-Wave Velocities in two beds of the Portland Group, Lulworth Cove	105
5.3	Comparison of Velocities at Swanworth Quarry and Lulworth Cove	105
5.4	Comparison of Elastic-Wave Velocities in some beds of the Portland Group, Central Dorset	106
5.5	Comparison of Elastic-Wave Velocities in some beds of the Portland Group, Isle of Portland	107
5.6	Comparison of Elastic-Wave Velocities in some lithostratigraphic units of the Portland Group, Vale of Wardour	109

TABLE		Page
5.7	Comparison of Elastic-Wave Velocities in three lithostratigraphic units of the Portland Group, Dorset and a summary of the Portland Group in Dorset and the Vale of Wardour	110
5.8	Coefficients of Aeolotropy and Results of Student's t-tests on Velocities for some beds of the Portland Group, Swanworth Quarry	113
5.9	Coefficients of Aeolotropy and Results of Student's t-tests on Velocities for two beds of the Portland Group, Lulworth Cove	114
5.10	Coefficients of Aeolotropy and Results of Student's t-tests on Velocities for some beds of the Portland Group, Central Dorset	115
5.11	Coefficients of Aeolotropy and Results of Student's t-tests on Velocities for some beds of the Portland Group, Isle of Portland	117
5.12	Coefficients of Aeolotropy and Results of Student's t-tests on Velocities for some lithostratigraphic units of the Portland Group, Vale of Wardour	118
5.13	Coefficients of Aeolotropy and Results of Student's t-tests on Velocities for three lithostratigraphic units of the Portland Group, Dorset, and for the Portland Group in Dorset and the Vale of Wardour ...	119
5.14	Comparison of Non-directional Elastic-Wave Velocities and Porosities in lithostratigraphic units of the Portland Group	121
6.1	Results of Simple Linear Regression Analysis between Porosity and Density for four Limestone-Types from the Portland Group	138
6.2	Results of Studies of Velocity/Porosity Relationships using Different Methods of Analysis on four Limestone-Types from the Portland Group	145
6.3	Results of Simple Linear Regression Analysis between Velocity and Porosity for four Limestone-Types from the Portland Group	150
6.4	Results of Pore-Structure Correlations for four Limestone Types from the Portland Group	163
7.1	Basic Statistics - Sparites (n=128)	188
7.2	Basic Statistics - Chalks (n=31)	189
7.3	Basic Statistics - Micrites (n=38)	190

TABLE		Page
7.4	Basic Statistics - Microsparites (n=48)	191
7.5	Simple Correlation Coefficients between Velocity and the Independent Variables	192
7.6	Results of Linear Multiple-Regression Analysis - Sparites (n=128)	195
7.7	Results of Linear Multiple-Regression Analysis - Chalks (n=31)	203
7.8	Results of Linear Multiple-Regression Analysis - Micrites (n=38)	207
7.9	Results of Linear Multiple-Regression Analysis - Microsparites (n=48)	212
A1.1	Velocities from Reversed Refraction lines at Swanworth Quarry	248
A1.2	Mean Velocities for some lithostratigraphic units at Swanworth Quarry using a Hammer-Seismic Method	250
A2.1	Velocity/percentage Water-Saturation Data for some Core-specimens of Micrites and Sparites	254
A2.2	Results of Simple Linear Regression Analysis on Velocity/percentage Water-Saturation Data for some Core-specimens of Micrites and Sparites	255

"Leave no Stone unturned."

Euripides

CHAPTER 1

INTRODUCTION

It is well known that ultrasonic velocities, measured in a wide range of rocks, are dependent upon numerous physical parameters, of which porosity or density are dominant. However, it is apparent that the degree of correlation between velocity and porosity or density, is lower for limestones than for many other rock-types. Only limited research has been made into possible factors causing this lower correlation and the consequent uncertainty in empirical relationships between velocity and porosity in limestones. As far as is known, no comprehensive laboratory study has been made of possible physical parameters affecting velocity in limestones. However, environmental effects such as depth, pressure, temperature, geological age, elastic-wave frequency, saturants and methods of determination on velocity, are well-documented for several rock-types including limestones.

A principal objective of this study is an investigation of velocity/porosity relationships in limestones. The limestones chosen are of limited stratigraphic range - late Jurassic, Portlandian, thus eliminating the geological-age factor. Other physical parameters, mainly petrographic, but including pore-structure, which were considered to be possible velocity-controlling variables, are also investigated in detail.

This investigation was limited entirely to surface-cropping limestones; thus the parameters depth, pressure and temperature are nominally constant. The effect of saturants on velocity, with the exception of a limited study of water-saturated specimens (Appendix 2), was eliminated by oven-drying of specimens for all velocity-determinations. The determinations were made at constant frequency using an ultrasonic transducer, but a limited number of determinations were made using a field-seismic method (Appendix 1) for comparative purposes.

Lower degrees of correlation between velocity and depth, pressure,

and degree of saturation in limestones, reported by previous workers, are possibly related to the lower velocity/porosity correlation described above and/or pore-structure (Chapter 2). Thus a study of the effect of porosity and pore-structure on velocity in limestones is of prime importance.

Four main limestone-types (Section 4.6.1), defined partly following the method of Folk (1959, 1962), were recognised in the Portland Group (Section 3.1). 898 specimens were used for velocity/porosity/density studies of these limestone-types. Statistical analysis of the resulting data established a series of empirical relationships, primarily using a simple linear function. A selection of 245 specimens from the total were used to investigate the possible effects of some 22 physical parameters, mainly petrographic but including porosity, on velocity. Additionally, 36 specimens of the 245 were used to assess the possible dependence of velocity on pore-structure and/or preferred pore-orientation.

Correlation of velocity with lithostratigraphic units of the Portland Group was attempted, since previous research indicates that identification of either stratigraphy or lithology from velocity is subject to considerable uncertainty. Also, an investigation of velocity-anisotropy in these lithostratigraphic units was made, since velocity-anisotropy often forms an important component in a wide range of rock-types including limestones. This investigation included a study of the effect of fabric on velocity-anisotropy.

CHAPTER 2

HISTORY OF PREVIOUS RESEARCH

2.1 Introduction

A review of previous literature indicates that ultrasonic velocities in rocks have been extensively investigated. These investigations have usually produced velocity/depth logs of boreholes without differentiating the rock types involved. Similarly, analyses of velocity-data from other sources have treated sedimentary rocks as a group, and in some instances have failed to separate them from igneous and metamorphic rocks.

Elastic-wave velocity in rocks is controlled by several widely-differing parameters. These are listed and reviewed in order, as follows:

Methods of velocity determination

Elastic-Wave Frequency

Bulk Lithology

Pressure

Temperature

Depth

Saturants

Porosity

Density

Fabric

Discrete Lithological Factors.

Finally, there is a discussion on pertinent results from recent marine sediments.

2.2 Effect of Methods of Determination on Elastic-Wave Velocity

It is evident that different techniques can produce differing velocity determinations for the same sample. For example, Wyllie et. al. (1958) found discrepancies between laboratory measurements and interval velocities from well-logs, for the same rock units. Nikitin (1962) found that ultrasonic methods gave greater velocity values for limestones than

field seismic refraction methods. Oliphant (1950) had previously shown similar variations, using a laboratory resonant-frequency method and a field seismic refraction method. In the Carboniferous System of Southwest Scotland, Hall (1970) investigated broad stratigraphic units by three field seismic methods:- hammer and explosive-charge refraction and explosive-charge reflection. Each stratigraphic unit gave different seismic velocities for the three methods used with a maximum difference of 50% between hammer and reflection methods. Greeley & Rinehart (1971) determined higher velocities in some vesicular basaltic lavas from California using an ultrasonic technique compared with a field hammer-seismic refraction technique. They concluded that the ultrasonic technique measured the properties of the matrix of the basalts, whereas the hammer-seismic technique measured the combined properties of matrix and vesicles. This conclusion can probably be applied generally to discrepancies in velocity, between field and laboratory determinations. Laboratory methods measure velocities in small unfractured and unweathered samples, whereas field methods measure velocities in much greater volumes of fractured, usually weathered, rock.

Hall's (1970) variations (see above) result from differences inherent in the actual methods used, rather than differences in sample volume. However, Hall found that velocity contrasts between rock units were almost independent of the methods of determination used.

2.3 Effect of Elastic-Wave Frequency on Velocity

Previous investigators have employed a wide spectrum of elastic-wave velocities and have shown that the effect of frequency on elastic-wave velocity is negligible. For example, Donata et. al. (1962) found less than 5% velocity-variation in several rocks, including a limestone from the Portland Group, over the frequency range 2Hz - 90kHz. Birch & Bancroft (1938), using forced-resonant vibrations of a long column of granite, showed that over the range 140Hz - 4.5kHz, velocity was independent of frequency to within 1%. Kubotera (1954) produced similar results for the range

50kHz - 300kHz and Hughes & Jones (1951) for the range 2MHz - 6MHz.

Koefoed et. al. (1963) found that although velocities in dry rock were unaffected by frequency, water-saturation resulted in a velocity-decrease at low frequencies and an increase at high frequencies.

It is concluded that velocity in dry rock is independent of frequency over a wide range. This can be further verified from the results of Peselnick & Outerbridge (1961), which showed that the elastic constants - Young's modulus and rigidity modulus, both of which can be directly related to elastic-wave velocity - were constant throughout the frequency range 4Hz - 10MHz.

2.4 Effect of Bulk Lithology on Elastic-Wave Velocity

The effect of bulk lithology on velocity is largely dependent upon the effects of individual physical parameters, each of which is a possible velocity-controlling variable. One of the earliest studies was made by Ewing & Crary (1935), the results of which showed that the local surface rock-types, consisting of cementstone, dolomite, shales, gneisses and sandstones, were each characterised by a discrete velocity. Oliphant (1950) recorded velocities in Permian sandstone, shale and limestone, using both field and laboratory techniques. He found that the limestone could be differentiated from the sandstone and shale on the basis of velocity, and that the limestone could be subdivided into two types, based upon density and laboratory-determined velocity.

In contrast, Leet (1938) did not find any correlation between interval velocity and bulk lithology, derived from well-data on Carboniferous rocks from West Virginia. Similarly McLemore (1963) found that lithology could not be identified on the basis of velocity, after applying probability theories of statistical inference to velocity-data determined from wells in the San Joaquin Valley, California. Press (1966) found that correlation of velocity with lithology was possible for sandstones and shales, but not for limestones, where the extent of recrystallisation resulted in large variations

in velocity.

Hall (1970) found that velocity contrasts, used in conjunction with absolute velocities, could be correlated with chrono-stratigraphic sequences, ranging in age from Dalradian to Triassic, in southwest Scotland. Absolute velocity did not correlate with specific chrono-stratigraphic units, due to large velocity deviations within individual units. This is to be expected, since a histogram of velocities in different rock-types, compiled by Grant & West (1965), shows considerable overlap in the velocity-ranges of each rock-type, and the majority of chrono-stratigraphic units studied by Hall contain several different rock-types.

2.5 Effect of Pressure on Elastic-Wave Velocity

There is a marked positive correlation between pressure, both hydrostatic and differential, i.e. difference between hydrostatic and internal pore pressures, and elastic-wave velocity, for all rock-types studied to date. One of the earliest studies is that of Hughes & Cross (1951) in which a uniform increase in elastic-wave velocity with increasing hydrostatic pressure, over the range 1 bar - 5 kilobars, was noted. Birch (1961) extended the observations to cover hydrostatic pressures up to 10 kilobars, and a non-linear relationship between velocity and pressure was revealed, with a marked increase in velocity between 1 bar and 3 kilobars, followed by a gradual decrease in the velocity gradient between 3 kilobars and 10 kilobars. Birch attributed this initial marked increase in velocity to the pressure closure of cracks and large pores within the rock samples.

The effect of differential pressure on elastic-wave velocity produces similar results to those of hydrostatic pressure. For example, Gardner et. al. (1965) found a positive correlation between velocity and differential pressure in dry sedimentary rocks, over the pressure range 34 bars - 170 bars, with velocity increasing most rapidly at the lower end of the range. A marked hysteresis effect on the velocity/pressure relationship was also noted, with higher velocities being recorded throughout the decreasing

pressure cycle, as compared with the corresponding increasing pressure cycle. Studies on sandstones (King, 1966) tend to confirm the observations of Gardner et. al. over the differential pressure range 68 bars - 340 bars. A non-linear relationship between velocity and hydrostatic pressure, similar to that described by Birch was also found.

Thus for a wide range of rock-types, there is a positive correlation and non-linear relationship between elastic-wave velocity and pressure, for the pressure range 1 bar to 10 kilobars. The non-linear relationship may be accounted for by the initial closure of cracks and pores, followed by a gradual increase in the elastic constants with increasing pressure.

2.6 Effect of Temperature on Elastic-Wave Velocity

By comparison with other velocity-dependent variables, studies of the effect of temperature are rather limited. The general conclusion here is that increasing temperature results in decreasing velocity, for a wide range of rock-types. An early investigation, that of Ide (1937), showed that velocity decreases with increasing temperature, over the temperature range $0^{\circ}C$ - $700^{\circ}C$. When the rock-samples were cooled, a permanent reduction in velocity was also noted, and this was explained by differential thermal expansion. Hughes & Cross (1951) recorded decreases in velocity when the temperature was increased from $25^{\circ}C$ to $300^{\circ}C$, although these decreases were found to fluctuate.

An investigation of velocities in rocks covering the temperature range $26^{\circ}C$ to $-36^{\circ}C$ (Timur, 1968) showed that velocities in water-saturated rocks increased with decreasing temperature, but in dry rocks velocity was found to be nearly independent of temperature. However, this temperature range is restricted, and falls below the freezing point of water, in contrast to the ranges used by other workers. The results for dry rocks probably do not affect the main conclusion of previous workers.

2.7 Effect of Depth on Elastic-Wave Velocity

Depth, in this context, refers to thickness of overburden and is

associated with both compaction and pressure. Previous research has concentrated upon data derived from well-logs, and there is general agreement that elastic-wave velocity always increases with thickness of overburden.

An early study by Weatherby & Faust (1935), on data from 50 wells in North America, showed that interval velocities in shale and sandstone increased with depth, but in limestone, velocity was nearly independent of depth. This absence of correlation in limestone could be due to the extent of recrystallisation (Press, 1966 & see Section 2.4).

Haskell (1941) derived gradients relating velocity to depth for Tertiary sandstones and shales in 62 wells from the San Joaquin Valley, California. It was found that sandstones had the steepest gradients, and that all gradients derived were linear down to 4.2 km. overburden, beyond which they diminished asymptotically. It was also shown that 78% of the total velocity gradient was due to the effect of pressure exerted by the existing overburden. West (1950) extended the analysis of velocity-variation with depth, down to the mantle/core boundary at 2900 km. Data on clastic sediments derived from several sources was used, and it was found that velocity (V) could be expressed as a function of depth (z) by the empirical equation:

$$V = Vo(1 + cz/Vo^4) \quad \ldots\ldots\ldots \quad \text{Eq.2.1}$$

where Vo is a constant characteristic of the rock, and $c = 3.3 km^3/sec^4$. This equation was valid for depths not exceeding 150 km., beyond which the function became:

$$V^5 = 180z \quad \ldots\ldots\ldots\ldots \quad \text{Eq.2.2}$$

The effect of the low velocity layer between 60 km. and 200 km. depth was not considered.

Faust (1951, 1953) analysed velocity data from approximately 200 km. of well-sections. The prediction of velocity from depth-determinations was improved by using the empirical equation:

$$V = 1948(zTL)^{1/6} \quad \ldots\ldots\ldots \quad \text{Eq.2.3}$$

where V is estimated velocity in ft./sec., z is depth, T is geological

time and L is a lithological factor based upon true electrical resistivity. This equation was only valid for shales and sandstones; velocities in limestones were found to show less definite increases with increasing depth, thus confirming the conclusions of Weatherby & Faust (1935).

Krumbein (1951) suggested that the positive correlation of velocity with thickness of overburden, observed for most rock-types except limestones, was caused by the elastic constants increasing at a greater rate than density.

The uncertainty over velocity-variation with depth for limestones is further confirmed by statistical analyses of velocity-data from wells in sandstone and limestone (Sarmiento, 1961). Correlation coefficients for velocity-depth relationships ranged between +0.27 and +0.67 for limestones, and between +0.58 and +0.80 for sandstones, with the exception of one sandstone with a correlation coefficient of +0.13.

There is thus considerable evidence to show that velocity increases with thickness of overburden, in sedimentary rocks excluding limestones, of a single stratigraphic system. This increase with depth has been found to be mostly non-linear, of the type described previously.

The effect of geological age on elastic-wave velocity is similar to that of depth (Faust, 1951, 1953). Increase in either geological age or depth usually increases the degree of compaction, and thus the elastic constants. Also, increasing geological age increases the probability of tectonism, which results in an increasing state of stress in the rocks, and in turn increases the elastic constants.

2.8 Effect of Saturants on Elastic-Wave Velocity

Previous research has concentrated upon the effect of water-saturation on elastic-wave velocity, and results indicate an uncertainty about the nature of this effect. Some results show evidence of a decrease in velocity with increasing degree of water saturation (Born & Owen, 1935; Oliphant, 1950; Peselnick, 1962; Usher, 1962; Koefoed et. al., 1963). However, the reverse is also observed (Murphy et. al., 1957; Wyllie et. al., 1958).

Oliphant (1950) found that velocities in limestones, shales and sandstones always decreased with increasing percentage water-saturation. The relation was non-linear, with a large initial decrease in velocity, followed by gradual decrease of the velocity gradient. It has been suggested that the decrease in velocity with increasing percentage water-saturation in rocks, is caused primarily by a reduction in matrix rigidity (Born & Owen, 1935; Peselnick, 1962; Usher, 1962).

Wyllie et. al. (1958) showed that increasing percentage water-saturation resulted in an increase in velocity, for a wide range of rock-types. Murphy et. al. (1957) derived similar conclusions, using synthetic sandstone cores, and showed that the velocity in cores of 10% porosity was twice the velocity in cores of 20% porosity, the cores being 100% saturated with water.

The shape of pores in crystalline rocks was found to be an important parameter affecting velocity/water-saturation relationships (Nur & Simmons, 1969). An increase in velocity with increasing percentage water-saturation was noted when the pores were in the form of cracks, but not when they were in the form of spheroidal holes. Differences in velocity between dry and water-saturated rock were found to approach 50%. The studies of both Nur & Simmons (1969) and Peselnick (1962) included velocity-data on the Solenhofen limestone, Germany, and the small decrease in velocity with increasing water-content found by Peselnick was therefore probably due to samples having pores in the form of spheroidal holes. In fact, the samples of Solenhofen limestone analysed by Nur & Simmons contained pores in the form of spheroidal holes only.

The effect of water-content on velocity was also found to be related to pressure (Hughes & Cross, 1951; Hughes & Kelly, 1952). At low pressures, water-saturation of sandstones resulted in an increase in velocity. This was explained by the fact that velocity in water is greater than velocity in air, which had previously occupied the pores. However at high

pressures, water in the saturated sandstones was subjected to compression, and because the compressibility of water is less than that of air, a reduction in velocity in the water-saturated sandstone was observed.

Possibly the most important parameter causing variation in velocity/water-saturation relationships is frequency. Koefoed et. al. (1963) showed that velocities in dry limestone samples decreased by 7% when subjected to water-saturation, using a pulse method of 20 KHz for velocity determinations, and by 12% when a resonant frequency method of unspecified low frequency was used. They suggested that these differences were due to the type of system applicable to the rock, i.e. open or closed. The type of system is dependent upon pore-geometry, nature of saturating fluid and frequency of elastic-waves (Gassmann, 1951). There is a gradual transition from open to closed systems, with increasing elastic-wave frequency. In open systems, the fluid contained in the pores is subjected to Poiseuille flow, but in closed systems, this flow breaks down (Biot, 1956). Biot predicted that the velocity through closed systems is higher when the fluid is water than when it is air, but the opposite is true in the case of open systems.

The results of previous research can be explained by the type of system and its dependent variables. All previous recorded increases in velocity resulting from water-saturation, used frequencies exceeding 1 MHz for velocity determination, indicating that closed systems operate above this frequency. Peselnick (1962) noted a decrease in velocity with water-saturation using a pulse method of 3 MHz, but as suggested earlier, pore geometry is probably an important parameter influencing these results. Frequencies of between 2Hz and 40 KHz were used by workers who found decreases in velocity resulting from water-saturation, so that open systems were probably operative here. It is thus obvious that frequency is an important parameter when water is the fluid present. However, in dry rocks, when air is the pore-fluid, velocity is independent of frequency (Section 2.3).

Research into the effects of saturants other than water shows

similar results to those for water-saturation. For example, Wyllie et. al. (1958) derived an empirical equation of the form:

$$\frac{1}{Vm} = \frac{\phi}{Vf} + \frac{1-\phi}{Vr} \qquad \text{..... Eq.2.4}$$

where Vm is measured velocity, Vf is fluid velocity, Vr is rock velocity and ϕ is volumetric porosity fraction. For all rock-types studied, the measured velocity in liquid-saturated rock exceeded that in dry rock. In the cases of sandstones, the measured velocity was found to be a function of the saturant velocity, when this exceeded 1490 m./sec. Total oil-saturation, compared with total water-saturation, produced a 2 - 4% decrease in velocity. Murphy et. al. (1957) found that the effect on velocity of saturating synthetic sandstone cores with alcohol, benzene, carbon tetrachloride and chloroform was similar to the results of water-saturation, using high frequencies. In contrast, Sarmiento (1961) found that oil-saturation had a negligible effect on velocity in dry sandstone cores, whereas gas-saturation under atmospheric conditions produced a 25% decrease in velocity.

King (1966) confirmed the predictions of Biot (1956) on velocity in fluid-saturated systems in relation to frequency. Sodium chloride solution and kerosene were the fluids used, and higher velocities were observed when sodium chloride solution was used as the saturant.

Variation of velocity with fluid-saturation in rocks thus depends upon the parameters controlling the type of system applicable to the rock; namely frequency, nature of the saturating fluid and pore-geometry. When water is the saturant, velocity becomes dependent on frequency, and to a lesser extent, on pressure and pore-geometry.

2.9 Effect of Porosity and Density on Elastic-Wave Velocity

Porosity and density are interdependent, and their effects on elastic-wave velocity are described together. In all cases, increasing porosity results in a reduction in velocity whereas the reciprocal effect is shown by density. In many cases, empirical equations have been established.

Previous research has concentrated upon sedimentary rocks, with considerable data being derived from well-logs. Wyllie et. al. (1958) obtained a linear relationship between velocity and porosity (Eq. 2.4), which included the effects of fluid saturation, and which was applicable to a wide range of sedimentary rocks.

Differences in velocity/porosity relationships between different sedimentary rock-types have been detected. Berry (1959) found a non-linear relationship between travel-time and porosity, and a linear relationship between velocity and porosity for sandstone. In homogeneous sandstones, no difference could be detected in porosity estimates using either relationship, but when appreciable amounts of shale were present, the travel-time/porosity curve gave the best estimates over the porosity range 10 - 25%. A similar study on limestones showed much uncertainty in velocity/porosity relationships. Velocities in limestones were found to be higher than in sandstones of similar porosity, and he suggested that this was caused by calcite having a higher velocity than quartz. Sarmiento (1961) found similar differences between sandstones and limestones, by computing linear relationships between travel-time and porosity from well-log data at depths exceeding 700 metres. Average correlation coefficients of +0.92 were found in the case of sandstones and +0.91 in the case of limestones with less than 12% porosity, for travel-time/porosity relationships. These relationships were uncertain in limestones with porosities exceeding 12%, and it was suggested that this was due to larger pores and vugs, causing the elastic-waves to follow least-time paths around the margins of the pores. However, Koefoed et. al. (1963) found a linear relationship between velocity and porosity for limestones, over the porosity range 4 - 23%.

Significant correlations have been found and linear relationships established for velocity as a function of density in limestones, over a range of density from 1.82 - 2.65 gm/c.c. (Kuiper et. al., 1959; Peselnick, 1962). Peselnick derived an empirical equation in the form:-

$$Vp = -7.41 + 5.11\ p \quad \ldots\ldots\ldots \quad \text{Eq.2.5}$$

where Vp is estimated velocity in m./sec. and p is density in gm./c.c. A correlation coefficient of +0.95 between velocity and density was computed. 24 samples of Solenhofen limestone were used, and by extrapolation to the density of calcite, it was found that the limestone acted as an aggregate of randomly-oriented calcite crystals, in terms of its elastic behaviour.

Velocities in metamorphic and igneous rocks also show a marked dependence on porosity and density. The classic analysis of Birch (1961) showed an approximately linear velocity/density function for materials having a common mean atomic weight. Nafe & Drake (1959) plotted velocity against density for a wide range of rock-types, and also included marine sediments from the Puerto Rico Trench. There was an initial decrease in velocity with increasing density over the range 1.0 - 1.5 gm./c.c., followed by a linear increase in velocity with density.

In conclusion, it is apparent that for most rock-types there is a significant positive correlation between velocity and density, and a corresponding negative correlation between velocity and porosity. These relationships can be best represented by a simple linear function. In the case of limestones, however, the relationships between velocity and porosity or density are subject to considerable uncertainty. These uncertainties are substantiated by the results of Wyllie et. al. (1958), which showed that velocities in vuggy and fractured limestone do not depend upon total porosity. Koefoed et. al. (1963) also suggested that pore-geometry was a velocity-dependent parameter in limestones, but provided no quantitative analysis.

2.10 Effect of Fabric on Elastic-Wave Velocity

Fabric includes both planar and linear elements such as bedding, cleavage and preferred orientation of minerals. Preferred orientation within the space lattice of individual crystals is also included in this section. Previous studies show that velocity is dependent upon the

orientation of fabric elements.

On the macroscale, there is considerable evidence to show that velocities in bedded sedimentary rocks are transversely isotropic (McCollum & Snell, 1932; Weatherby et. al., 1934; Hagedoorn, 1954; Uhrig & Van Melle, 1955; Kleyn, 1956; Dunoyer et. al., 1959). Velocity determinations were usually made parallel and perpendicular to bedding, and the results obtained were irrespective of the magnitude of sedimentary dip. For example, Kleyn found that velocity was transversely isotropic for a horizontal sedimentary sequence in South Sumatra, whereas Weatherby et. al. reached similar conclusions for a vertically-dipping limestone in Oklahoma. Kleyn used the results of a seismic refraction profile, a well-velocity survey and a radial well survey to show that the anisotropy factor, defined as the ratio:

Velocity parallel to bedding / Velocity perpendicular to bedding

varied with thickness of overburden. He suggested that this was caused by the vertical velocity, which was perpendicular to bedding, increasing with depth, whereas the horizontal velocity remained constant. Differences in rock type could also account for variation in the anisotropy factor with depth, as implied by the results of Dunoyer et.al., which showed an anisotropy factor of 1.00 for sandstone, 1.08 - 1.12 for limestone, 1.00 - 1.05 for halite and 1.15 - 1.20 for anhydrite.

The transversely isotropic nature of bedded rocks with reference to velocity, is probably dependent upon the frequency and distribution of bedding planes, which act as planes of discontinuity in the media transmitting the elastic-waves. This is implied by an anisotropy factor of 1.4 reported for shale, which has a higher frequency of bedding or foliation planes than other sedimentary rocks (Uhrig & Van Melle, 1955).

Hagedoorn (1954) suggested that lower vertical than horizontal velocities noted in horizontally-bedded rocks could be due to different

methods of measurement. Horizontal velocities, computed from seismic refraction profiles, are always the maximum velocities, whereas vertical velocities, computed from well-logs, are usually mean velocities.

The effect of fabric on velocity has been studied on a laboratory scale. Prasada Rao (1947) determined velocities in cores taken from three orthogonal directions, with reference to bedding, cleavage or foliation, in a wide range of rock-types. The velocity anisotropy of each sample was computed using the formula:

$$\% \text{ anisotropy} = \frac{V_{max} - V_{min}}{1/3\ (V_{max} + V_{int} + V_{min})} \times 100 \quad \ldots\ldots \quad \text{Eq.2.6}$$

and these attained values of 41%. Densities were also determined but in individual samples there was no variation of density with direction. He concluded that velocity anisotropy was related to the state of residual tectonic stress in each rock sample, and this was controlled by bedding, cleavage or foliation. This conclusion is partially confirmed by the results of Tocher (1957) which showed that velocity increased with increasing compression, at a higher rate in the direction parallel to compression than in the direction perpendicular to compression, for several different rock-types.

A close relationship was found to exist between velocity anisotropy and preferred orientation of mineral grains, in tectonically-deformed sandstones (Giesel, 1963). A model was constructed, which fitted mathematically the elastic behaviour and velocity anisotropy of the tectonically-deformed sandstones.

The effect of pressure on velocity anisotropy has been studied. King (1966) showed that velocity anisotropy in sandstones, which was related to bedding, decreased with increasing confining pressure, and suggested that this was caused by the bedding planes closing with increasing pressure, in a manner analogous to the closure of cracks. In contrast, Christensen (1965) analysed velocities determined in three orthogonal directions in metamorphic rocks, covering the hydrostatic pressure range 1 - 10 kilobars. Most

samples exhibited velocity anisotropy, and he concluded that at low pressures, anisotropy resulted from preferred orientation of planar voids, coupled with a partly parallel crystal-orientation of minerals. At pressures above 4 kilobars, velocity anisotropy was related to degree of mineral-orientation and the velocity anisotropies of the oriented minerals.

The effect of petrofabrics on velocity have been extensively investigated. For example, several workers (Pros & Babuska, 1967; Klima & Kulhanek, 1968; Thill et. al., 1969) studied spherical samples of marble. By constructing contoured equal-area projections of elastic-wave velocities and corresponding petrofabric diagrams of calcite $\langle\bar{0}001\rangle$ crystallographic axes, they showed that the minimum velocity coincided with the direction of maximum concentration of $\langle\bar{0}001\rangle$ axes. This conclusion was predicted from the results of Peselnick & Robie (1962), which showed that the velocity anisotropy of calcite was approximately 28%, with the minimum velocity occurring in the $\langle\bar{0}001\rangle$ crystallographic direction. Thill et. al. also used the same technique on spherical samples of pumice and granite. An orthorhombic velocity-symmetry pattern was found for pumice, and this corresponded to a preferred orientation of elongate vesicles. A similar pattern was found for granite, corresponding to the symmetry-pattern of preferred orientation of a set of microfractures in quartz. Christensen (1965) analysed velocities in three orthogonal directions in metamorphic rocks, related to the petrofabrics. Velocity variation in schists was found to be a direct result of the abundance and degree of preferred orientation of mica. In amphibolites, marked concentrations of c - axes of hornblende were found to coincide with the direction of maximum velocity whereas concentrations of a - axes coincided with the direction of minimum velocity. These observations were consistent with measured velocities in single crystals of hornblende.

Studies have been made of the effect of preferred lattice orientation of olivine crystals on velocity. Woeber et. al. (1963) found

that velocity anisotropies in samples of dunite were dependent upon this preferred orientation. Christensen & Ramananantoandro (1971) divided dunite into two distinct types, based upon the elastic properties of olivine. In one type, olivine showed a preferred orientation of a - axes, and a uniaxial pattern of velocity. In the other type, in which there were preferred orientations of all three crystallographic axes, there was a corresponding orthorhombic pattern of velocity, with maxima parallel to the a - axes, and minima parallel to the b - axes.

Lappin (1971) suggested that the preferred orientations of olivine formed during purely magmatic crystallisation, were accompanied by high temperature and low temperature orientation patterns, probably produced by recrystallisation. He tentatively suggested that the observed velocity anisotropy of the Mantle near Mid-Ocean Ridges, where velocities perpendicular to the Ridges exceed velocities parallel to the Ridges, could be due to olivine recrystallisation under low-temperature conditions.

It is concluded that fabric forms an important velocity-controlling variable and therefore it is essential in any study or application of velocity, to use consistent orientations for velocity determinations, in order to correct for fabric effects.

2.11 Effect of Discrete Lithological Factors on Elastic-Wave Velocity

The term lithological factors includes discrete physical parameters such as the calcite/dolomite ratio in limestones, clay content, and type and amount of cement.

Previous research has dealt mostly with lithological factors in limestones and their effect on velocity, possibly because studies of velocity/porosity/density relationships in various rock-types, show that minimum correlations occur in the case of limestones (Kuiper et. al., 1959). There is agreement that, other than porosity or density, an important parameter influencing velocity in limestones is the amount of clay, shale or marl present (Oliphant, 1950; Schwaetzer, 1958; Kuiper et. al., 1959; Nikitin,

1962; Jankowsky, 1970). Such a conclusion is supported by the results of both field and laboratory studies. More recently, Jankowsky analysed travel-time and depth-data from wells in some Upper Cretaceous carbonate rocks of northwest Germany and derived an equation in the form:

$$\frac{1}{V} = 10^{\frac{(Z - A)}{B}} \qquad \ldots\ldots\ldots \quad \text{Eq. 2.7}$$

where Z = depth, $\frac{1}{V}$ = reciprocal of interval velocity or travel-time per depth unit, A = constant, depending probably on the particular matrix velocity, and B = slope of the regression lines representing travel-time of carbonate and shaly sediments versus depth. The constant A was found to be higher for "pure" limestones than for shaly limestones, whereas the corresponding slopes, B, were approximately equal within the depth range 800 - 2000 metres. A shale/carbonate ratio was computed using the expression:

$$\frac{\text{shale}}{\text{carbonate}} = \frac{\text{Travel Time (shale)}}{\text{Travel Time (carbonate)}}$$

and an upper limit of 1.927 was found in the case of travel-times for "pure" shale and "pure" limestone. This suggests that velocity in "pure" limestone is almost twice that in "pure" shale, at the same depth. The effect of an increasing shale content, and also an increasing clay or marl content, in causing a decrease in the velocity of "pure" limestones, had also been previously observed by several other workers (Nikitin, 1962; Schwaetzer, 1958; Kuiper et. al., 1959). Oliphant (1950) suggested additionally that in certain limestones, variation in lithoclast size resulted in differences in velocity.

The effects of mineral composition, particularly calcite/dolomite ratios, on velocity in limestones, can be important (Kisslinger, 1953; Sarmiento, 1961). Kisslinger found that, provided a sufficient range of data was available, there was a tendency for velocity to decrease with increasing magnesium carbonate content, with a regression coefficient of

- 29.3 metres/second/percent $MgCO_3$. This relationship applied only to dolomites which had developed local porosity. Non-porous dolomites, where volume-for-volume replacement had occurred, showed a velocity increase with increasing magnesium carbonate content. Increasing content of residual material also reduced velocity, and a regression coefficient of - 55.0 metres/second/percent was computed. Sarmiento confirmed Kisslinger's main conclusions by showing that velocities in pure dolomites were higher than those in limestones of equal porosity. From a consideration of the elastic constants of dolomite, which are higher than those of calcite (Birch, 1942), these results are to be expected. For example, Kisslinger calculated that the velocity in an isotropic, homogenous, pure dolomite rock, would be 6% higher than in a similar calcite rock. Press (1966) suggested that velocities in limestone depended on the degree of crystallisation. He showed that, in non-crystalline limestones, velocities varied between 2,800 and 6,400 metres per second, whereas in crystalline limestones, predominantly high velocities, 5,670 - 6,400 metres per second, were encountered.

Research into rock-types other than limestones has been limited. Sarmiento (1961) studied velocity/porosity relationships in sandstones from well-log data, and concluded that depth and shaliness were the most important parameters affecting these relationships. Shaliness had a similar effect in sandstones to that in limestones, with increasing shale content resulting in a decrease in velocity. Wyllie et. al. (1956) predicted that mineral composition of rocks would affect the elastic-wave velocity. For example, randomly oriented calcite crystals should yield a matrix velocity of 6.8 km./sec., whereas similarly oriented quartz crystals should yield a matrix velocity of 5.9 km./sec. However, it would appear that no investigation of the effect of calcite/quartz ratios on velocity in sedimentary rocks has been undertaken.

Studies of synthetic sandstones (Murphy et. al., 1957; Viksne et. al., 1961) showed that velocity depends upon porosity, manufacturing pressure, grain contacts, and the amount and type of cement. Velocity decreased with

increasing porosity and decreasing cement content, and both these parameters were closely interrelated. An increase in manufacturing pressure resulted in an increase in velocity, and this was related to both area of grain contact, which increased with pressure, and porosity, which decreased with pressure. Murphy et. al. studied the effects of various saturants, and found that the experimental data could be fitted to the equation:

$$V_T = kV_F + c \quad \ldots\ldots\ldots\ldots \text{Eq. 2.8}$$

where V_T is velocity in a saturated core of synthetic sandstone, and V_F is velocity in the saturating fluid. k is a constant dependent upon porosity and cement-type, and c another constant dependent upon the nature of the rock-frame, which consisted of the cement and the sorted quartz sand grains, in varying degrees of contact. Analogies with natural sandstones are dubious, since in cores exceeding 17.5% cement content, the sand grains float in the cement (Viksne et. al., 1961).

A theoretical approach to the problem of elastic-wave propagation was made by Paterson (1956). In porous granular aggregates, two waves of volume-expansion were observed. These waves were termed frame-waves and air-waves or liquid-waves, depending upon the nature of the pore-filler. Frame-wave velocity was dependent on the strength of the frame, the densities of the solid and the pore-filling materials, and the texture of the medium. Air- and liquid-wave velocities were related to the texture of the medium and the density and viscosity of the pore-filler. Application of this theoretical approach to a beach sand showed that porosity and permeability could be inferred from velocity determinations.

Analyses of sedimentary rocks have been limited to discrete parameters and no comprehensive study, comparable to those on synthetic sandstones (Murphy et. al. 1957; Viksne et. al., 1961) has been made. Velocity variation with lithological parameters in igneous and metamorphic rocks seem not to have been investigated.

2.12 Elastic-Wave Velocities in Unconsolidated Marine Sediments

An attempt is made to relate pertinent results of velocity variation in unconsolidated marine sediments to velocity studies in lithified sediments.

It is generally concluded that velocities are minimum in sediments with porosities between 75% and 90%, and that these velocities are usually 2 to 3% lower than the velocity in water (Hamilton, 1970). Hamilton (1956) suggested that scattering and viscous drag resulted in high-porosity sediments acting acoustically as a suspension, with a resulting velocity less than that of water. He also reported a large increase in velocity in unconsolidated marine sediments upon lithification (Hamilton, 1959).

Several parameters affecting velocity in sedimentary rocks can be equally applied to unconsolidated marine sediments. For example, Nafe & Drake (1957) found a linear velocity-increase with thickness of overburden in marine sediments. Shumway (1958) showed a velocity-decrease with increasing temperature similar to the velocity-decrease in water. He suggested that this was due to the predominance of a water compressibility component in the compressibility of the water-sediment mixture. In marine sediments with porosities less than 75%, a linear increase in velocity with decreasing porosity has been observed (Sutton et.al., 1957; Horn et. al., 1968; Schreiber, 1968; Hamilton, 1970). There is a complementary increase in velocity with increasing bulk density (Hamilton, 1970). Similar conclusions to those of Murphy et. al. (1957) and Viksne et. al. (1961) for synthetic sandstone cores, were drawn by Shumway (1960), who proposed that the rigidity and thus the velocity of marine sediments was increased by increasing the area of contact between the particles, particularly sand- and silt-sized particles. In contrast to sedimentary rocks, the effect of fabric on velocities in marine sediments was negligible through a thickness of 500 metres, in which velocities were determined in three orthogonal directions (Hamilton, 1970).

Previous research has shown that velocity in unconsolidated marine

sediments is dependent upon several parameters, a study of which has not been applied to sedimentary rocks. For example, there is widespread agreement that velocity in marine sediments is related to grain-size (Sutton et. al., 1957; Hamilton, 1959; Horn et. al., 1968; Schreiber, 1968; Hamilton, 1970; Buchan et. al., 1972). Increases in grain-size result in linear increases in velocity. Velocity in marine sediments was also found to be indirectly related to calcium carbonate content. Sutton et. al. (1957), Hamilton (1959) and Buchan et. al. (1972) found positive correlations between velocity and calcium carbonate content and between velocity and grain-size. The calcium carbonate occurs as bioclasts whose grain-size is coarser than the rest of the sediment. Thus coarse sediment is automatically richer in calcium carbonate and the two correlations are interrelated.

2.13 Conclusions

Elastic-wave velocity in rock is dependent upon several physical parameters, of which density and porosity are the most important, as shown by significant correlations with velocity. This is only true provided that determinations of velocity, porosity and density are made in a consistent direction in dry rock, at equal depths, and at the same pressure and temperature. However, limestones normally exhibit a low degree of correlation between velocity and density or porosity, thus implying that other physical parameters affect significantly the velocity. Previous studies show that shaliness, mineral composition and pore-geometry can be related to velocity in limestones, but a comprehensive study of limestones has not apparently been made.

Correlation of velocity with stratigraphy is also subject to considerable uncertainty, principally because there is usually variation in velocity-dependent parameters such as porosity within a single stratigraphic unit.

CHAPTER 3

GEOLOGICAL BACKGROUND AND SAMPLE LOCALITIES

3.1 Introduction

An essential prerequisite to a comprehensive study of elastic-wave velocity variation in limestones was the selection of samples covering a wide range of limestone-types (Folk, 1959, 1962). A further constraint was imposed by the need for samples to be of approximately the same geological age, since age can affect velocity (Section 2.7). Limestones from the Portlandian Stage of the Jurassic System were found to satisfy these criteria. These limestones are extensively quarried both for building stone and road aggregate, resulting in numerous exposures of fresh, unweathered rock, in addition to natural cliff-sections, thus facilitating a more comprehensive sampling-program. The degree of induration and the individual bed-thickness, generally exceeding 0.3m, greatly assisted sample-preparation (Chapter 4).

The sampling-program was conducted on a lithostratigraphic basis, made easy by reference to the numerous published stratigraphic descriptions (Blake, 1880; Huddleston, 1883; Woodward, 1895; Strahan, 1898; Arkell, 1933, 1935, 1947; Davies, 1956; House, 1969; Townson, 1971). These descriptions are mostly lithostratigraphic, and the units recognised and described generally comply with the American Code of Stratigraphic Nomenclature (1961). In a few instances the units are informally renamed and redefined in accordance with the code.

The limestones sampled are stratigraphically part of the Portland "Beds" (Fitton, 1836 and subsequent workers). Two formations can be defined, a younger Portland Limestone resting conformably on the Portland Sandstone. A type-section is designated (Section 3.2.1). These formations can be ranked into a group, the Portland Group.

3.2 Regional Geology of the Portland Group

3.2.1 Stratigraphy

The two formations of the Portland Group are well exposed at the West Weare Cliffs /SY 682720/ on the Isle of Portland. This section is here designated the type-section for both Formations and for the Group.

The Portland Limestone, 33 metres thick at the type-section, is a limestone with chert in the lower part, whereas the underlying Portland Sandstone, 32 metres thick, consists of alternating sequences of calcareous sandstone, marl and clay. These formations correspond approximately to the Portland Stone and Portland Sand as defined by Arkell (1933, Fig. 84). Unfortunately, Arkell used both lithostratigraphic and biostratigraphic criteria to define these units, and the biostratigraphic range zones have subsequently been revised (Cope in Torrens, 1969), (Table 3.1).

At the type-section, the upper boundary of the Portland Limestone is defined by a clay bed, 0.04 metres thick, described by Arkell (1933, Fig. 89) as the "Lower Dirt Bed". This clay bed is traceable throughout the areas in which the Portland Limestone outcrops. It forms the lowest clay bed in a sequence of interbedded limestones, marls and clays, defined by Arkell (1933, p.518) and previous workers as the Purbeck "Beds". The stratigraphic position of this lowest clay bed is such that at the type-section, 0.70 metres of limestone (named the "Skull Cap"), assigned to the Purbeck "Beds" by Arkell, are included in the Portland Limestone. This applies to most other areas in which the Portland Limestone outcrops. The beds overlying the Portland Limestone are redefined in this thesis, as the Purbeck beds.

The boundary between the Portland Limestone and the underlying Portland Sandstone is conformable but abrupt, calcareous sandstone being overlain by limestone containing neither quartz sand nor chert nodules. At the type locality, West Weare Cliffs, the lowest limestone has been designated the "Basal Shell Bed" (Arkell, 1933, Fig. 84) and is separated from the

highest calcareous sandstone by 3.9 metres of clay (Fig. 3.3).

The base of the Portland Sandstone is defined at the type-section by the base of the lowest sandstone bed in the sequence of calcareous sandstones, clays and marls underlying the Portland Limestone. This bed has been designated the "Black Nore Sandstone" (Arkell, 1933, Fig. 84). The underlying beds are termed the Kimmeridge beds in this thesis, and are equivalent to the Kimmeridge Clay as defined by Arkell (1933, p. 440, 497).

The Portland Sandstone and Portland Limestone can be divided into a sequence of beds, which have been described and defined by previous authors. The nomenclature previously used, e.g. Arkell (1933), is retained where possible, but modified informally to comply with the American code.

The beds of the Portland Limestone can be ranked into two members at the type-section, the Oolitic Limestone Member (10 metres thick) and the Cherty Limestone Member (20 metres thick) based respectively upon Arkell's "Freestone Series" and "Cherty Series". The Oolitic Limestone Member consists predominantly of oolitic and shelly limestone beds, with the top coinciding with that of the Portland Limestone, and the base defined by the base of the lowest limestone bed without chert nodules. This bed has been referred to as the "Base Bed" (Arkell, 1933, p. 494). The Cherty Limestone Member consists of limestone beds with chert nodules and stringers. The base is defined by the top of the "Basal Shell Bed" (Arkell, 1933, Fig. 84).

Further details of the type-section are presented in Section 3.3.7 together with descriptions of the sample localities. The two formations of the Portland Group underlie the whole Isle of Portland, and form extensive outcrops in Dorset, several outcrops in Wiltshire, and isolated outliers northeastwards from Swindon to Stewkley, Buckinghamshire. The two members of the Portland Limestone cannot be traced beyond Dorset.

The sampling-program was restricted to outcrops of the Portland

Group in Dorset and the Vale of Wardour, Wiltshire (Fig. 3.1). Due to lateral variation in both lithology and bed thickness within the two formations of the Portland Group, lithostratigraphic descriptions of sections at each sampling-locality are presented. A summary of the stratigraphy of the Portland Group in Dorset and the Vale of Wardour is given in Table 3.1.

TABLE 3.1

Generalised Stratigraphy of the Portland Group in Dorset and the Vale of Wardour

LITHOSTRATIGRAPHY	BIOSTRATIGRAPHIC RANGE ZONES	THICKNESS RANGE (metres)
PURBECK beds (Purbeck "Beds" of Arkell, 1933)		
PORTLAND LIMESTONE	Titanites giganteus	10 - 37
	Glaucolithites gorei	
PORTLAND SANDSTONE	Progalbanites albani	15 - 37
KIMMERIDGE beds (Kimmeridge Clay of Arkell, 1933)		

3.2.2 Structure

Two episodes of tectonism can be recognised, (i) pre-Albian, which resulted in a series of east-west symmetrical folds, and (ii) Tertiary, which resulted in east-west asymmetrical and monoclinal folds with steep north-facing limbs.

The outcrops on the Isle of Portland and in east Purbeck (Fig. 3.1), form part of the gently-dipping ($\leq 5^{o}$) southern limbs of two major asymmetrical folds, the Weymouth Anticline and the Purbeck Anticline,

respectively. In west Purbeck the outcrops, with dips in the range 20° - 50°, form part of the steeply-dipping north-facing limb of the Purbeck Anticline. The remaining outcrops in Dorset between Ringstead and Portesham form both north- and south-facing limbs of a series of asymmetrical folds, except in cases where the north-facing limbs are cut out by strike faults of Tertiary age. In the Vale of Wardour, the east-west trending Vale of Wardour Anticline affects both Upper Jurassic and Cretaceous strata. Outcrops of the Portland Group occur on both northern and southern limbs with dips in the range 3° - 5° south and 6° - 15° north. In addition, several pre-Albian northwest-southeast trending flexures affect the main anticline.

In the areas described above, the Portland Group forms a conformable sequence with both the underlying Kimmeridge beds and the overlying Purbeck beds. However, the pre-Albian tectonic episode has resulted in an overstep of Upper Cretaceous strata. In Dorset, the amount of overstep increases westwards, with Upper Cretaceous strata unconformably overlying strata of Oxfordian Age in the vicinity of Upwey, whereas in the Vale of Wardour, Upper Cretaceous strata overstep progressively from Aptian strata in the east, to Kimmeridgian in the west.

3.3 Sampling Localities

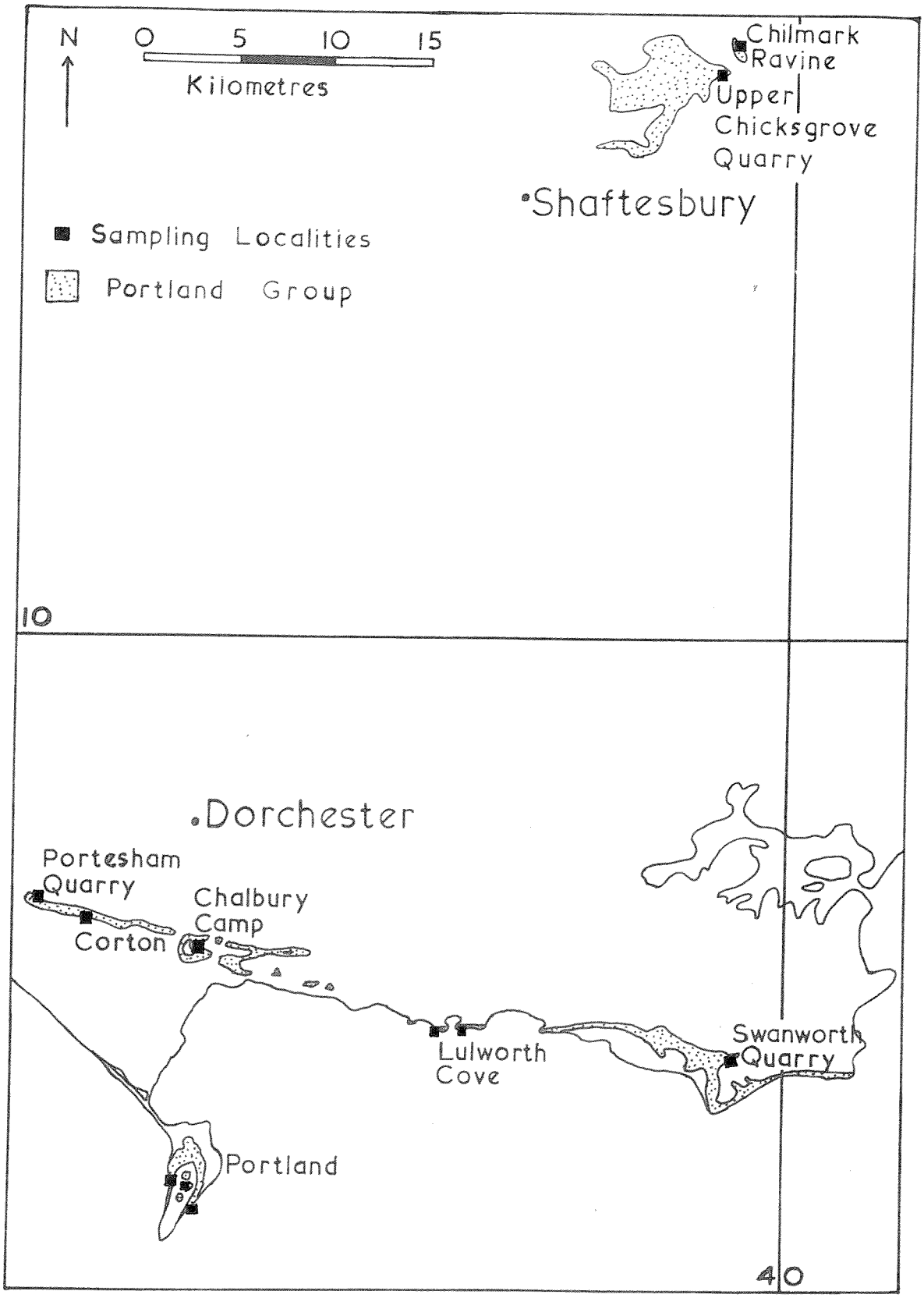
3.3.1 Introduction

The collection of samples was influenced by several factors:

1. Only surface outcrops were sampled, in order to eliminate the effect of depth of overburden on elastic-wave velocity (See Section 2.7).
2. A wide range of limestone-types (Folk, 1959, 1962) was sought. The location of these different limestone-types was such that samples were taken from exposures of the Portland Group over a considerable area (Fig. 3.1). However, because of the predominance of sandstones and marls in the Portland Sandstone, sampling was restricted to the Portland Limestone and the highest beds of the Portland Sandstone, which are calcareous and dolomitic sandstones.

Fig. 3.1

Outcrops of the Portland Group in Dorset and the
Vale of Wardour, Wiltshire with positions of sampling localities

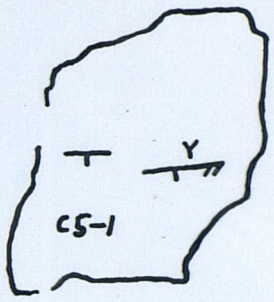


3. In order to minimise the effects of tectonism on velocity, samples were taken where the dip of the strata is less than 10°. This usually resulted in sample localities being restricted to the southern limbs of the asymmetrical folds described in Section 3.2.2. For comparative purposes, three samples were taken from exposures where the strata dip at angles between 22° and 48°.

A total of 72 limestone samples (Appendix 3) was collected. The dimensions of these samples ranged from 20 x 15 x 10 cm. to 35 x 25 x 20 cm., thus facilitating the extraction of several cylindrical cores of approximately 6 cm. length. The samples were oriented in situ (Plate 3.1) and, as far as possible, only unweathered samples were selected, since the work of Nikitin (1962) indicates that elastic-wave velocity can vary by as much as 50% between weathered and unweathered samples of the same rock.

3.3.2 Locality 1 - Swanworth Quarry /SY 969784/

Swanworth Quarry, Purbeck (Fig. 3.1), provides a continuous section in the Portland Group, from the highest beds of the Portland Sandstone to the basal Purbeck beds (Plate 3.2). The section is shown in Table 3.2 and the beds recognised are based on units defined by Arkell (1933, 1935, 1947) throughout Purbeck. The maximum dip recorded was 5° to the south.


Y
CS-1

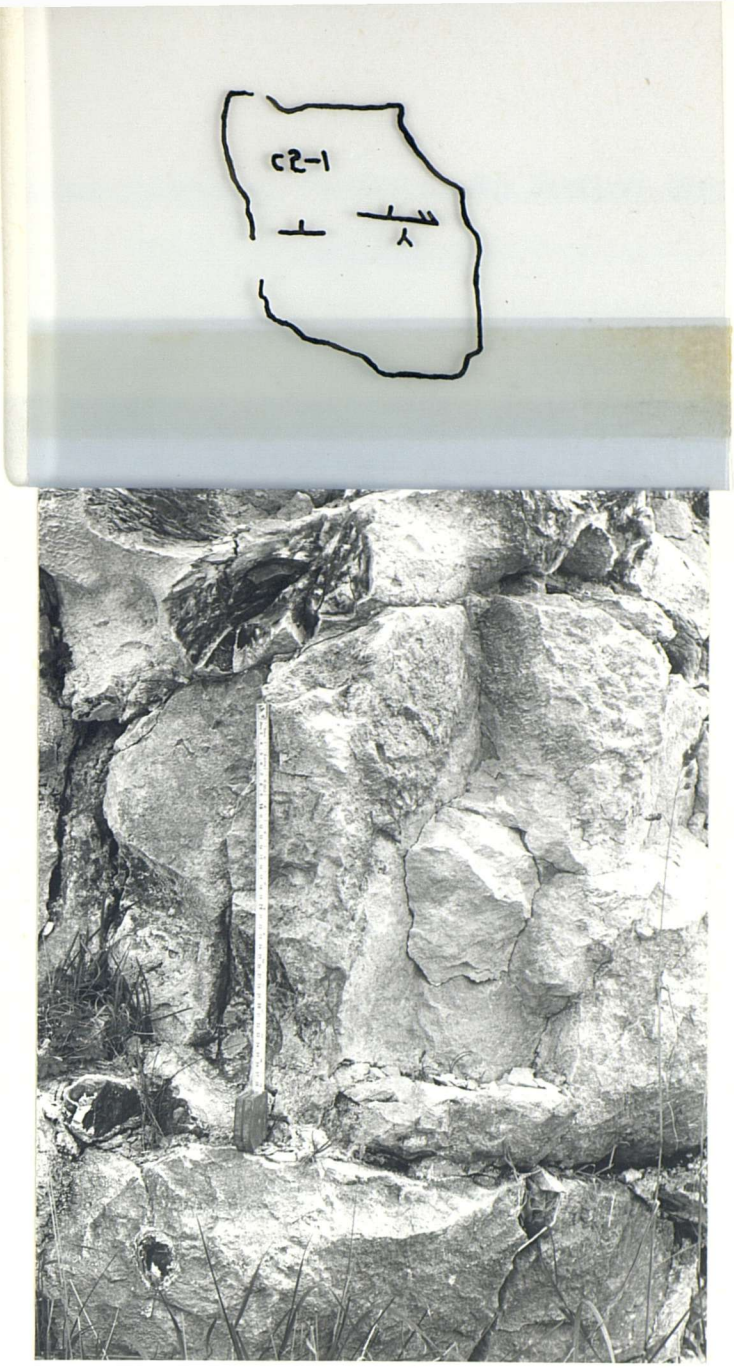


Plate 3.1 SAMPLING.

Size and shape of a typical sample <u>in situ</u> with orientation marks. The sample field orientation, designated Y , is one of the three orthogonal directions of coring (see Section 4.2)

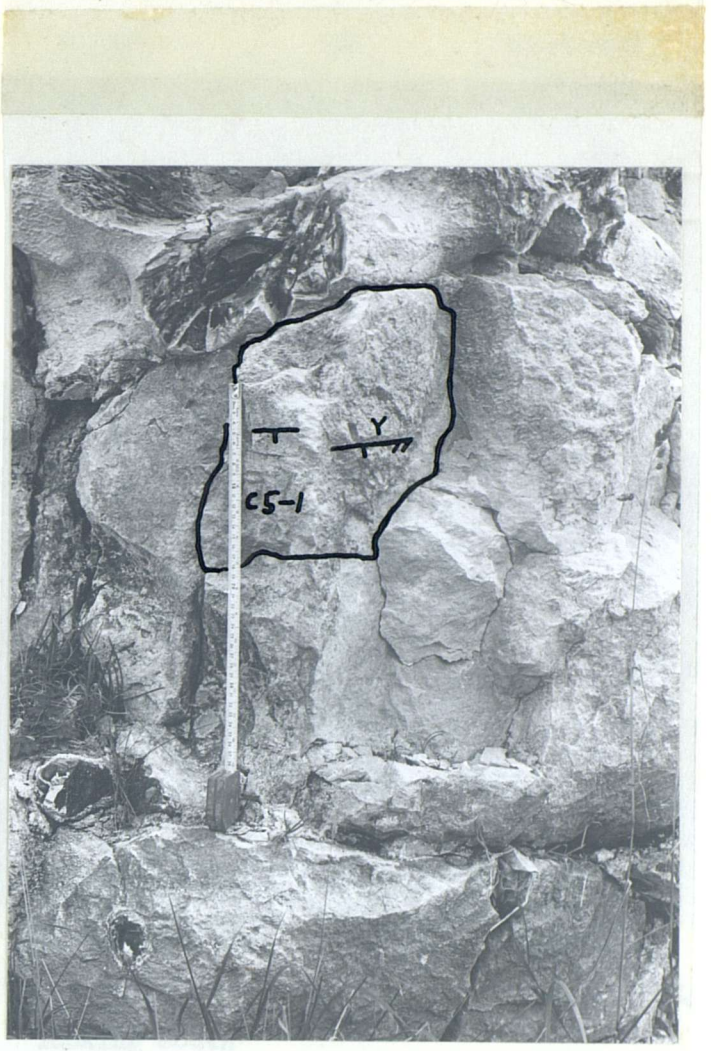


Plate 3.1 SAMPLING.

Size and shape of a typical sample <u>in situ</u> with orientation marks. The sample field orientation, designated Y , is one of the three orthogonal directions of coring (see Section 4.2)

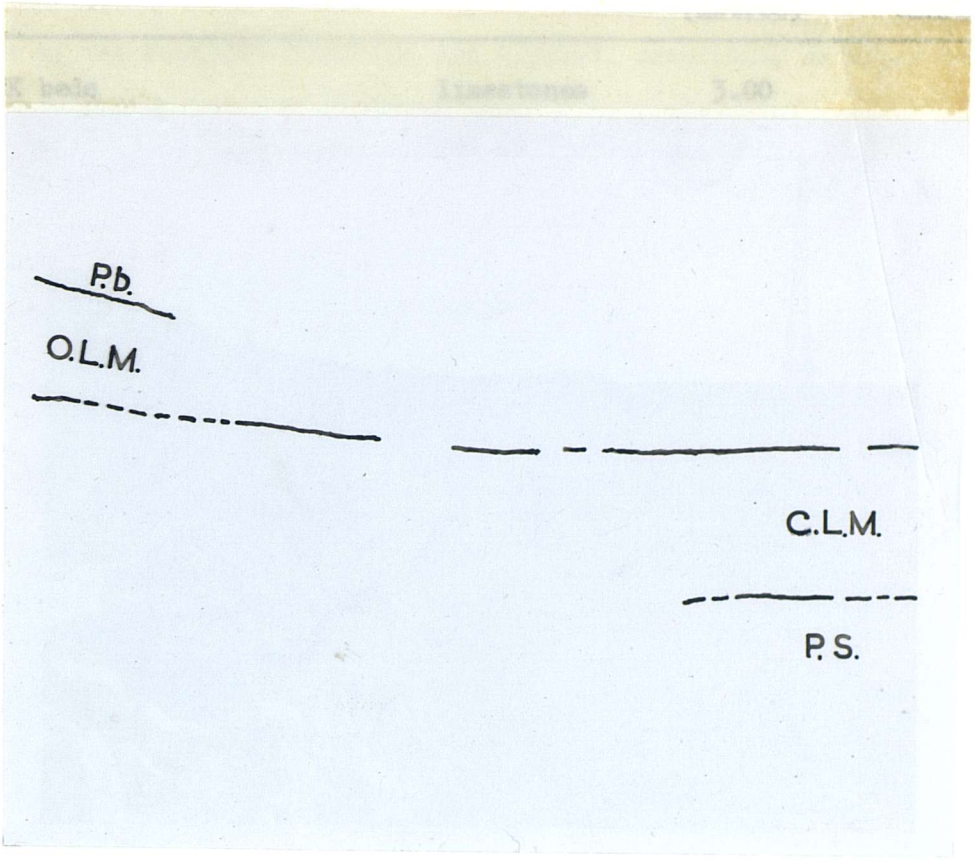

P.b.
O.L.M.
C.L.M.
P.S.



Plate 3.2 Exposure of the Portland Group, Swanworth Quarry, looking south

KEY

P.b. —— Purbeck beds

O.L.M. —— Oolitic Limestone Member

C.L.M. —— Cherty Limestone Member

P.S. —— Portland Sandstone

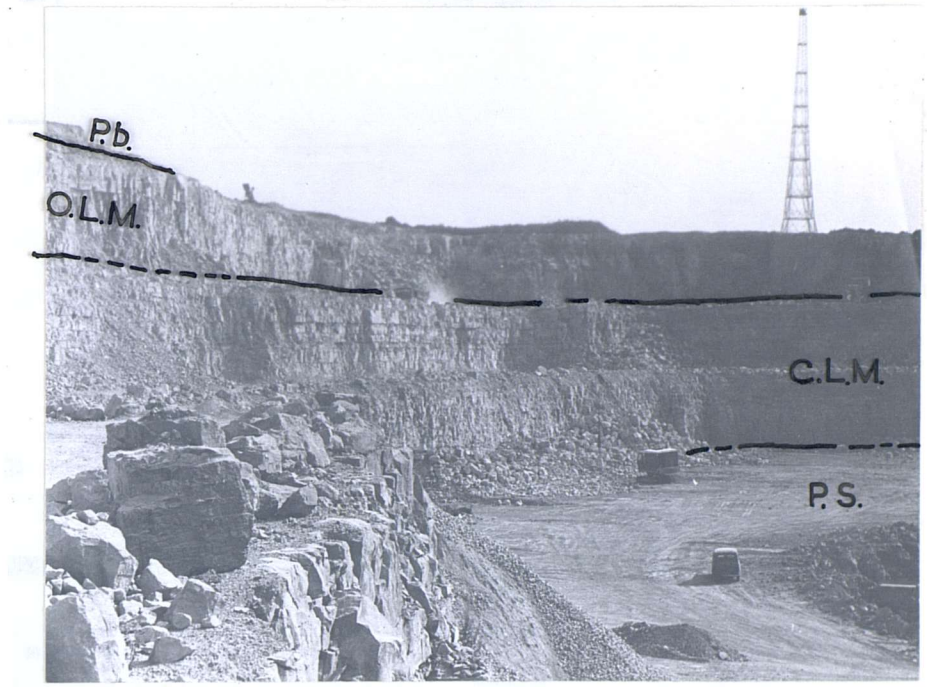


Plate 3.2 Exposure of the Portland Group, Swanworth Quarry, looking south

KEY

P.b. ——— Purbeck beds
O.L.M. —— Oolitic Limestone Member
C.L.M. —— Cherty Limestone Member
P.S. ——— Portland Sandstone

TABLE 3.2

Lithostratigraphic Section in the Portland Group,

Swanworth Quarry

FORMATION	MEMBER	BED	THICKNESS (metres)	NUMBER OF SAMPLES
PURBECK beds (3.05 m.)		limestones	3.00	
		black clay bed (Arkell's "Dirt Bed")	0.05	
PORTLAND	OOLITIC LIMESTONE (14.77 m.)	bed V	3.48	5
		bed U	2.94	3
		bed T	2.29	3
		bed S	0.67	2
		bed Q	2.44	3
		bed P	0.59	3
		bed O	2.36	3
LIMESTONE (33.95 m.)	CHERTY LIMESTONE (19.18 m.)	bed N	3.45	3
		bed M	1.15	
		bed L	1.39	
		bed K	0.46	
		bed J'	0.52	
		bed J	1.38	
		bed H	1.22	
		bed G	1.20	
		bed F	2.45	
		bed E	2.74	
		bed D	1.07	
		bed C	2.15	
PORTLAND SANDSTONE (2.32 m.) to quarry floor		bed B	0.57	2
		bed A 28	1.75	2

The Oolitic Limestone Member consists of both shelly and oolitic limestone beds with the exception of bed S, which is a limestone with chert stringers. The Cherty Limestone Member consists mainly of fine-grained, shelly limestone beds with chert nodules and stringers. Only the highest two beds of the Portland Sandstone are exposed, comprising an upper bed (bed B) of grey calcareous sandstone with chert nodules and a lower bed (bed A 28) of black dolomitic sandstone.

A total of 29 samples, representative of the main limestone-types exposed at Swanworth Quarry, were taken. The beds sampled are indicated in Table 3.2, and detailed lithological descriptions of the samples are presented in Appendix 3.

3.3.3. Locality 2 - Lulworth Cove Area [SY 8279]

The Portland Group, dipping at between 22° and 48°, forms part of the northern limb of the Purbeck Anticline. Three samples were taken for comparison with outcrops of negligible dip. Two samples were taken from a small exposure [SY 828797], approximately 200 metres west of the Fossil Forest, and one sample from a cliff exposure at Dungy Head [SY 816799]. A generalised section combining personal observations and the work of Arkell (1935), is presented in Table 3.3. The bed-terminology of Arkell (1935) is retained. The section is a condensed sequence of that at Swanworth Quarry.

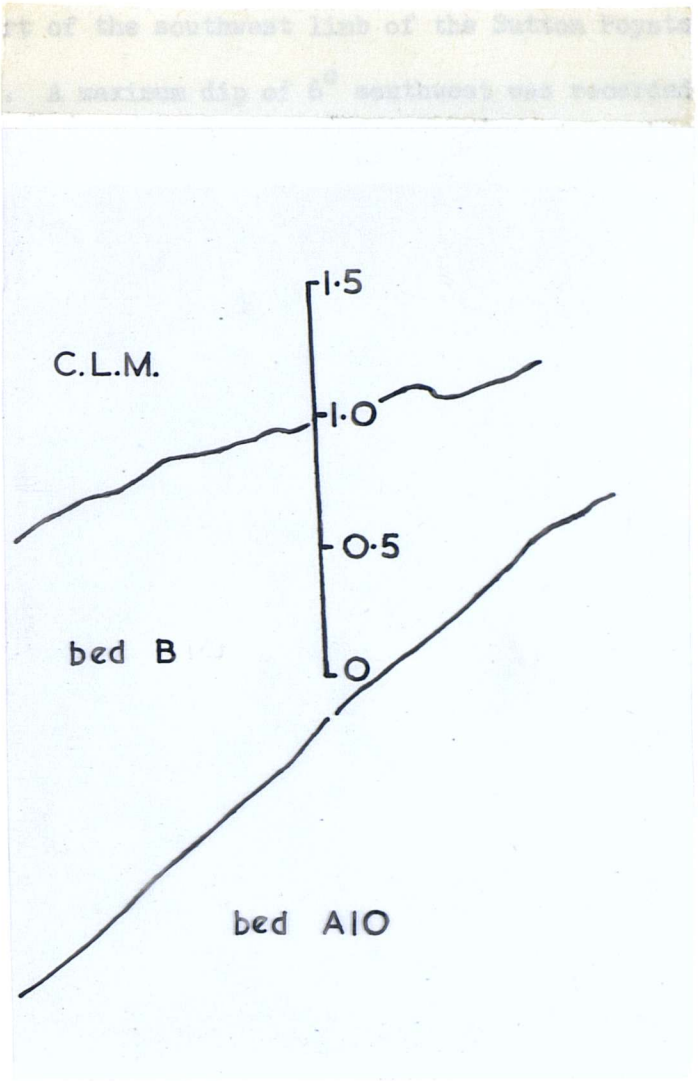
Two samples were taken from bed V at the exposure west of the Fossil Forest and one sample from bed A10 at Dungy Head (Plate 3.3), (Appendix 3).

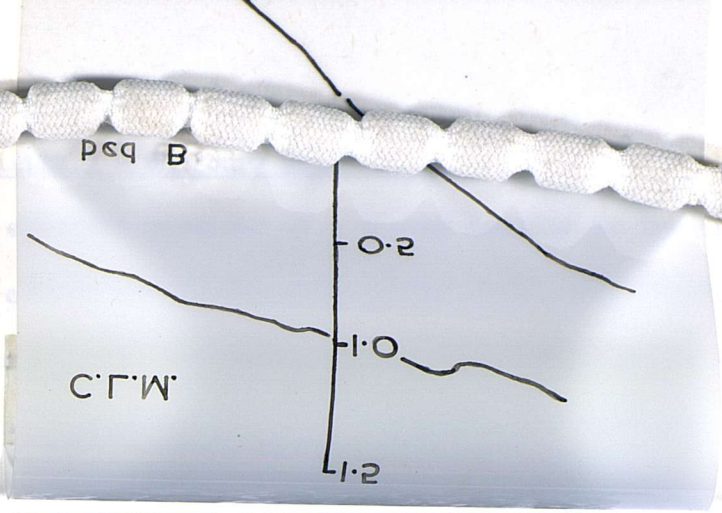
TABLE 3.3.

Generalised Section in the Portland Group,

Lulworth Cove Area

FORMATION	MEMBER	BED	THICKNESS (Metres)	NUMBER OF SAMPLES
PURBECK beds (11.10 m.)		limestones	11.00	
		black clay bed (Arkell's "Dirt Bed")	0.10	
PORTLAND LIMESTONE (16.32 m.)	OOLITIC LIMESTONE (6.65 m.)	bed V	2.08	2
		bed U	1.37	
		bed S	0.15	
		bed O(= beds O, P,Q at Swanworth Quarry)	3.05	
	CHERTY LIMESTONE (9.67 m.)	bed N	3.54	
		bed L (= beds L,M at Swanworth Quarry)	0.91	
		bed K	0.61	
		bed J'	0.53	
		bed J	1.30	
		bed G (= beds G,H at Swanworth Quarry)	0.76	
		bed C (= beds C,D, E,F at Swanworth Quarry)	2.02	
PORTLAND SANDSTONE (3.48 m.) to top of Boulder Talus above sea level		bed B	1.03	
		bed A10 (= bed A28 at Swanworth Quarry)	2.45	1


1·5
C.L.M.
1·0
0·5
bed B
0
bed A10



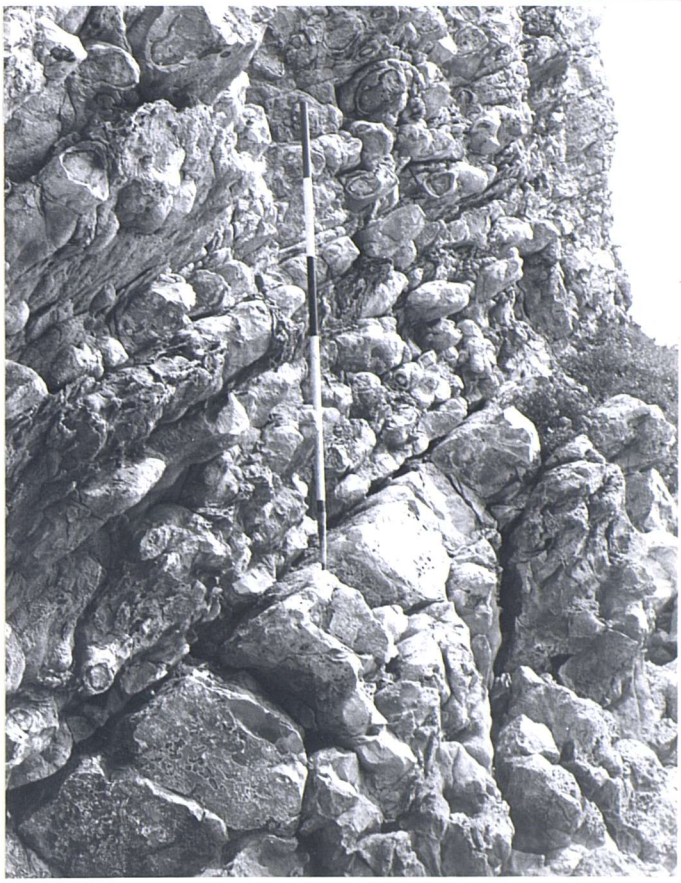


Plate 3.3 Exposure of the sampled part of the section in the Portland Group, Dungy Head.

KEY

C.L.M. --- Cherty Limestone Member

Scale is in metres.

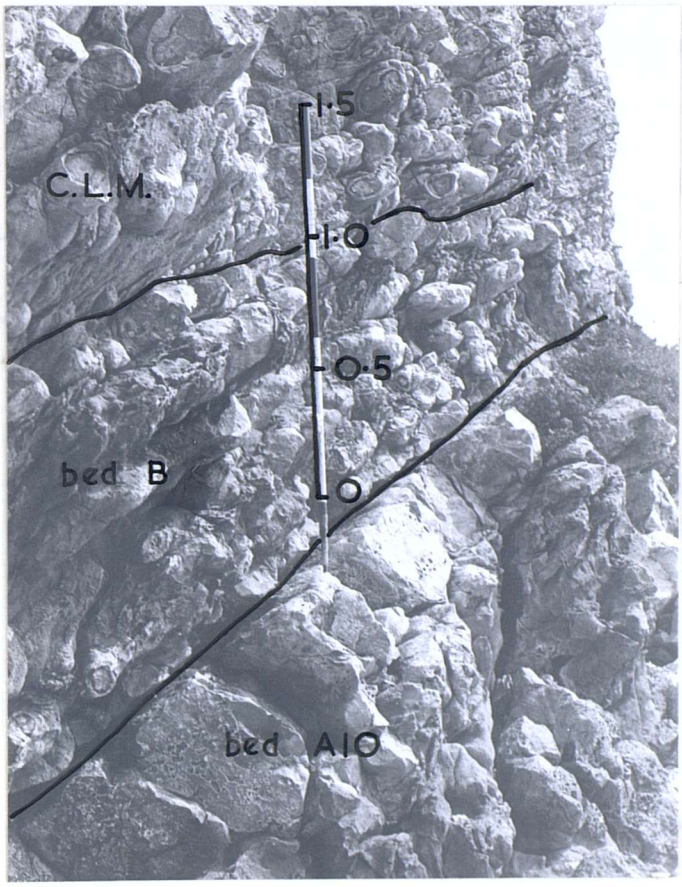


Plate 3.3 Exposure of the sampled part of the section in the Portland Group, Dungy Head

KEY

C.L.M. —— Cherty Limestone Member

Scale is in metres.

3.3.4 Locality 3 - Chalbury Camp /SY 694838/

This exposure consists of a quarry section in the Portland Limestone and overlying Purbeck beds (Plate 3.4). Structurally these strata form part of the southwest limb of the Sutton Poyntz Anticline (Arkell, 1947). A maximum dip of 6° southwest was recorded for the sampled strata. The lithostratigraphic section is presented in Table 3.4, the local bed terminology (Arkell, 1935) being retained.

TABLE 3.4

Section in the Portland Group, Chalbury Camp

FORMATION	MEMBER	BED	THICKNESS (metres)	NUMBER OF SAMPLES
PURBECK beds (3.54m)		limestones	3.50	
		black marly clay bed (Arkell's "Dirt Bed")	0.04	
PORTLAND LIMESTONE (16.70 m)	OOLITIC LIMESTONE (8.47 m)	bed 11	0.36	
		bed 10	1.02	2
		bed 9	0.16	
		bed 8	3.24	2
		bed 7	0.45	
		bed 6	3.34	2
	CHERTY LIMESTONE (7.47 m)	bed 5	1.22	3
		bed 4	3.66	
		bed 3	2.59	
		bed 2 (Arkell's "Basal Shell Bed")	0.76	
PORTLAND SANDSTONE (1.83 m. to quarry floor)		bed 1 (Arkell's "Portland Clay")	1.83	

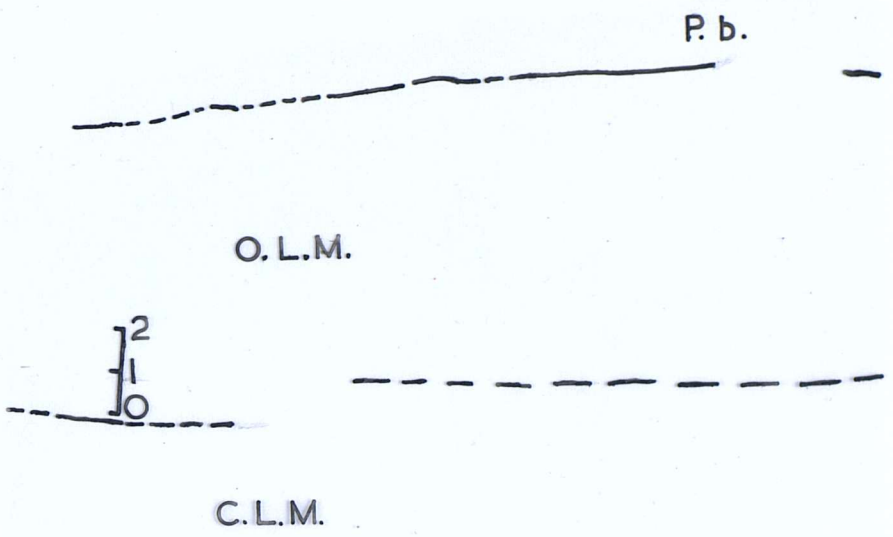

P. b.
O. L. M.
2
1
0
C. L. M.



Plate 3.4 Exposure of the sampled part of the section in the Portland Limestone, Chalbury Camp

KEY

P.b. —— Purbeck beds

O.L.M. —— Oolitic Limestone Member

C.L.M. —— Cherty Limestone Member

Scale is in metres

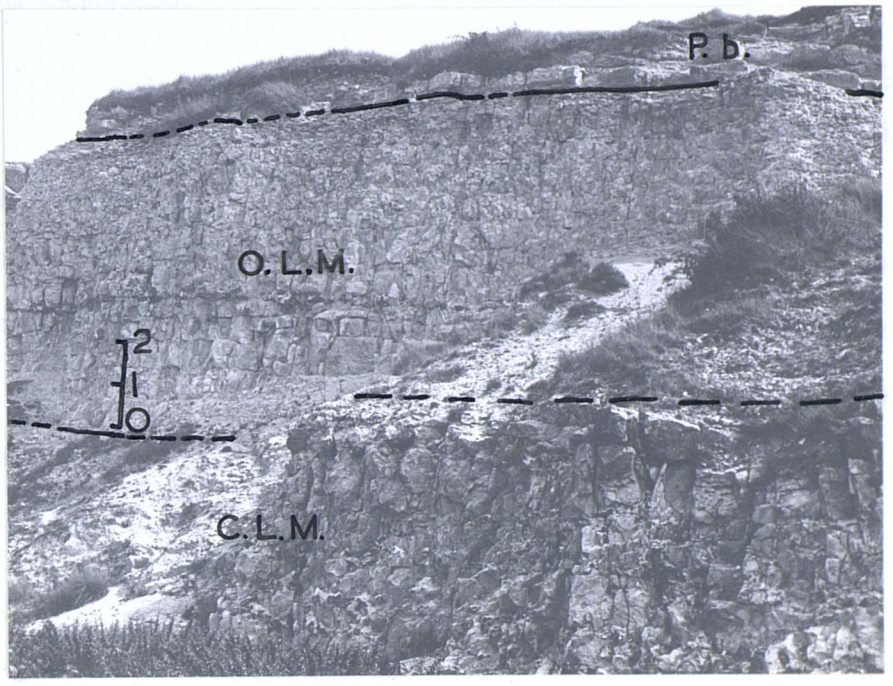


Plate 3.4 Exposure of the sampled part of the section in the Portland Limestone, Chalbury Camp

KEY

P.b. —— Purbeck beds

O.L.M. —— Oolitic Limestone Member

C.L.M. —— Cherty Limestone Member

Scale is in metres

The Oolitic Limestone Member consists of interbedded, white, chalky limestones with chert stringers, overlain by a bed of laminated limestone (bed 11). The Cherty Limestone Member consists of 3 beds of hard chalky limestone containing scattered, irregular chert nodules. This is underlain by bed 2, a beige-coloured, shelly limestone at the base of the Portland Limestone and bed 1, a greenish-black clay at the top of the Portland Sandstone.

3.3.5 Locality 4 - Road-cutting near Corton Farm /SY 636855/

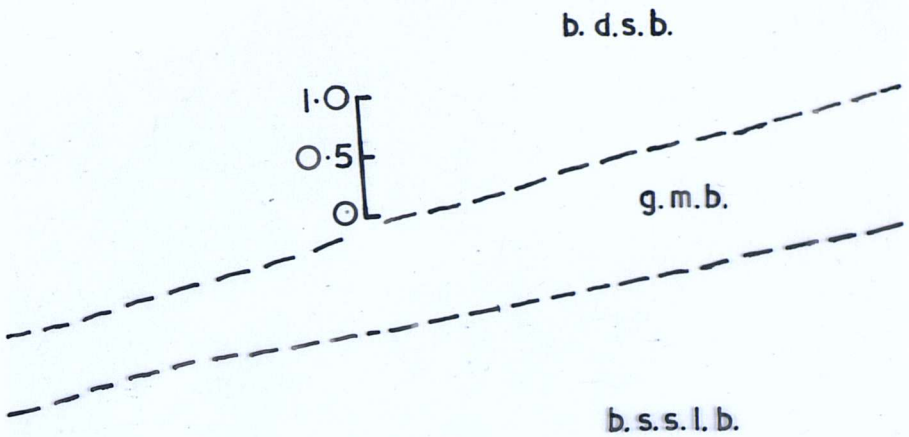
This section is restricted to the Portland Sandstone, here forming part of the southern limb of the Upwey Syncline (Arkell, 1947), with maximum dip of 13° north. Plate 3.5 illustrates the sampled part of the section, given in detail in Table 3.5. Reference was made to Arkell (1935) and Townson (1971) in order to interpret gaps in the present section.

TABLE 3.5

Section in the Portland Sandstone at top of road-cutting, Corton Farm

FORMATION	BED	THICKNESS (metres)	NUMBER OF SAMPLES
PORTLAND	black dolomitic sandstone bed	2.00	2
SANDSTONE (7.90 m)	grey marl bed (Arkell's "Cast Beds")	1.80	
(Total thickness approx 29 m. according to Arkell, 1935)	beige sandy shelly limestone bed	4.10	

Studies of more extensive sections throughout Dorset (Arkell, 1935; Townson, 1971) indicate that the black dolomitic sandstone bed, from which 2 samples were taken, is probably equivalent to bed A 28 at Swanworth Quarry and bed A 10 at Dungy Head. It thus is part of the highest beds of the Portland Sandstone.


b. d.s. b.
1·0
0·5
0
g. m. b.
b. s. s. l. b.

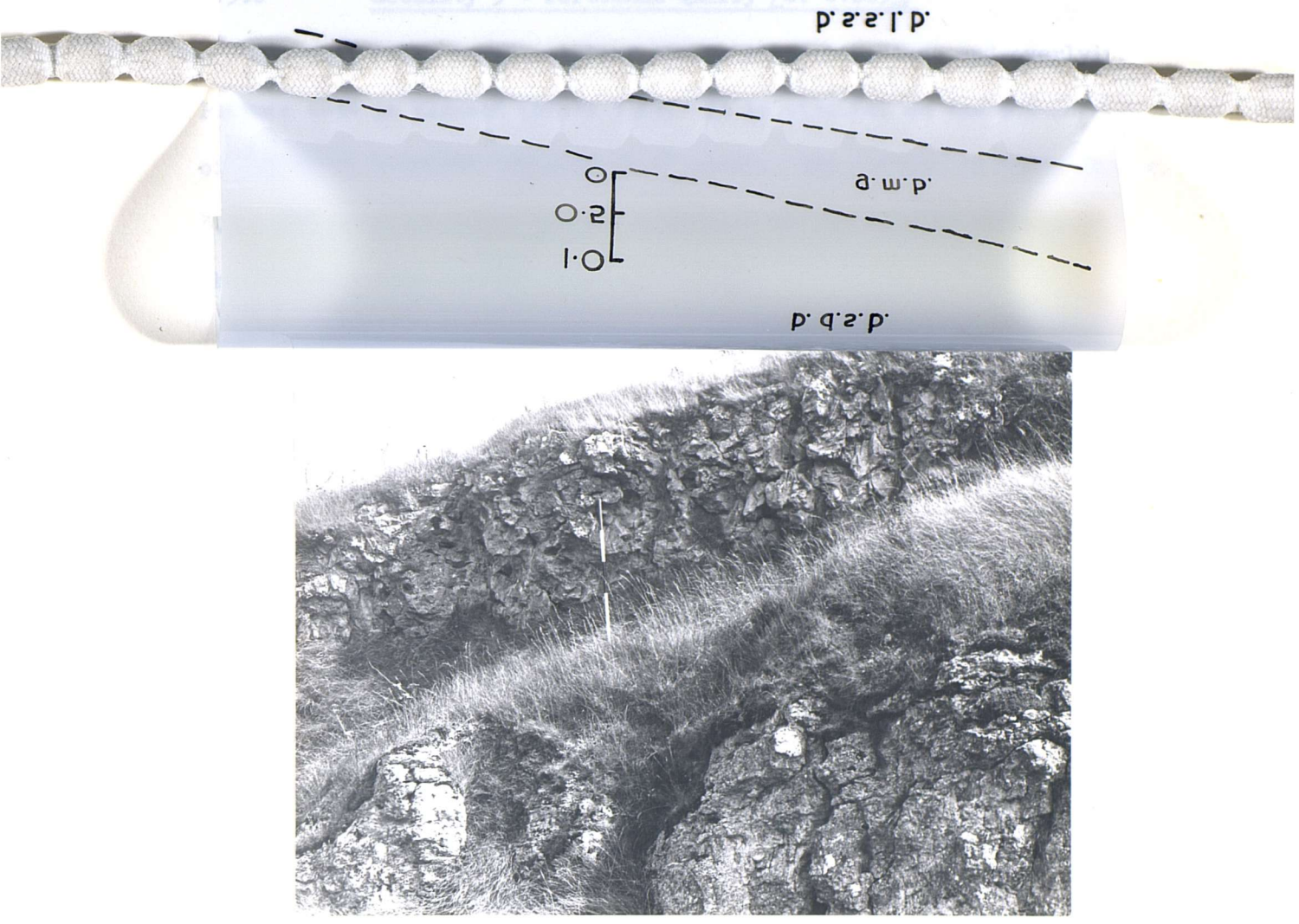


Plate 3.5 Exposure at top of road-cutting, Corton Farm, showing the sampled part of the section in the Portland Sandstone

KEY

b.d.s.b. — black dolomitic sandstone bed

g.m.b. — grey marl bed

b.s.s.l.b. — beige sandy shelly limestone bed

Scale is in metres

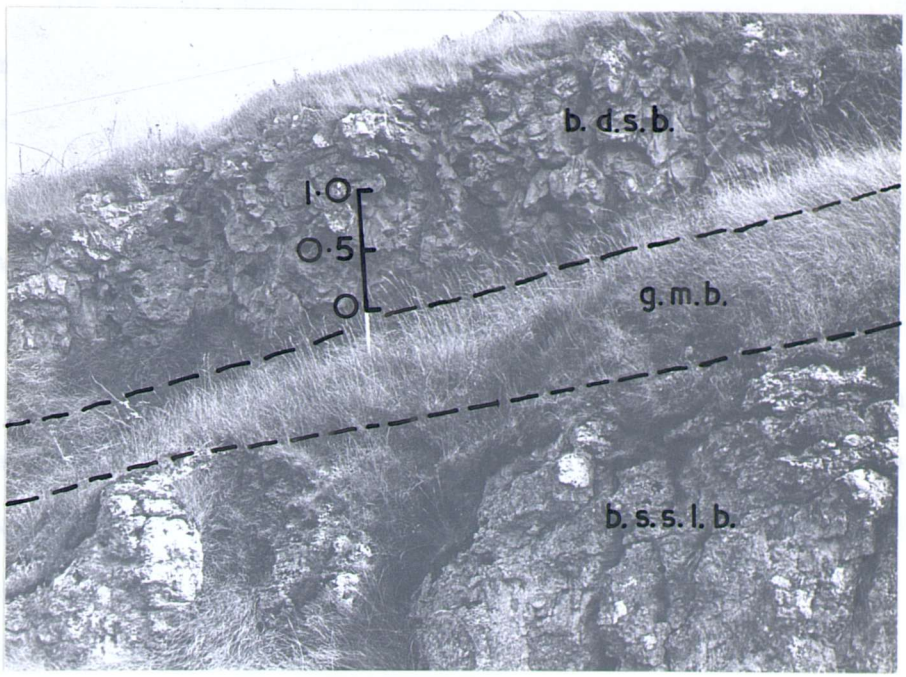


Plate 3.5 Exposure at top of road-cutting, Corton Farm, showing the sampled part of the section in the Portland Sandstone

KEY

b.d.s.b. — black dolomitic sandstone bed

g.m.b. — grey marl bed

b.s.s.l.b. — beige sandy shelly limestone bed

Scale is in metres

3.3.6 Locality 5 - Portesham Quarry [SY 610859]

At this quarry, part of the Portland Limestone and overlying Purbeck beds is exposed (Plate 3.6). It is situated on the southern limb of the Upwey Syncline and dips at 5° north. The section is shown in Fig. 3.2. The sequence here, though condensed, is the lateral equivalent of the Chalbury Camp section (Section 3.3.4).

The Oolitic Limestone Member consists of chalky limestones with chert stringers overlain by a bed of grey laminated limestone (bed 11). This laminated limestone grades into the top of the chalky limestone. Only the top of the Cherty Limestone Member is exposed in this section (bed 5), consisting of a hard chalky limestone with chert nodules.

3.3.7 Locality 6 - Isle of Portland

The most extensive exposures of the Portland Group in Dorset are found on the Isle of Portland. The Isle of Portland is located on the southern limb of the Weymouth Anticline, with a maximum dip of 4° south. Three localities were sampled as follows:

a) West Weare Cliffs [SY 682724]

b) Freshwater Bay [SY 692702]

c) Perryfield Quarries [SY 694712]

These sections show very similar successions to the type-locality on West Weare Cliffs [SY 682720]. The presence of several clays and marls in the Portland Sandstone and of chert nodules and hollow shell moulds in beds of the Portland Limestone, restricted sampling. The relevant sections are described.

a) West Weare Cliffs [SY 682724]

This locality is approximately 400 metres north of the type-locality, but nevertheless an almost continuous exposure of the upper part of the Portland Sandstone and most of the Portland Limestone is present. Plate 3.7 and Fig. 3.3 give details of the sampled section.

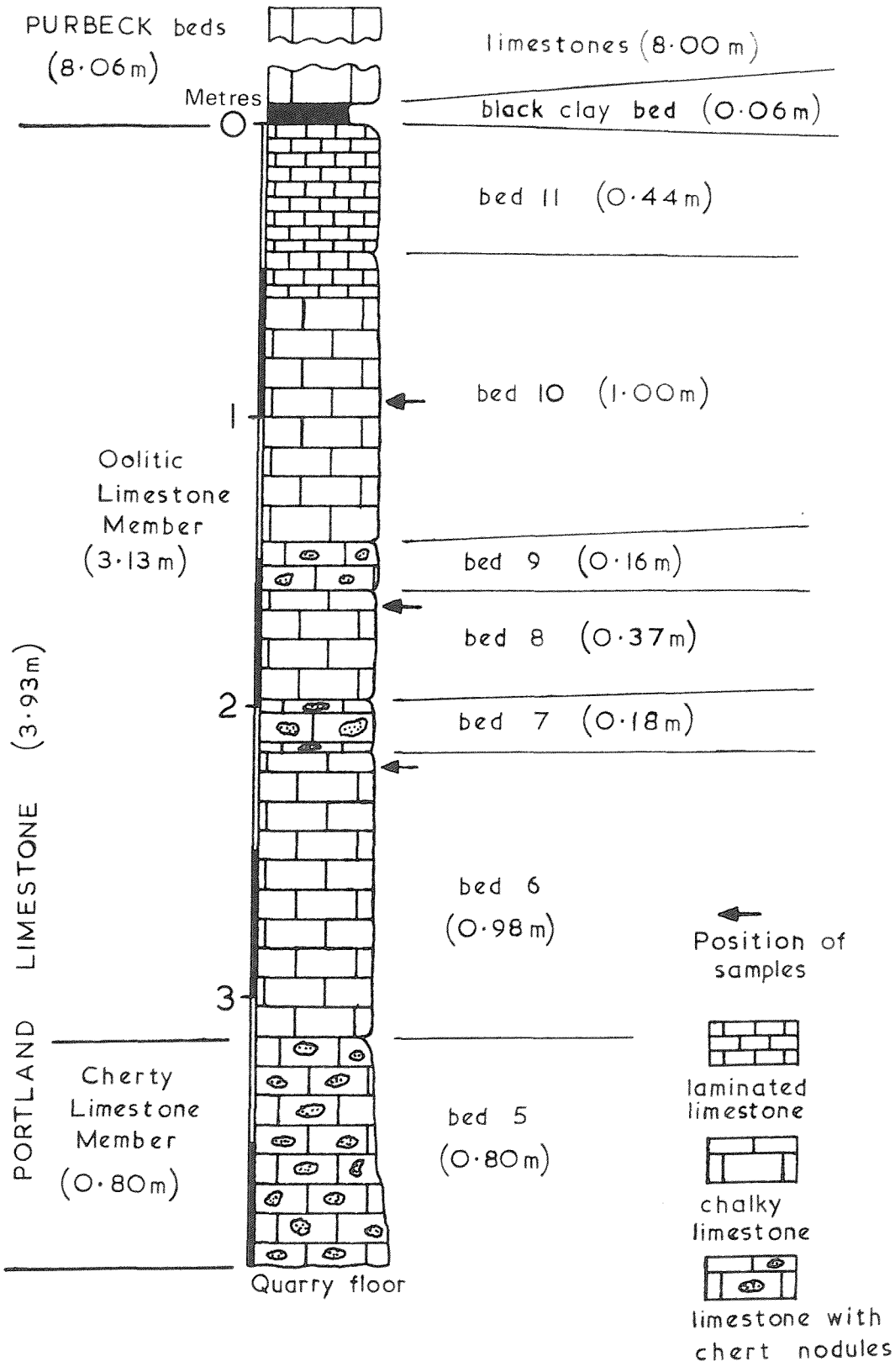
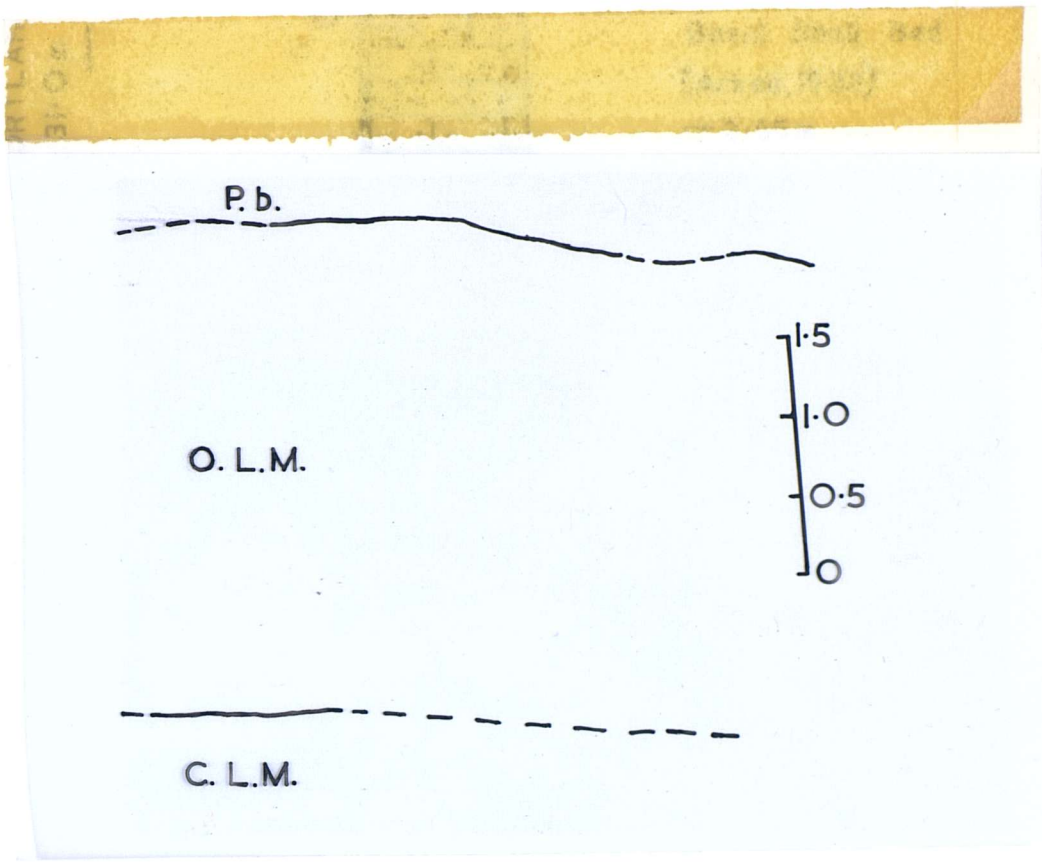


Fig. 3.2 Section of the Portland Limestone, Portesham Quarry


P. b.
1·5
1·0
0·5
0
O. L. M.
C. L. M.

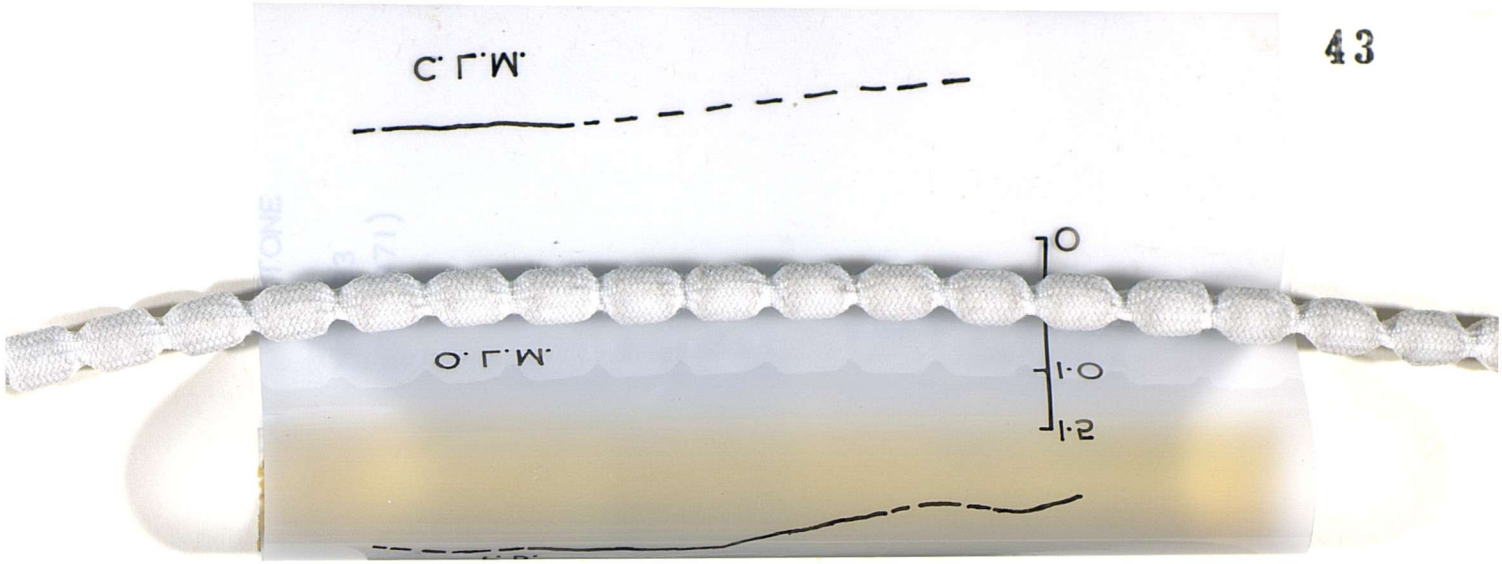




Plate 3.6 Exposure of the section in the Portland Limestone, Portesham Quarry

KEY

P.b. —— Purbeck beds

O.L.M. —— Oolitic Limestone Member

C.L.M. —— Cherty Limestone Member

Scale is in metres

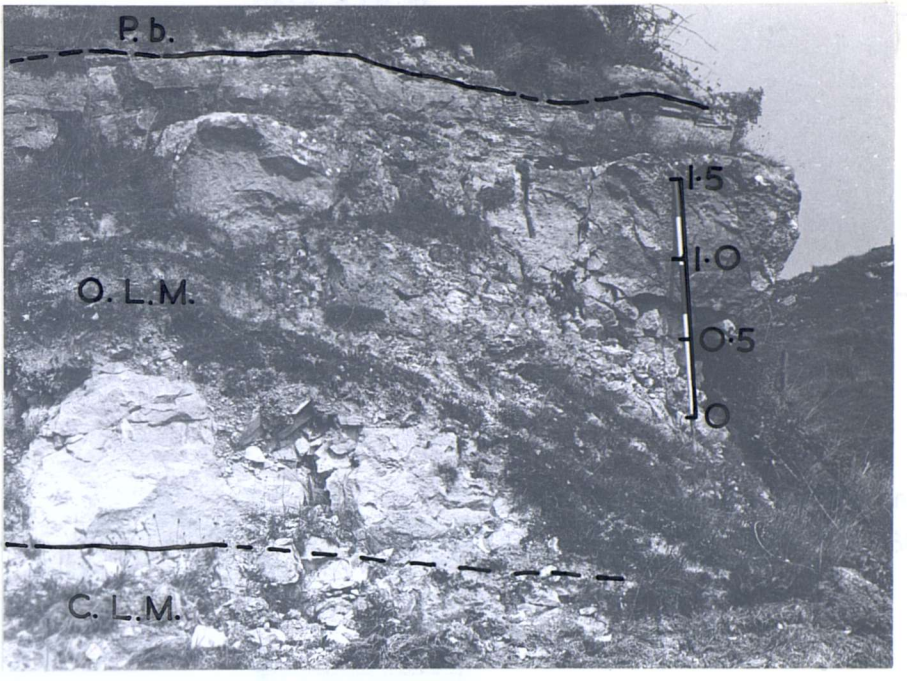


Plate 3.6 Exposure of the section in the Portland Limestone, Portesham Quarry

KEY

P.b. —— Purbeck beds

O.L.M. —— Oolitic Limestone Member

C.L.M. —— Cherty Limestone Member

Scale is in metres

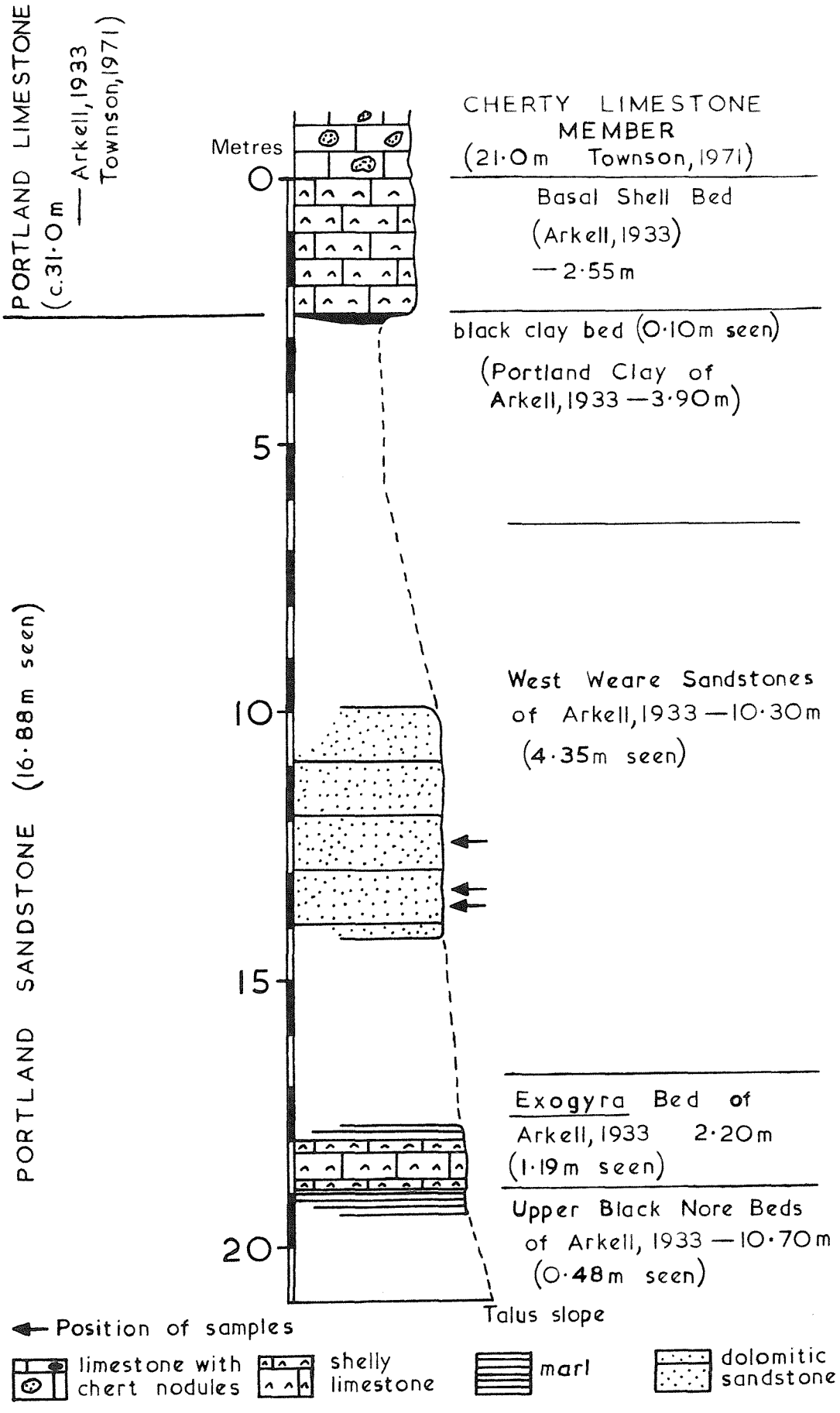
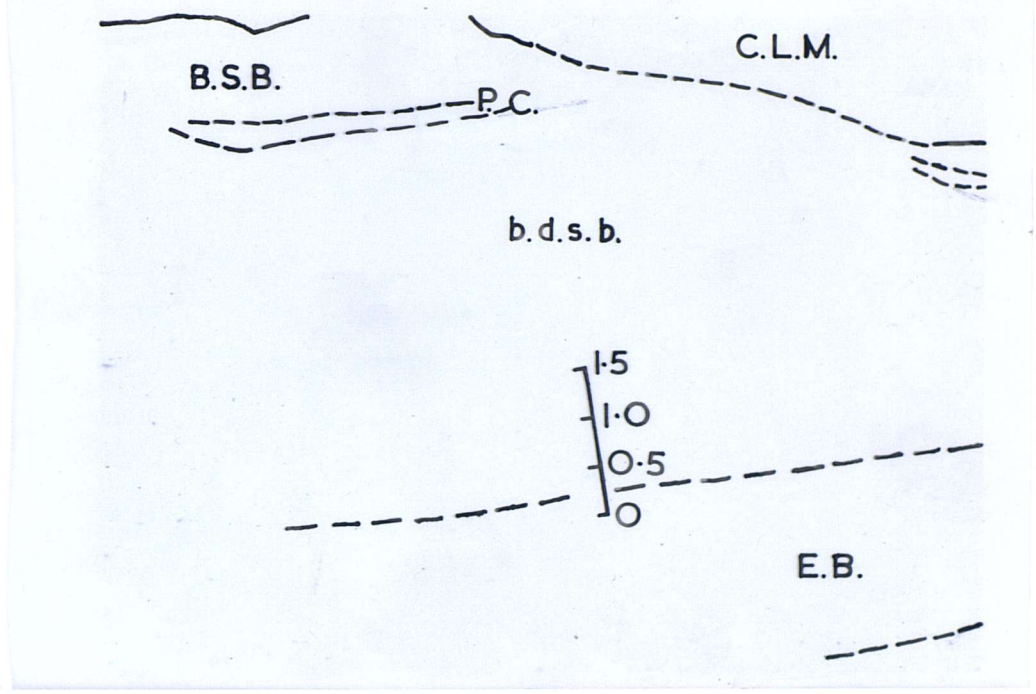


Fig. 3.3 Sampled section of the Portland Group, West Weare Cliffs


B.S.B.
P.C.
C.L.M.
b.d.s.b.
1·5
1·0
0·5
0
E.B.

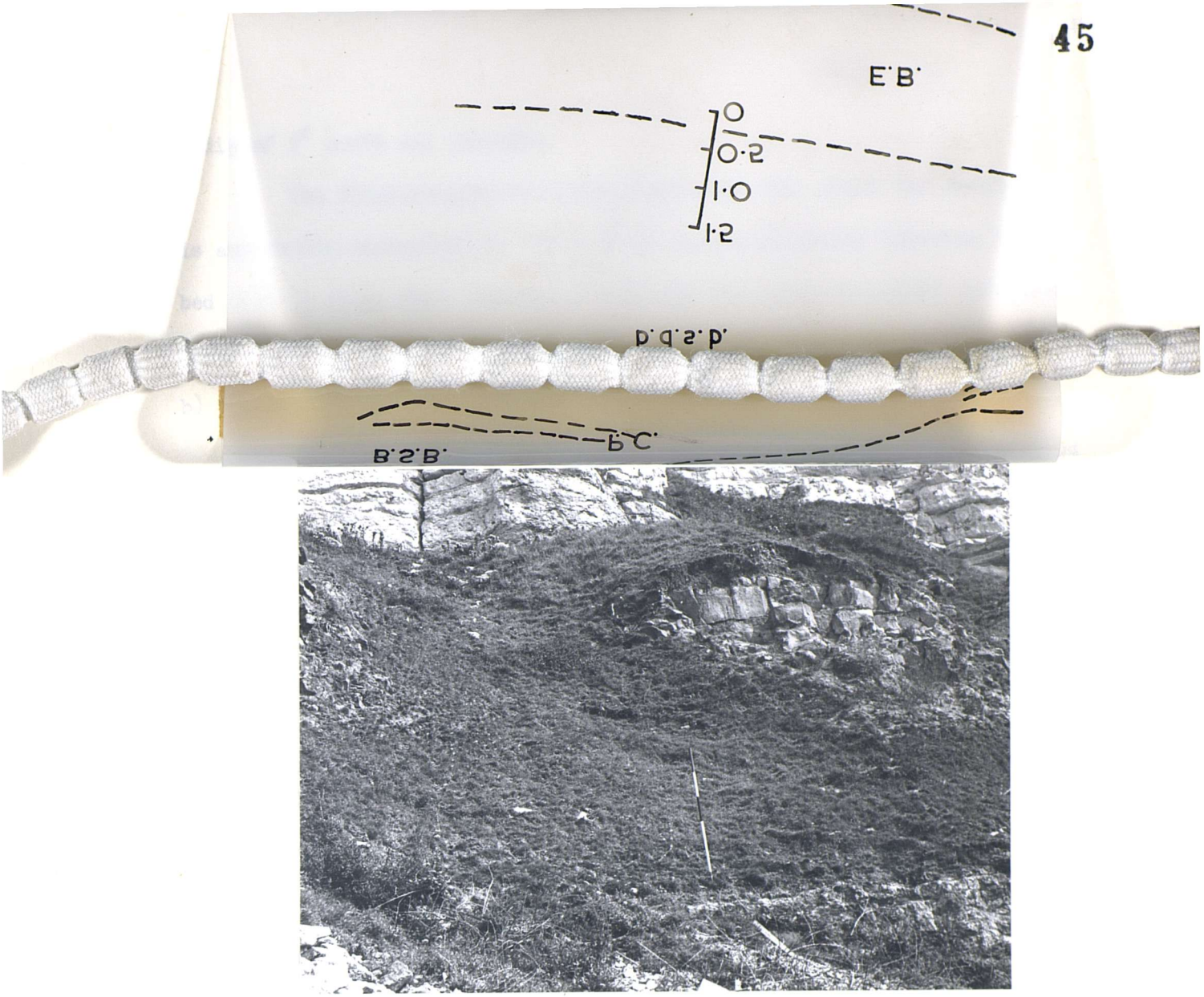


Plate 3.7 Exposure of the sampled part of the section in the Portland Group, West Weare Cliffs

KEY

C.L.M. — Cherty Limestone Member

B.S.B. — Arkell's Basal Shell Bed

P.C. — Arkell's Portland Clay

b.d.s.b. — blackish-grey dolomitic sandstone bed

E.B. — Arkell's *Exogyra* Bed

Scale is in metres

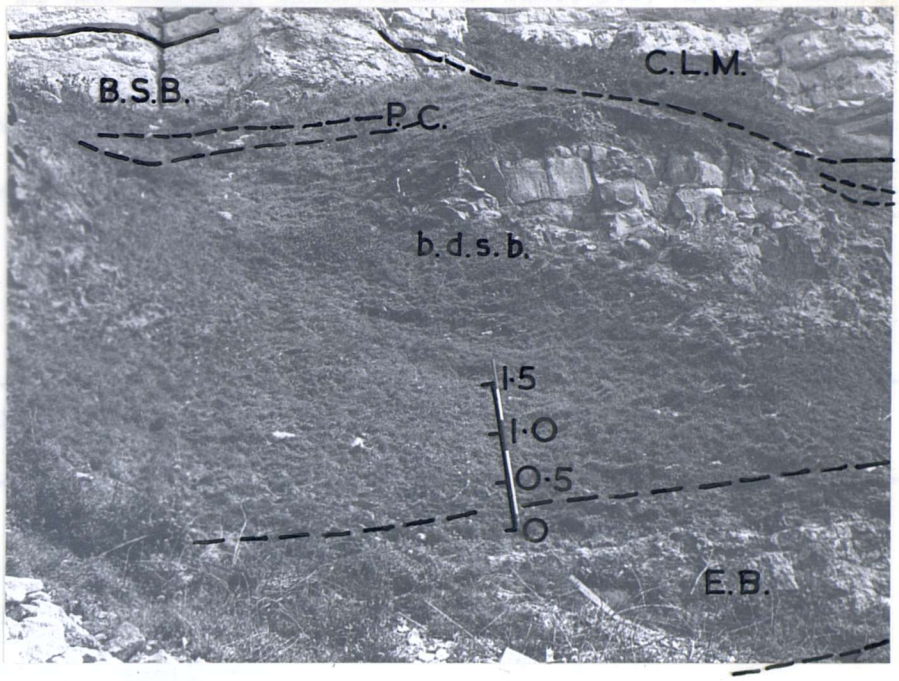


Plate 3.7 Exposure of the sampled part of the section in the Portland Group, West Weare Cliffs

KEY

C.L.M. — Cherty Limestone Member
B.S.B. — Arkell's Basal Shell Bed
P.C. — Arkell's Portland Clay
b.d.s.b. — blackish-grey dolomitic sandstone bed
E.B. — Arkell's *Exogyra* Bed
Scale is in metres

A dip of 2° south was recorded.

The blackish-grey dolomitic sandstone bed, which was sampled, is apparently equivalent to bed A 28 at Swanworth Quarry (Section 3.3.2), bed A 10 at Dungy Head (Section 3.3.3) and the black dolomitic sandstone bed at Corton Farm road-cutting (Section 3.3.5), (Townson, 1971).

b) Freshwater Bay /SY 692702/

In this section, illustrated in Plate 3.8, most of the Portland Limestone and the highest bed of the Portland Sandstone are exposed. Sampling was restricted to the lowest bed of the Portland Limestone (Table 3.6). The maximum dip recorded was 4° south.

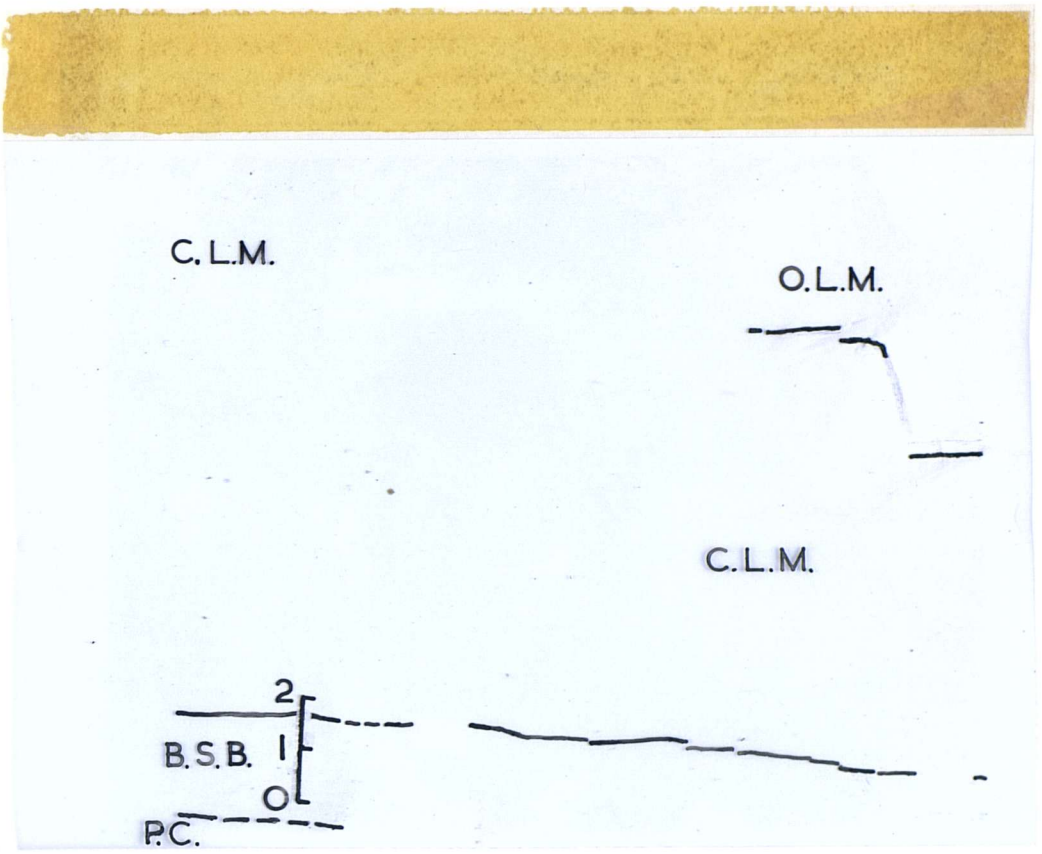
TABLE 3.6

Section in Part of the Portland Group, Freshwater Bay

FORMATION	MEMBER	BED	THICKNESS (metres)	NUMBER OF SAMPLES
PORTLAND LIMESTONE (26.0 m, according to Townson, 1971)	CHERTY LIMESTONE (15.0 m. according to Townson, 1971)	Beds of limestone with chert nodules and stringers		
		grey shelly limestone bed (Arkell's "Basal Shell Bed")	2.80	3
PORTLAND SANDSTONE (0.82 m.) (to beach level)		black clay bed (Arkell's "Portland Clay")	0.82	

c) Perryfield Quarries /SY 694712/

A section in part of the Portland Limestone and the overlying Purbeck beds is exposed, with the strata dipping south at 3°. The section is shown in Table 3.7 and illustrated in Plate 3.9.


C. L.M.
O.L.M.
C.L.M.
2
B.S.B. 1
O
P.C.

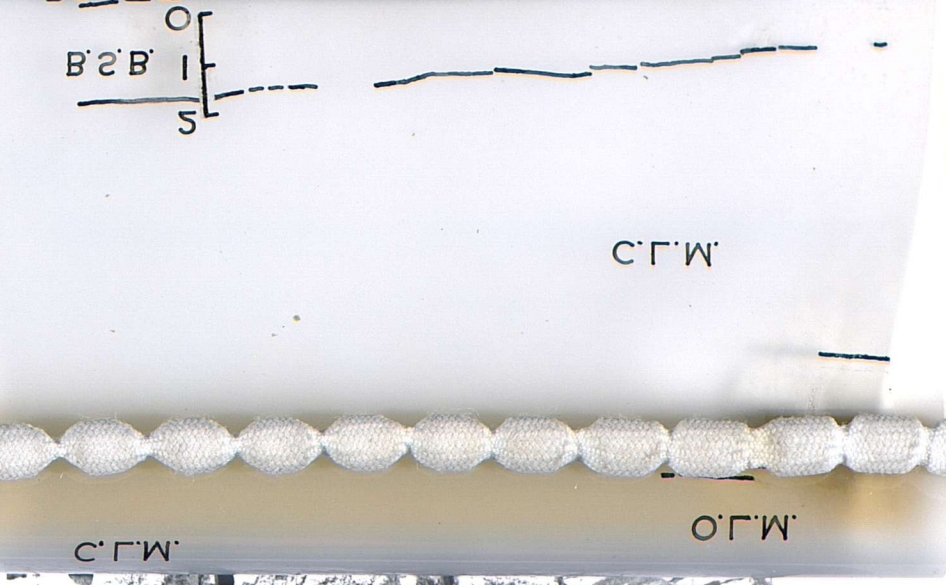


Plate 3.8 Exposure of the section in the Portland Group, Freshwater Bay

KEY

O.L.M. —— Oolitic Limestone Member

C.L.M. —— Cherty Limestone Member

B.S.B. —— Arkell's Basal Shell Bed

P.C. —— Arkell's Portland Clay

Scale is in metres

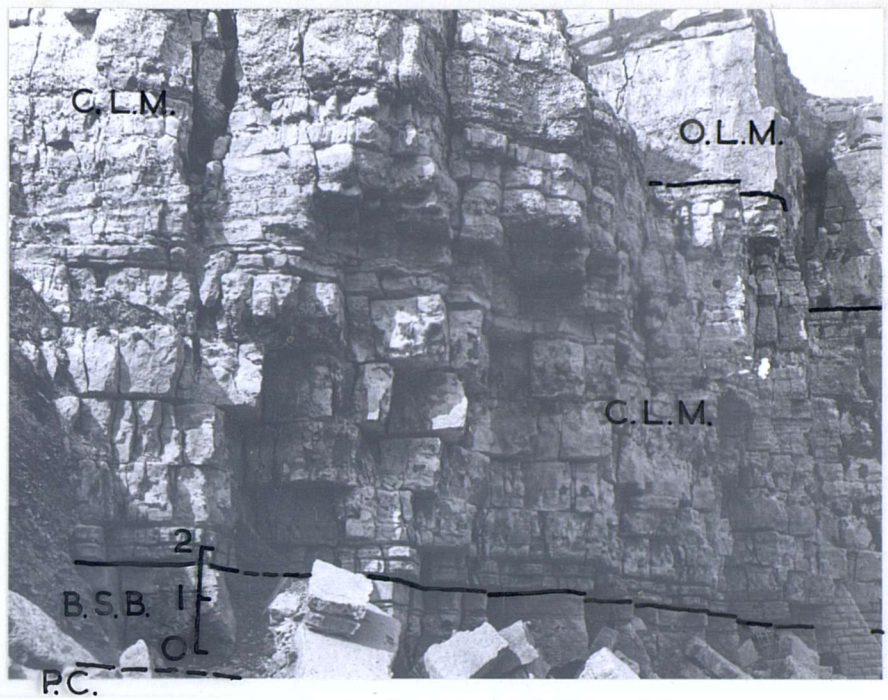


Plate 3.8 Exposure of the section in the Portland Group, Freshwater Bay

KEY

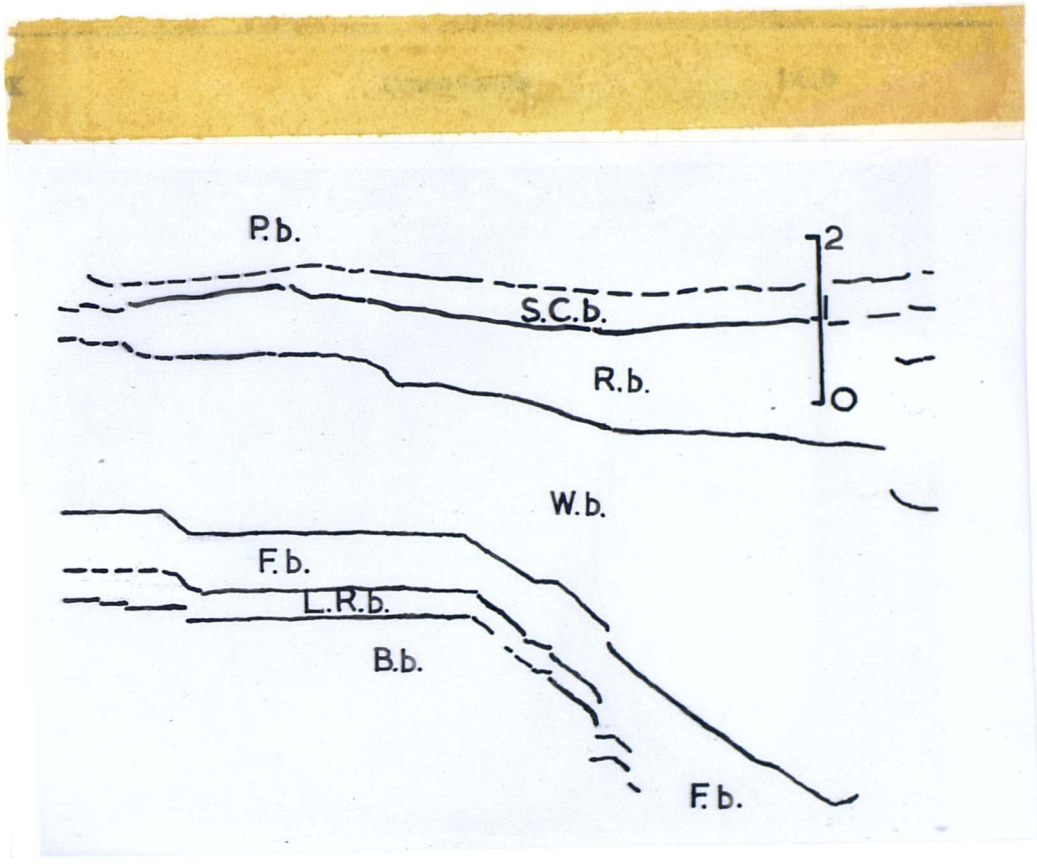
O.L.M. —— Oolitic Limestone Member

C.L.M. —— Cherty Limestone Member

B.S.B. —— Arkell's Basal Shell Bed

P.C. —— Arkell's Portland Clay

Scale is in metres


P.b.
2
S.C.b.
1
R.b.
O
W.b.
F.b.
L.R.b.
B.b.
F.b.

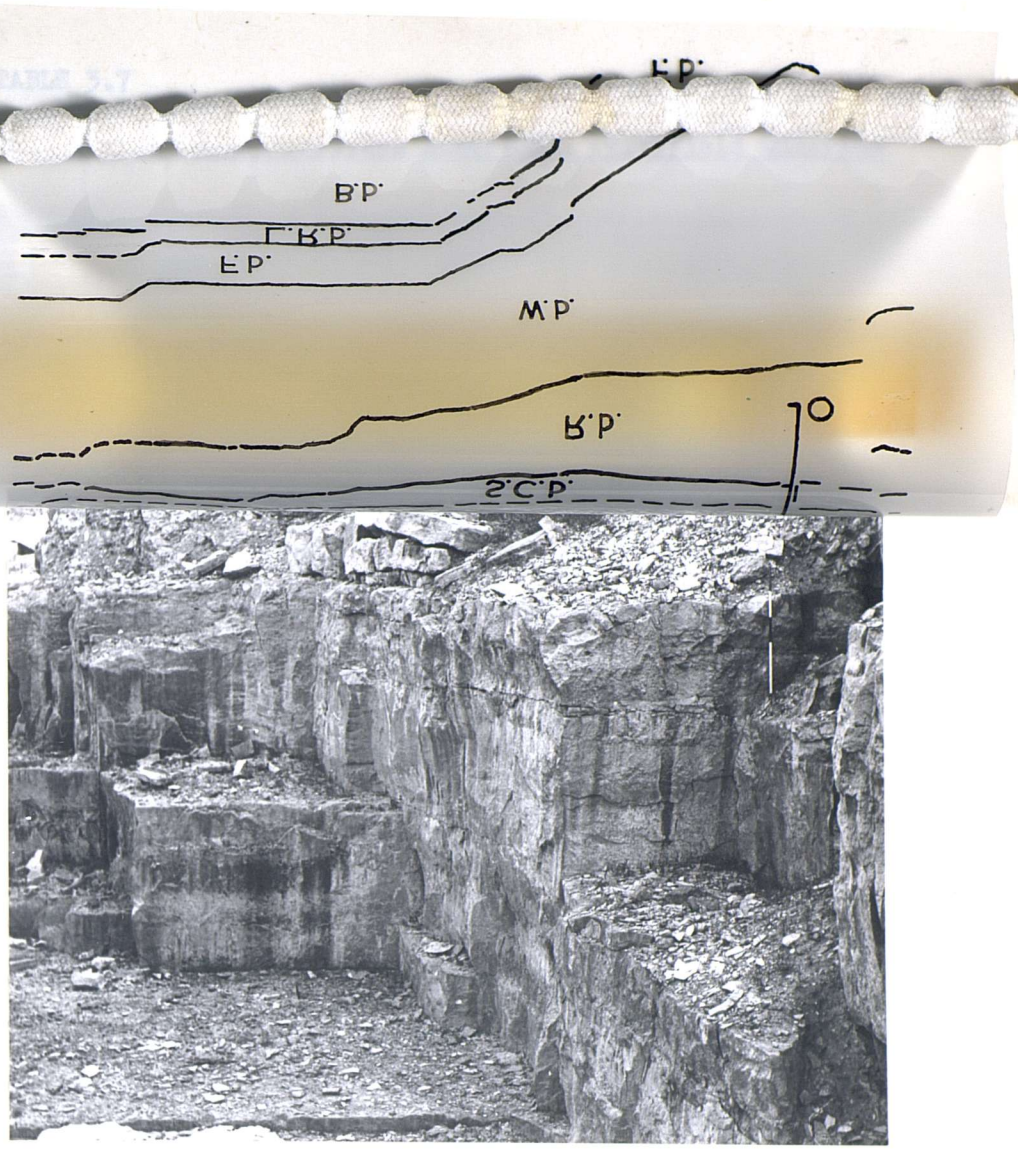


Plate 3.9 Exposure of the section in the Portland Limestone, Perryfield Quarries

KEY

P.b. — Purbeck beds
S.C.b. — Skull Cap bed
R.b. — Roach bed
W.b. — Whit bed
F.b. — Flinty bed
L.R.b. — Little Roach bed
B.b. — Base bed
Scale is in metres

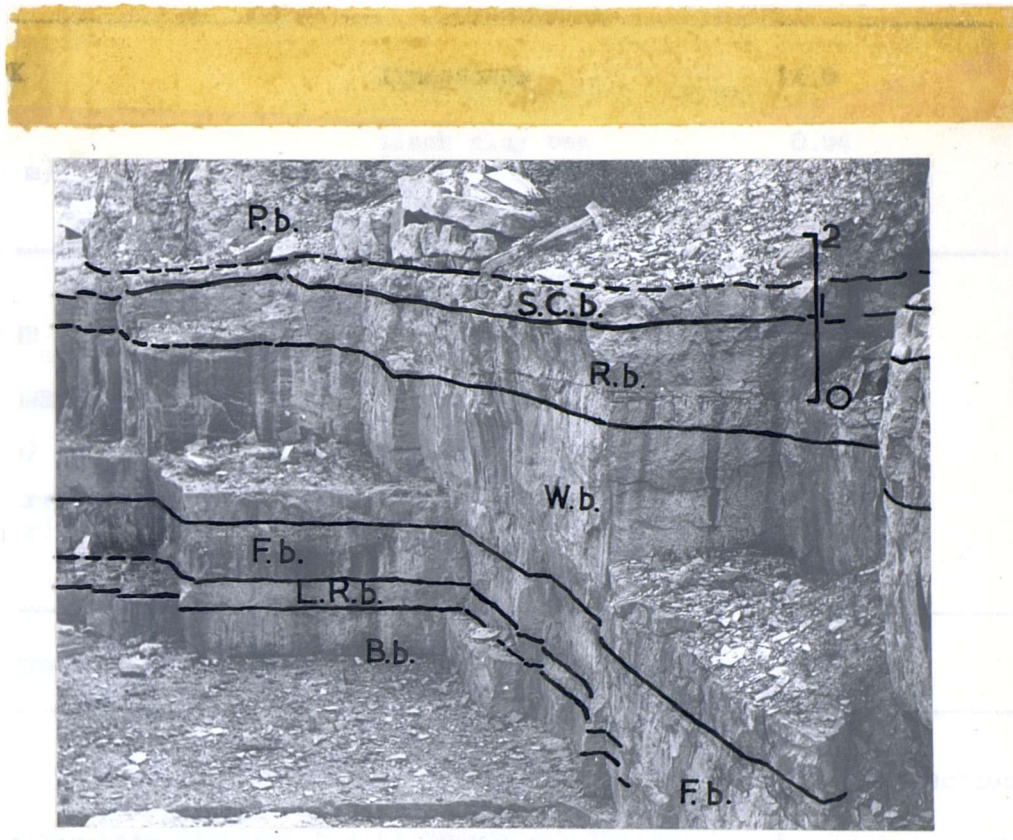


Plate 3.9 Exposure of the section in the Portland Limestone, Perryfield Quarries

KEY

P.b. —— Purbeck beds
S.C.b. —— Skull Cap bed
R.b. —— Roach bed
W.b. —— Whit bed
F.b. —— Flinty bed
L.R.b. —— Little Roach bed
B.b. —— Base bed

Scale is in metres

TABLE 3.7

Section in the Portland Limestone, Perryfield Quarries

FORMATION	MEMBER	BED	THICKNESS (metres)	NUMBER OF SAMPLES
PURBECK beds (14.04 m)		limestones	14.0	
		black clay bed (Arkell's "Lower Dirt Bed")	0.04	
PORTLAND LIMESTONE (6.61 m) (to quarry floor)	OOLITIC LIMESTONE (6.61 m)	Skull Cap bed*	0.43	
		Roach bed*	1.48	
		Whit bed*	2.42	2
		Flinty bed*	1.01	
		Little Roach bed*	0.45	
		Base bed*	0.82	2

* quarrymen's names for beds

The section at Perryfield Quarries is comparable to the section at the type locality (Section 3.2.1) except for the Roach bed, which is a shelly, oolitic limestone with an absence of shell moulds, and the Flinty bed, an oolitic limestone containing two horizons of chert nodules.

3.3.8 Locality 7 - Chilmark Ravine /ST 974313/

Isolated exposures of the Portland Group occur in several disused quarries and underground galleries on Ministry of Defence property. The strata, forming part of a northwest - southeast trending flexure on the northern limb of the Vale of Wardour Anticline, lie almost horizontally. A generalised section is shown in Table 3.8, based upon sections described by previous workers (Huddleston, 1883; Woodward, 1895; Arkell, 1933; Townson, 1971), supplemented by personal observations.

TABLE 3.8

Generalised Section in the Portland Group, Chilmark Ravine

FORMATION	BED older terminology	BED description	THICKNESS (metres)	NUMBER OF SAMPLES
PURBECK beds (4.43 m)		limestones	4.40(Woodward,1895)	
		brown clay bed	0.03	
PORTLAND LIMESTONE (15.98 m)	Upper Building Stones	beige oolitic limestone beds	4.88	4
	Cherty Series	chalky limestone beds with occasional chert nodules	7.30	3
	Ragstones	Ragstone beds (shelly and oolitic limestones with interbedded marls)	3.00	1
	Main Building Stones	Trough bed (sandy oolitic limestone)	0.80	
PORTLAND SANDSTONE (4.70 m to quarry floor)		glauconitic sandy limestone beds	4.70	

Earlier workers identified two formations here - Portland Stone conformably overlying Portland Sand. The boundary was placed at the top of the Trough bed. This bed shows greater resemblance to the overlying Ragstones than to the glauconitic sandy limestones beneath. The boundary between Portland Limestone and Portland Sandstone is accordingly moved to the base of the Trough bed.

3.3.9 Locality 8 - Upper Chicksgrove Quarry /ST 962296/

Upper Chicksgrove Quarry consists of one main face exposing nearly 10 metres of Portland Sandstone (Plate 3.10), and several small

isolated exposures, which together give an almost continuous section of the Portland Limestone and the basal part of the overlying Purbeck beds (Plate 3.11). The strata are situated on the southern limb of the Vale of Wardour Anticline and dip at 4° southsoutheast.

This quarry has only recently been opened, and description is limited to Townson (1971). The section given in Fig. 3.4 is based partly on Townson's observations together with further measurements made by the author. Small discrepancies exist between the recorded thicknesses and those noted by Townson. Existing bed nomenclature applicable to the Vale of Wardour (Huddleston, 1883; Woodward, 1895; Arkell, 1933), was used where possible.

Earlier workers recognised Purbeck Beds, with a laminated limestone bed at the base (Townson, 1971) resting on Portland Stone which in turn rests on the Portland Sand with the Trough bed at its top. The Portland Limestone, as defined here, includes both the laminated limestone and the Trough bed (Fig. 3.4).

Correlation of the lower part of the Portland Sandstone underlying the glauconitic sandy limestone beds (Fig. 3.4) at Upper Chicksgrove Quarry with other exposures in the Vale of Wardour is uncertain. Townson (1971) recorded approximately 7.5 metres of Basement beds (Fig. 3.4), termed the "Sandy Limestone Beds", resting on 3.8 metres of shelly limestones termed the "Wardour Exogyra Beds". He suggested that these shelly limestones were equivalent to the Upper Lydite Bed, as defined by Arkell (1933), elsewhere in the Vale of Wardour. The Upper Lydite Bed was first described by Huddleston (1883) as 0.91 metres of "greenish concretionary limestone grit, with occasional lydite", at a section near Haselton [ST 935280] which is 2.7 Km. west of Upper Chicksgrove Quarry. Here, the Upper Lydite Bed was separated from the Main Building Stones (see Fig. 3.4) by 2.13 metres of "loose sands with doggers", which formed part of the Basement Beds (Huddleston, 1883).

The base of the Portland Sandstone is not now exposed anywhere in the Vale of Wardour so that its total thickness is indeterminate. It seems very unlikely that the 3 metres seen at Haselton (Huddleston, 1883) could thicken to the 11.3 metres (Townson, 1971) seen at Chicksgrove. Accordingly, the shelly limestones at the base of the Chicksgrove section are informally designated the Basal Shell beds and are thought to be unexposed at Haselton.

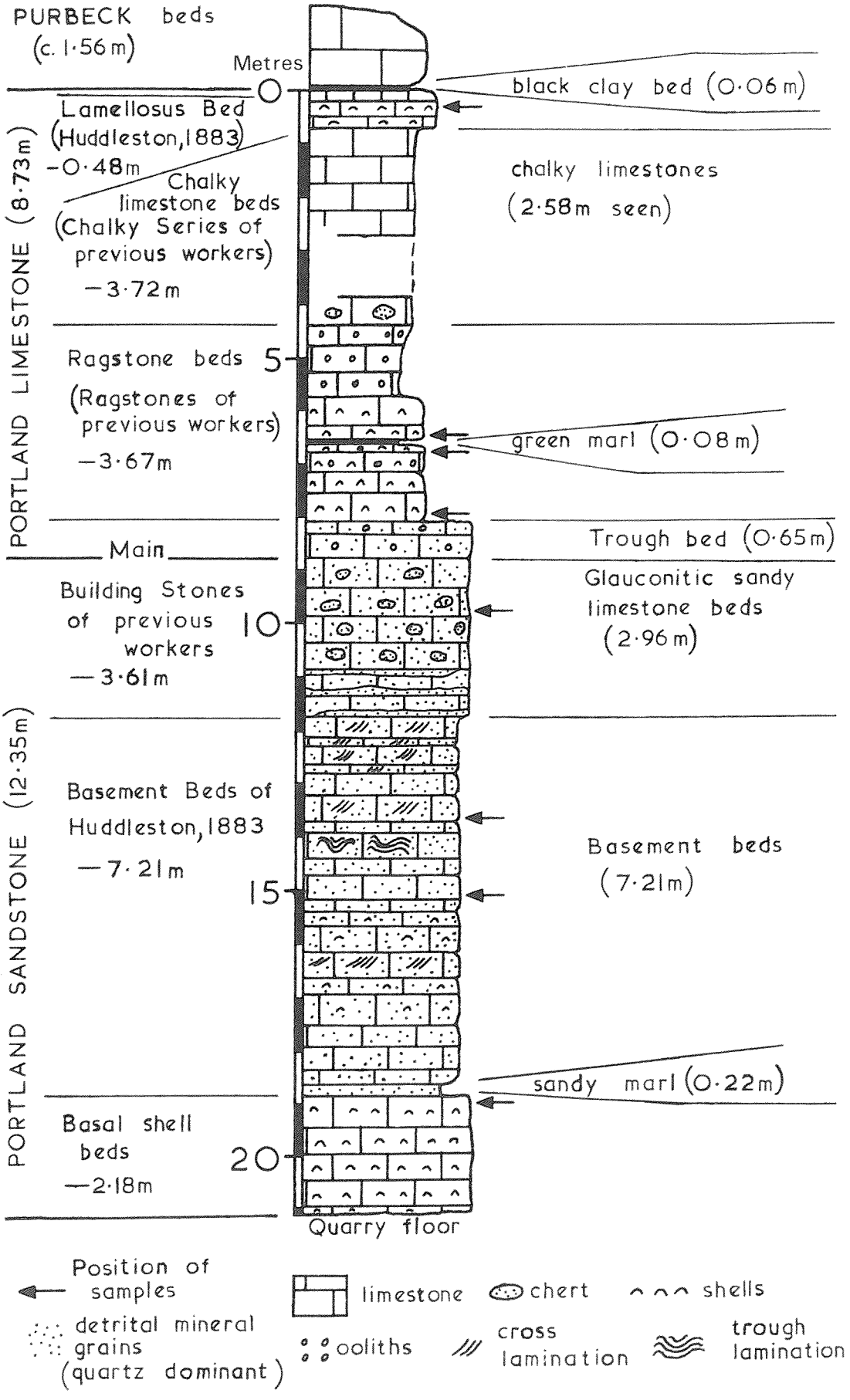


Fig. 3.4 Section of the Portland Group, Upper Chicksgrove Quarry

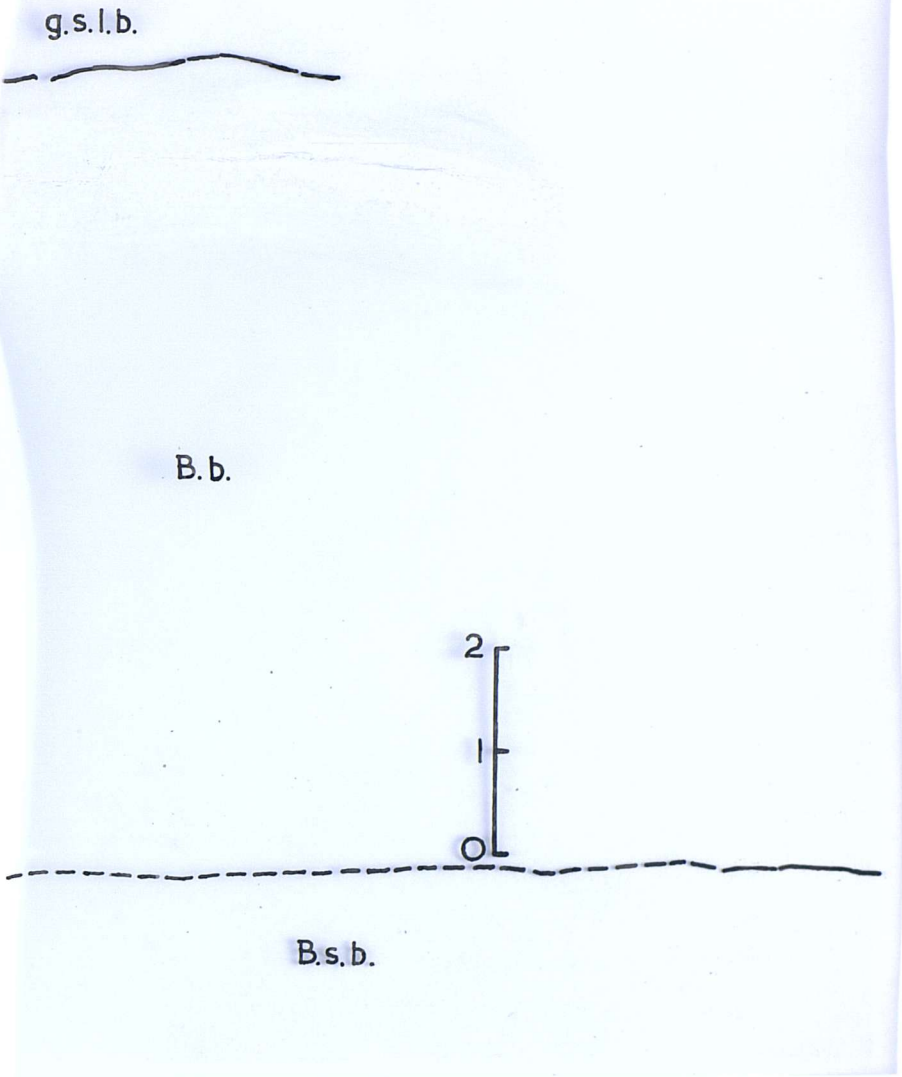

g.s.l.b.
B.b.
2
1
0
B.s.b.



Plate 3.10 Exposure of part of the section in the Portland Sandstone, main face, Upper Chicksgrove Quarry

KEY

g.s.l.b. —— glauconitic sandy limestone beds

B.b. —— Basement beds

B.s.b. —— Basal shell beds

Scale is in metres



Plate 3.10 Exposure of part of the section in the Portland Sandstone, main face, Upper Chicksgrove Quarry

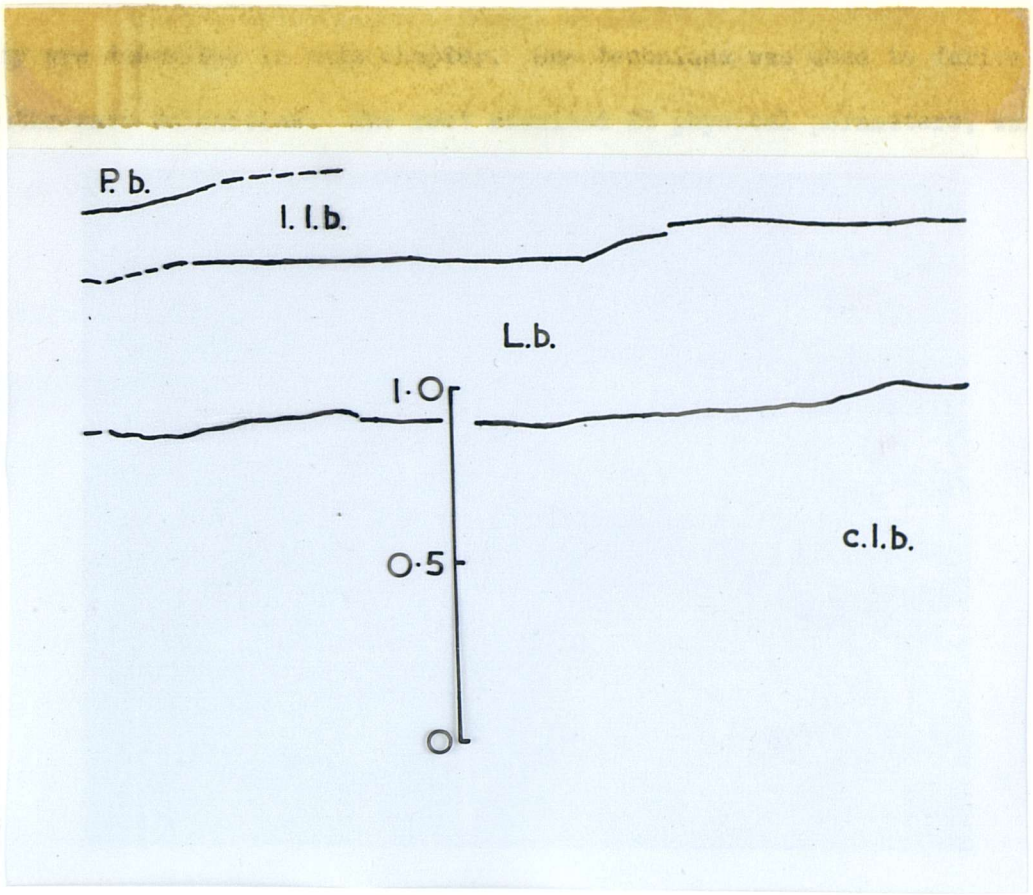
KEY

g.s.l.b. — glauconitic sandy limestone beds

B.b. — Basement beds

B.s.b. — Basal shell beds

Scale is in metres


P. b.
I. I. b.
L. b.
1·0
0·5
c. l. b.

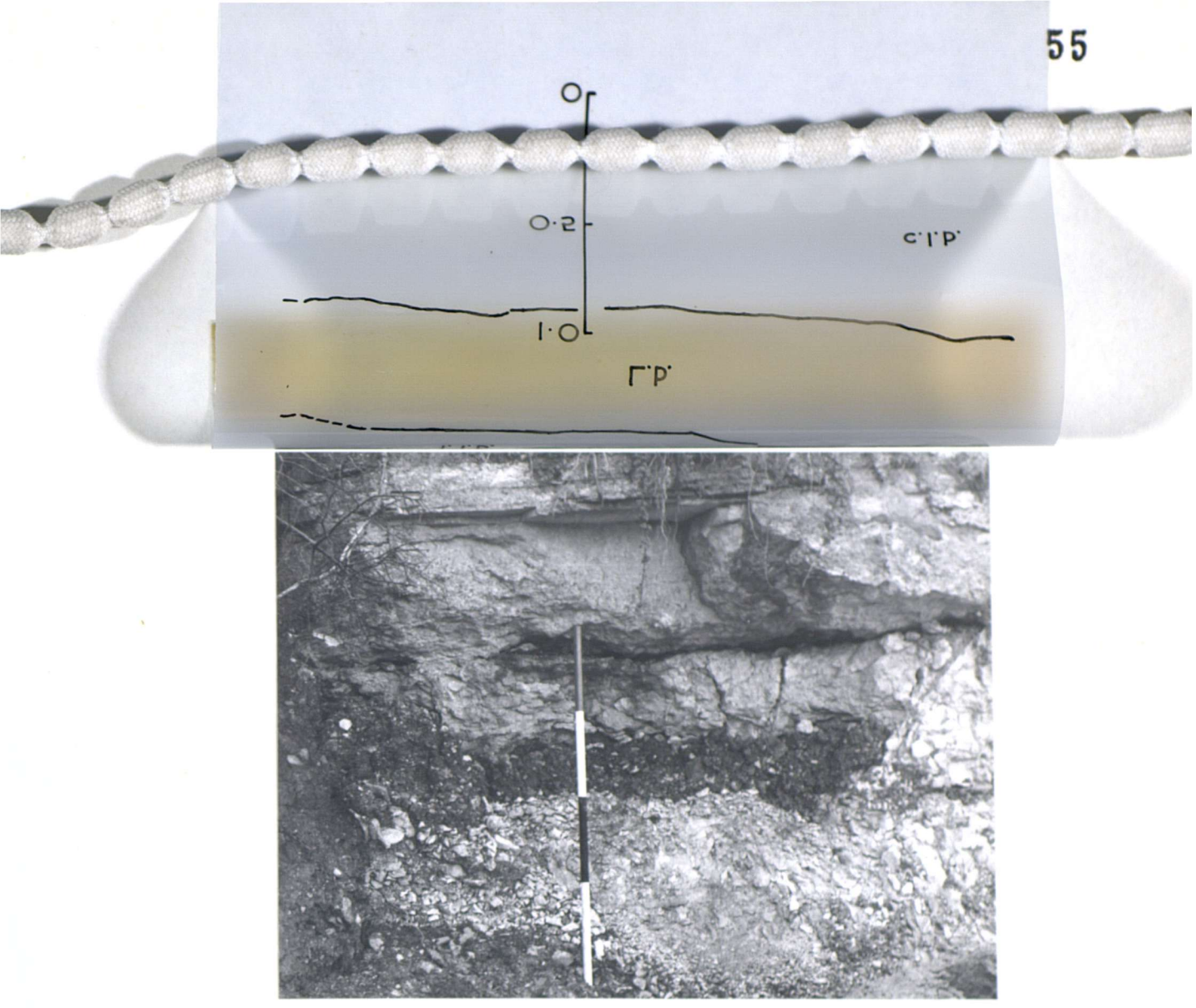


Plate 3.11 Exposure of the Portland Limestone/Purbeck beds contact, Upper Chicksgrove Quarry

KEY

P.b. —— Purbeck beds

l.l.b. —— laminated limestone bed

L.b. —— Lamellosus bed

c.l.b. —— chalky limestone beds

Scale is in metres

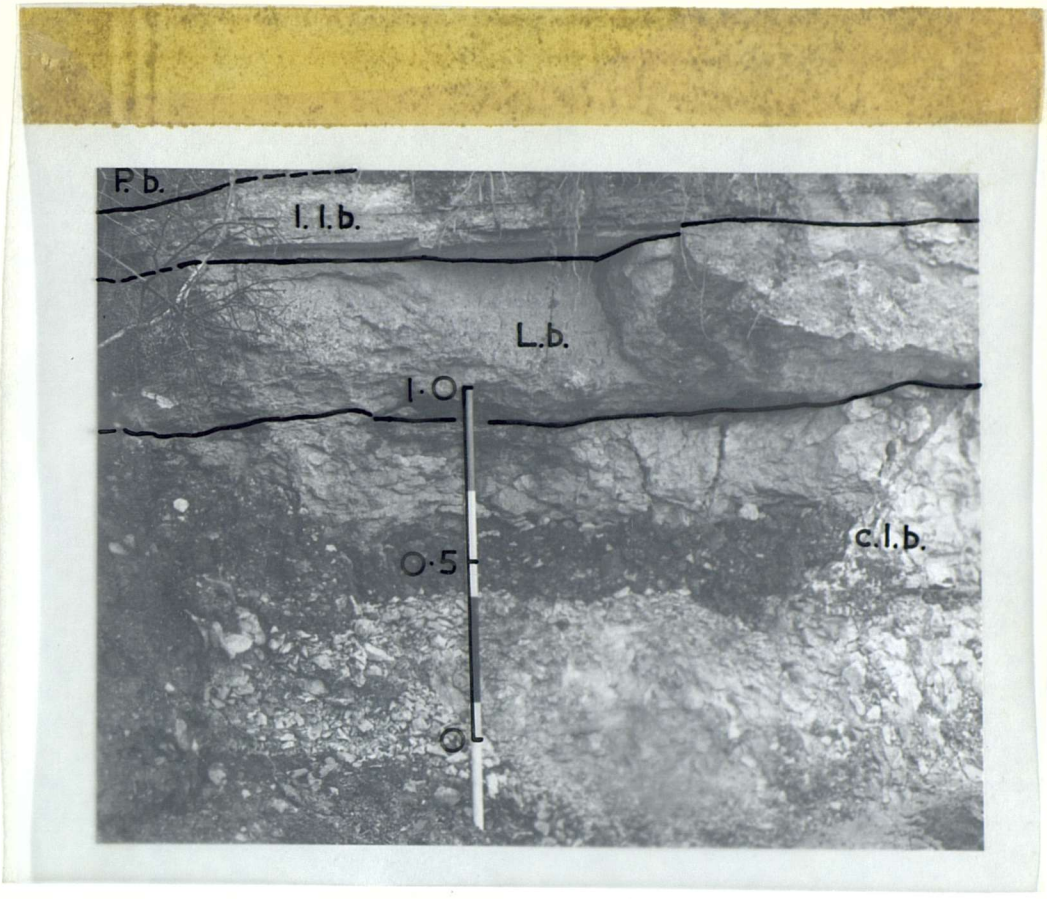


Plate 3.11 Exposure of the Portland Limestone/Purbeck beds contact, Upper Chicksgrove Quarry

KEY

P.b. — Purbeck beds

l.l.b. — laminated limestone bed

L.b. — Lamellosus bed

c.l.b. — chalky limestone beds

Scale is in metres

CHAPTER 4

EXPERIMENTAL TECHNIQUES

4.1 Introduction

All the principal experimental techniques utilised during the study are described in this chapter. One technique was used to derive elastic-wave velocities. The rest examined 28 physical parameters, which were considered to be possible velocity-controlling variables.

The parameters analysed are defined and, where appropriate, classifications are presented. An indication of the accuracy of the experimental techniques is given, together with the percentage errors to be expected.

4.2 Sample Preparation

Cylindrical core-specimens, nominally 2.54 cm. in diameter, were drilled from the samples (Appendix 3) by means of a standard diamond-tipped rotary drill (Plate 4.1). Cores were taken in three orthogonal directions, X and Y being horizontal and Z vertical, controlled by the field orientation of the sample (Section 3.3.1). The number of cores from each sample was limited by sample size. At least one core was taken in each of the three orthogonal directions from every sample. One large sample gave 33 cores. The original coring scheme aimed at producing cores having an optimum length of 10 cm. This was frustrated by premature fracturing across the cores or limitations imposed by sample size. A total of 814 cores were obtained with an average length of 6.5 cm.

The cores in each sample were oriented before extraction, by means of a simple core-orientation device (Plate 4.2) which enabled the trend and plunge of the core-axis to be found. The core-axis orientations were then related to the sample orientations by means of a Schmidt stereographic net. These directions are listed in Appendix 4, from which it can be seen that departure of core-axis orientation from orthogonality



Plate 4.1 Diamond-tipped rotary drill used for extracting 2.54 cm. diameter cores from the samples. The field orientation as marked on the sample, determines the three orthogonal directions of drilling.

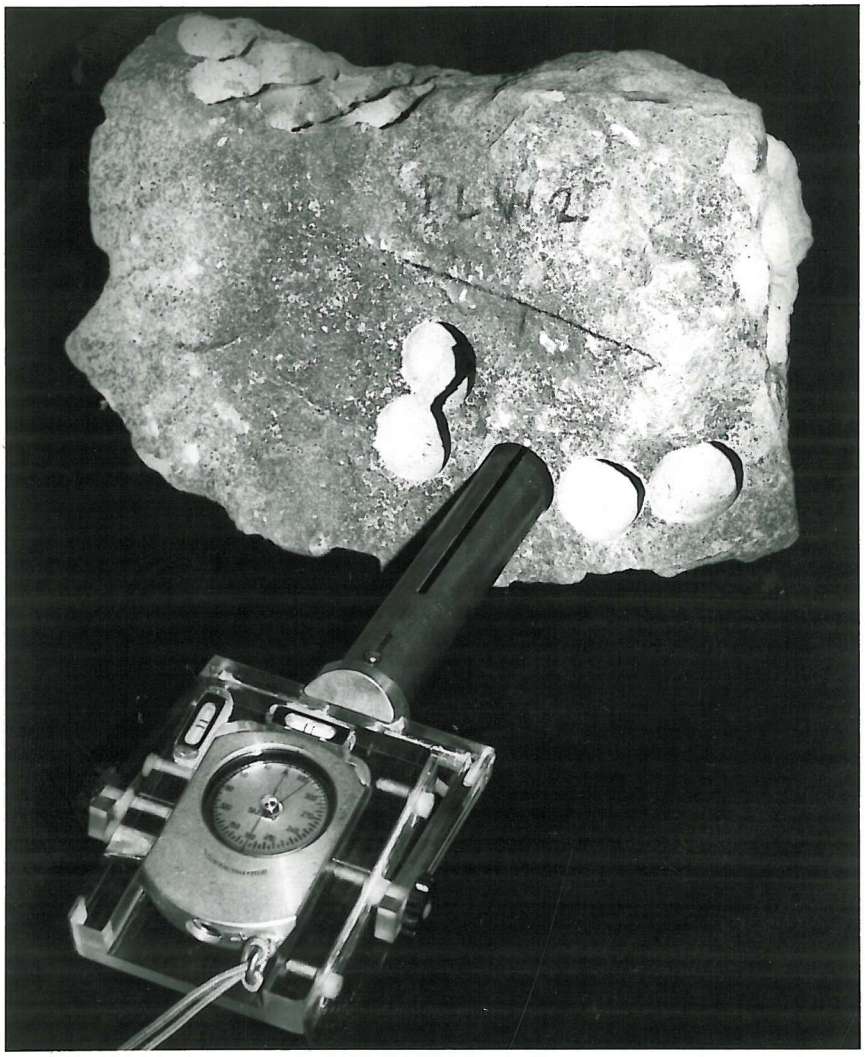


Plate 4.2 Core-orientation device
This enables any departure of core-axis orientation from orthogonality to be determined.

is always less than 10^{o}.

The extracted cores were carefully squared into right circular cylinders by use of a diamond-saw and trim-wheel. This involved a certain loss of material, and final core-lengths ranged from 1.9 cm. to 10.2 cm., with a constant diameter of 2.54 cm. Birch (1960) has shown that for velocity-measurements on cores using an ultrasonic transducer system, the length/diameter ratio should not exceed 4, if elastic-wave energy is not to be attenuated by boundary reflection. The maximum ratio in this study is 4.0; thus all the cores used for velocity-measurements satisfy the above conditions.

4.3 Velocity Determinations

4.3.1 Instrumentation

A Dawe ultrasonic materials tester, type UCT2/1822, was used (Plate 4.3). A trigger generator, producing a negative rectangular pulse at a repetition rate equal to the mains frequency (50 - 60Hz) is used to trigger transmitter, time-base and time-marker circuits. The transmitter discharges the charged capacitance of a transducer through 1000 V, which causes the transducer to produce a seismic wave pulse. This travels through the core under measurement and is then received by another transducer. The received pulse, together with a transmitted pulse, time-base and time-markers are displayed on a cathode-ray tube (Plate 4.4). The time-measuring system is calibrated by means of a quartz oscillator (frequency 100 KHz), which results in 10 microsecond and 50 microsecond markers being displayed on the cathode-ray tube.

Barium titanate transducers, enclosed in suitable protective housings, were used. The resonant frequency of these transducers is 150 KHz and the mode of propagation of the seismic wave-pulse is longitudinal. Pulse transit-times were measured from the difference in the on-set instants of transmitted and received pulses as shown in Plate 4.4. The transmitted pulse acts as a "zero time marker", travelling direct from transmitter to

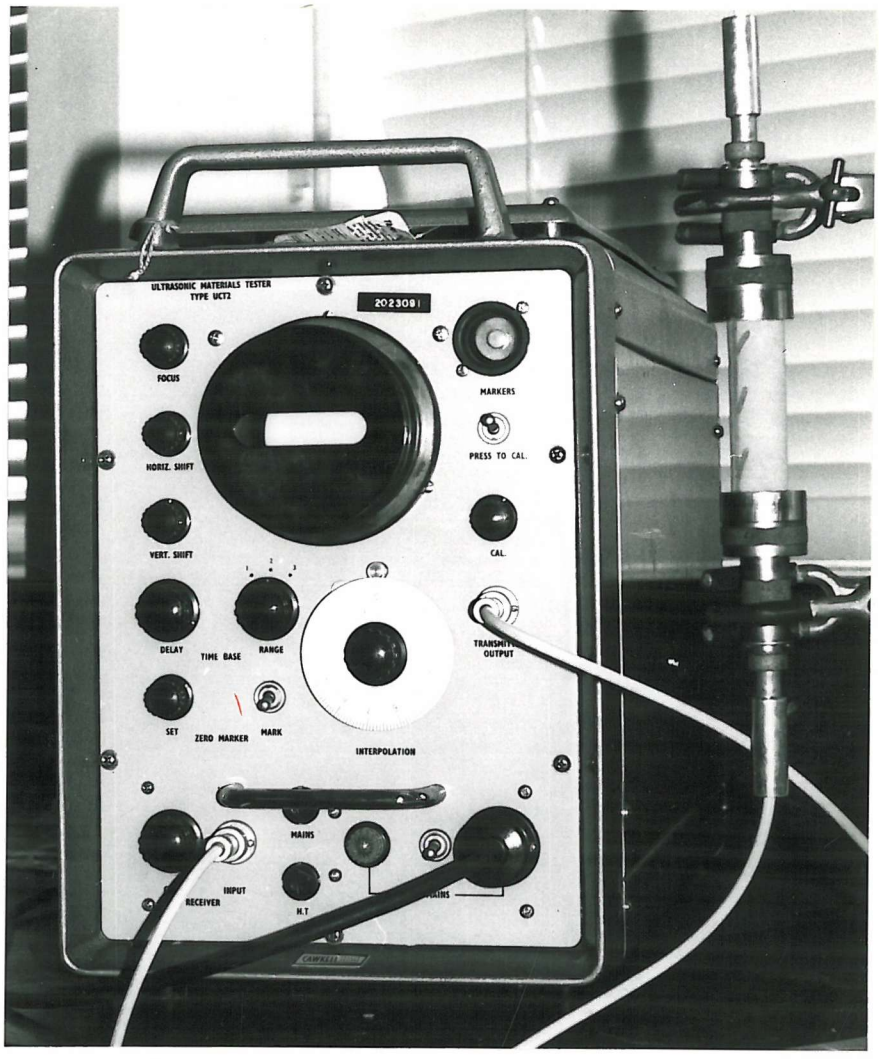


Plate 4.3 Ultrasonic materials tester, with a core-specimen in position between the transducers. The transit-time of compressional elastic-wave energy travelling through the core-specimen between the transducers is measured.

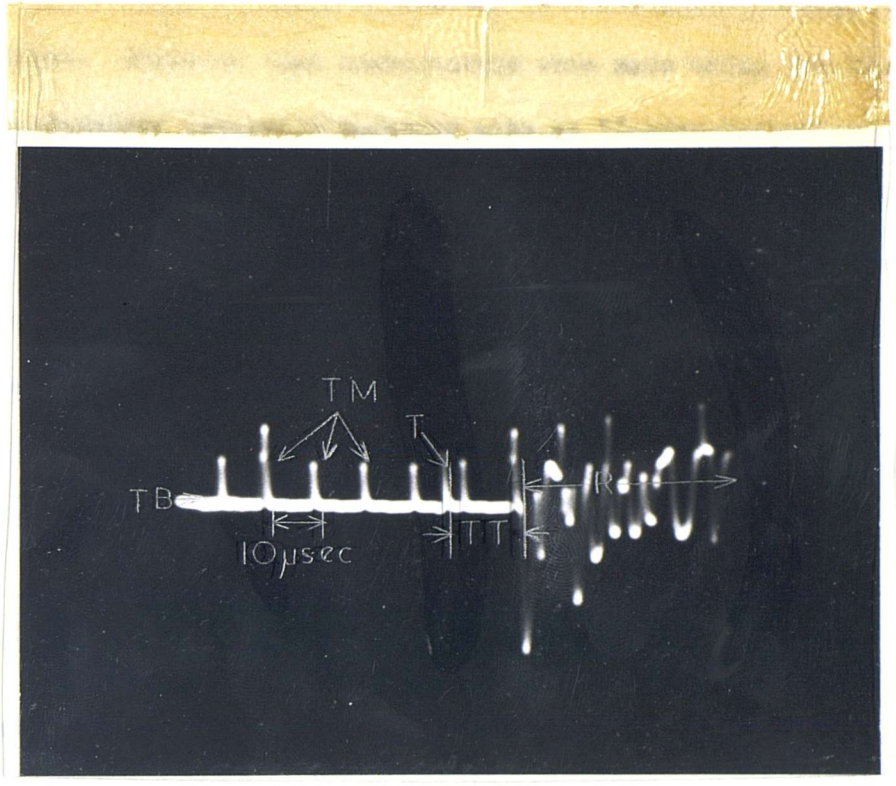


Plate 4.4 Oscilloscope trace of received pulse R, after travel through core-specimen, transmitted pulse T, time-base TB, and time-markers TM. Pulse transit-time TT, is measured as the difference between the on-set instants of the transmitted pulse and the received pulse.

oscilloscope. In order to obtain a correct pulse transit-time, 1.3 microseconds were subtracted from the observed measurement in order to allow for the delay in transmitting the received pulse through the transducers. Observed time measurements were made using the time markers at 10 microsecond intervals together with an "Interpolation" control (Plate 4.3), which divides the 10 microsecond interval between two time markers into units of 0.1 microseconds, and enables measurements to be made to an accuracy of $\pm$0.05 microseconds. The time markers at 50 microsecond intervals were not used, since pulse transit-times did not exceed 50 microseconds for the cores studied. The transit-times are well within the time-calibration range (5 - 1000 microseconds) of the instrument.

4.3.2 Velocity-Measurement Procedure

Prior to making velocity determinations, the cores were oven-dried at 110°C for 24 hours, and dessicated under vacuum for 2 hours, following a method described by King (1966). This procedure leaves only negligible amounts of solvent and moisture in the cores.

Velocity-measurements were carried out under dry-atmosphere conditions. The core-lengths were measured using Vernier jaw-calipers, in two mutually-perpendicular directions, and an average length computed. This minimised errors in non-parallelism of the cut core-ends. The lengths were measured to an accuracy of $\pm$ 1/40 mm.

For velocity determinations, an individual core was firmly clamped between the transmitting and receiving transducers as shown in Plate 4.3. Vacuum grease was applied to the transducer faces to improve the elastic-energy coupling. Six readings of pulse transit-time, i.e. corrected pulse transit-time (Section 4.3.1), were taken for each core, over a period of five hours, to allow for operator and instrument error. The precision of pulse transit-time readings was assessed by use of two standards, consisting of machined cylinders of aluminium alloy and brass

with lengths of 10.00 cm. and diameters of 2.54 cm. On every occasion that core-specimen velocities were determined, the standards were included. Readings for the standards were found to be consistent over a period of approximately two years, indicating a high degree of precision (Section 4.3.3).

The pulse transit-times and average length of each core were used to compute the elastic-wave velocity from the simple formula:

$$\text{VELOCITY} = \frac{\text{AVERAGE CORE LENGTH} \times 10^{-2}}{\text{TRANSIT-TIME} \times 10^{-6}} \quad (\text{m.sec}^{-1}) \qquad \text{.....Eq. 4.1}$$

This was calculated for each of the six pulse transit times recorded, and the mean, variance, standard deviation and standard error of the velocity were computed. These statistics are recorded in Appendix 5.

4.3.3 Errors in Velocity-Determinations

The velocities of individual cores are subject to errors inherent in the instrument used, in core-preparation and its placing in the instrument and in the read-out system.

Variations due to non-parallelism of the core-ends were small, with maximum differences of 0.3% between the two lengths measured.

Pulse transit-times could be read to an accuracy of 0.05 microseconds, leading to maximum errors of approximately 1%.

Instrument and operator error leading to differences between the six pulse transit-times recorded for each core did not exceed 3%. The two standards, which were used to assess precision in pulse transit-time readings, were measured on 28 occasions, and an overall mean velocity calculated. The 28 individual mean velocities were compared statistically with the overall mean velocity, using a Student's t-test. The results of these tests together with overall mean velocity and density of the standards are given in Table 4.1. It can be shown that on every occasion when pulse transit-time readings were taken, the individual mean velocity of at least one standard was statistically from the same population as the overall

velocity mean. This infers a high degree of precision in pulse transit-time readings over a period of two years, with individual velocity means deviating by a maximum of 0.8% from the overall velocity mean of either standard.

TABLE 4.1

Student's t-test Results for Velocity Statistics on 2 Standards

STANDARD	OVERALL MEAN VELOCITY AND STANDARD ERROR (N = 28)	DENSITY (gm/c.c.)
BRASS	4656 ± 4 metres / sec.	8.7
ALUMINIUM	6768 ± 6 metres / sec.	2.8

INDIVIDUAL MEAN VELOCITIES AND STANDARD DEVIATIONS FOR ALUMINIUM (metres per second)	STUDENT'S T-TEST RESULT +	INDIVIDUAL MEAN VELOCITIES AND STANDARD DEVIATIONS FOR BRASS (metres per second)	STUDENT'S T-TEST RESULT +
6727 ± 67	*	4657 ± 66	****
6735 ± 28	**	4617 ± 12	–
6740 ± 17	**	4640 ± 8	*
6761 ± 37	****	4649 ± 16	****
6730 ± 43	–	4640 ± 18	**
6746 ± 14	**	4649 ± 9	****
6743 ± 20	**	4635 ± 8	–
6727 ± 22	–	4645 ± 11	***
6746 ± 14	**	4649 ± 6	****
6757 ± 25	****	4657 ± 6	****
6784 ± 23	****	4666 ± 9	****
6787 ± 19	***	4673 ± 7	*
6776 ± 27	****	4644 ± 12	***
6768 ± 31	****	4667 ± 9	***
6787 ± 27	***	4677 ± 6	–
6753 ± 17	****	4655 ± 6	****
6772 ± 28	****	4657 ± 9	****
6772 ± 35	****	4671 ± 16	**
6803 ± 25	–	4669 ± 23	***
6794 ± 68	****	4682 ± 8	–
6784 ± 40	****	4666 ± 11	****
6780 ± 41	****	4669 ± 6	***

/cont.

INDIVIDUAL MEAN VELOCITIES AND STANDARD DEVIATIONS FOR ALUMINIUM(metres per second)	STUDENT'S T-TEST RESULT +	INDIVIDUAL MEAN VELOCITIES AND STANDARD DEVIATIONS FOR BRASS (metres per second)	STUDENT'S T-TEST RESULT +
6787 ± 28	***	4657 ± 13	****
6784 ± 23	****	4644 ± 11	***
6795 ± 24	**	4660 ± 20	****
6749 ± 31	***	4655 ± 24	****
6815 ± 43	–	4671 ± 11	**
6799 ± 40	*	4658 ± 9	****

+ Probability levels of t for samples from same population

****	***	**	*	–
P > 0.2	P > 0.1 < 0.2	P > 0.05 < 0.1	P > 0.02 < 0.05	P < 0.02

P < 0.05 taken as significant with samples not from same population.

The accuracy of the method (Hurley, 1967) could not be assessed, since no other methods for determining velocity were available for comparison.

Total error thus does not exceed a maximum of 5.1%. The bulk of this error is due to instrument and operator errors, leading to variations in the individual pulse transit-time readings.

4.4 Porosity and Density Determinations

4.4.1 Terminology

Two types of porosity are recognised, namely absolute and effective. Absolute porosity of a rock is defined as the ratio of total void space to bulk volume. Effective porosity is defined as the ratio of intercommunicating void space to bulk volume. These ratios are usually expressed as percentages. Most procedures for porosity determination measure the effective and not the absolute porosity.

The density of a rock can be defined as the ratio of dry weight to bulk volume. As with porosity, two types of density are

distinguished. Absolute density is the density of a substance in which there is a complete absence of void space, whereas effective or bulk density is that of a substance containing void space. The density usually measured in rocks is the effective density.

4.4.2 Methods of Determination

A combined density and porosity determination method (Pirson, 1958) has been used in this study. Measurements were made on all 814 cores used for velocity determinations.

The method involves determinations of both bulk and grain volumes of each core, from which porosity can be derived from the expression:

$$\% \text{ POROSITY} = 100 \left(\frac{\text{(Bulk Volume - Grain Volume)}}{\text{Bulk Volume}} \right) \quad \ldots\ldots \quad \text{Eq. 4.2}$$

Measurements of the dry weight of each core enable density to be calculated from the ratio:

$$\text{DENSITY (gm./c.c.)} = \frac{\text{DRY WEIGHT (gm.)}}{\text{BULK VOLUME (c.c.)}} \quad \ldots\ldots \quad \text{Eq. 4.3}$$

The cores were initially oven-dried at 110°C for 24 hours and then dessicated using a method identical to that described in Section 4.3.2. The dry weight of each core was measured, as were all other weighings, to an accuracy of one milligram. The cores were then oven-dried for a further 12 hours, saturated with paraffin, under vacuum for 12 hours, and then reweighed whilst immersed in paraffin. This was recorded as "apparent weight". The grain volume could then be calculated from the expression:

$$\text{GRAIN VOLUME (c.c.)} = \left(\frac{\text{(Dry Weight (gm.) - Apparent Weight (gm.)}}{\text{(Density of Paraffin (gm./c.c.)}} \right) \quad \ldots\ldots \quad \text{Eq. 4.4}$$

Standard methods were used to determine the density of paraffin for each set of weighings.

The saturated cores were then used for bulk volume determinations, by submerging the saturated core in a paraffin-filled flask. The weight of paraffin displaced was measured, and the bulk volume calculated from the ratio:

$$\text{BULK VOLUME (c.c.)} = \frac{\text{Weight of Paraffin Displaced (gm.)}}{\text{Density of Paraffin (gm./c.c.)}} \quad \ldots\ldots\ldots \text{Eq. 4.5}$$

The porosity and density of each core were then calculated using the equations 4.2 and 4.3. The results are tabulated in Appendix 5.

This method, which is basically a liquid-saturation method, measures effective porosity, since only the intercommunicating void space of the cores is penetrated by paraffin. Paraffin, which has a low viscosity and low surface tension, was used as a saturant because this permitted easier and more complete penetration of the cores. The method has the advantage of being rapid. Approximately seven cores per hour could be measured.

4.4.3 Errors in Density and Porosity Determinations

The precision was checked by conducting repeat measurements on ten cores, and both sets of results are listed in Table 4.2.

TABLE 4.2

Results of Initial and Repeat Porosity and Density Measurements made on ten Cores

CORE NUMBER	INITIAL % POROSITY	INITIAL DENSITY (gm./c.c.)	REPEAT % POROSITY	REPEAT DENSITY (gm./c.c.)
W03Y4	3.9	2.52	3.7	2.53
W03X1	6.3	2.48	6.1	2.53
WP1X5	8.0	2.40	7.6	2.46
W03Z5	10.4	2.43	11.4	2.46
W02Z1	12.3	2.28	12.7	2.27
WA28-2X5	15.4	2.19	16.8	2.15
WA28-2Y4	19.5	2.10	18.4	2.10
WB2X3	22.0	1.95	21.5	1.96
WB2Y4	25.7	1.85	24.5	1.82
WB2Z3	28.7	1.92	29.7	1.97

The results show that deviations in the consistency of porosity measurements do not exceed 9.6% and in the consistency of density measurements, only 2.6%. The ten cores cover a wide range of porosity and, assuming that they are representative of the total 814 cores, the precision of the method is probably 10% for porosity determinations and 3% for density determinations.

An estimate of the accuracy of the results was obtained by using different techniques for determining porosity and density. The bulk volume of each core was calculated from the dimensions, since all cores are approximately right-angle cylinders. These volumes were found to deviate by less than 3% from the displacement determinations which indicates that the density determination is subject to a 3% error. The results of X-Ray diffraction analysis (Section 4.5.43) show that approximately 400 cores are composed of at least 98% calcite. Taking the density of calcite as 2.712 gm./c.c. (Peselnick & Robie, 1962) the grain volumes of these cores were calculated from the ratio:

$$\text{Grain Volume (c.c.)} = \frac{\text{Dry Weight (gm.)}}{\text{Density of Calcite (gm./c.c.)}} \quad \ldots \text{ Eq. 4.6}$$

These grain volumes deviated from the values determined using the liquid-saturation method by a maximum of 3%. The calculation of porosity involves both grain and bulk volumes (Eq. 4.2), resulting in maximum errors in porosity determinations, of approximately 9%.

All weighings could be read to an accuracy of ± 1 mg, and a total of three weighings was necessary for density determinations and four weighings for porosity determinations. This gives maximum errors, due to accuracy to which readings could be taken of 0.01% in the case of density determinations and 0.04% in the case of porosity determinations.

Total maximum errors in porosity determinations are thus approximately 19%, and in density determinations approximately 6%. These

errors are mainly derived from two sources, precision and accuracy of determinations, both of which are dependent upon errors inherent in the method used. The most important error inherent in the liquid-saturation method, is probably the degree of paraffin-saturation achieved prior to measurement of bulk and grain volumes. A decreasing degree of paraffin-saturation results in an increasing magnitude of error.

4.5 Petrographic Analysis

4.5.1 Introduction

Analysis of 21 physical parameters, which were considered as possible factors controlling elastic-wave velocity, was made quantitatively using thin-sections supplemented by X-Ray diffraction and ultra-violet fluorescence. 245 cores were selected for analysis. These were considered fully representative both of the velocity and porosity range and of the limestone-types (Section 4.6.1) sampled from the Portland Group.

The recognition and definition of most of the components analysed were based largely upon the petrographic classification of Folk (1959, 1962). This classification was adopted since it provides a more detailed physical description of the core-specimens than other classifications.

4.5.2 Terminology and Classification of Carbonate Rocks (Folk, 1959, 1962)

The main components recognised by Folk are as follows:

(i) Allochem - Grains formed by chemical or biochemical precipitation within a depositional basin. These are usually the dominant components of limestones. Four types of allochem have been recognised, intraclasts, ooliths, bioclasts and pellets.

(ii) Intraclast - Fragment of weakly-consolidated carbonate mud that has been reworked and deposited within a depositional basin.

(iii) Oolith - Spherical or ellipsoidal particle, usually 125 μ to

2.0 mm. in diameter, comprising a concentrically laminated envelope surrounding a nucleus. The envelope is usually calcareous and shows either radial and/or concentric structure. The nucleus is very variable in size, shape and mineral composition.

(iv) Bioclast - Called fossil by Folk. It includes entire fossils, in or near their growth positions, and transported fragments, both usually composed of calcium carbonate. For the purposes of this study, it was found convenient to include trace fossils such as burrows, and non-carbonate fossil fragments such as fish-scales.

(v) Pellet - Ovoid or rod-shaped particle composed of microcrystalline calcite lacking any internal structure. The size ranges from 30 μ to 150 μ. Pellets are usually considered to be the excreta of invertebrates. They can also be defined as any allochem less than 200 μ in diameter, composed of lime mud.

(vi) Orthochem - Precipitate formed within a depositional basin or within the rock itself. Three types are recognised, micrite, sparite and calcite replacement or recrystallisation products.

(vii) Micrite - Microcrystalline calcite ooze, forming grains 1 - 4 μ in diameter. It is also defined as a limestone-type in which there are less than 1% of allochems (Fig. 4.1). Intraclasts, ooliths and pellets are usually composed of micrite.

(viii) Sparite - Chemically-precipitated pore-filling calcite cement in the form of grains or crystals of at least 10 μ diameter, but commonly ranging from 20 - 100 μ.

(ix) Microspar - Microcrystalline calcite averaging 5 - 15 μ in diameter, usually equidimensional and uniform in size. It probably represents recrystallisation of microcrystalline calcite ooze.

Folk's classification is based upon a combination of the four variables shown below:

1. Ratio of sparite to micrite
2. % allochems in the rock
3. Amount of sorting and abrasion
4. Volumetric composition of the allochems.

Fig. 4.1 shows the classification after Folk (1962). Appendix 6 lists all 245 specimens analysed and classifies them according to the Folk system. Examples of the components defined above are illustrated in Plates 4.5 to 4.18, 4.20, 4.21, 6.8, 6.12, 6.13 and 6.18.

4.5.3 Descriptions and Determinations of Possible Velocity-controlling Parameters

In the petrographic analysis of the core-specimens, the following components were identified:

grains - intraclasts, ooliths, bioclasts, pellets, detrital grains

cements - micrite, microspar, sparite

others - dolomite, calcite veins, silica replacements, calcite replacements

Percentages and grain-sizes of individual components and groups of related components were calculated (Tables 7.1, 7.2 and 7.4). Multiple-regression analysis (Section 7.2) was then applied to the data obtained. Those components not defined in Section 4.5.2, are defined as follows:

(i) Dolomite - Percentage and grain-size were determined, and in the core-specimens, any dolomite present was always in the form of rhombic crystals (Plates 4.18, 6.4, 6.5, 6.16 and 6.17) uniform in size, with long axes ranging from 20 - 40 μ. It was usually associated

NOTES TO FIG. 4.1

* Designates rare rock types.

1. Names and symbols in the body of Table 1 refer to limestones. If the rock contains more than 10 per cent replacement dolomite, prefix the term "dolomitised" to the rock name, and use DLr or DLa for the symbol (e.g. dolomitised intrasparite, Ii:DLa). If the rock contains more than 10 per cent dolomite of uncertain origin, prefix the term "dolomitic" to the rock name, and use dLr or dLa for the symbol (e.g. dolomitic pelsparite, Ip:dLa). If the rock consists of primary (directly deposited) dolomite, prefix the term "primary dolomite" to the rock name, and use Dr or Da for the symbol (e.g. primary dolomite intramicrite, IIi:Da). Instead of "primary dolomite micrite" (IIIm:D) the term "dolomicrite" may be used.

2. Upper name in each box of Table 1 refers to calcirudites (median allochem size larger than 1·0 mm.); and lower name refers to all rocks with median allochem size smaller than 1·0 mm. Grain size and quantity of ooze matrix, cements or terrigenous grains are ignored.

3. If the rock contains 10-50 per cent terrigenous material, prefix "sandy", "silty" or "clayey" to the rock name, and "Ts", "Tz", or "Tc" to the symbol depending on which is dominant (e.g. sandy biosparite, TsIb:La, or silty dolomitised pelmicrite, TzIIp:DLa). If the rock contains more than 50 per cent terrigenous material, it is classified as a terrigenous rock.

4. If the rock contains other allochems in significant quantities (10% in this study) that are not mentioned in the main rock name, these should be prefixed as qualifiers preceding the main rock name (e.g. fossiliferous intrasparite, oolitic pelmicrite, pelletiferous oosparite, or intraclastic biomicrudite). This can be shown symbolically as Ii(b), IIp(o), Io(p), IIb(i), respectively.

5. If the fossils are of rather uniform type or one type is dominant, this fact should be shown in the rock name (e.g. pelecypod biosparrudite, crinoid biomicrite).

6. If the rock was originally microcrystalline and can be shown to have recrystallised to microspar (5-15 micron, clear calcite), the terms "microsparite", biomicrosparite", etc. can be used instead of "micrite" or "biomicrite". The letter "R" is prefixed to the symbol (e.g. RIIIm:L, RIIb:La).

7. Specify crystal size as shown in the examples.(1-aphano-crystalline ($<$ 0·004 mm.), 2 - v.finely crystalline (0·004 - 0·016 mm.), 3 - finely crystalline (0·016 - 0·062 mm.), 4 - medium crystalline (0·062 - 0·25 mm.), 5 - coarsely crystalline (0·25 - 1·0 mm.), 6 - v.coarsely crystalline (1·0 - 4·0 mm.))

Fig. 4.1 Classification of Carbonate Rocks (after Folk, 1962)

TABLE I. CLASSIFICATION OF CARBONATE ROCKS

Volumetric Allochem Composition				Limestones, Partly Dolomitized Limestones, and Primary Dolomites (see Notes 1 to 6)				Replacement Dolomites[7] (V)	
				>10% Allochems Allochemical Rocks (I and II)		<10% Allochems Microcrystalline Rocks (III)			
				Sparry Calcite Cement >Microcrystalline Ooze Matrix	Microcrystalline Ooze Matrix >Sparry Calcite Cement	1–10% Allochems	<1% Allochems	Allochem Ghosts	No Allochem Ghosts
				Sparry Allochemical Rocks (I)	Microcrystalline Alochemical Rocks (II)				
<25% Intraclasts			>25% Intraclasts (i)	Intrasparrudite (Ii:Lr) Intrasparite (Ii:La)	Intramicrudite* (IIi:Lr) Intramicrite* (IIi:La)	Intraclasts: Intraclast-bearing Micrite* (IIIi:Lr or La)	Micrite (IIIm:L); if disturbed, Dismicrite (IIImX:L); if primary dolomite, Dolomicrite (IIIm:D)	Finely Crystalline Intraclastic Dolomite (Vi:D3) etc.	Medium Crystalline Dolomite (V:D4)
	<25% Oölites		>25% Oölites (o)	Oösparrudite (Io:Lr) Cösparite (Io:La)	Oömicrudite* (IIo:Lr) Oömicrite* (IIo:La)	Oölites: Oölite-bearing Micrite* (IIIo:Lr or La)		Coarsely Crystalline Oölitic Dolomite (Vo:D5) etc.	Finely Crystalline Dolomite (V:D3)
		Volume Ratio of Fossils to Pellets	>3:1 (b)	Biosparrudite (Ib:Lr) Biosparite (Ib:La)	Biomicrudite (IIb:Lr) Biomicrite (IIb:La)	Fossils: Fossiliferous Micrite (IIIb: Lr, La, or Ll)		Aphanocrystalline Biogenic Dolomite (Vb:Dl) etc.	
			3:1–1:3 (bp)	Biopelsparite (Ibp:La)	Biopelmicrite (IIbp:La)	Pellets: Pelletiferous Micrite (IIIp:La)		Very Finely Crystalline Pellet Dolomite (Vp:D2) etc.	etc.
			<1:3 (p)	Pelsparite (Ip:La)	Pelmicrite (IIp:La)				
				Most Abundant Allochem				Evident Allochem	
							Biolithite (IV:L)		

	Undisturbed Bioherm Rocks (IV)

CARBONATE TEXTURAL SPECTRUM

	OVER 2/3 LIME MUD MATRIX				SUBEQUAL SPAR & LIME MUD	OVER 2/3 SPAR CEMENT		
Percent Allochems	0-1 %	1-10 %	10-50%	OVER 50%		SORTING POOR	SORTING GOOD	ROUNDED & ABRADED
Representative Rock Terms	MICRITE & DISMICRITE	FOSSILIFEROUS MICRITE	SPARSE BIOMICRITE	PACKED BIOMICRITE	POORLY WASHED BIOSPARITE	UNSORTED BIOSPARITE	SORTED BIOSPARITE	ROUNDED BIOSPARITE
1959 Terminology	Micrite & Dismicrite	Fossiliferous Micrite	Biomicrite			Biosparite		
Terrigenous Analogues	Claystone		Sandy Claystone	Clayey or Immature Sandstone		Submature Sandstone	Mature Sandstone	Supermature Sandstone

LIME MUD MATRIX
SPARRY CALCITE CEMENT

A textural spectrum for carbonate sediments, showing eight proposed sequential stages. In general, "low-energy" sediments occur to the left, with successively "higher-energy" sediments to the right. These stages are quite analogous to the textural maturity sequence in terrigenous rocks. Because of lack of space, only the biomicrite-biosparite terms are used as representative examples; for these terms, one can substitute the other allochemical limestone types (for example, the cell labeled "packed biomicrite" can equally well stand for packed intramicrite, packed oömicrite, and packed pelmicrite). Comparison with the fourfold division used in Folk, 1959, is also shown.

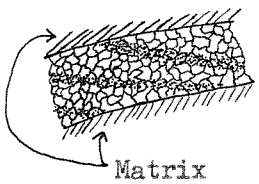
with microspar (Plate 6.12), and the presence of micritic nuclei in the rhombs suggested replacement of microcrystalline calcite ooze, possibly at the time of formation of the microspar. Allochems were always unaffected by the dolomite. It was restricted to the microsparite limestone-type (Section 4.6.1), and for part of the multiple regression analysis, percentages and grain-sizes of both dolomite and calcite were combined, since both are carbonates and have similar grain-sizes (Table 7.4).

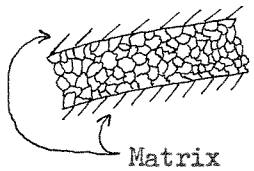
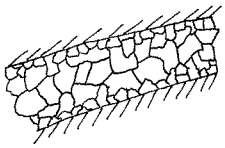
(ii) Detrital grains - These include quartz, feldspar and glauconite, with quartz forming at least 90% of the detrital grains (Plates 4.11, 4.12, 4.14, 4.15, 4.18). Group percentages and grain-sizes of the three minerals were determined.

(iii) Calcite Replacement and Recrystallisation - In the study of possible parameters affecting velocity, consideration of the type of component affected by calcite replacement or recrystallisation, together with the type of calcite cement present, were found to be more important than genetic considerations. It was found that bioclasts were the components affected by calcite replacement or recrystallisation. Wilson's (1967) classification of bioclast-modification fabrics is adopted (Table 4.3).

TABLE 4.3

Classification of Calcite Replacement and Recrystallisation Fabrics in Bioclasts (After Wilson, 1967).

TYPE	BIOCLAST	Description
I		Fabrics show sutured calcite grain boundaries, and bands of inclusions as relicts of the original life structure of the shell. It can be continuous with the matrix, i.e. calcite cement. It is usually formed by inversion of aragonite to calcite (Folk, 1965).

TYPE	BIOCLAST	DESCRIPTION
II		Fabrics show sutured grain boundaries but no relicts of the original life structure. It is not continuous with the matrix and is usually formed by <u>in situ</u> replacement of aragonite by calcite (Folk, 1965).
III		Fabrics possess straight grain boundaries, and the grain-size increases towards the centre of the shell. It can be continuous with the matrix, and triple enfacial junctions with one angle of 180° are common (Bathurst, 1964). It is usually formed by passive precipitation (Folk, 1965).

The grain-sizes of Type I and Type II fabrics were determined irrespective of matrix-type, since these fabrics showed marked morphological and size differences from the calcite cement. Similarly, Type III fabrics were determined independently in the case of core-specimens with micrite or microspar. However, in the case of core-specimens with a sparry calcite cement Type III fabrics were included with the calcite cement, since no distinction could be made between them, and there was evidence, such as optical continuity between the fabric and the cement, to indicate that they were genetically related. All bioclasts showed evidence of calcite replacement or recrystallisation, and for this reason only grain-sizes were determined, since an estimation of the percentage of replacement or recrystallisation could be made from the determinations of bioclast percentages. A small proportion of the other allochem-types showed evidence of calcite replacement and/or recrystallisation, usually in the form of Type II fabrics. Type I fabrics are illustrated in Plates 4.9,

4.12, Type II fabrics in Plates 4.5 - 4.8 and Type III fabrics in Plates 4.6, 4.20, 6.14 and 6.15.

(iv) Silica Replacement - Percentages and grain-sizes of silica replacement were determined, and the replacement-types (Wilson, 1966, Fig. 2) mosaic quartz, lutecite and microcrystalline granular quartz were recognised. Silica replacement was found to be only a minor component of the rocks studied (Tables 7.1 - 7.3). The replacement-types are illustrated in Plates 4.6, 4.9, 4.12 and 4.17.

(v) Sponge Spicules - These include the genera Rhaxella and Pachastrella. Rhaxella spicules consist of reniform bodies, 60 to 100 μ in diameter. They were initially siliceous but, in the core-specimens studied, often took the form of calcite-filled casts (Plate 4.16). Pachastrella spicules consist of hollow siliceous tetraxons, $\frac{1}{2}$ to 2 mm. in length (Plates 4.10, 4.17 and 6.7).

Only hollow siliceous spicules were included in the analysis since their presence increases the amount of pore-space, and is pore-space which cannot be determined by the liquid-saturation method, thus forming a possible velocity-controlling parameter (Section 7.3.2a). The analysis was limited to determinations of spicule percentages, since grain-sizes were included in bioclast grain-size determinations.

(vi) Calcite Veins - Several core-specimens contain calcite veins discordantly intersecting all other components. In some specimens, two stages of veining are recognised. Calcite vein percentages and diameters of calcite crystals forming these veins, were determined. Calcite veins are illustrated in Plates 4.13 and 4.16.

(vii) Fabric - This term was applied to planar structures, excepting fractures and veins, in the core-specimens analysed. These

planar structures usually consisted of planes of preferred mineral orientation in the form of normal bedding and cross-lamination (Plate 4.19). They were common in core-specimens with detrital grain contents exceeding 20%. These structures were also defined by alignment of bioclasts, which were parallel to normal bedding in some core-specimens. The effect of fabric on elastic-wave velocity has previously been discussed (Section 2.10). A fabric frequency factor, defined as the number of planar structures per centimetre perpendicular to the core-axis, was determined.

4.5.4 Methods of Analysis

4.5.4.1 Thin-Section Analysis

Thin-sections were made of the 245 cores selected for analysis. The cores were sliced longitudinally through their centres, since all pulse transit-time readings and thus velocity determinations, were made in this direction.

A Zeiss (Jena) Standard Universal - Pol microscope was used, fitted with a micrometer eyepiece. The following parameters were measured on the longer of the two visible dimensions:

Intraclasts

Ooliths

Bioclasts

Pellets

Calcite Cement

Dolomite

Detrital Grains

Calcite Replacement and Recrystallisation

Silica Replacement

Calcite Veins.

Where possible, 100 measurements of each parameter were taken and a mean size computed. Modal analysis using a point-counter was made on each thin-section, and an average of 400 counts was taken. The parameters listed for size measurement, excluding calcite replacement and recrystallisation but with the addition of sponge spicules, were analysed. The readings were converted to percentages and from these results, each core was classified according to the method of Folk (1962) (Appendix 6). In order to avoid duplication of results, both silica-replacement and sponge spicule contents were included in the bioclast component.

4.5.4.2 Errors in Thin-Section Analysis

Errors due to limitations in the accuracy to which readings could be taken did not exceed approximately 6% for size measurements, since the micrometer could be read to an accuracy of $\pm$ 0.06 or $\pm$ 0.7 μ, depending on the magnification used.

Precision of readings was assessed by repeat analysis of 10 thin-sections. Both the initial and repeat results are listed in Table 4.4.

TABLE 4.4

Results of Initial and Repeat Thin-Section Analyses of 10 Core-Specimens

Specimen No.	PETROGRAPHIC PARAMETERS							
	INTRACLASTS				OOLITHS			
	% of total rock		Mean size (μ)		% of total rock		Mean size (μ)	
	Readings 1	2	Readings 1	2	Readings 1	2	Readings 1	2
WV 2Y2	0.0	0.0	-	-	0.0	0.0	-	-
WV 5Y1	0.0	0.0	-	-	0.0	0.0	-	-
WA28-1X1	0.0	0.0	-	-	0.0	0.0	-	-
WB 1Z1	0.0	0.0	-	-	0.0	0.0	-	-
WN1Y1	4.5	4.7	372	387	51.0	53.2	215	213
WO 3Z2	4.8	5.1	413	430	36.0	37.1	319	325

TABLE 4.4 cont.

PETROGRAPHIC PARAMETERS

Specimen No.	INTRACLASTS				OOLITHS			
	% of total rock		Mean size (μ)		% of total rock		Mean size (μ)	
	Readings 1	2	Readings 1	2	Readings 1	2	Readings 1	2
WP2Y1	6.8	6.5	384	400	51.0	47.7	335	311
WQ2X2	4.8	4.7	520	536	13.0	12.1	316	295
WT3X2	5.4	5.8	537	557	52.2	50.6	398	409
WU1Y1	9.0	8.6	551	526	44.0	46.5	384	370
	BIOCLASTS				PELLETS			
Specimen No.	% of total rock		Mean size (μ)		% of totalrock		Mean size (μ)	
	Readings 1	2	Readings 1	2	Readings 1	2	Readings 1	2
WV2Y2	12.5	12.4	416	402	0.0	0.0	-	-
WV5Y1	20.0	21.1	316	320	0.0	0.0	-	-
WA28-1X1	3.9	4.2	260	273	0.0	0.0	-	-
WB1Z1	8.9	8.8	253	241	0.0	0.0	-	-
WN1Y1	16.0	16.7	586	601	0.0	0.0	-	-
WO3Z2	24.7	23.9	672	690	0.0	0.0	-	-
WP2Y1	21.8	22.3	1499	1460	0.0	0.0	-	-
WQ2X2	45.7	47.6	1684	1720	0.0	0.0	-	-
WT3X2	17.4	18.9	660	692	0.0	0.0	-	-
WU1Y1	16.0	15.0	1322	1285	0.0	0.0	-	-

TABLE 4.4 cont.

PETROGRAPHIC PARAMETERS

Specimen No.	DETRITAL GRAINS				CALCITE CEMENT			
	% of total rock		Mean size (μ)		% of total rock		Mean size (μ)	
	Readings 1	2	Readings 1	2	Readings 1	2	Readings 1	2
WV2Y2	0.0	0.0	-	-	87.5	89.0	1	1
WV5Y1	0.0	0.0	-	-	80.0	75.5	1	1
WA28-1X1	11.3	10.2	51	53	12.2	13.1	21	22
WB1Z1	24.0	23.1	51	54	62.7	65.3	17	16
WN1Y1	3.5	3.2	183	193	25.0	24.0	238	250
WO3Z2	2.0	2.0	175	170	10.0	10.5	163	151
WP2Y1	2.0	2.1	144	150	12.5	11.8	77	70
WQ2X2	1.5	1.6	207	190	35.0	33.5	192	180
WT3X2	3.0	2.9	229	226	22.0	21.5	338	351
WU1Y1	1.5	1.6	245	250	29.5	30.2	352	370

Specimen No.	DOLOMITE				CALCITE VEINS			
	% of total rock		Mean size (μ)		% of total rock		Mean size(μ)	
	Readings 1	2	Readings 1	2	Readings 1	2	Readings 1	2
WV2Y2	0.0	0.0	-	-	0.0	0.0	-	-
WV5Y1	0.0	0.0	-	-	0.0	0.0	-	-
WA28-1X1	72.6	70.0	27	28	0.0	0.0	-	-
WB1Z1	0.0	0.0	-	-	4.4	4.7	17	18
WN1Y1	0.0	0.0	-	-	0.0	0.0	-	-
WO3Z2	0.0	0.0	-	-	0.0	0.0	-	-
WP2Y1	0.0	0.0	-	-	0.0	0.0	-	-
WQ2X2	0.0	0.0	-	-	0.0	0.0	-	-
WT3X2	0.0	0.0	-	-	0.0	0.0	-	-
WU1Y1	0.0	0.0	-	-	0.0	0.0	-	-

TABLE 4.4 cont.

Specimen No.	PETROGRAPHIC PARAMETERS							
	SILICA REPLACEMENT				SPONGE SPICULES		CALCITE REPLACEMENT	
	% of total rock		Mean size (μ)		% of total rock		Mean size (μ)	
	Readings		Readings		Readings		Readings	
	1	2	1	2	1	2	1	2
WV2Y2	0.0	0.0	-	-	0.0	0.0	109	114
WV5Y1	0.0	0.0	-	-	0.0	0.0	132	138
WA28-1X1	0.0	0.0	-	-	0.0	0.0	-	-
WB1Z1	0.0	0.0	-	-	0.0	0.0	-	-
WN1Y1	0.0	0.0	-	-	6.3	6.0	16	17
WO3Z2	0.2	0.2	180	190	0.0	0.0	22	20
WP2Y1	1.0	1.0	209	195	0.3	0.3	33	35
WQ2X2	2.0	2.2	118	116	0.5	0.5	224	210
WT3X2	0.0	0.0	-	-	3.3	3.0	14	15
WU1Y1	0.3	0.3	103	100	0.2	0.1	26	27

The results shown in Table 4.4 indicate that maximum differences between initial and repeat determinations are of the order of 9% for mean sizes and 8% for percentages of the petrographic parameters.

4.5.4.3 X-Ray Diffraction Analysis

This was used in conjunction with thin-section analysis in order to determine qualitatively the minerals present in each core-specimen.

The application of X-Ray diffraction techniques to the study of sedimentary rocks is described by Brown (1961). Calcite, quartz and dolomite were found to be the dominant minerals with minor amounts of feldspar and glauconite. X-Ray diffraction analysis of the acid-insoluble residues from 26 samples, selected from the main sampling localities and representative of the limestone-types (Section 4.6.1), showed that

quartz was the most abundant mineral present, and that feldspar and glauconite occurred in minor amounts, with traces of clay minerals.

Those core-specimens shown to contain dolomite were subsequently stained in a solution of Alizarin Red-S in dilute hydrochloric acid (Friedman, 1959). This enabled dolomite to be distinguished from calcite under the microscope.

4.5.4.4 Ultra-Violet Fluorescence

Fabrics in the core-specimens could be more clearly identified under ultra-violet light. This is probably due to impurities, which tend to concentrate along planar fabric elements, increasing the amount of fluorescence.

The core-specimens, which were initially bisected longitudinally for thin-sectioning, were used in the analysis, with both halves of each core placed under ultra-violet light. In each half, the number of planar fabric elements transverse to the core-axis was counted, and the fabric frequency factor (Section 4.5.3) was calculated from the ratio:

$$\text{Fabric Frequency Factor} = \frac{\text{Total number of planar fabric elements transverse to core-axis}}{\text{Total length of both core-halves}} \quad \ldots \text{ Eq.4.7}$$

4.6 Pore-Structure Analysis

4.6.1 Introduction

The influence of pore-structure on elastic-wave velocity was investigated by reflected-light microscopy on polished surfaces of the core-specimens. Some cores were further examined by scanning-electron microscopy.

36 core-specimens, representing four main limestone-types, defined partly according to Folk's classification, were analysed. These four limestone-types are defined as follows:

1. SPARITES - limestones with more than 2/3 sparry calcite
2. MICRITES - limestones with more than 2/3 lime mud

3. CHALKS - limestones with a chalky texture, composed of pellets and lime mud with bioclast content less than 50%.

4. MICROSPARITES - limestones with a matrix of microspar. Some specimens are dolomitised, with up to 87% dolomite.

The 36 specimens were chosen to give as wide a range of porosity as possible.

Several classifications of porosity have been formulated, e.g. Waldschmidt et. al. (1956), Thomas (1962), Jodry (1966). Choquette & Pray (1970) devised a comprehensive classification of porosity in sedimentary carbonates, recognising 15 basic porosity-types. Their system has been followed in this study. Certain aspects of the classification were omitted, e.g. code designation, since only a descriptive classification is necessary for the investigation of pore-structure as a possible velocity-influencing variable. The final classification used is presented in Fig. 4.2, and the porosity-types recognised are defined in Section 4.6.2.

4.6.2 Terminology

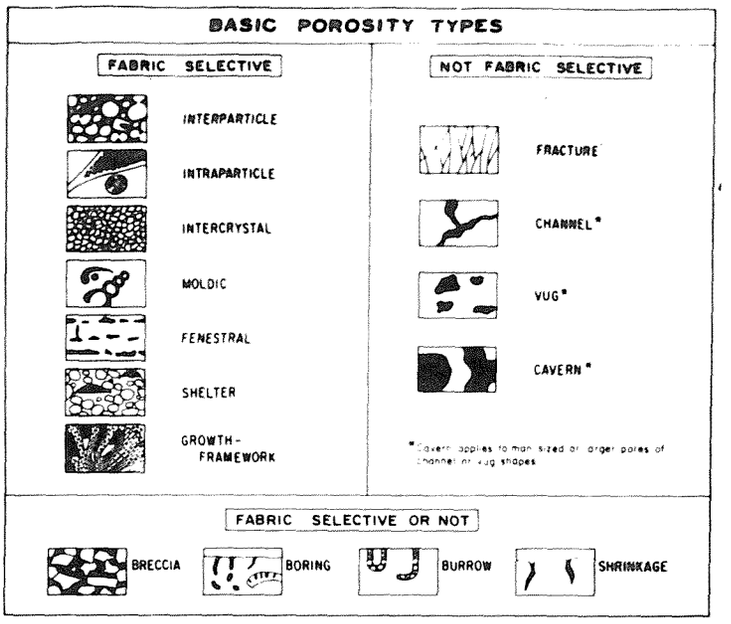
The basic porosity-types recognised in this study are defined as follows, and an indication of the abundance of these porosity types is given:

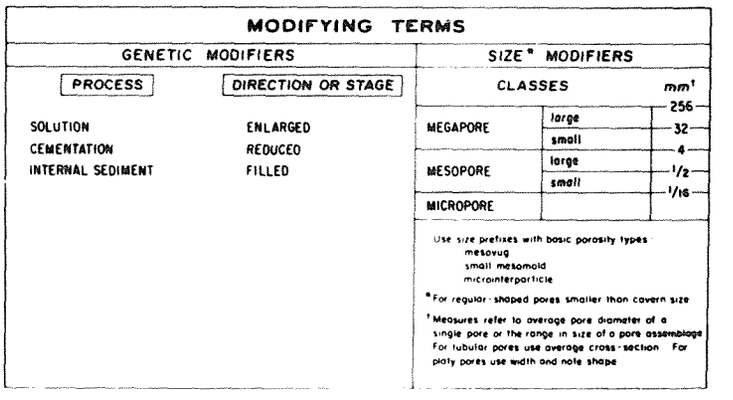
1. Interparticle: Porosity between particles, which generally refers to allochems and detrital grains. This type is present in most core-specimens.

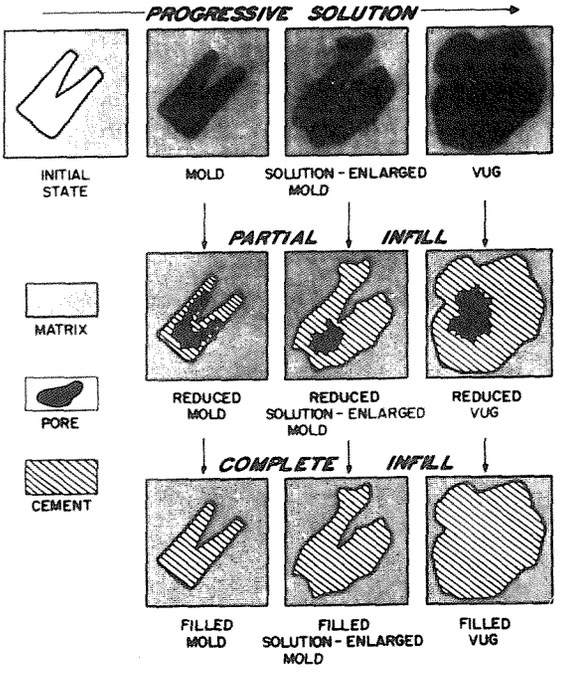
2. Intraparticle: Porosity within individual particles. This occurs within all four allochem-types, particularly bioclasts, and it is found to be very abundant in most core-specimens.

3. Intercrystal: Porosity between crystals, restricted to equidimensional crystal fabrics with no allochems. This type occurs in core-specimens of microsparite and, to a lesser extent, of sparite limestone-types (Section 4.6.1). On a

Fig. 4.2 Geologic Classification of Porosity in Carbonate Rocks (after Choquette & Pray, 1970)







Common stages in evolution of one basic type of pore, a mold, showing applications of genetic modifiers and classification code. Starting material is crinoid columnal (top left). It, and matrix adjoining it, then may be dissolved in varying degrees. Depending on extent of solution (top row), resulting pore is classed as mold, solution-enlarged mold, or vug if precursor's identity is lost. Filling by cement could occur after each solution stage.

microscale, it occurs in micrites and chalks (Section 6.3.3; Plates 6.13, 6.18).

4. Moldic: Porosity formed by the selective removal, normally in solution, of a former individual allochem. It is identified on the basis of shape, size, wall-ornamentation or relict features. It is common in the core-specimens studied.

5. Fracture: Porosity occurring along breaks in a rock, where there has been little mutual displacement of the opposite blocks. This type is limited to one core-specimen.

6. Vug: A somewhat equant pore, with a diameter greater than 60 microns. It does not conform specifically in position, shape or boundaries to particular fabric elements of the host-rock. Solution is the dominant process of formation. Vugs are found to be common in the core-specimens analysed, and usually grade into other basic porosity-types.

7. Boring: Openings created in relatively rigid allochems or rock, by boring organisms. This type is recognised in both ooliths and bioclasts in a few core-specimens, but it accounts for a very small proportion of the total porosity.

8. Burrow: Pores created by organic burrowing in relatively unconsolidated sediment. This type, where present in the core-specimens, is generally completely infilled by calcite-cement.

Examples of the basic porosity-types present in the core-specimens, together with modifications produced by solution and infilling by calcite cement, are illustrated in Plates 4.20 - 4.23; 6.1 - 6.18.

4.6.3 Methods of Analysis

The cores selected had all been previously used in the

petrographic analysis, and polished surfaces were made of the longitudinally-bisected core-halves, on which fabric determinations had been made (Section 4.5.4.4). These were studied under reflected light, using a Zeiss (Jena) NU Universal Research Microscope, and the basic porosity-types, together with any modifications to these types, were recorded.

Each core-specimen was oriented on the microscope stage with respect to the core-axis, and orientations of the longest dimensions of 50 pores were determined. The exact position of the longest dimension was difficult to define, and this resulted in orientation readings being made to an accuracy of 5°. Since the orientations are not vectors, measurements were taken only in the northern hemisphere, 270° through 360° to 090°.

A micrometer eyepiece was used to measure both the longest and shortest dimensions of the 50 pores. This eyepiece could be read to the same accuracy as that used in the thin-section analysis (Section 4.5.4.2) and this resulted in maximum errors of 5% in the pore-dimension readings. The mean and standard deviation of these dimensions were calculated for each core-specimen, together with the mean and standard deviation of the ratio: Long Dimension / Short Dimension.

A method described by Curray (1956) was used to compute the vector magnitude and vector resultant of the 50 pore-orientation readings for each core-specimen. The vector magnitudes for each core-specimen were tested statistically for departure from randomness (Section 6.3.3).

In order to ascertain the validity of using only 50 readings in the pore-structure analysis of each core, additional sets of 100 readings were made on 12 cores and 150 readings on 2 cores, the results of which are shown in Table 4.5. The means and vector resultants were compared statistically, using a student's t-test and an F-test (Steinmetz, 1962) respectively. These tests showed that both sets of readings were

statistically from the same population, inferring that statistically-valid means and vector resultants of the pore-dimensions could be computed using only 50 readings. The tests also indicated a high degree of precision in the readings taken.

The parameters described above, pore-classification and percentage porosity for each core-specimen, are listed in Appendix 7.

TABLE 4.5

Pore-Structure Determinations

No.*	N = 50			N = 100			N = 150		
	Mean & Std.Dev. (μ)		Vector res.(°)	Mean & Std.Dev. (μ)		Vector res.(°)	Mean & Std.Dev. (μ)		Vector res.(°)
	Length	Width		Length	Width		Length	Width	
1	147±171	66±40	284.4	127±137	62±39	301.1	113±118	58±36	287.2
2	129±109	69±43	351.2	115± 96	58±39	343.3	not determined		
3	105±121	52±39	005.7	104±216	42±31	024.2	n. d.		
4	119±84	60±32	294.1	121±99	60±35	307.7	n. d.		
5	126±124	57±29	051.8	123±138	55±26	057.5	n. d.		
6	91±69	47±29	306.8	129±119	55±32	280.2	n. d.		
7	76±57	39±37	074.7	84±62	47±37	083.8	80±55	45±33	086.2
8	83±70	41±28	323.9	91±69	45±32	318.6	n. d.		
9	63±39	33±15	039.6	70±45	37±18	010.7	n. d.		
10	255±212	88±50	044.6	229±192	83±47	023.0	n. d.		
11	347±247	127±60	044.6	321±228	122±63	044.0	n. d.		
12	243±158	96±65	288.5	251±194	99±65	300.0	n. d.		

*The specimens referred to are as follows:

1. PLBS 3Z1
2. PLBS 3Y2
3. PLBS 3X4
4. C5 - 1X3
5. C5 - 1Y1
6. C5 - 1Z1
7. WA28 - 2Z2
8. WA28 - 2Y3
9. WA28 - 2X1B
10. UCB1 X4
11. UCB1 Y4
12. UCB1 Z1

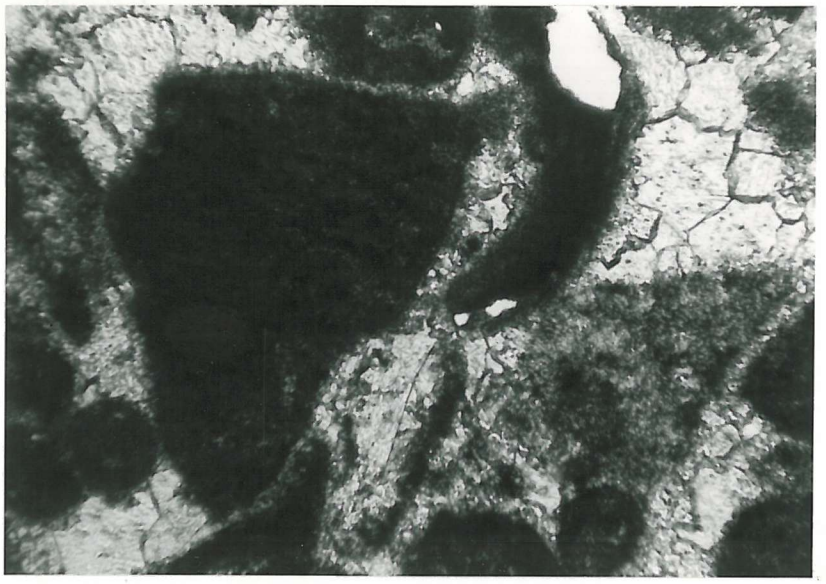
The limit of resolution of the NU microscope is about 5 μ. Thus the smaller micropores could not be recognised. They were investigated by use of a Cambridge Scanning Electron Microscope, Model S4, with magnification factors ranging between 20 and 20,000, which enabled objects including pores with diameters of the order of 0.01 μ. to be identified. This large range of magnification, together with a large depth of focus, has the additional advantage of revealing pores in three dimensions. The use of Scanning Electron Microscopy in the study of pore-systems in rocks is described by Timur et al. (1971).

13 specimens covering a wide porosity range and the basic porosity-types recognised in the core-specimens using reflected light, were taken from these core-specimens, as recorded in Appendix 7. Preparation of these specimens consisted of coating under vacuum with gold and carbon in order to improve the surface conductivity. Each specimen was mounted on the goniometer stage of the Scanning Electron Microscope, and identification of any micropores in the specimen was made. The basic porosity-types previously identified were also studied in detail under high magnification. Results were recorded in the form of photomicrographs (Plates 4.21; 6.4; 6.5; 6.7; 6.8; 6.12-6.18). The microporosity identified is described in Section 6.3.3.

Plates 4.5 — 4.23

These photographic plates mainly illustrate the petrographic components described in this chapter, and which were considered to be possible velocity-controlling parameters. Plates 4.5 - 4.8, 4.11 - 4.14, 4.16 and 4.18 are photomicrographs using plane polarised light, and plates 4.9, 4.10, 4.15, 4.17 and 4.20 are photomicrographs using crossed polarised light. Plate 4.19 is a photograph of a cross-laminated bed in the Basement beds at Upper Chicksgrove Quarry (Section 3.3.9). Plate 4.21 is a scanning electron micrograph and plates 4.22 and 4.23 are photomicrographs using reflected light. With the exception of plate 4.19, the core-specimens used for the plates e.g. WP3X2 together with the limestone-type are indicated. The porosity (ϕ) of the core-specimens used for plates 4.20 - 4.23, which illustrate porosity-types, is also given. All scales are given in microns (μ) with the exception of plate 4.19, where centimetres are used.

Plate 4.5 WP3X2 (Sparite)

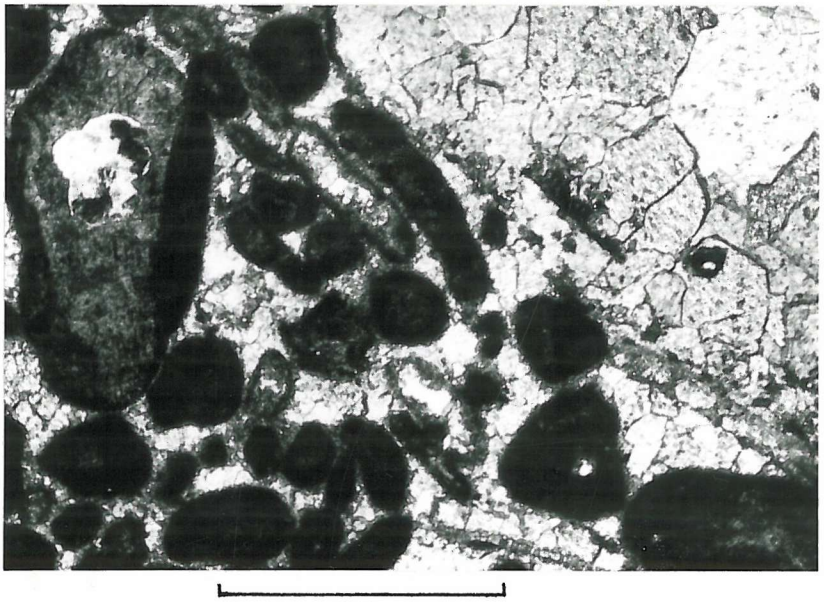


500μ

Large irregular-shaped intraclast, elongate bioclasts and rounded ooliths with clear, sparry calcite crystals (sparite) forming the cement. Some bioclasts show fine-grained Type II calcite replacement fabrics.

Photomicrograph (x 91)

Plate 4.6 WP1Z2 (Sparite)



1000μ

Rounded to ovoid ooliths and elongate bioclasts set in a clear, sparry calcite cement, which shows optical continuity with Type III calcite replacement fabrics. These fabrics which replace a large bioclast seen in the upper right half of the plate, were probably formed by passive precipitation. Large ovoid bioclast near left margin of plate has been replaced by fine-grained Type II calcite fabrics, followed by silica replacement in the form of lutecite, which is approx. rounded in shape.

Photomicrograph (x 38)

Plate 4.7 PLW1X2 (Sparite)



500μ

Ovoid to elongate bioclasts, which show Type II calcite replacement fabrics, and rounded ooliths. Some of the intervening pore-space (interparticle porosity) is filled with sparry calcite cement (upper left margin of plate).

Photomicrograph (x 91)

Plate 4.8 PLW1X2 (Sparite)

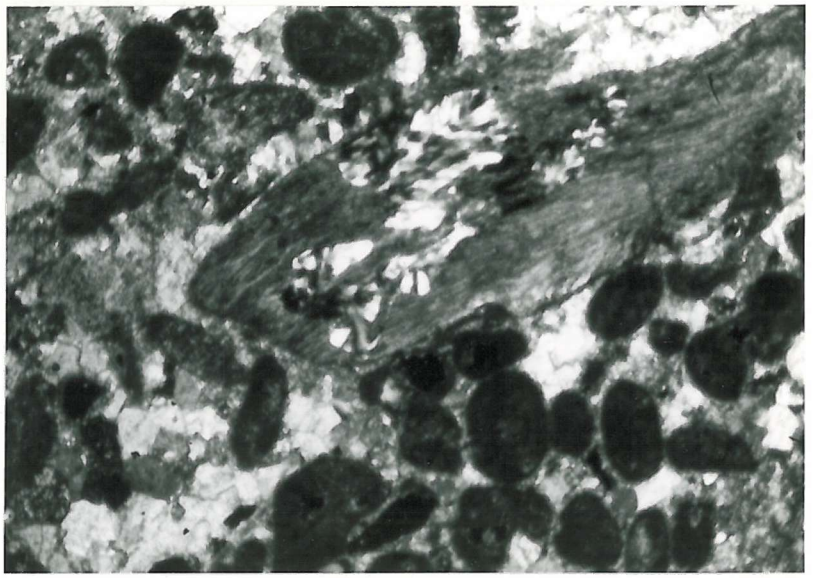


1000μ

Elongate to irregular-shaped bioclasts and rounded to ovoid ooliths. Most bioclasts show fine-grained Type II calcite replacement fabrics, and some of the interparticle porosity is filled with sparry calcite cement.

Photomicrograph (x 38)

Plate 4.9 WP1Z3 (Sparite)

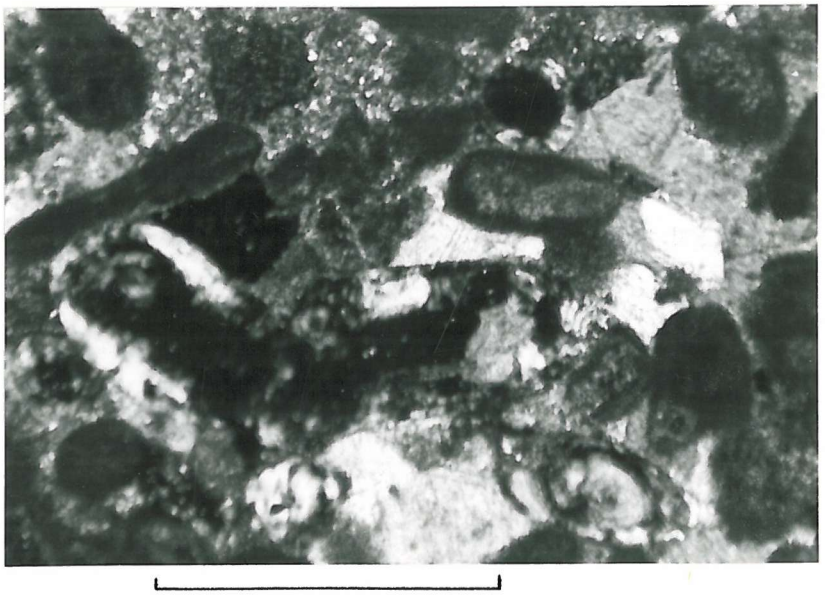


1000μ

Rounded to ovoid ooliths and a large elongate bioclast set in a clear, sparry calcite cement. The bioclast shows banded, fine-grained, Type I calcite replacement fabrics and irregular-shaped silica replacement fabrics in the form of lutecite.

Photomicrograph (x 38)

Plate 4.10 WN1Y1 (Sparite)



500μ

Rounded ooliths and large elongate to irregular-shaped bioclasts set in a sparry calcite cement. Several hollow siliceous sponge (Pachastrella) spicules seen in section, with a large tetraxon present in lower half of plate.

Photomicrograph (x 91)

Plate 4.11 UCM1Y5 (Sparite)

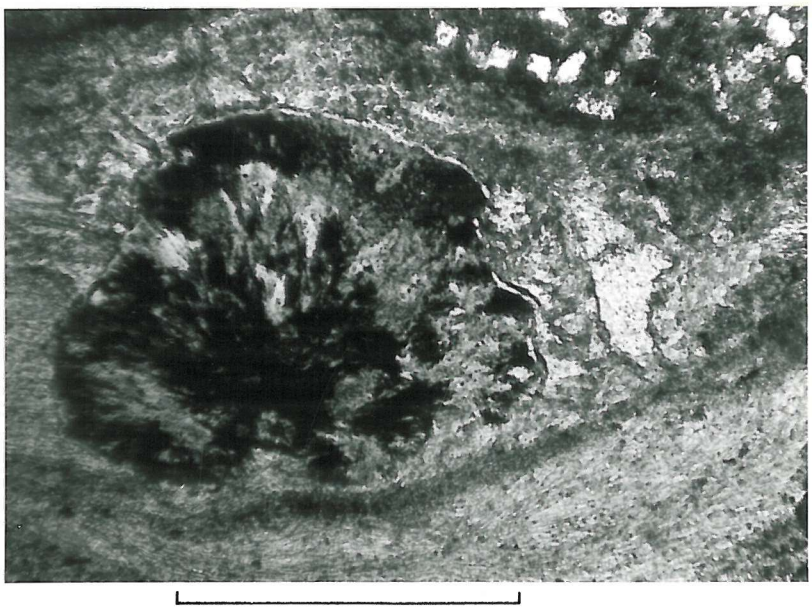


300μ

Rounded to ovoid ooliths and detrital grains of quartz (anhedral and clear) and glauconite (elongate, mottled grain in upper right half of plate) set in a sparry calcite cement (showing high relief).

Photomicrograph (x 150)

Plate 4.12 UCBS1Z1 (Sparite)

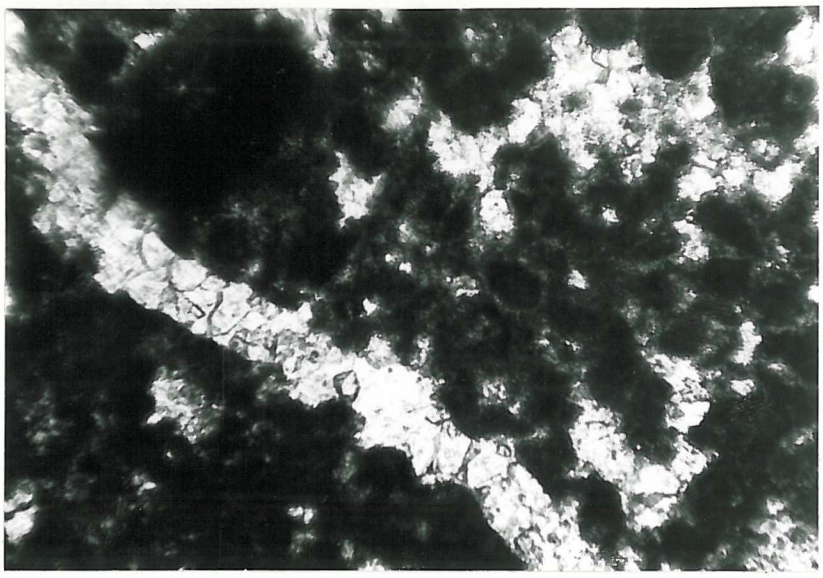


500μ

Part of bioclast showing fine-grained, Type I calcite replacement fabrics post-dated by silica replacement in the form of circular-shaped lutecite. Detrital grains of anhedral, clear quartz set in a sub-equal sparite and micrite cement (Appendix 6; Folk, 1962) present near right upper margin of plate.

Photomicrograph (x 91)

Plate 4.13 LCV1X5 (Sparite)

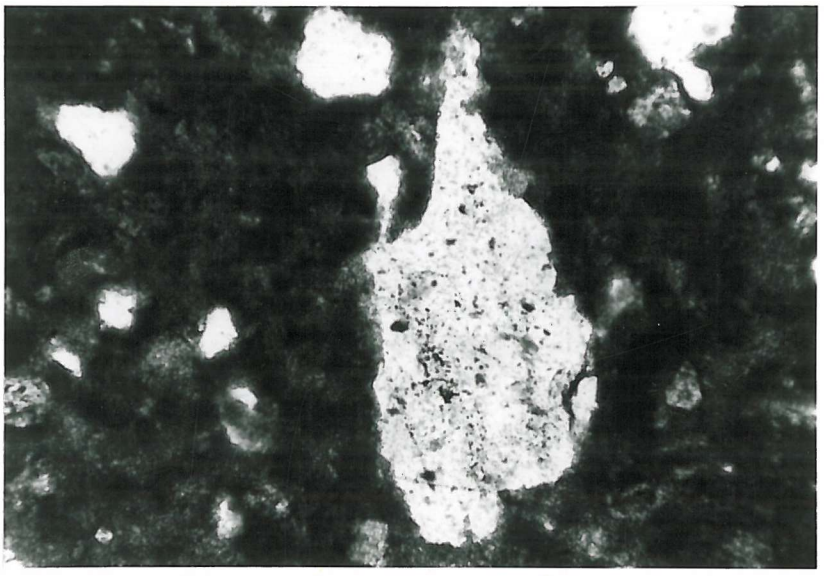


500μ

Irregular mass of rounded to ovoid pellets, with a few ooliths, set in a clear sparry calcite cement. Discordant vein of sparry calcite crystals also present.

Photomicrograph (x 91)

Plate 4.14 CRC1Z1 (Chalk)

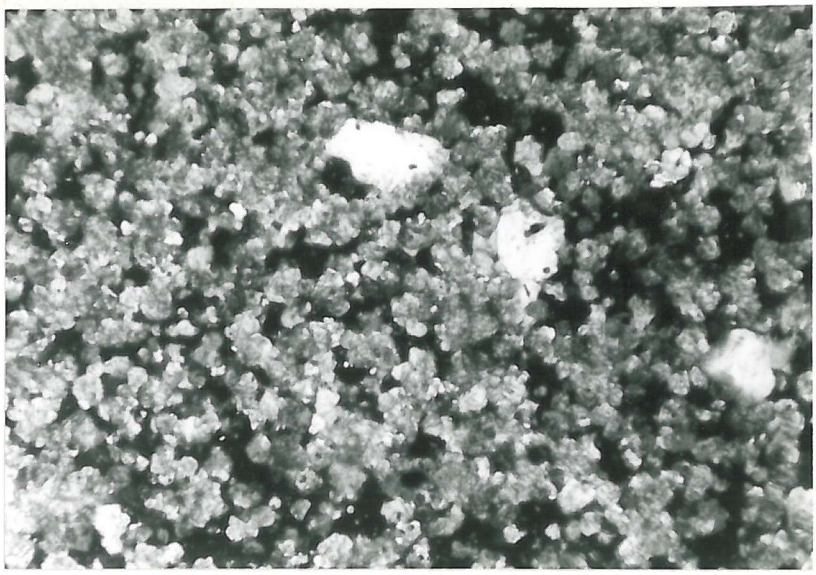


300μ

Irregular mass of rounded to ovoid pellets and detrital grains of anhedral, clear quartz, set in a microcrystalline calcite (micrite) cement.

Photomicrograph (x 150)

Plate 4.15 WB1X4A (Microsparite)

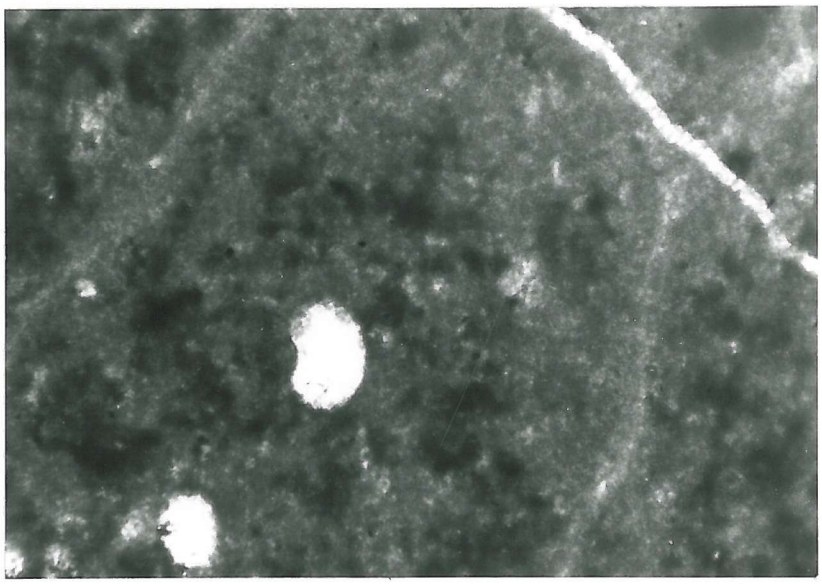


300μ

Equidimensional, finely-crystalline calcite (microspar) with three larger detrital grains of anhedral, clear quartz.

Photomicrograph (x 150)

Plate 4.16 WV1Y1 (Micrite)



300μ

Reniform casts of sponge (Rhaxella) spicules infilled with sparry calcite (Type III replacement fabrics) set in a microcrystalline calcite (micrite) cement. Discordant vein of sparry calcite also present.

Photomicrograph (x 150)

Plate 4.17 WS2X2 (Sparite)

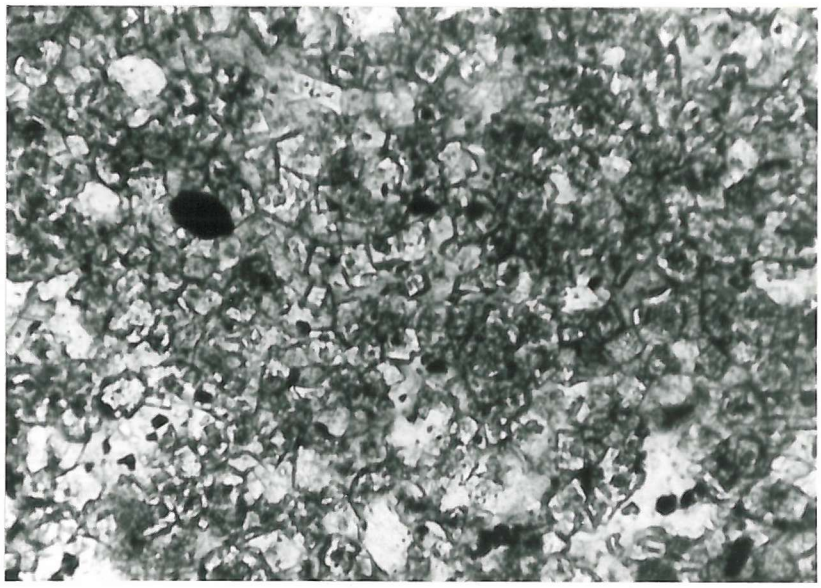


300μ

Large bioclast showing silica replacement in the form of mosaic quartz, mainly on the margins, and microcrystalline granular quartz. Sparry calcite forms the surrounding cement, and the cross-section of a hollow, siliceous, sponge (Pachastrella) spicule is present on lower left margin of plate.

Photomicrograph (x 150)

Plate 4.18 LCA10-1Z4A (Microsparite)



300μ

Equidimensional, finely-crystalline calcite (microspar) and rhombic dolomite, with detrital grains of anhedral, clear quartz and anhedral, opaque magnetite.

Photomicrograph (x 150)

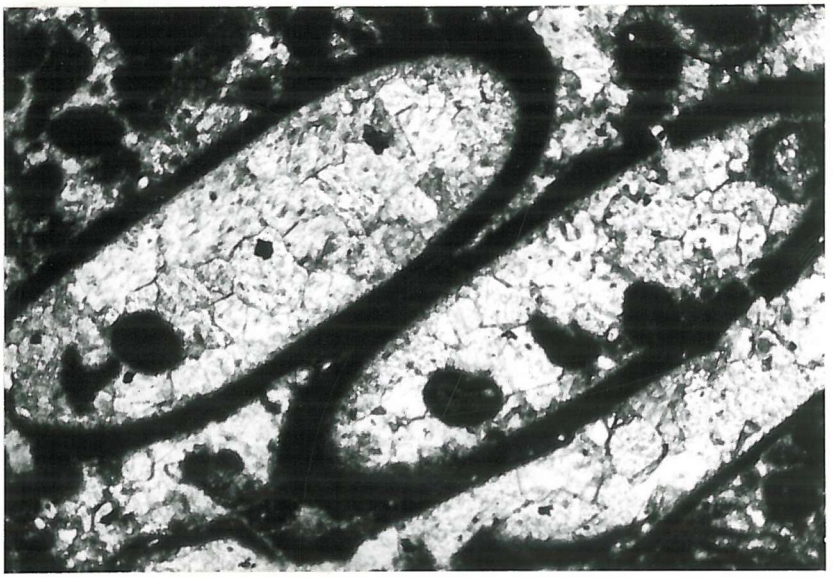
Plate 4.19 FABRIC



50cm

An example of fabric defined by preferred orientation of quartz grains in the form of cross-lamination.

Plate 4.20 WP1Y6 (Sparite) $\phi = 8.9\%$



1000μ

Sparry calcite crystals forming the cement and Type III replacement fabrics, which completely infill burrow mesopores, classed as bioclasts in this study. Rounded to ovoid ooliths also present.

Photomicrograph (x 38)

Plate 4.21 CRU2Z2 (Sparite) ϕ = 31.0%



50μ

Boring micropore in oolith, which shows a marked concentric structure and to a lesser extent, a radial structure.

Scanning Electron Micrograph (x 980)

Plate 4.22 WV3Y5 (Micrite) ϕ = 9.0%

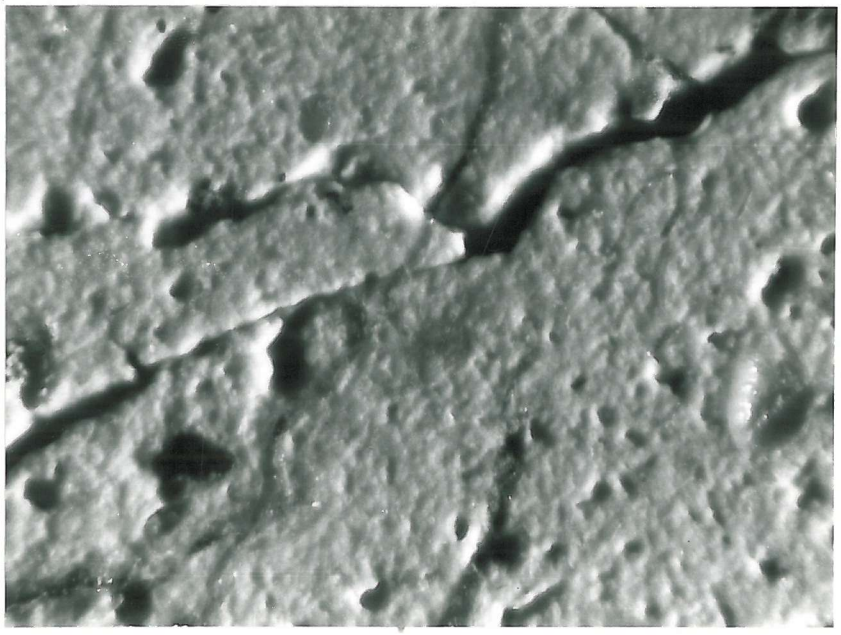


1000μ

Isolated, evenly-distributed, rounded micromolds with some elongate mesomolds showing partial and complete infill with sparry calcite. These elongate molds are derived from shell-fragments (bioclasts).

Photomicrograph (x 46)

Plate 4.23 UCR3Z2 (Micrite) ϕ = 12.8%



1000μ

Solution-enlarged micro-mesofracture and irregular-shaped micro-mesomolds, most of which are solution-enlarged.

Photomicrograph (x 46)

CHAPTER 5

VARIATION OF ELASTIC-WAVE VELOCITY WITH LITHOSTRATIGRAPHY

5.1 Introduction

An attempt is made to correlate elastic-wave velocity with individual lithostratigraphic units. Velocity anisotropy within these units is also studied.

The Portland Group shows considerable lateral variation in lithostratigraphy, complicated at Lulworth Cove by involvement in a major monocline (Chapter 3). Data were analysed from five separate areas -

East Purbeck, Dorset

Lulworth Cove, Dorset

Central Dorset

Isle of Portland, Dorset

Vale of Wardour, Wiltshire

Three lithostratigraphic units, the black dolomitic sandstone bed, the Portland oolitic limestone member and the Portland cherty limestone member (Chapter 3) can be traced laterally throughout Dorset. The data from these units were aggregated to determine any possible correlation with velocity.

Mean velocities in both a horizontal plane and a vertical direction were computed for each lithostratigraphic unit from the individual core-specimen velocity data (Appendix 5). A mean velocity irrespective of direction was finally calculated for each unit together with the corresponding mean porosities for these units. Velocity anisotropy in the lithostratigraphic units was assessed by means of the coefficient of aeolotropy calculated separately for each unit.

5.2 Elastic-Wave Velocity Variation with Lithostratigraphy

5.2.1 Introduction

Samples cored in three orthogonal directions (section 4.2) enabled mean velocities to be computed in these directions for each sample. Unfortunately, only the vertical direction (Z) is identical in all the samples; the horizontal directions (X and Y) were arbitarily allocated for each sample. The study of velocity in the sampled units was therefore made with reference to the horizontal plane and the vertical direction. For the horizontal plane, a mean velocity was computed from the combined individual velocity-determinations for the 'X' and 'Y' cores. Similarly, for the vertical direction, mean velocities were computed from individual velocity-determinations for the 'Z' cores.

Tables of mean, standard error and range of velocity are listed (Section 5.2.2) for the areas previously defined (Section 5.1). Any possible correlations between velocity and lithostratigraphic units were investigated by use of Student's t-tests applied at a 5% probability level. Those units which had velocities statistically from the same population were deduced.

5.2.2 Results

(a) East Purbeck

The lithostratigraphic units recognised at Swanworth Quarry (Section 3.3.2) are considered to be representative of the East Purbeck area, since they can be traced throughout this area (Arkell, 1935, 1947).

Velocity data are presented in Table 5.1. This table indicates that the mean velocities can be grouped into five populations.

However, overlapping ranges prevent unique correlations being made between lithostratigraphy and velocity for any given bed. It is also apparent that velocity contrasts between beds are not of sufficient

TABLE 5.1

Comparison of Elastic-Wave Velocities in some beds of the Portland Group, Swanworth Quarry

BED	No. of core spec.	VERTICAL DIRECTION — VELOCITY (metres/sec.) Mean & S.E.	Range	Index. No.*
V	14	5204 ± 104	4538 - 5792	1
U	14	4819 ± 78	4257 - 5162	2
T	5	5441 ± 387	4326 - 6505	3
S	5	5671 ± 122	5321 - 5950	3
Q	9	4701 ± 134	4075 - 5398	2
P	9	5548 ± 61	5258 - 5784	3
O	14	4752 ± 66	4407 - 5168	2
N	11	4512 ± 35	4311 - 4692	4
C-M	not sampled	-	-	-
B	9	3233 ± 195	2685 - 4072	5
A28	6	3152 ± 135	2831 - 3664	5

BED	No. of core spec.	HORIZONTAL PLANE — VELOCITY (metres/sec.) Mean & S.E.	Range	Index. No.*
V	29	5257 ± 45	4358 - 5864	1
U	26	5204 ± 53	4596 - 5935	1
T	11	5492 ± 138	4608 - 6112	2
S	5	5688 ± 152	5334 - 6200	2
Q	19	4966 ± 122	4379 - 5854	3
P	17	5463 ± 60	4932 - 5761	2
O	29	4681 ± 88	4008 - 5462	3
N	22	4456 ± 39	4152 - 4708	4
C-M	not sampled	-	-	-
B	19	3489 ± 101	3030 - 4351	5
A28	14	3459 ± 88	2851 - 4051	5

* Population Index Number

magnitude to enable an identification of the bed-sequence to be made positively from velocity data alone.

(b) Lulworth Cove

The Portland Limestone Formation is a condensed sequence compared to that at Swanworth Quarry and dips at a much greater angle (Section 3.3.3.). Two lithostratigraphic units were examined at Lulworth Cove, beds V and A10.

Table 5.2 gives the results. They show that the two beds can be differentiated on the basis of mean velocity, but an identification of the beds from individual velocity measurements is marred in the case of the horizontal plane by overlapping velocity-ranges.

Comparisons of the results from Swanworth Quarry and Lulworth Cove are presented in Table 5.3. Velocities are generally higher at Lulworth. This increase in velocity at Lulworth, particularly in bed A10 could be related to tectonism (section 3.3.3.). This is further discussed in section 5.4.2b with reference to porosity.

(c) Central Dorset

This includes Chalbury Camp, Corton Farm road-cutting and Portesham Quarry, since bed-by-bed correlation is possible between these localities (Sections 3.3.4; 3.3.5; 3.3.6). Five beds were sampled: the black dolomitic sandstone bed and beds 5, 6, 8 and 10 of the Portland Limestone. The relevant results are listed in Table 5.4. Vertical velocity means can be grouped into two populations whereas the horizontal-plane velocity means show no grouping. Overlapping velocity-ranges prevent any correlation between velocity and individual beds.

(d) Isle of Portland

The velocity statistics for the beds sampled on the Isle of Portland are given in Table 5.5. The results show that in a vertical direction only the "Basal Shell Bed" (Arkell, 1933) which has velocities in a higher range, and the black dolomitic sandstone bed which has velocities in a

TABLE 5.2

Comparison of Elastic-Wave Velocities in two beds of the Portland Group, Lulworth Cove

BED	No. of core specs.	VERTICAL DIRECTION VELOCITY (metres/sec.) Mean & S.E.	Range	Index No.
V	11	5595 ± 59	5331 - 5789	1
B-U	not sampled	-	-	-
A10	6	5265 ± 38	5101 - 5339	2

BED	No. of core specs.	HORIZONTAL PLANE VELOCITY (metres/sec.) Mean & S.E.	Range	Index No.
V	18	5577 ± 53	5212 - 5822	1
B-U	not sampled	-	-	-
A10	11	5004 ± 65	4675 - 5374	2

TABLE 5.3

Comparison of Velocities at Swanworth Quarry and Lulworth Cove

		Bed V, Swanworth	Bed V, Lulworth	Bed A28 Swanworth	Bed A10 Lulworth
Vertical Direction	Mean	5204 ± 104	5595 ± 59	3152 ± 135	5265 ± 38
	Range	4538 - 5792	5331 - 5789	2831 -3664	5101-5339
Horizontal Plane	Mean	5257 ± 45	5577 ± 53	3459 ± 88	5004 ± 65
	Range	4358 - 5864	5212 - 5822	2851 -4051	4675-5374

TABLE 5.4

Comparison of Elastic-Wave Velocities in some beds of the Portland Group, Central Dorset

BED	No. of core specs.	VERTICAL DIRECTION VELOCITY (metres/sec.) Mean & S.E.	Range	Index No.
10	11	4370 ± 200	3870 - 5717	1
9	not sampled	-	-	-
8	11	4253 ± 88	3797 - 4667	1
7	not sampled	-	-	-
6	12	3483 ± 33	3325 - 3686	2
5	8	3612 ± 92	3307 - 4108	2
1-4	not sampled	-	-	-
BDSB*	3	4363 ± 207	3948 - 4575	1

BED	No. of core specs.	HORIZONTAL PLANE VELOCITY (metres/sec.) Mean & S.E.	Range	Index No.
10	19	4352 ± 82	3838 - 5204	1
9	not sampled	-	-	-
8	25	4116 ± 78	3679 - 5108	2
7	not sampled	-	-	-
6	25	3529 ± 43	3181 - 3899	3
5	17	3814 ± 96	3326 - 4726	4
1-4	not sampled	-	-	-
BDSB*	9	4670 ± 47	4488 - 4865	5

* BDSB = Black dolomitic sandstone bed

TABLE 5.5

Comparison of Elastic-Wave Velocities in some beds of the Portland Group, Isle of Portland

BED	No. of core specs.	VERTICAL DIRECTION VELOCITY (metres/sec.) Mean & S.E.	Range	Index No.
Whit bed	9	4492 ± 35	4349 - 4685	1
Flinty bed	not sampled	-	-	-
Little Roach bed - not sampled			-	-
Base bed	10	4566 ± 61	4209 - 4781	1
Beds of limestone with chert nodules - not sampled				-
ABSB	16	5383 ± 57	5096 - 5746	2
Arkell's "Portland Clay" - not sampled			-	-
BDSB	13	3821 ± 71	3751 - 4209	3

BED	No. of core specs.	HORIZONTAL PLANE VELOCITY (metres/sec.) Mean & S.E.	Range	Index No.
Whit bed	18	3965 ± 33	3805 - 4319	1
Flinty bed - not sampled		-	-	-
Little Roach bed - not sampled			-	-
Base bed	20	4475 ± 45	4039 - 4729	2
Beds of limestone with chert nodules - not sampled				-
ABSB	27	5621 ± 48	4843 - 6079	3
Arkell's "Portland Clay" - not sampled			-	-
BDSB	30	4021 ± 38	3527 - 4495	1

ABSB = Arkell's "Basal Shell Bed"
BDSB = Black dolomitic sandstone bed

lower range than those of the other two beds, can be identified using velocity. In the horizontal plane, only the "Basal Shell Bed" (Arkell, 1933) can be clearly distinguished, having velocities in a higher range than those of the other three beds. However a positive identification of these beds from velocity is made uncertain by lack of data from the unsampled beds in the sequence (Table 5.5).

(e) Vale of Wardour

The velocity data from core-specimens of samples from both the Chilmark Ravine (Section 3.3.8) and Upper Chicksgrove Quarry (Section 3.3.9) cover an almost continuous sequence of lithostratigraphic units. The results are presented in Table 5.6.

The results show that the mean velocities fall statistically within several populations. However, individual velocities cannot be correlated with specific lithostratigraphic units because of overlapping ranges.

Comparisons can be drawn with East Purbeck (Section 5.2.2a), in that velocity contrasts between units (Table 5.6) are not of sufficient magnitude to enable the sequence of units in the Vale of Wardour to be identified.

(f) Regional Correlations

Three lithostratigraphic units can be traced laterally throughout Dorset, the black dolomitic sandstone bed, the Portland cherty limestone member and the Portland oolitic limestone member (Chapter 3). The velocity statistics of these units, together with those of the Portland Group throughout the areas studies, are summarised in Table 5.7.

The results indicate that the higher mean velocity of the Portland oolitic limestone member is not statistically from the same population as the other two units. However overlapping velocity-ranges between units prevent an identification of these units from individual velocity measurements.

TABLE 5.6

Comparison of Elastic-Wave Velocities in some lithostratigraphic units of the Portland Group, Vale of Wardour

UNIT	No. of core specs.	VERTICAL DIRECTION VELOCITY (metres/sec.) Mean & S.E.	Range	Index No.
LB	4	3978 ± 197	3452 - 4407	1
AUBS	25	3536 ± 33	3147 - 3830	2
CLB	11	3002 ± 22	2896 - 3111	3
RB	11	4227 ± 209	3319 - 5013	1
TB	not sampled	-	-	-
GSLB	6	2269 ± 91	1876 - 2453	4
BB	7	2645 ± 228	1992 - 3776	4
BSB	4	3516 ± 29	3453 - 3594	2

UNIT	No. of core specs.	HORIZONTAL PLANE VELOCITY (metres/sec.) Mean & S.E.	Range	Index No.
LB	7	5380 ± 131	5030 - 6025	1
AUBS	45	3340 ± 68	2690 - 4157	2
CLB	23	2894 ± 36	2598 - 3130	3
RB	22	4534 ± 164	3452 - 5447	4
TB	not sampled	-	-	-
GSLB	12	2577 ± 98	2010 - 3201	5
BB	17	3367 ± 201	2144 - 5505	2
BSB	6	4502 ± 56	4278 - 4642	4

LB = Lamellosus bed
AUBS = Arkell's "Upper Building Stones"
CLB = Chalky limestone beds
RB = Ragstone beds
TB = Trough bed
GSLB = Glauconitic sandy limestone beds
BB = Basement beds
BSB = Basal shell beds

TABLE 5.7

Comparison of Elastic-Wave Velocities in three lithostratigraphic units of the Portland Group, Dorset and a summary of the Portland Group in Dorset and the Vale of Wardour

VERTICAL DIRECTION

UNIT	No. of core specs.	VELOCITY (metres/sec.) Mean & S.E.	Range	Index No.
POLM	132	4757 ± 60	3325 - 6505	1
PCLM	19	4133 ± 113	3307 - 4692	2
BDSB	28	4045 ± 147	2831 - 5339	2
PORT-LAND GROUP	272	4281 ± 56	1876 - 6505	-

HORIZONTAL PLANE

UNIT	No. of core specs.	VELOCITY (metres/sec.) Mean & S.E.	Range	Index No.
POLM	261	4730 ± 45	3181 - 6200	1
PCLM	39	4176 ± 69	3326 - 4726	2
BDSB	64	4158 ± 72	2851 - 5374	2
PORT-LAND GROUP	542	4338 ± 40	2010 - 6200	-

POLM = Portland oolitic limestone member
PCLM = Portland cherty limestone member
BDSB = Black dolomitic sandstone bed

The Portland Group shows approximately equal mean velocities in the vertical direction and horizontal plane, indicating that it has no velocity anisotropy; see also Section 5.3.2 f and the summary of Table 5.14 f.

5.2.3 Conclusions

The lithostratigraphic units of the Portland Group studied, can be distinguished either singly or in sets, which are statistically from the same population, on the basis of mean velocity. In the case of determinations in a vertical direction, a positive identification of individual units, using individual velocities, is limited to three units or 10% of those studied. In the case of determinations in the horizontal plane, only one unit, the "Basal Shell Bed" (Arkell, 1933), Isle of Portland, can be characterised by its velocity value. Obviously, any attempt at velocity correlation with lithostratigraphy is severely limited by overlapping velocity-ranges between units.

5.3 Velocity Anisotropy in relation to Lithostratigraphy

5.3.1 Introduction and Methods

An investigation of velocity anisotropy within lithostratigraphic units of the Portland Group is made.

Velocity anisotropy is commonly defined by the equation:

$$\% \text{ Anisotropy} = \frac{V_{max} - V_{min}}{\bar{V}} \times 100 \quad \ldots \text{ Eq. 5.1}$$

where Vmax is the maximum, Vmin is the minimum and $\bar{V}$ is the mean of velocities determined in three orthogonal directions. The maximum and minimum velocities should come from statistically independent populations for a true anisotropy to exist. Here, the study of velocity anisotropy is limited to variation between mean velocity magnitude in the vertical direction and in the horizontal plane. This

SOUTHAMPTON UNIVERSITY LIBRARY

variation is represented quantitatively for each unit by a coefficient of aeolotropy defined as the ratio:

$$\frac{\text{Mean Velocity in the Vertical Direction}}{\text{Mean Velocity in the Horizontal Plane}} \quad \ldots\ldots \text{Eq. 5.2}$$

However, the coefficient of aeolotropy is only valid statistically if the two mean velocities are not from the same population. This was tested for each lithostratigraphic unit studied, by means of a Student's t-test at the 5% probability level. Coefficients of velocity aeolotropy together with the results of Student's t-tests, for each unit studied, are listed in tabular form. Mean velocities are given in Tables 5.1 - 5.7.

5.3.2. Results and Discussions

The study was made on both a local and regional basis because of lateral variations in lithostratigraphy, following the methods used in Section 5.2.

(a) East Purbeck

The results (Table 5.8) show that with the exception of bed U, all beds of the Portland Group studied are isotropic. Bed U is anisotropic with a mean velocity in the vertical direction 7% less than that in the horizontal plane. This is probably a result of the effects of planar fabric elements in the form of preferred shell-orientation. A visual study of core-specimens taken from bed U, shows that they consist of shelly, oolitic limestones with isolated shells lying in the horizontal plane, which is parallel to bedding since the maximum dip recorded was 5 degrees (Section 3.3.2). In some cases, these shells extend over the entire cross-sectional area of the cores. It is inferred from this that vertical velocities in core-specimens and thus the mean velocity of bed U in a vertical direction will be less than

TABLE 5.8

Coefficients of Aeolotropy and Results of Student's t-tests on Velocities for some beds of the Portland Group, Swanworth Quarry

BED	Student's *t* & Probability level (p)	Coefficient of aeolotropy
V	-0.547; p > 20%	0.990
U	-4.161; p < 1%	0.926*
T	-0.157; p > 20%	0.991
S	+0.087; p > 20%	0.997
Q	+1.321; 10% < p < 20%	0.947
P	-0.907; p > 20%	1.016
O	-0.524; p > 20%	1.015
N	-0.927; p > 20%	1.013
C-M	not sampled	
B	-1.294; p > 20%	0.927
A28	-1.911; 5% < p < 10%	0.911

* statistically valid

the horizontal velocities because of the greater number of discontinuities to the transmission of elastic-wave energy in the vertical direction. Further discussion with reference to fabric is given in Sections 7.3.1; 7.3.2a.

(b) Lulworth Cove

TABLE 5.9

Coefficients of Aeolotropy and Results of Student's t-tests on Velocities for two beds of the Portland Group, Lulworth Cove

BED	Student's t & Probability level (p)	Coefficient of aeolotropy
V	-0.943; $p > 20\%$	1.003
B-U	not sampled	-
A10	-2.812; $1\% < p < 2\%$	1.052*

* statistically valid

The results show that bed V is isotropic, whereas bed A10 is anisotropic with a velocity in the vertical direction 5% greater than that in the horizontal plane. As no evidence of any planar fabric elements was found in core-specimens taken from bed A10, it is suggested that fortuitous sampling resulting in apparent porosity differences between cores taken in the vertical direction and in the horizontal plane may be a possible cause of these velocity differences.

Bed A10 in the Lulworth Cove area is situated on the northern limb of the Purbeck Anticline (Section 3.2.2.), and vertically-oriented core-specimens are thus perpendicular to the direction of maximum tectonic compression (Arkell, 1938). The mean velocity perpendicular to maximum compression is therefore up to 5% greater than that parallel to maximum compression. Bedding is probably not an

important factor affecting velocity anisotropy in bed A10, since apparent dips of bedding traces within the three orthogonal directions of coring, are almost constant, varying between 28° and 33°.

(c) Central Dorset

TABLE 5.10

Coefficients of Aeolotropy and Results of Student's t-tests on Velocities for some beds of the Portland Group, Central Dorset

BED	Student's t & Probability level (p)	Coefficient of aeolotropy
10	+0.097; p > 20%	1.004
9	not sampled	-
8	-1.036; p > 20%	1.033
7	not sampled	-
6	+0.691; p > 20%	0.987
5	+1.299; p > 20%	0.948
1-4	not sampled	-
BDSB	+2.252; 2% < p < 5%	0.934*

* statistically valid
BDSB = Black dolomitic sandstone bed

With the exception of the black dolomitic sandstone bed, the beds sampled in Central Dorset are isotropic. For the black dolomitic sandstone bed, the mean velocity in the horizontal plane is 7% greater than that in the vertical direction. Since the dip of this bed is approximately 13 degrees (Section 3.3.5), the lower mean velocity in the vertical direction could be related to a greater frequency of planar fabric elements in the form of laminae, as suggested previously for bed U, East Purbeck (Section 5.3.2a). This is further discussed in Sections 7.3.1; 7.3.2d with reference to preferred mineral-orientation parallel to primary bedding and cross lamination.

(d) Isle of Portland

With the single exception of the Base bed, the beds studied on the Isle of Portland exhibit velocity anisotropy.

The Whit bed has a mean velocity in the vertical direction some 13% greater than that in the horizontal plane. Cores taken from this bed do not show any planar fabric elements and it is possible that, as in the case of bed A10, Lulworth Cove, the velocity anisotropy is an artefact of apparent differences in porosity due to specimen sampling procedure.

The velocity anisotropy of the "Basal Shell Bed" (Arkell, 1933) may be related to preferred shell-orientation parallel to bedding as described in Sections 7.3.1; 7.3.2c.

In the case of the velocity anisotropy of the black dolomitic sandstone bed, the effects of pore-orientation (Section 6.3.3b) and fabric, in the form of preferred mineral-orientation (Section 7.3.2d) are probably both of importance.

(e) Vale of Wardour

Four units of the Portland Group show velocity anisotropy and of these, the Lamellosus bed, the Basement beds and the Basal shell beds are probably anisotropic as a result of fabric (Section 4.5.3.). The fabric elements are usually in the horizontal plane, which is parallel to bedding (Section 3.3.9), and this results in the mean velocities in the vertical direction being less than those in the horizontal plane. In the case of the Lamellosus bed, the fabric elements consist of preferred pore-orientation (Section 6.3.3b), which is probably related to preferred shell-orientation (Sections 7.3.1; 7.3.2c). Similarly, in the Basal shell beds, the fabric elements consist of preferred shell-orientation, (Section 7.3.2a). In the case of the Basement beds, preferred mineral-orientation apparently forms the fabric elements (Sections 7.3.1; 7.3.2a).

TABLE 5.11

Coefficients of Aeolotropy and Results of Student's t-tests on Velocities for some beds of the Portland Group, Isle of Portland

BED	Student's *t* & Probability level (p)	Coefficient of aeolotropy
WB	-9.953; p < 1%	1.133*
FB	not sampled	-
LRB	not sampled	-
BB	-1.183; p > 20%	1.020
CLB	not sampled	-
ABSB	+3.096; p < 1%	0.958*
APC	not sampled	-
BDSB	-2.704 p = 1%	0.950*

*statistically valid

WB = Whit bed
FB = Flinty bed
LRB= Little Roach bed
BB = Base bed
CLB = Beds of limestone with chert nodules
ABSB = Arkell's "Basal Shell Bed"
APC = Arkell's "Portland Clay"
BDSB = Black dolomitic sandstone bed

TABLE 5.12

Coefficients of Aeolotropy and Results of Student's t-tests on Velocities for some lithostratigraphic units of the Portland Group, Vale of Wardour

UNIT	Student's *t* & Probability level (p)	Coefficient of aeolotropy
LB	-6.168; $p < 1\%$	0.739*
AUBS	-2.060; $2\% < p < 5\%$	1.059*
CLB	-1.979; $5\% < p < 10\%$	1.037
RB	+1.114; $p > 20\%$	0.932
TB	not sampled	
GSLB	+2.007; $5\% < p < 10\%$	0.880
BB	+2.076; $2\% < p < 5\%$	0.786*
BSB	+13.470; $p < 1\%$	0.781*

* statistically valid

LB = *Lamellosus* bed

AUBS = Arkell's "Upper Building Stones"

CLB = Chalky limestone beds

RB = Ragstone beds

TB = Trough bed

GSLB = Glauconite sandy limestone beds

BB = Basement beds

BSB = Basal shell beds

The "Upper Building Stones" (Arkell, 1933) have higher mean velocities in the vertical direction than in the horizontal plane. This is similar to the results obtained for the Whit bed (Section 5.3.2d) and bed A10 (Section 5.3.2b).

(f) Regional correlations

TABLE 5.13

Coefficients of Aeolotropy and Results of Student's t-tests on Velocities for three Lithostratigraphic Units of the Portland Group, Dorset, and for the Portland Group in Dorset and the Vale of Wardour

UNIT	Student's t and Probability level (p)	Coefficient of aeolotropy
POLM	+0.590; p > 20%	1.006
POCM	+0.045; p > 20%	0.990
BDSB	-0.998; p > 20%	0.973
PORT-LAND GROUP	-0.825; p > 20%	0.987

POLM = Portland oolitic limestone member

POCM = Portland cherty limestone member

BDSB = Black dolomitic sandstone bed

The units described are as given in Table 5.7 (Section 5.2.2f). The results show that these units, including the Portland Group as a whole, are isotropic with respect to mean velocity. A study is therefore made (Section 5.4) of mean velocities, irrespective of direction, in lithostratigraphic units of the Portland Group for the areas defined in Section 5.1.

5.3.3 Conclusions

The majority of lithostratigraphic units of the Portland Group are isotropic. This is to be expected, since the units consist mainly

of massive homogenous limestone beds of at least 0.3 metres in thickness, and generally lack any planar fabric elements.

Most of the velocity anisotropy that did occur was of the transverse isotropic type, i.e. velocities in the horizontal plane exceeding those in the vertical direction. In all cases, the units involved showed planar fabric elements, usually parallel to bedding. In only three instances (10% of the units studied) was the velocity in the vertical direction found to exceed that in the horizontal plane. These units lacked visible planar fabric elements, so that the anisotropy must be accounted for in some other manner. It is suggested that this may be fortuitously related to sampling, in that apparent differences in porosity between cores taken in mutually perpendicular directions, may be contributing to the observed velocity differences.

Comparison with earlier work is made in Section 5.5.

5.4. Analysis of Velocities in Lithostratigraphic Units of the Portland Group, including the Effect of Porosity.

5.4.1. Introduction

The results of the previous section indicate that 65% of the lithostratigraphic units studied, show velocity isotropy. A summary is therefore made of mean velocities, computed from core-specimen velocities in each unit, irrespective of core-axis direction, together with the corresponding mean porosities in order to assess the degree of dependence of velocity on porosity in the units studied.

Means, standard errors, and ranges of both velocity and porosity for all units studied, are given in Table 5.14, together with the results of Student's t-tests as described previously (Section 5.2.1).

5.4.2. Results

The results are given and discussed for each of the areas previously defined (Section 5.1), following the methods used in Section 5.2.

TABLE 5.14

Comparison of Non-directional Elastic-Wave Velocities and Porosities in Lithostratigraphic Units of the Portland Group

UNIT	No. of core specs.	VELOCITY (metres/sec)			POROSITY (%)		
		Mean & S.E.	Range	Index no.*	Mean & S.E.	Range	Index no.*
a) EAST PURBECK							
V	43	5240±45	4358–5864	E1	9.4±0.2	4.9–12.1	E1
U	40	5069±53	4257–5935	E2	7.9±0.4	3.4–13.5	E2
T	16	5476±146	4326–6505	E3	7.3±0.7	3.5–13.5	E2
S	10	5680±92	5321–6200	E3	5.0±0.8	1.7–8.7	E3
Q	28	4880±95	4075–5854	E4	8.5±0.6	2.4–12.4	E2
P	26	5492±44	4932–5784	E3	5.5±0.4	3.0–9.9	E3
O	43	4704±63	4008–5462	E4	8.9±0.3	3.9–13.7	E1
N	33	4474±28	4152–4708	E5	10.3±0.4	7.1–19.8	E4
C–M not sampled							
B	28	3407±94	2685–4351	E6	24.6±0.6	18.7–29.4	E5
A28	20	3367±79	2831–4051	E6	17.7±1.0	11.5–25.5	E6
b) LULWORTH COVE							
V	27	5583±40	5212–5822	L1	6.4±0.2	5.2–8.0	L1
B–U not sampled							
A10	17	5096±53	4675–5374	L2	7.9±0.3	6.0–11.2	L1
c) CENTRAL DORSET							
10	30	4359±88	3838–5717	C1	21.6±0.9	7.8–27.0	C1
9 not sampled							
8	36	4158±61	3679–5108	C2	22.9±0.6	14.9–27.6	C1
7 not sampled							
6	37	3514±31	3181–3899	C3	28.3±0.3	25.3–32.8	C2
5	25	3750±73	3307–4726	C4	24.4±0.9	14.7–31.3	C1
1–4 not sampled							
black dolomitic sandstone bed	12	4593±69	3948–4865	C1	16.0±0.7	14.0–21.5	C3
d) ISLE OF PORTLAND							
Whit bed	27	4141±54	3805–4685	P1	19.5±0.3	17.0–22.7	P1
Flinty bed not sampled							
Little Roach bed not sampled							
Base bed	30	4505±37	4039–4781	P2	14.5±0.3	11.5–18.0	P2
beds of limestone with chert nodules not sampled							
Arkell's "Basal Shell Bed"	43	5532±41	4843–6079	P3	7.9±0.6	4.3–16.8	P3
Arkell's "Portland Clay" not sampled							
black dolomitic sandstone bed	43	3961±36	3527–4495	P4	18.0±0.4	12.1–25.0	P4
e) VALE OF WARDOUR							
Lamellosus bed	11	4870±237	3452–6025	W1	16.0±2.2	9.6–30.2	W1
"Upper Building Stones" (Arkell, 1933)	70	3410±47	2690–4157	W2	29.6±0.3	24.8–34.4	W2
chalky limestone beds	34	2929±27	2598–3130	W3	35.3±0.3	31.7–38.9	W3
Ragstone beds	33	4432±130	3319–5447	W1	16.5±1.2	6.2–27.9	W1
Trough bed not sampled							
glauconitic sandy limestone beds	18	2474±79	1876–3201	W4	28.7±0.6	25.2–32.9	W2
Basement beds	24	3156±169	1992–5505	W3	27.6±1.1	15.4–39.2	W2
Basal shell beds	10	4108±165	3453–4642	W1	14.4±1.1	9.7–18.6	W1
f) DORSET & TOTAL PORTLAND GROUP							
Portland oolitic limestone member	393	4739±36	3181–6505	1	13.5±0.4	1.7–32.8	1
Portland cherty limestone member	58	4162±59	3307–4726	2	16.4±1.0	7.1–31.3	2
black dolomitic sandstone bed	92	4124±67	2831–5374	2	15.8±0.5	6.0–25.5	2
PORTLAND GROUP	814	4319±32	1876–6505		17.3±0.3	1.7–39.2	

* Population Index Number

(a) East Purbeck

Velocity and porosity data for the units studied are illustrated in Fig. 5.1, and presented in Table 5.14a. It is apparent from this table, that each set of results can be grouped into six populations. However, there is no identity of populations between the sets. Identification of beds from either individual velocity or porosity measurements is prevented by overlapping ranges (Fig. 5.1).

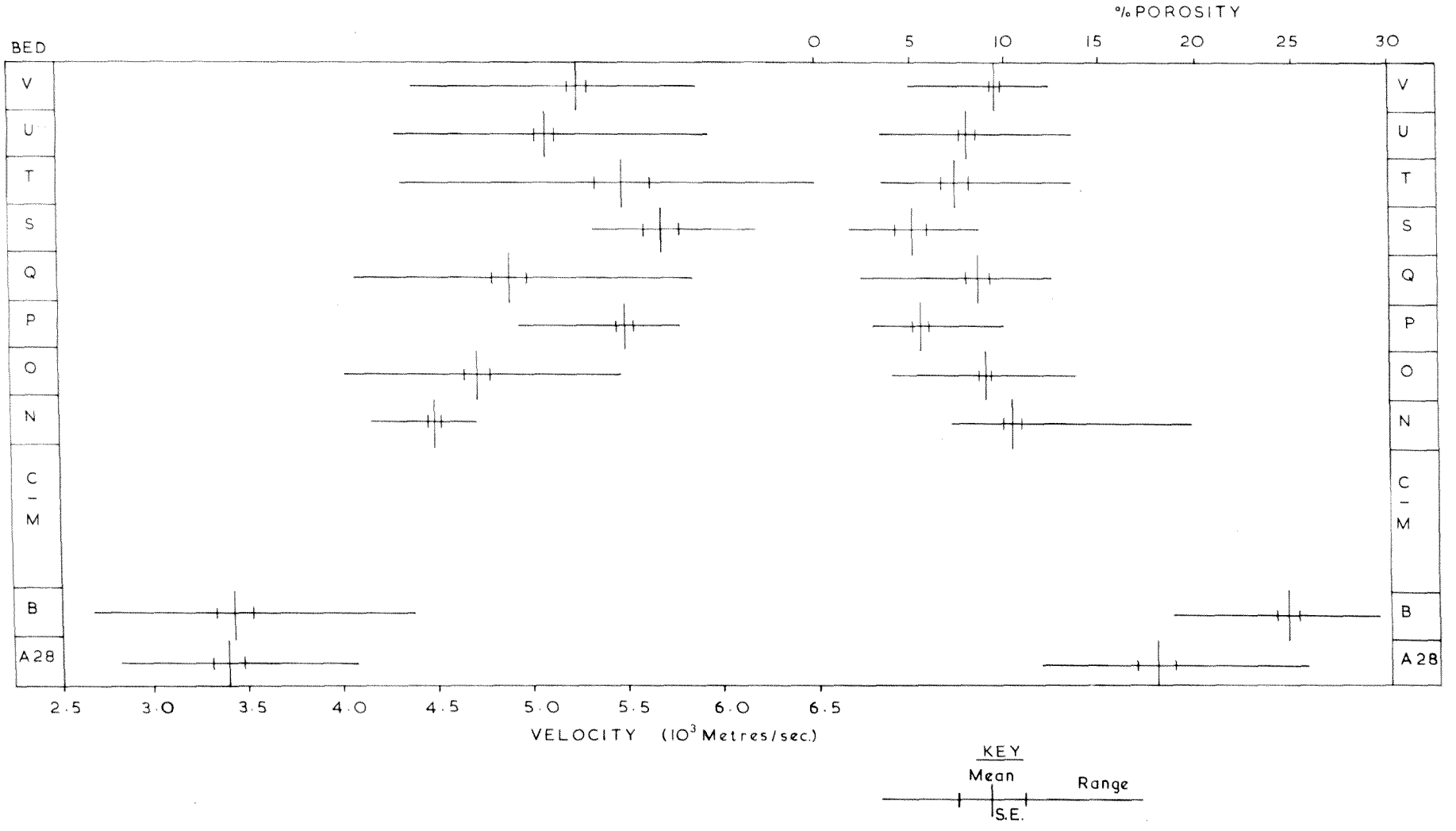
There is a tendency for mean velocity to decrease with increasing mean porosity between beds, with the exception of beds V and A28 (Fig. 5.1). Bed V is a micrite (Section 4.6.1; Appendix 6) which shows a low degree of correlation between velocity and porosity (Section 6.3.2). Bed A28 is a microsparite in which velocity is affected by mineral content (Section 6.2) and other petrographical parameters (Section 7.3.2d). These factors, which tend to reduce the dependence of velocity on porosity, are further discussed in Chapters 6 and 7.

Fig. 5.1 indicates that both velocity and porosity contrasts between beds are not of sufficient magnitude to enable identification of the bed-sequence to be made from velocity or porosity data alone. This is similar to the conclusion obtained from studies of directional velocity described in Section 5.2.2a.

(b) Lulworth Cove

Only two beds, bed V and bed A10, were considered and a study of the mean velocities (Table 5.14b) shows that they are statistically-independent. However, as in the case of velocities in the horizontal plane (Section 5.2.2b), overlapping ranges prevent any correlation between velocity and lithostratigraphy. No differentiation is possible on the basis of mean porosity since the means of both beds are from the same population (Table 5.14b). Correlation between individual

Fig. 5.1 Elastic-wave velocities and porosities in some beds of the Portland Group, Swanworth Quarry



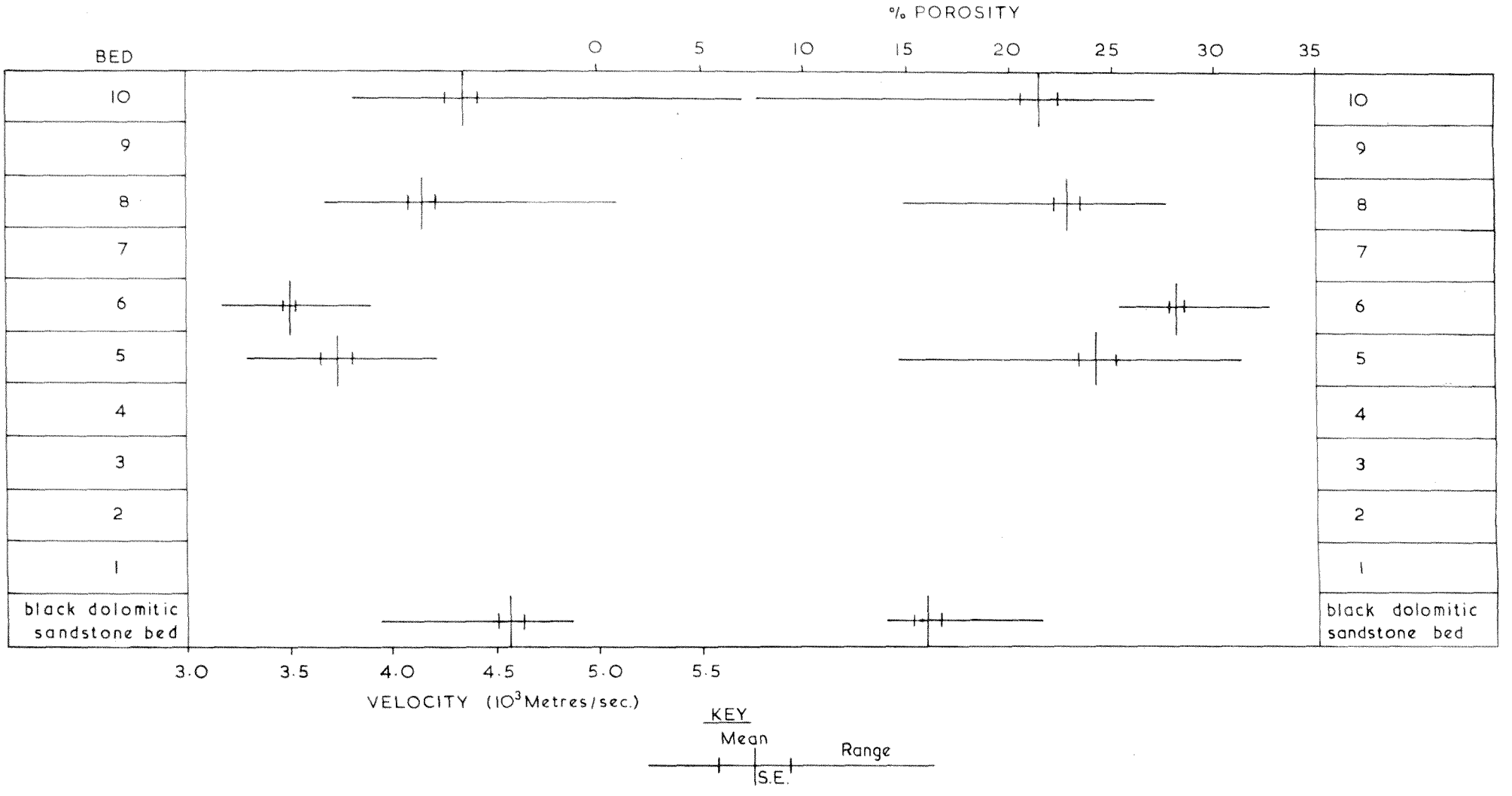
porosities and lithostratigraphy is also marred by overlapping ranges but clearly velocity increases with decreasing porosity.

Comparisons of the velocities at Lulworth with those of the lithostratigraphically-equivalent beds (see Table 5.3) at Swanworth Quarry, show similar results to those for velocities measured in the vertical direction and in the horizontal plane (Section 5.2.2b). Velocities at Lulworth are generally higher. This is probably a result of the usual inverse velocity/porosity relationship as indicated by the lower mean porosities at Lulworth compared with those at Swanworth Quarry (Table 5.14). This decrease in porosity at Lulworth may be related to differences in the intensity of folding. As explained in Section 3.2.2, dips at Lulworth vary between 22° and 48°, whilst minimal dips of $0^{\circ} - 5^{\circ}$ are encountered at Swanworth Quarry. However, Stereoscan studies (Sections 4.6.3; 6.3.3c; Plate 6.15) show no indication of increased tectonism. The decrease in porosity is apparently due to an increase in cement in the case of bed V, and to a denser interlocking of dolomite crystals, possibly caused by compaction, in the case of bed A10 (Plates 6.4; 6.5). Similar decreases in porosity in bed A10 are also noted when compared with the low-dipping, lithostratigraphically-equivalent black dolomitic sandstone bed at two other localities in Dorset, Corton Farm road-cutting (Section 3.3.5.; Table 5.14c) and West Weare Cliffs, Portland (Section 3.3.7a; Table 5.14d).

(c) Central Dorset

The results are presented in Table 5.14c and illustrated in Fig. 5.2. Both the mean velocities and mean porosities of the beds sampled can be grouped into several populations, but, as in the case of East Purbeck (Section 5.4.2a) there is no identity of populations between the sets of velocity/porosity means. There is a tendency for

Fig. 5.2 Elastic-wave velocities and porosities in some beds of the Portland Group, Central Dorset



mean velocity to increase with decreasing mean porosity (Fig. 5.2), with the possible exception of the black dolomitic sandstone bed, which shows a lower mean velocity than expected from the corresponding mean porosity. This slight departure from the normal inverse velocity/porosity relationship may be attributed to the influence of mineral content and fabric.

(d) Isle of Portland

The results are presented in Table 5.14d and illustrated in Fig. 5.3. The mean velocity and mean porosity of each bed are statistically-independent, and there is a complete identity of populations between the sets of velocity/porosity means (Table 5, 14d). Again, with the exception of the "Basal Shell Bed" (Arkell, 1933), individual beds cannot be identified uniquely from velocity or porosity because of overlapping ranges (Fig. 5.3). The "Basal Shell Bed" (Arkell, 1933) has a distinct velocity-range but no corresponding distinct porosity-range and it is not possible to say that this velocity-range is unique in view of the lack of data from several beds in the local sequence.

The usual inverse velocity/porosity relationship is noted with the exception of the black dolomitic sandstone bed, which shows very similar results to those for Central Dorset (Section 5.4.2c; Figs. 5.2.; 5.3).

(e) Vale of Wardour

The results are shown in Table 5.14e and illustrated in Fig. 5.4. Both the mean velocities and mean porosities fall statistically within four populations, and with the exception of population W1 (Table 5.14) there is no identity of populations between the sets of velocity/porosity means. It is apparent (Fig. 5.4) that individual beds cannot be correlated with either velocity or porosity, because of

Fig. 5.3 Elastic-wave velocities and porosities in some beds of the Portland Group, Isle of Portland

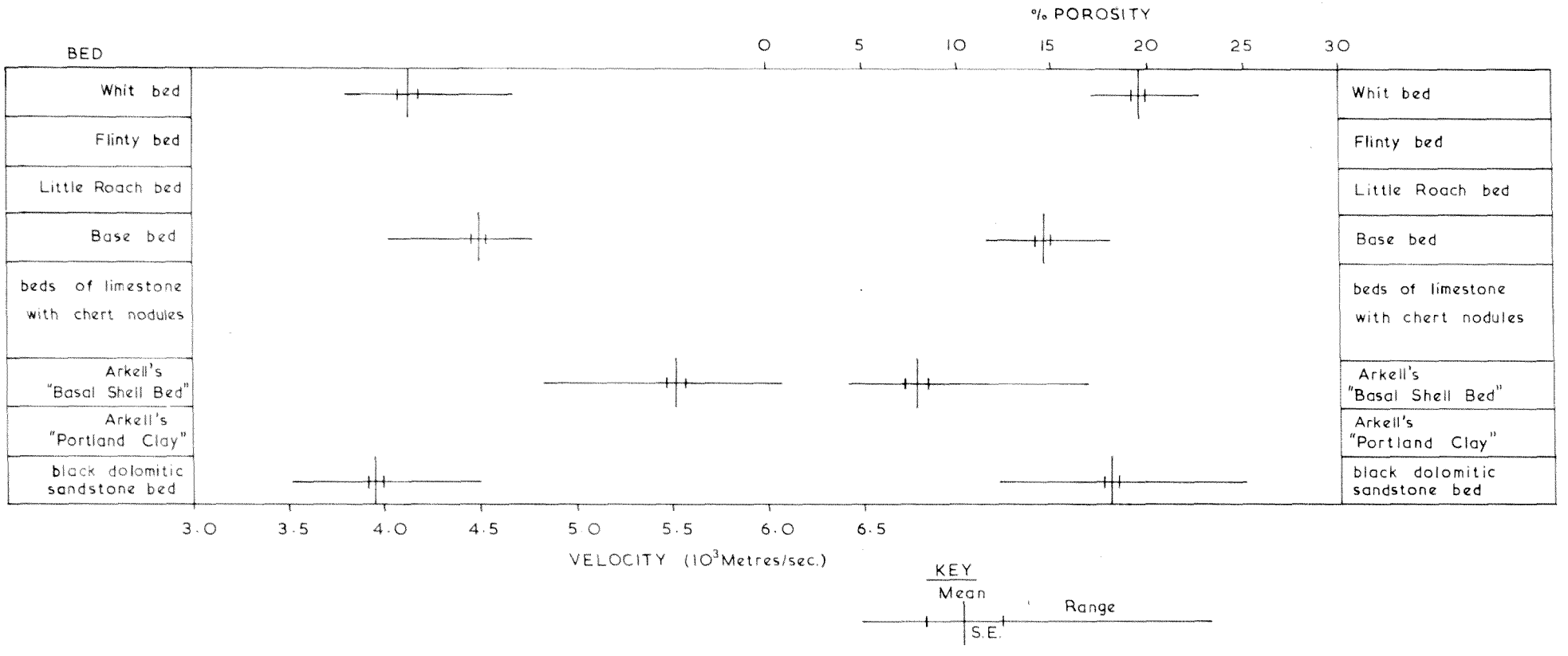
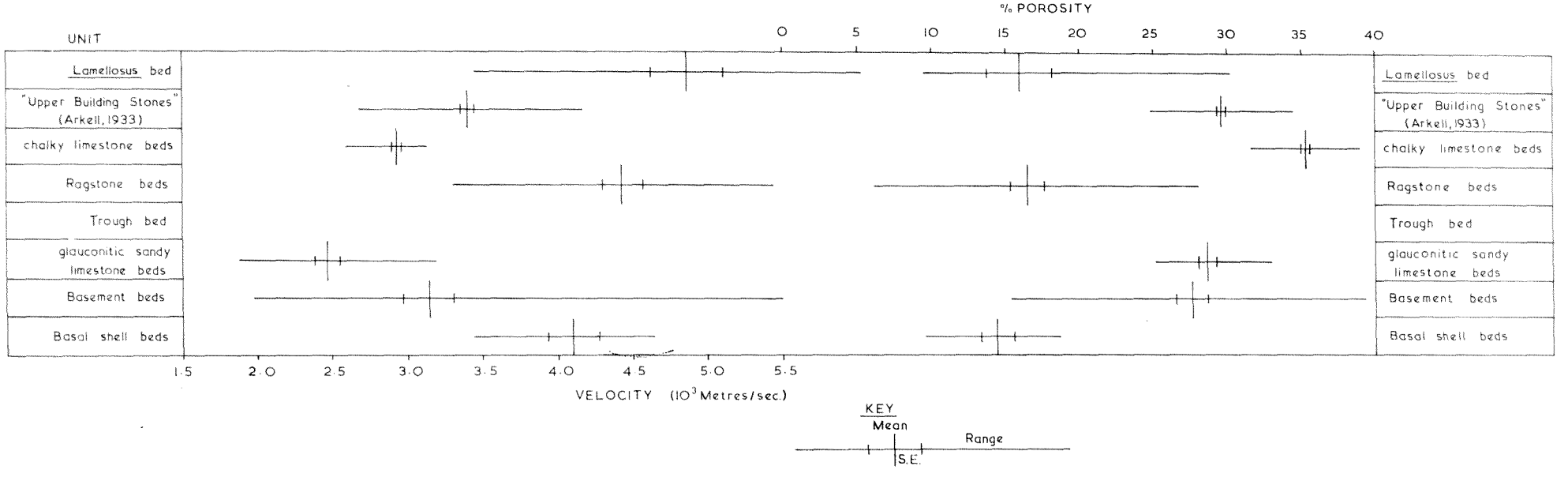


Fig. 5.4 Elastic-wave velocities and porosities in some lithostratigraphic units of the Portland Group, Vale of Wardour.



overlapping ranges.

The inverse relationship between mean velocity and mean porosity, previously recognised, is present (Fig. 5.4). However, the lowest three units, i.e. Basal shell beds, Basement beds and glauconitic sandy limestone beds, in contrast to the remaining units, have lower mean velocities than expected from the corresponding mean porosities. Also, the Lamellosus bed has a slightly higher mean velocity than expected. The Basal shell beds and Basement beds probably show the effects of fabric on velocity as shown by the anisotropic nature of these beds (Section 5.3.2e). The presence of quartz in the Basement beds and glauconite sandy limestone beds could be expected to cause a decrease in velocity. A tendency for the Lamellosus bed to be associated with a higher mean velocity, could be related to its predominantly micritic character (Section 4.6.1; Appendix 6). This result shows similarities to that of bed V, East Purbeck (Section 5.4.2a).

(f) Regional Correlations

On a regional basis, the results (Table 5.14f) show that the velocity/porosity means of the three units are statistically from two populations, and that there is a complete identity of populations between these velocity/porosity means. The Portland oolitic limestone member has a higher mean velocity than the other two units. This is similar to the results obtained when the variation of velocity with direction was considered (Section 5.2.2f). It is also apparent that this higher mean velocity is related to a lower mean porosity (Table 5.14f).

No correlation between the units and either individual velocities or porosities is possible, owing to overlapping ranges between units.

5.5. Discussion and Conclusions

It is apparent that lithostratigraphy cannot be correlated with elastic-wave velocity in the Portland Group. This applies to both velocities in a specific direction and those independent of direction. Although 10% of the lithostratigraphic units studied can be identified from velocity in a vertical direction, 3% from velocity in a horizontal plane and 3% from velocity in three orthogonal directions combined, lack of data for several units in the local sequences studied, renders this identification imprecise. These results tend to agree with the work of Hall (1970), but direct comparisons cannot be made, since he used field-seismic prospecting methods for velocity-determinations, and the units studied consisted of chronostratigraphic units, e.g. the Permian System. However, a limited study of outcrop velocities using a hammer-seismic technique (Appendix 1) provides further information that lithostratigraphy cannot be correlated with velocity, because of overlapping velocity-ranges caused by fracturing (Section A1.4). The results of analyses made by Leet (1938) which showed that lithology could not be correlated with velocity, and by Faust (1953), which showed correlations between velocity and lithology with the exception of limestones, tend to be confirmed by the results of the present study. However, previous research also indicates that correlations can be made between velocity and gross lithology (limestone, shale, sandstone, etc.), but these tend to be related to local geological and stratigraphical factors (Ewing & Cary, 1935).

Several workers (Beers, 1940; Oliphant, 1950; Krumbein, 1951) were able to recognise velocity-stratigraphic units, which either included several lithostratigraphic units of differing lithology but similar velocity (Beers, 1940) or subdivided existing lithostratigraphic units, which consisted of limestones (Oliphant, 1950), into

microlayers approximately 0.3 metres thick, of similar velocity and density. An analysis of the velocity-ranges in samples from individual lithostratigraphic units of the Portland Group (Appendix 5), shows that 35% of these units can be subdivided into microlayers approximately 0.3 metres thick with similar velocities in the horizontal plane, 40% with similar velocities in the vertical direction and 25% with similar velocities irrespective of direction. This subdivision is subject to error, as shown by samples taken from the same microlayer (Appendices 3; 5) having different velocity-ranges in the horizontal plane in 7% of the relevant microlayers and different velocity-ranges in the vertical direction in 43% of the relevant microlayers.

The inclusion of mean porosities of units into the study does not substantially influence the absence of correlation between velocity and lithostratigraphy due to an inverse relationship between velocity and porosity, described in detail in Section 6.3. Porosity is considered to be the most important factor causing variation in mean velocity between lithostratigraphic units. In certain cases, the effects on planar fabric elements (Section 4.5.3) and mineral content (Section 6.2) also contribute to this variation. These effects are further discussed in Chapters 6 and 7.

The wide ranges of velocities both in a horizontal plane and in a vertical direction within lithostratigraphic units of the Portland Group, has meant that velocity anisotropy as defined in this study by the coefficient of aeolotropy, cannot be correlated with lithostratigraphy. This would appear to contradict the results of Dunoyer et. al. (1959) which showed velocity anisotropy to be a function of lithology. However, their results were obtained for gross lithologies - sandstones, limestones, halite and anhydrite -

and a differentiation of the limestones was not made. The wide range of coefficients of aeolotropy noted in the present study, was also found by Koefoed et. al. (1963) for a variety of limestones.

Velocity anisotropy within the Portland Group, as evidenced by this study, is restricted to 35% of the lithostratigraphic units. Of these units, the bulk (25% of all units) show anisotropy of the transverse isotropic type, in that velocities in the horizontal plane exceed those in the vertical direction. It is likely that planar fabric elements are the major cause of this. This confirms the results of previous workers (Weatherby et. al. 1934; White & Sengbush, 1953; Uhrig & van Melle, 1955; Dunoyer et. al., 1959), excepting that their data was acquired using field-seismic prospecting methods. Their results show that bedded strata, including limestones, nearly always exhibit velocity anistropy. In the present study 10% of the units are anisotropic, with velocities in the vertical direction exceeding those in the horizontal plane. These velocity differences are related to corresponding porosity differences, probably as a result of fortuitous sampling. The remainder of the Portland Group units (65%) show no statistical difference in mean velocities in the horizontal plane and vertical direction. This confirms the results of Koefoed et. al. (1963), that the majority of limestones are isotropic.

In conclusion, all units studied cannot be uniquely correlated with either velocity or porosity. This is a result of velocity-and porosity-variations within units exceeding those between units.

CHAPTER 6

VARIATION OF ELASTIC-WAVE VELOCITY WITH POROSITY

6.1 Introduction

Analysis of elastic-wave velocity-variation with lithostratigraphy described in the previous chapter, indicates the importance of porosity as a dominant velocity-controlling parameter. Details of this velocity/porosity relationship are explained here on the basis of measurements made on 898 core-specimens. Emphasis is placed on both velocity-variation with percentage porosity and possible effects of pore-structure.

It is well known that a highly significant inverse correlation usually exists between porosity and density. The present investigation supports this (Section 6.2). Previous workers have concentrated on velocity-variation with either porosity or density. This study concentrates on porosity.

Statistical analysis was completed on the data from core-specimens assigned to the four physically-distinct limestone-types described previously (Section 4.6.1), i.e. sparites, micrites, chalks and microsparites. Core-specimen orientation was omitted from the study since the results of Chapter 5 (Section 5.5) indicate that of the lithostratigraphic units studied, only 35% show velocity anisotropy.

6.2 Porosity/Density Relationships

The study of porosity/density relationships in the four limestone-types was made using simple correlation coefficients and simple linear-regression analysis. Table 6.1 gives the results of this analysis; porosity/density plots are given in Figs. 6.1 - 6.4. It is apparent that porosity and density are highly correlated ($r_{\phi\rho}$ values significant at $p < 0.001$). According to Hoel (1947) the values of r^2 indicate that, in the limestone-types studied, but excluding microsparites, at least 93% of

TABLE 6.1

Results of Simple Linear Regression Analysis between Porosity and Density for four Limestone-Types from the Portland Group

LIMESTONE TYPE	SPARITES	MICRITES	CHALKS	MICRO SPARITES	ALL
No. of specimens	460	128	162	148	898
POROSITY (%) ϕ mean	14.8 ± 0.4	9.3 ± 0.4	26.7 ± 0.5	17.4 ± 0.5	16.6 ± 0.3
range	1.7 - 32.2	1.9 - 30.2	7.8 - 38.9	5.5 - 29.4	1.7 - 39.2
DENSITY (gm/c.c.) p mean	2.24 ± 0.01	2.40 ± 0.01	1.95 ± 0.01	2.16 ± 0.02	2.20 ± 0.01
range	1.60 - 2.58	1.87 - 2.58	1.62 - 2.47	1.76 - 2.43	1.60 - 2.58
corr. coefft. $r_{\phi p}$	- 0.9872	- 0.9898	-0.9979	-0.8726	-0.9791
regression equation	$\phi = -37p + 98$ ±1.5%	$\phi = -40p+105$ ±0.6%	$\phi = -37p+99$ ±0.4%	$\phi = -28p+77$ ±3.1%	$\phi = -37p+98$ ±1.9%

Fig. 6.1 Variation of density with porosity
—— Sparites (n = 460)

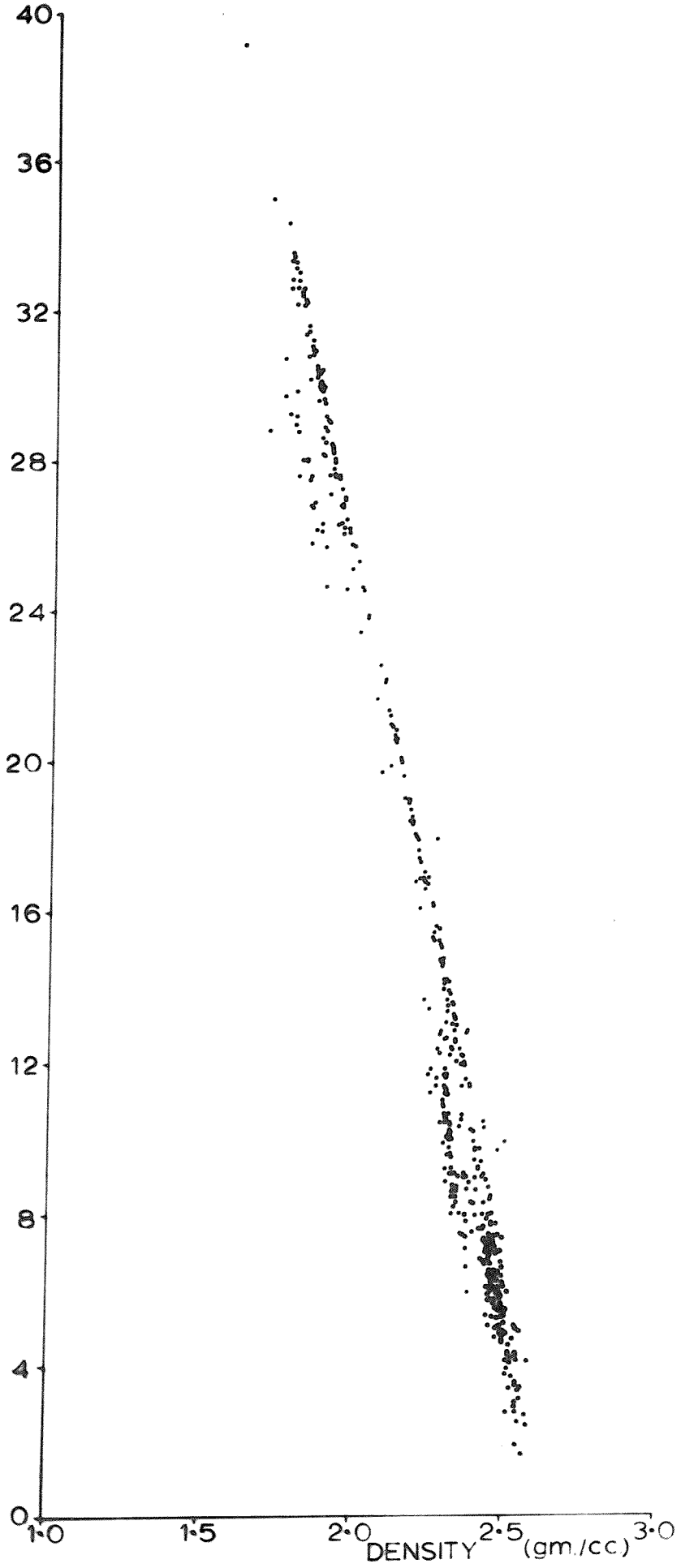


Fig. 6.2 Variation of density with porosity
—— Chalks (n = 162)

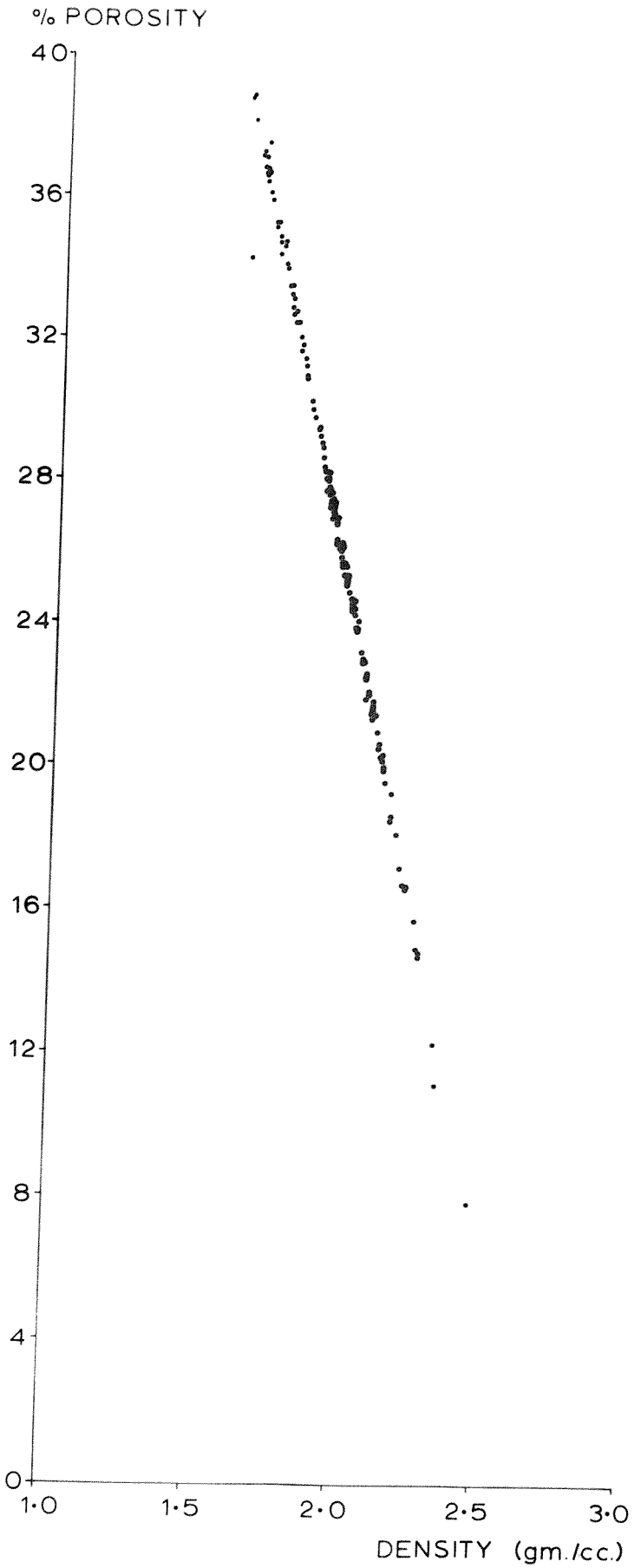


Fig. 6.3 Variation of density with porosity
—— Micrites (n = 128)

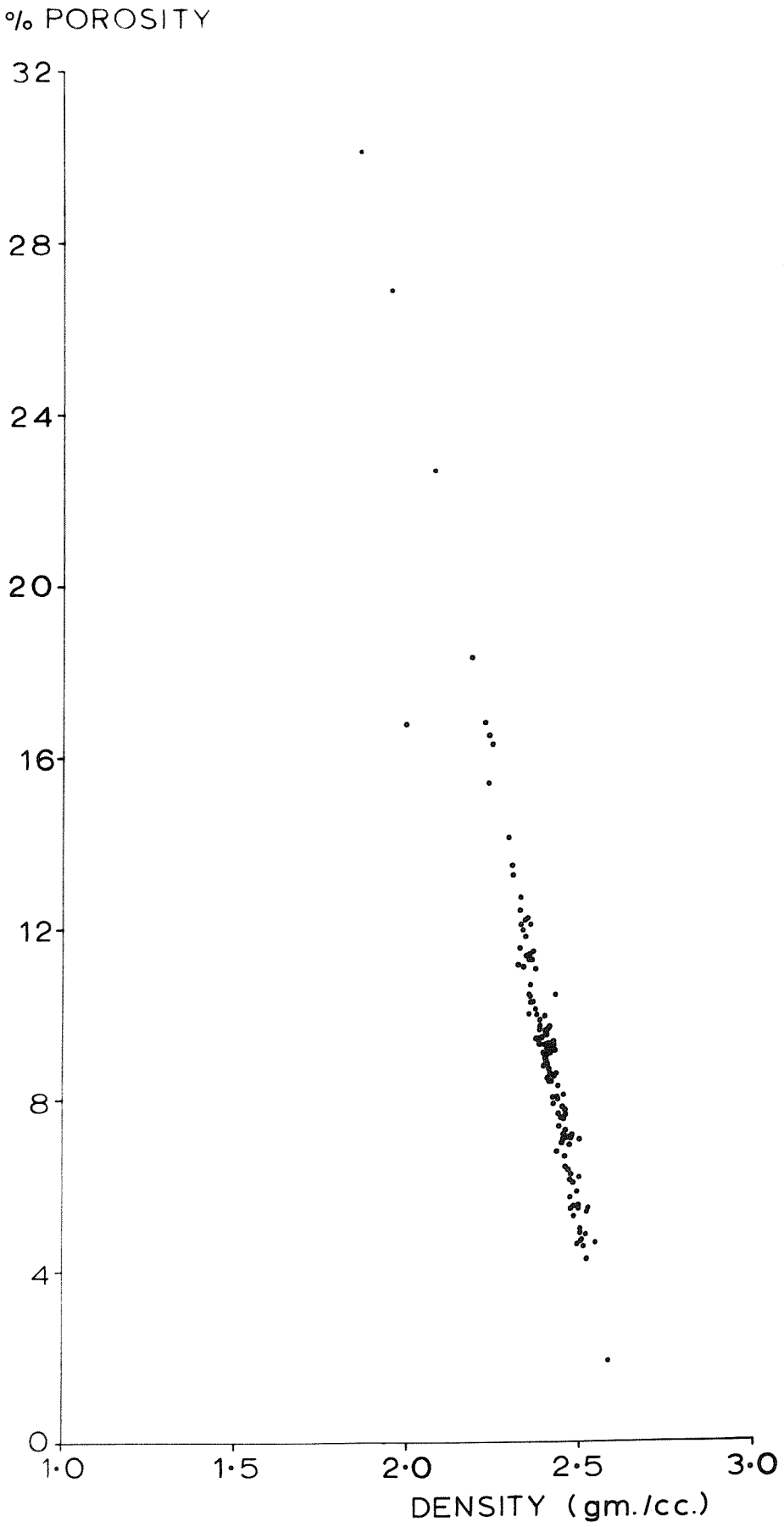


Fig. 6.4 Variation of density with porosity
—— Microsparites (n = 148)

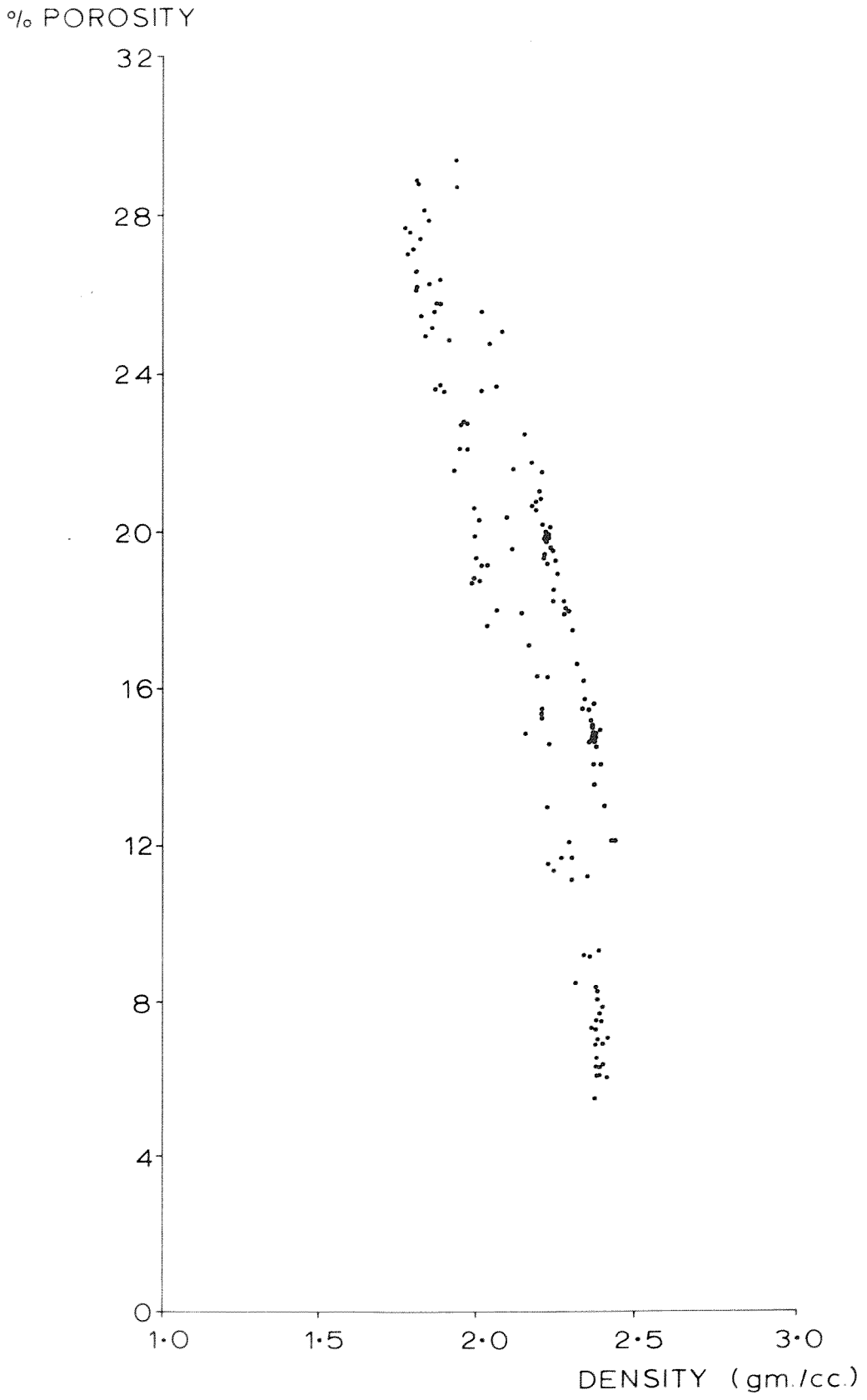
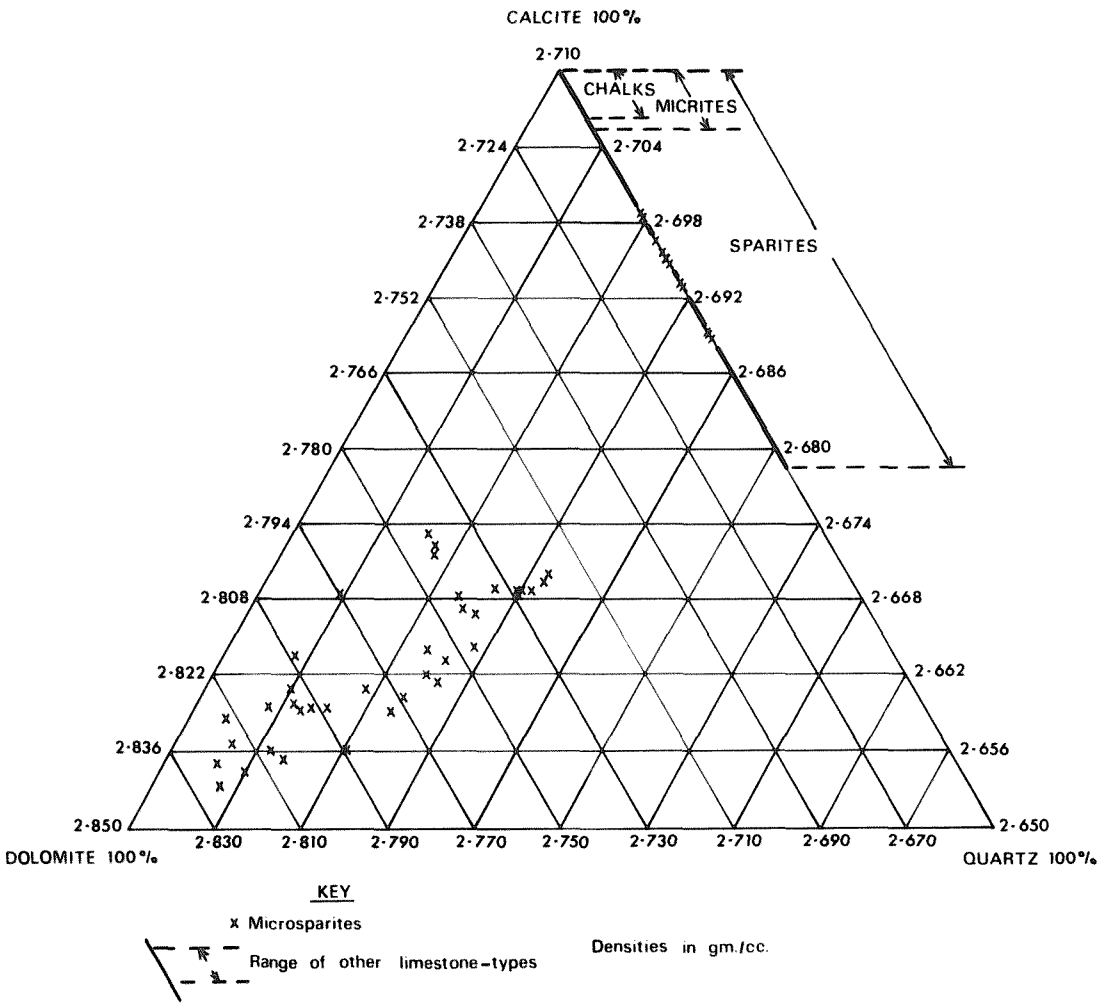


Fig. 6.5 Plot of calcite, dolomite and quartz contents showing variation in absolute density of the Portland Group limestone-types



the variation in porosity is accounted for by linear regression between porosity and density. Differences between the regression equations for these limestone-types are small, but significant ($p < 0.05$), as shown by F-tests (Griffiths, 1967). This high degree of dependence of porosity on density is shown by extrapolating the regression curves to zero density, where the porosity should be 100%. Values obtained always exceeded 95%.

Microsparites differ from the other limestone-types in that only 76% of the variation in porosity is accounted for by linear regression between porosity and density. There is a lower gradient in the regression equation and at zero density, the predicted porosity is only 77%, again indicating a low degree of dependence of porosity on density. The remaining 24% variation in porosity is probably attributable to experimental error and the influence of other factors. Variation in mineral content may be a dominant factor reducing the correlation between porosity and density in this instance. A triangular plot (Fig. 6.5) of calcite, quartz and dolomite contents (recalculated to 100%) for some 245 core-specimens shows that microsparites have the widest absolute density range, caused by the occurrence of dolomite only in this particular group.

This density range (2.689 to 2.826 gm./c.c.) contrasts with the other limestone-types, where the range is 2.678 to 2.710 gm./c.c. These rocks are simple mixtures of quartz and calcite. In microsparites, the bulk density of a core-specimen of given porosity could thus vary substantially with changing mineral content, resulting in the lower degree of dependence of porosity on density described above. These conclusions agree with the results of Sarmiento(1961), which showed mineralogical composition in some Palaeozoic dolomites to be important in affecting travel-time/porosity relationships.

6.3 Velocity/Porosity Relationships

6.3.1 Methods of Statistical Analysis

Velocity/porosity relationships have been studied by computation

TABLE 6.2

Results of Studies of Velocity/Porosity Relationships using Different Methods of Analysis on four Limestone-Types from the Portland Group

SPARITES

n = 460

Mean Velocity ($\bar{V}$) = 4483 $\pm$ 45 m/sec

Mean Porosity ($\bar{\phi}$) = 14.8 $\pm$ 0.4%

Simple linear regression

$$V = -90\phi + 5816 \pm 439$$

$r = -0.8899$

Polynomial function

in form $V = A_0 + A_1\phi + A_2\phi^2 + A_3\phi^3 + A_4\phi^4$ where A_0 etc. are constants.

$$V = 5973 - 116\phi + 0.71\phi^2 \pm 437$$

$r = -0.8910$

Exponential function

in form $V = e^{K\phi}$ or $\log_{10}V = K\phi \log_{10}e$ where K is a constant

$$\log_{10}V = 3.7832 - 0.022\ \phi \log_{10}e \pm 0.0490$$

$r = -0.8827$

Logarithmic function (log -linear)

in form $V = C + K \log_{10} \phi$ where C and K are constants

$$V = 7519 - 2826 \log_{10} \phi \pm 480$$

$r = -0.8665$

Logarithmic function (log - log)

in form $\log_{10}V = C + K \log_{10} \phi$ where C and K are constants

$$\log_{10}V = 3.9590 - 0.296 \log_{10} \phi \pm 0.0567$$

$r = -0.8393$

Reciprocal-Velocity function

$$\frac{1}{V} = 10^{-6} (150 + 6\ \phi \pm 34)$$

$r = +0.8474$

TABLE 6.2 cont.

CHALKS

n = 162

Mean Velocity $(\bar{V})$ = 3727 $\pm$ 47 m/sec

Mean Porosity $(\bar{\phi})$ = 26.7 $\pm$ 0.5%

Simple linear regression

$$V = -92\phi + 6173 \pm 239$$

$r = -0.9189$

Polynomial function

in form $V = A_0 + A_1\phi + A_2\phi^2 + A_3\phi^3 + A_4\phi^4$ where A_0 etc. are constants.

$$V = 6467 - 107\phi + 0.0002\phi^4 \pm 237$$

$r = -0.9210$

Exponential function

in form $V = e^{K\phi}$ or $\log_{10}V = K\phi \log_{10}e$ where K is a constant.

$$\log_{10}V = 3.8490 - 0.024\ \phi \log_{10}e \pm 0.0274$$

$r = -0.9203$

Logarithmic function (log - linear)

in form $V = C + K \log_{10} \phi$ where C and K are constants.

$$V = 10794 - 4997 \log_{10} \phi \pm 255$$

$r = -0.9072$

Logarithmic function (log - log)

in form $\log_{10}V = C + K \log_{10} \phi$ where C and K are constants.

$$\log_{10}V = 4.3700 - 0.568 \log_{10} \phi \pm 0.0317$$

$r = -0.8919$

Reciprocal-Velocity function

$$\frac{1}{V} = 10^{-6} (97 + 6.7\ \phi \pm 18)$$

$r = +0.9119$

TABLE 6.2 cont.

MICRITES

n = 128

Mean Velocity ($\bar{V}$) = 5300 $\pm$ 36 m/sec

Mean Porosity ($\bar{\phi}$) = 9.3 $\pm$ 0.4 %

Simple linear regression

$V = -68\,\phi + 5959 \pm 312$

$r = -0.6563$

Polynomial function

in form $V = A_0 + A_1\phi + A_2\phi^2 + A_3\phi^3 + A_4\phi^4$ where A_0 etc. are constants.

$V = 5540 - 2.37\,\phi^2 \pm 311$

$r = -0.6600$

Exponential function

in form $V = e^{K\phi}$ or $\log_{10}V = K\phi \log_{10}e$ where K is a constant

$\log_{10}V = 3.7800 - 0.014\,\phi \log_{10}e \pm 0.0266$

$r = -0.6809$

Logarithmic function (log - linear)

in form $V = C + K \log_{10}\phi$ where C and K are constants

$V = 6629 - 1423 \log_{10}\phi \pm 338$

$r = -0.5764$

Logarithmic function (log - log)

in form $\log_{10}V = C + K\log_{10}\phi$ where C and K are constants.

$\log_{10}V = 3.8410 - 0.1265 \log_{10}\phi \pm 0.0295$

$r = -0.5840$

Reciprocal-Velocity function

$\frac{1}{V} = 10^{-6}\,(160 + 3\,\phi \pm 12)$

$r = +0.7026$

TABLE 6.2 cont.

MICROSPARITES

n = 148

Mean Velocity ($\bar{V}$) = 3988 $\pm$ 59 m/sec

Mean Porosity ($\bar{\phi}$) = 17.4 $\pm$ 0.5 %

Simple linear regression

$$V = -93\,\phi + 5613 \pm 394$$

$r = -0.8357$

Polynomial function

in form $V = A_0 + A_1\phi + A_2\phi^2 + A_3\phi^3 + A_4\phi^4$ where A_0 etc. are constants.

$$V = 10039 - 1265\,\phi + 105\,\phi^2 - 4\,\phi^3 + 0.05\,\phi^4 \pm 377$$

$r = -0.8540$

Exponential function

in form $V = e^{K\phi}$ or $\log_{10}V = K\phi \log_{10}e$ where K is a constant.

$$\log_{10}V = 3.7690 - 0.023\,\phi \log_{10}e \pm 0.0445$$

$r = -0.8230$

Logarithmic function (log - linear)

in form $V = C + K \log_{10} \phi$ where C and K are constants.

$$V = 7804 - 3166 \log_{10} \phi \pm 384$$

$r = -0.8447$

Logarithmic function (log - log)

in form $\log_{10}V = C + K \log_{10} \phi$ where C and K are constants.

$$\log_{10}V = 3.9972 - 0.3347 \log_{10} \phi \pm 0.0451$$

$r = -0.8179$

Reciprocal-Velocity function

$$\frac{1}{V} = 10^{-6}\,(157 + 6\,\phi \pm 28)$$

$r = +0.8019$

of simple correlation coefficients, and by simple linear regression analysis. Polynomial, exponential, logarithmic and reciprocal-velocity functions were also computed. The results are given in Table 6.2.

All the calculated correlation coefficients are statistically significant at the 5% probability level. Further, the magnitude of individual correlation coefficients for each separate function is not appreciably different from that calculated for simple linear regression. Any of the chosen functions provide a useful empirical relationship between the two variables. The simple linear relationship has the advantage of direct use of the basic data. All other methods involve transformations of the basic data. This is in accordance with previous studies on limestones, which show that velocity/porosity relationships can be best represented by a simple linear function (Berry, 1959; Koefoed et. al., 1963). Wyllie et. al. (1956) and Sarmiento (1961) found simple linear relationships between reciprocal-velocity and porosity, but this was a direct result of the form of the basic data, velocity-log travel-times and percentage porosity.

6.3.2 Simple Linear Regression Analysis between Velocity and Percentage Porosity

Assessment of the form of simple linear relationships between velocity and porosity is made, with particular reference to differences between limestone-types. The results of the analysis are summarised in Table 6.3, and illustrated in Figs. 6.6 - 6.10.

Frequency distributions of the velocity/porosity data used in the analysis are given in Fig. 6.11. These show that both velocity and porosity are unimodally distributed, except for sparites. Sparites show a bimodal porosity distribution, possibly caused by inadequate sampling. It is also apparent that each limestone-type is characterised by a wide spectrum of velocities and porosities. The overall bimodal distribution of porosity in the Portland Group is a combination of the sparite-bimodality, the unimodal low porosities of micrites and the unimodal

TABLE 6.3

Results of Simple Linear Regression Analysis between Velocity and Porosity for four Limestone-Types from the Portland Group

Limestone-Type		SPARITES	MICRITES	CHALKS	MICRO SPARITES	ALL
No. of specimens		460	128	162	148	898
VELOCITY (m/sec) V	Mean	4483 ± 45	5300 ± 36	3727 ± 47	3988 ± 59	4382 ± 31
	Range	1876 - 6505	3452 - 6079	2598 - 5717	2685 - 5439	1876 - 6505
POROSITY (%) ø	Mean	14.8 ± 0.4	9.3 ± 0.4	26.7 ± 0.5	17.4 ± 0.5	16.6 ± 0.3
	Range	1.7 - 39.2	1.9 - 30.2	7.8 - 38.9	5.5 - 29.4	1.7 - 39.2
Corr. Coeff. $r_{V\phi}$		-0.8899	-0.6563	-0.9189	-0.8357	-0.8859
Regression Equation		V = -90ø+5816 ±439 m/sec.	V = -68ø+5929 ±312 m/sec.	V = -92ø+6173 ±239 m/sec	V = -93ø+5613 ±394 m/sec	V = -88ø+5833 ±434 m/sec
Max.difference between observed & estimated velocity (%)		37.9	17.8	17.1	29.6	39.7

Fig. 6.6 Relationship between velocity and porosity

— Sparites (n = 460)

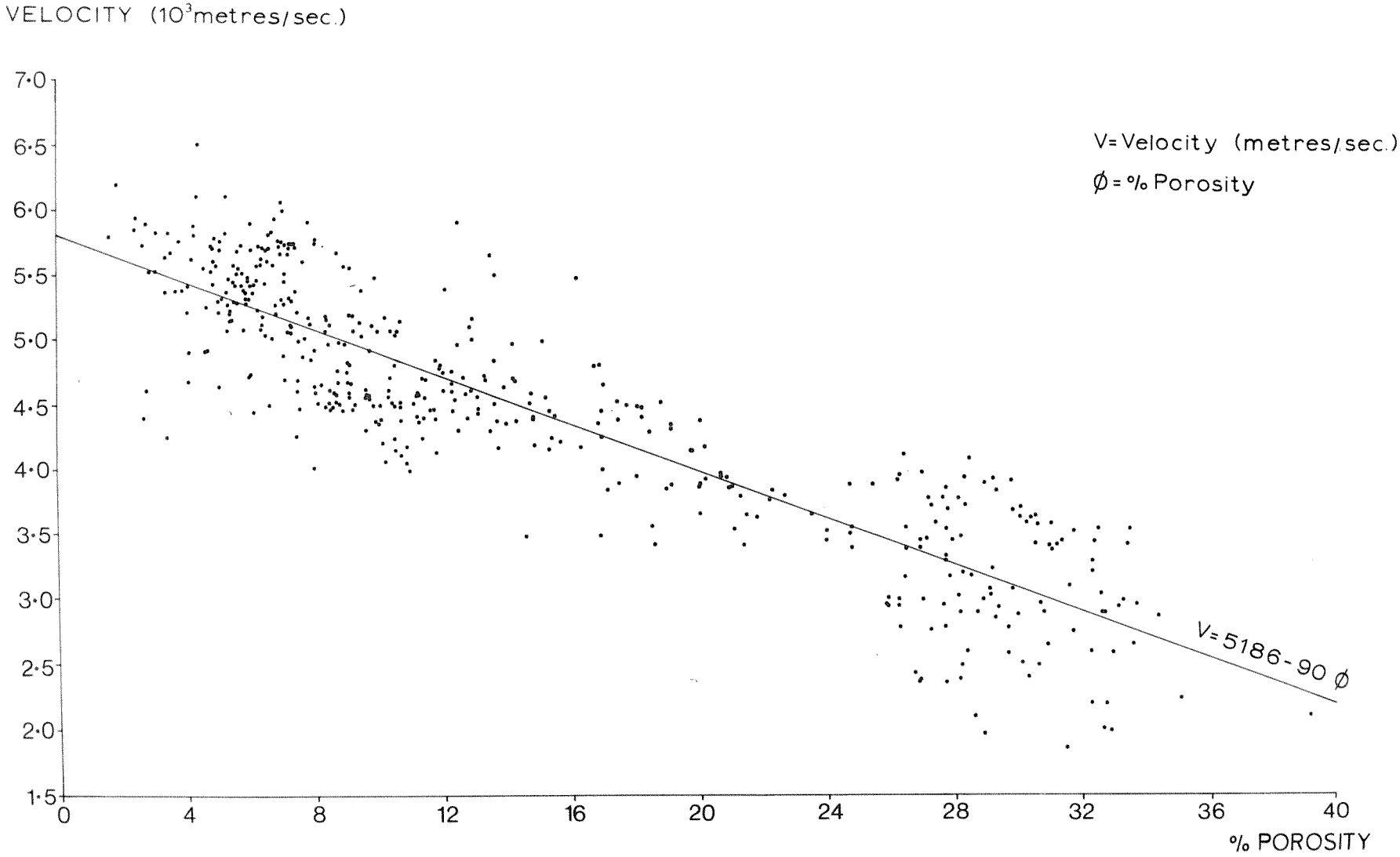


Fig. 6.7 Relationship between velocity and porosity

— Chalks (n = 162)

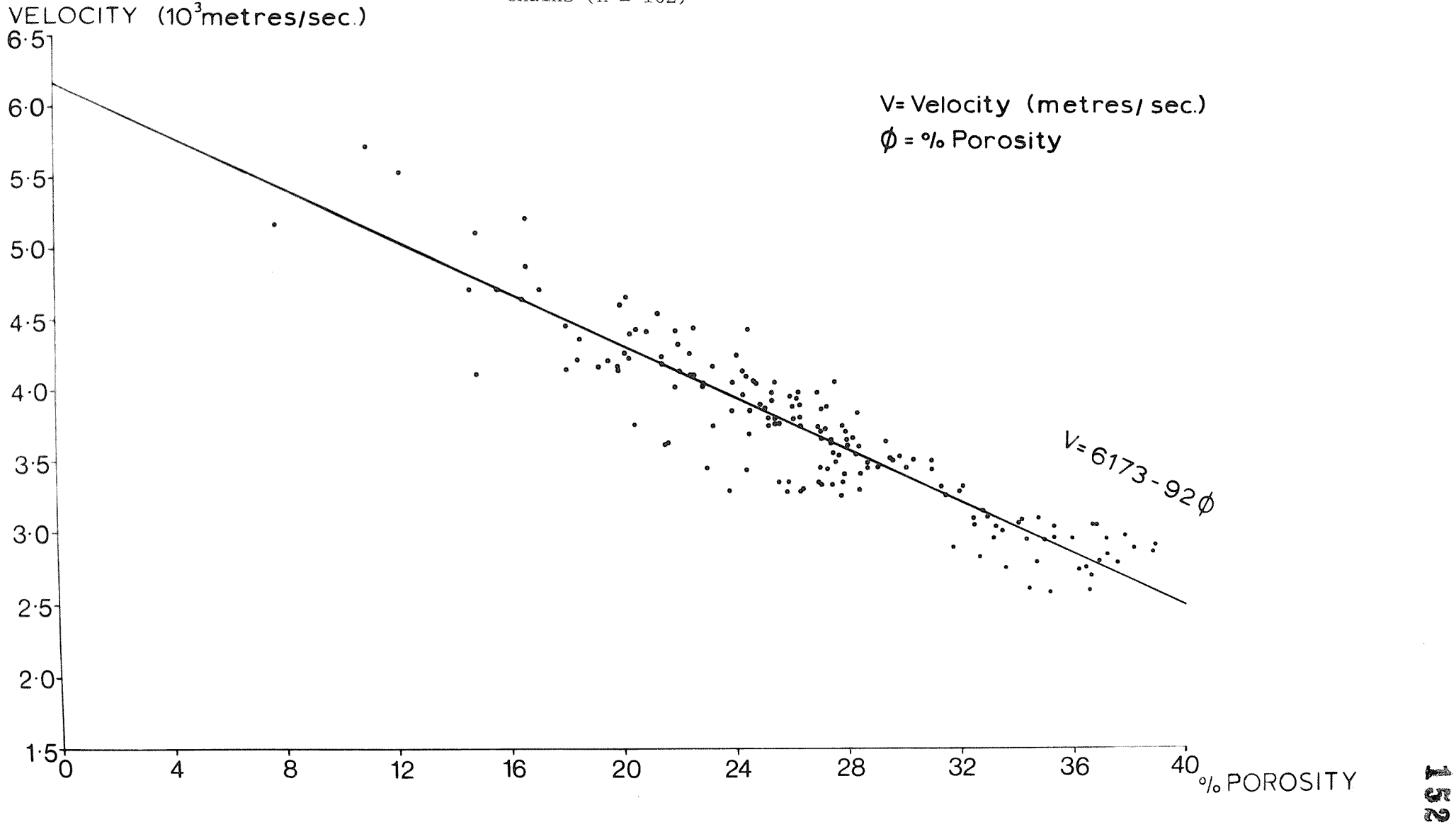


Fig. 6.8 Relationship between velocity and porosity

— Micrites (n = 128)

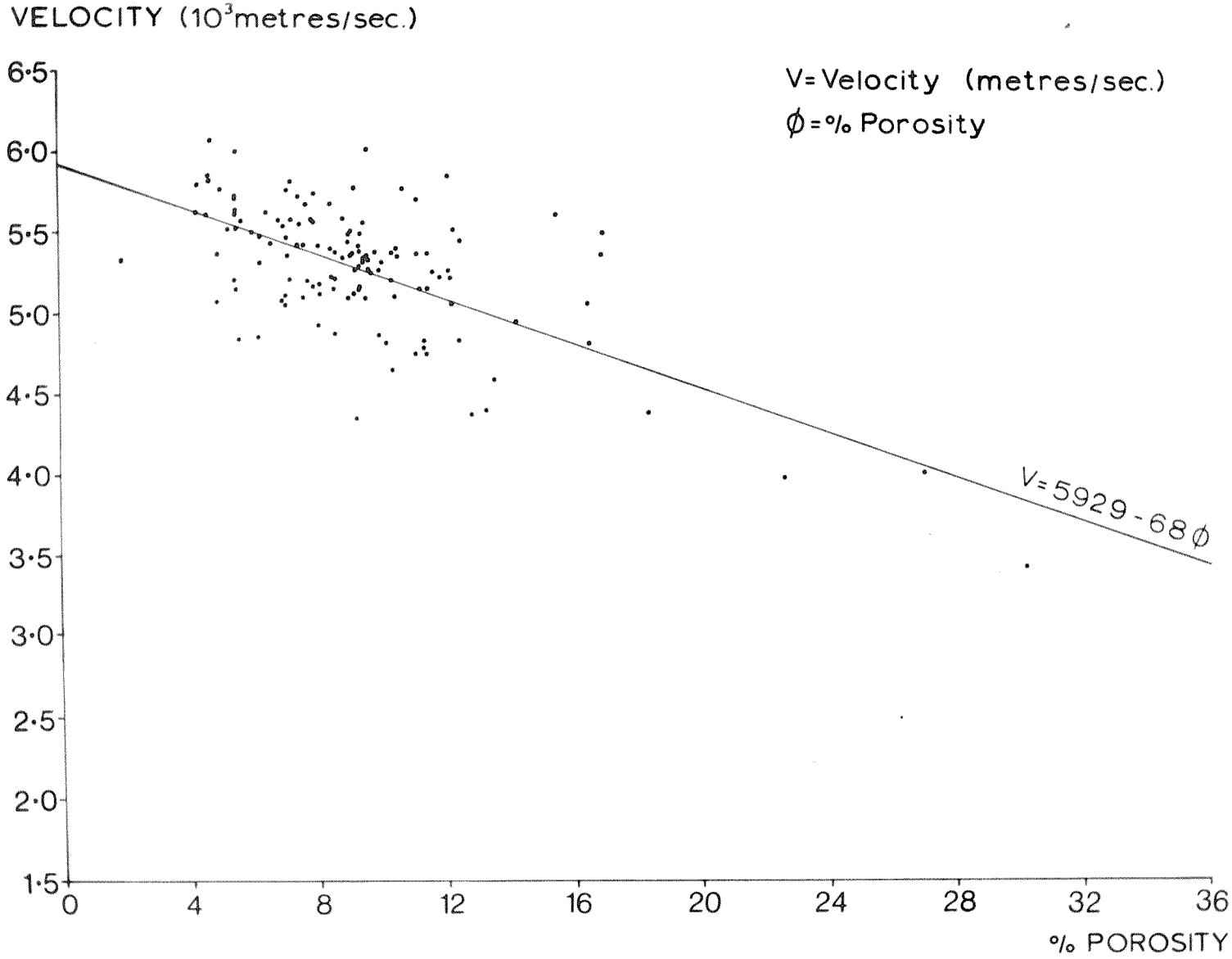


Fig. 6.9 Relationship between velocity and porosity

—— Microsparites (n = 148)

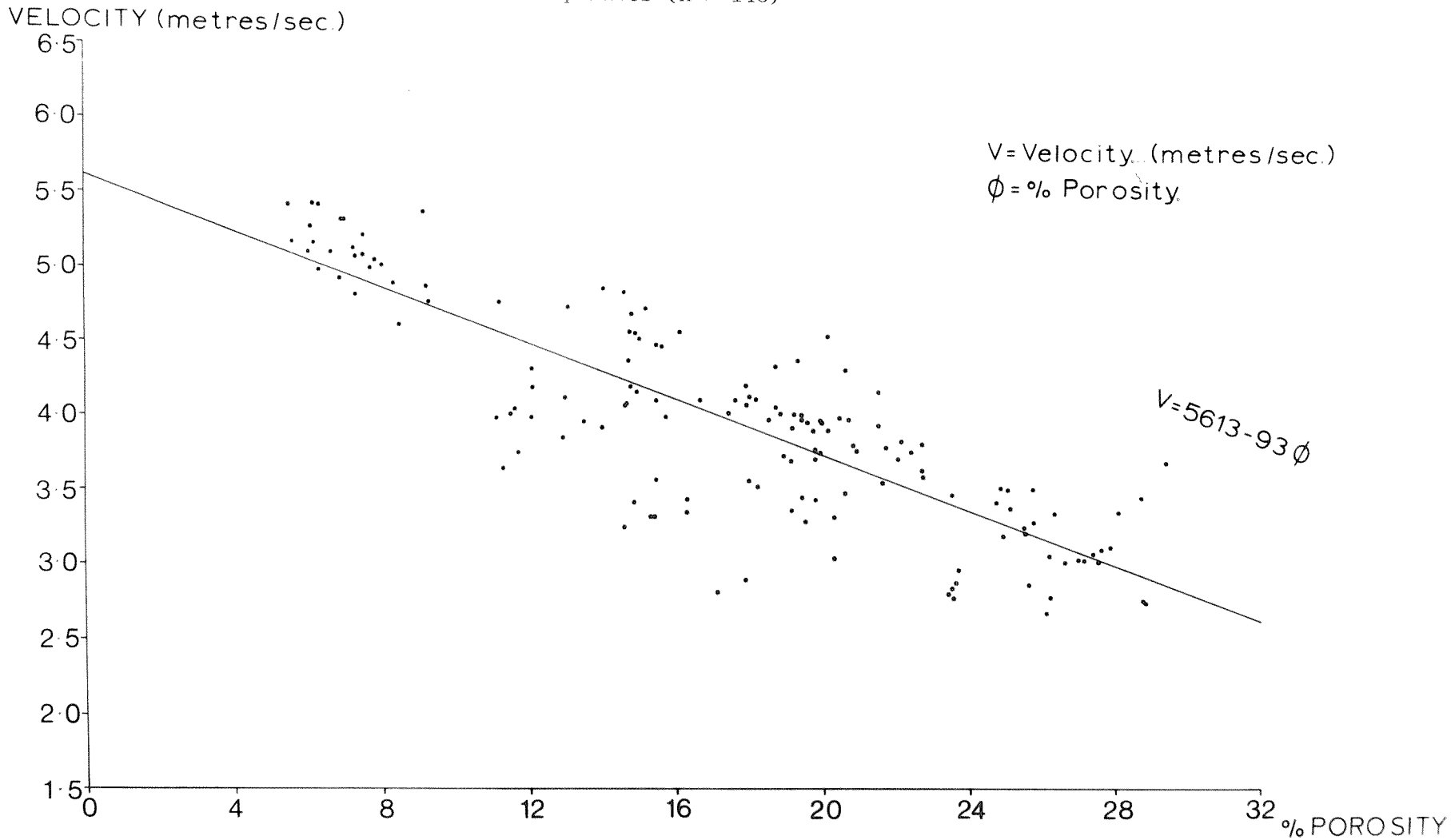


Fig. 6.10 Relationship between velocity and porosity

—— Total data, Portland Group (n = 898)

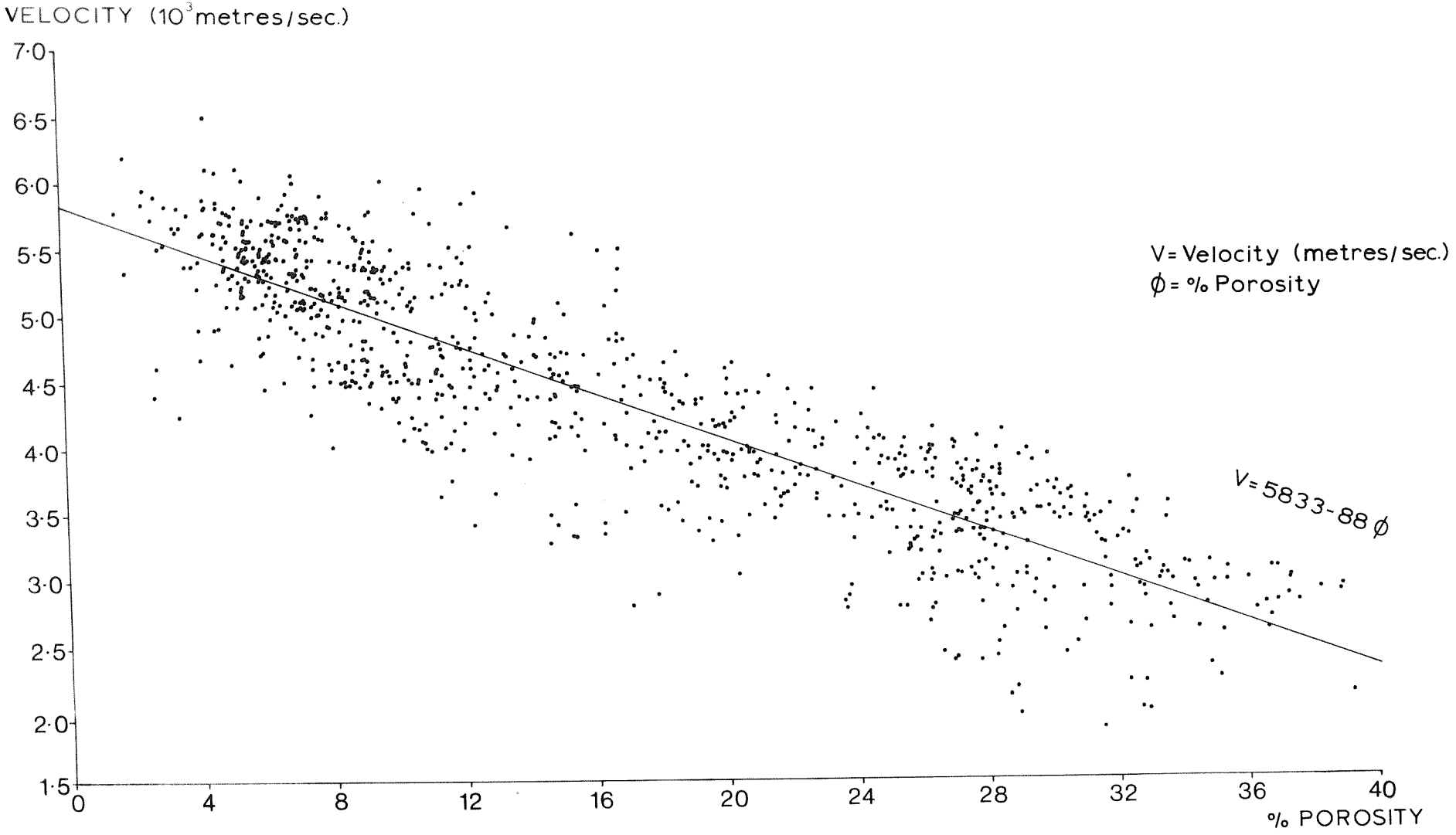
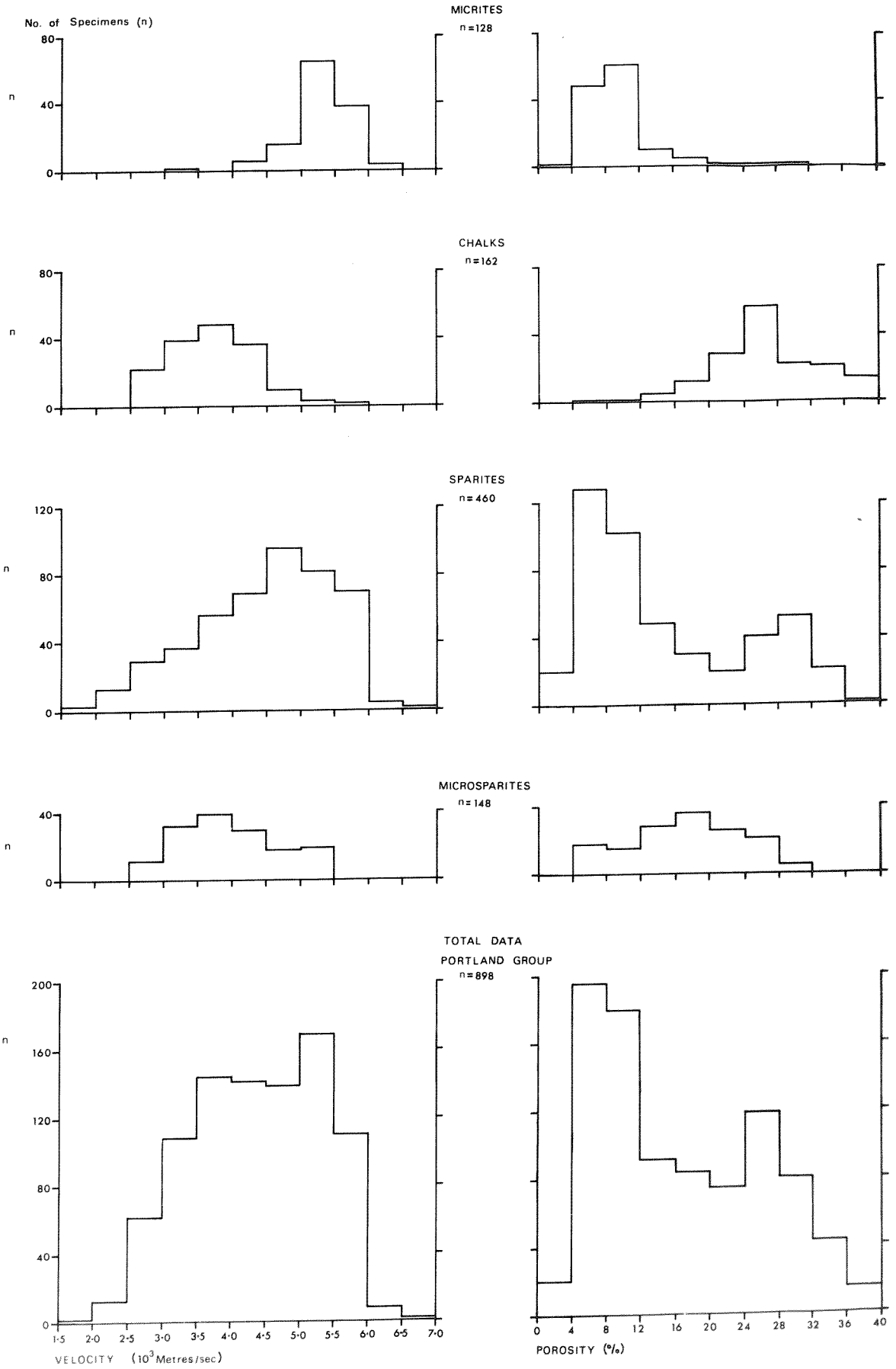


Fig. 6.11 Frequency distributions of velocity and porosity of the Portland Group limestone-types



high porosities of chalks.

The correlation coefficients between velocity and porosity for the four limestone-types (Table 6.3) are highly significant ($p < 0.001$), and each regression equation is statistically-different ($p < 0.01$) on the basis of F-tests (Griffiths, 1967). The limestone-types thus possess distinct empirical velocity/porosity relationships. Linear regression between velocity and porosity accounts for 79% of velocity-variation in sparites, 43% in micrites, 84% in chalks and 70% in microsparites. Errors in velocity and porosity determinations (Sections 4.3.3; 4.4.3) may account for a large proportion of the remaining velocity-variation in sparites and chalks. However, factors other than porosity and experimental error most probably affect velocity in micrites and microsparites. These factors are probably related to pore-structure, i.e. pore-size, pore-morphology and pore-distribution (Section 6.3.3c) and to a lesser degree fabric (Section 7.3.2c) in the case of micrites, and to mineral content (Section 6.2) and other petrographical parameters (Section 7.3.2d) in the case of microsparites. The marked differences both in degree of correlation and regression equation (Table 6.3) for micrites compared with the other limestone-types, indicate that these factors are probably important in controlling velocity.

Direct comparison with previous work is not entirely possible, since in many cases the limestones studied were undifferentiated. Additionally, a large proportion of previous work was derived from well-logs. Several workers have made velocity/porosity plots (Berry, 1959; Koefoed et. al., 1963) without deriving correlation coefficients or regression equations for the limestones studied. However, the plots indicate qualitative agreement with the results of the present study.

Wyllie et. al. (1956) found a linear relationship between velocity and porosity, but direct comparisons cannot be made with the present results, since the velocity of fluid contained in the pores was also included in the regression equation. Sarmiento (1961) derived

empirical relationships between reciprocal velocity ($1/V$) and porosity (ϕ) for some Palaeozoic limestones and dolomites using well-log data at depths exceeding 700 metres. The equation for limestones included a depth-dependent term; when extrapolated to zero depth, the expression has the form:

$$\frac{1}{V} = 10^{-6} (160 + 3.7\,\phi) \text{ secs/metre} \quad .... \quad \text{Eq. 6.1}$$

For dolomites, the equation is:

$$\frac{1}{V} = 10^{-6} (130 + 4.1\,\phi) \text{ secs/metre} \quad .... \quad \text{Eq. 6.2}$$

The porosity gradients, when compared with the corresponding gradients for the Portland Group limestone-types (Table 6.2), are lower in magnitude except in the case of micrites. The correlation coefficient (+0.91) derived by Sarmiento for both limestones and dolomites individually, indicates a high dependence of velocity on porosity, in contrast to micrites where the low porosity gradient is a direct result of the low degree of dependence of velocity on porosity. The lower porosity gradients found by Sarmiento could therefore be the result of differences either in data-source or in geological age. The correlation coefficients for the limestone-types from the Portland Group (Table 6.2) with the exception of chalks, are lower in magnitude than those derived by Sarmiento. However, the correlation coefficient (-0.886) between velocity and porosity for the total data of the Portland Group (Table 6.3) is similar to those for the Palaeozoic limestones and dolomites. This contrasts with the conclusions of Sarmiento (1961, Fig. 4), which suggest <u>no</u> correlation between travel-time and porosity at depths of less than 700 metres, presumable including outcrops.

The equations relating velocity to porosity for the limestone-types of the Portland Group (Table 6.3), when extrapolated to zero porosity, give the following results:

Sparites $V = 5816 \pm 439$ m/sec

Micrites $V = 5929 \pm 312$ m/sec

Chalks $V = 6173 \pm 239$ m/sec

Microsparites $V = 5613 \pm 394$ m/sec

These velocities are less than the limiting velocity (6450 m/sec) for a quasi-isotropic aggregate of randomly-oriented calcite crystals with zero porosity (Peselnick, 1962), the velocities predicted by Voigt (1928) - 6710 m/sec - and Reuss (1929) - 6240 m/sec - from the elastic constants of a single calcite crystal, and the velocity predicted by Wyllie et. al. (1956) - 6800 m/sec - for a random distribution of calcite crystals. This suggests that sparites, micrites and chalks, which are composed predominantly of calcite (Fig. 6.5), do not behave as perfect models in terms of elastic-wave velocity at zero porosity. The low limiting velocity of microsparites is probably a result of variations in mineral-content (Section 6.2). These results are to be expected, since a study of the petrography of core-specimens shows that there is considerable departure from a quasi-isotropic aggregate of randomly-oriented calcite crystals (Plates 4.5 - 4.18, & 4.20). The results contrast with those for the Solenhofen Limestone, Germany (Peselnick, 1962), which is 98.5% calcite, and has a limiting velocity of 6450 m/sec, thus behaving as a quasi-isotropic aggregate of randomly-oriented single calcite crystals with zero porosity.

6.3.3 Analysis of the Effects of Pore-Orientation, Pore-Structure and Pore-Type on Velocity

6.3.3a Introduction

A limited analysis was made on a total of 36 core-specimens representative of the four limestone-types (Section 4.6.1). A study of pore-orientation and its possible effect on velocity-aeolotropy, was made initially. The major part of the study concentrated upon the effect of pore-structure and pore-type (Section 4.6) on velocity, particularly

in the case of micrites, where a low degree of correlation between velocity and porosity exists. The basic data is given in Appendix 7.

6.3.3b Pore-Orientation

Pore-orientation was defined as the orientation of the long axis. A vector-resultant was calculated for each of the 36 cores studied (Section 4.6). Analysis of the vector-resultants using a Rayleigh test (Curray, 1956) showed that, at a 5% probability level, sparites and chalks have a random pore-orientation, whereas 25% of microsparites and 40% of micrites have significantly non-random preferred orientations. These preferred orientations are apparently related to bedding, since in all cases, they are aligned approximately in directions within the XY plane of the core-specimens. For specimens UCLI Z4 (micrite) and PLPS 1Z4 (microsparite) (Appendix 7), these preferred orientations are probably related to the velocity-aeolotropy observed in the Lamellosus bed (Vale of Wardour) and black dolomitic sandstone bed (Isle of Portland) respectively, by increasing the frequency of discontinuities to elastic-wave transmission in the vertical direction (Sections 5.3.2e; 5.3.2d). Similarly, the preferred pore-orientation in specimen WA28-2Z2 (microsparite) is probably related to the resulting coefficient of aeolotropy (Section 5.3.1) of 0.945 for the sample from which this specimen was taken. The preferred orientations in the XY plane noted in specimens WV4X1, WV4Y1 and WV4Z1 (micrites) do not apparently affect the transmission of elastic-wave energy in the sample, since the coefficient of velocity-aeolotropy (1.008) for the sample is not statistically significant. The effect of preferred pore-orientation on elastic-wave velocity within micrites is thus variable. A study of pore-type (Section 4.6.2; Fig. 4.2) indicates that in low porosity micrites ($\phi < 12\%$), rounded micromolds are dominant, with elongate micro- and mesomolds. With increasing percentage-porosity, these grade into elongate and irregular, solution-enlarged micro- and mesomolds, and micro-

and mesovugs (Plates 6.1 - 6.3). Since specimens WV4X1, WV4Y1 and WV4Z1 have porosities less than 12% (Appendix 7), preferred pore-orientation in low-porosity micrites has no effect on velocity. The relationship between velocity-aeolotropy and preferred orientation noted in specimen UCL1Z4, which has a porosity of 27%, indicates that in high-porosity micrites, pore-orientation is important, and is probably the result of preferred orientation of elongate molds, usually of molluscan debris, coinciding with bedding (Sections 5.3.2e; 7.3.2c).

Microsparites are the only other limestone-type to exhibit preferred pore-orientation A study of pore-type indicates that intercrystal micro- and mesopores grading into mesovugs are dominant (Fig. 4.2; Plates 6.4; 6.5; 6.12) over a wide percentage-porosity range. The preferred orientation is probably related to preferred mineral-orientation (Section 7.3.2d) and in one case, results in velocity-aeolotropy in a lithostratigraphic unit (Section 5.3.2d).

Preferred pore-orientation is thus related to pore-type in the form of moldic and intercrystal porosity. This preferred orientation always occurs in directions within the horizontal (XY) plane, and is probably related to preferred shell-orientation (Section 7.3.1) in the case of moldic porosity (micrites) and to preferred mineral-orientation (Section 7.3.1) in the case of intercrystal porosity (microsparites). This conclusion is enhanced by the fact that sparites are characterised by randomly-distributed interparticle and intraparticle pores (Fig. 4.2, Plates 6.6 - 6.8), and chalks by randomly-distributed regular and irregular micro- and mesomolds, some of which are solution-enlarged and grade into vugs, over a wide percentage-porosity range (Plates 6.9 - 6.11). Although chalks possess a moldic-type porosity, an absence of preferred pore-orientation is to be expected, since planar fabric elements in the form of preferred shell-orientation do not have a highly-significant correlation with velocity (Section 7.3.1). This is reflected by the fact that all lithostratigraphic units from which samples of chalks

were taken (Appendix 6) display velocity-isotropy (Section 5.3).

6.3.3c Pore-Structure and Pore-Type

The effect of pore-structure, i.e. pore-size, pore-morphology and pore-distribution, on velocity was assessed by simple correlation coefficients. The appropriate results are given in Table 6.4. These results show that, excluding microsparites, increasing porosity correlates with increasing pore-size at the 5% probability level. Microsparites show a lower correlation (Table 6.4). This is to be expected since the dominant pore-type is intercrystal, and crystal sizes are nearly constant throughout the percentage-porosity range studied (Plates 6.4; 6.5; 6.12; Table 7.4). Correlation between porosity and pore-size found in micrites and chalks could be related to solution-enlargement of moldic porosity.

The positive correlation between porosity and pore-size in sparites probably depends upon the amount of sparry calcite cement (Section 4.5.2) occupying the interparticle and intraparticle pores, these forming the main pore-types.

Velocity/porosity correlation coefficients are significant at the 5% probability level for the four limestone-types, with the usual velocity/porosity inverse relationship present. The importance of these results is limited by the small number of specimens used, but nevertheless, there is close agreement between these correlation coefficients and those given in Table 6.3, derived from the total data available for each limestone-type.

Photomicrographs of micrites suggest that the low degree of correlation between velocity and percentage porosity (Section 6.3.2; Tables 6.3; 6.4) could be a result of pore-structure and pore-type. As previously described, in low-porosity micrites ($\phi < 12\%$), rounded micromolds form the major pore-type. These are evenly distributed throughout the core-specimens (Plate 6.1), and thus probably do not form

TABLE 6.4

Results of Pore-Structure Correlations for Four Limestone-Types from the Portland Group

Limestone-Type		SPARITES	MICRITES	CHALKS	MICROSPARITES
No. of specimens		10	10	8	8
VELOCITY (m./sec) V	Mean	4124 ± 329	4843 ± 154	4098 ± 383	3887 ± 281
	Range	2511 - 5546	4048 - 5774	2946 - 5717	2831 - 5319
POROSITY (%) ϕ	Mean	17.7 ± 3.1	12.7 ± 2.1	22.7 ± 3.8	16.8 ± 2.5
	Range	3.0 - 32.3	4.9 - 26.9	7.8 - 38.9	6.3 - 27.8
PORE LONG AXIS (μ) L	Mean	219 ± 22	182 ± 43	163 ± 27	85 ± 6
	Range	124 - 321	65 - 484	112 - 311	66 - 107
PORE SHORT AXIS (μ) S	Mean	87 ± 8	71 ± 9	72 ± 9	40 ± 2
	Range	60 - 134	42 - 132	55 - 126	32 - 45
L/S	Mean	2.6 ± 0.1	3.7 ± 1.6	2.2 ± 0.1	2.1 ± 0.1
	Range	2.0 - 3.6	1.5 - 18.2	1.9 - 2.8	1.9 - 2.3
CORRELATION COEFFICIENT (r) & PROBABILITY LEVEL (p)	$r_{V\phi}$	-0.9417* p<0.001	-0.7009* 0.05>p>0.02	-0.9053* 0.01>p>0.001	-0.7530* 0.05>p>0.02
	r_{VL}	-0.6092 0.1>p>0.05	-0.6919* 0.05>p>0.02	-0.6126 p > 0.1	-0.1225 p > 0.1
	r_{VS}	-0.4293 p > 0.1	-0.8456* 0.01>p>0.001	-0.4246 p > 0.1	-0.6458 0.1 > p > 0.05
	$r_{VL/S}$	-0.5204 p > 0.1	-0.3609 p > 0.1	-0.6439 0.1>p>0.05	-0.1229 p > 0.1
	$r_{\phi L}$	+0.6833* 0.05>p>0.02	+0.4921 p > 0.1	+0.7146* 0.05>p>0.02	+0.2950 p > 0.1
	$r_{\phi S}$	+0.4872 p > 0.1	+0.7923* 0.01>p>0.001	+0.5265 p > 0.1	+0.3843 p > 0.1

*Correlation coefficient significant.

appreciable discontinuities to the transmission of elastic-wave energy in the matrix. Low-porosity micrites with preferred pore-orientation, probably caused by the occurrence of elongate micro- and mesomolds, show no velocity-aeolotropy (Section 6.3.3b). Thus the elongate micro- and mesomolds can be only a minor component of the porosity. With increasing porosity ($\phi > 12\%$), there is an increase in the number of elongate molds, mainly formed from molluscan debris, and both rounded and elongate molds are solution-enlarged and grade into vugs (Plates 6.2; 6.3). This results in an increase in the discontinuities to the transmission of elastic-wave energy and an association between preferred pore-orientation and velocity-aeolotropy as previously described. The effect of these changes in pore-structure is probably gradual, as implied by a positive correlation (Table 6.4) between percentage porosity and pore-size. However, the most rapid changes occur at approximately 12% porosity and this is reflected by marked differences in correlation coefficients above 12% (-0.6993) and below 12% (-0.4004) using the total velocity/porosity data for micrites (Appendices 5 & 6). The importance of pore-size and its effect on elastic-wave transmission is substantiated by a significant negative correlation coefficient between velocity and pore-size (Table 6.4). The importance of pore-structure, which results in a low degree of correlation between velocity and porosity in low-porosity micrites, is also inferred from a limited study of velocity-variation with degree of water-saturation (Appendix 2). This study, made on four micrite cores and four sparite cores, all with porosities less than 12%, gave the results shown in Fig. A2.1. There is a low degree of dependence of velocity on degree of water-saturation in micrites, but a high degree of dependence in sparites. This limited observation supports the conclusion reached above that transmission of the elastic-wave energy is largely confined to the matrix of micrites with less than 12% porosity. As a result, there is a low degree of correlation between velocity and percentage porosity.

Pore-structure and pore-type do not apparently affect velocity in microsparites. This is implied by an absence of significant correlations between velocity and pore-size as well as between porosity and pore-size. Also, pore-distribution, pore-morphology and pore-type (intercrystal) are nearly constant (plates 6.4; 6.5; 6.12) over a wide porosity range. The velocity-variation not attributed to linear regression between velocity and porosity and to experimental error (Section 6.3.2) is therefore probably related to mineral content (Section 6.2) and other petrographical parameters (Section 7.3.2d).

The high degree of correlation between velocity and porosity in sparites and chalks (Tables 6.3; 6.4) indicates that factors other than porosity and experimental error (Section 6.3.2) do not substantially affect these relationships. This is supported by the results of pore-structure analysis, which show an absence of significant correlation between velocity and pore-size, a random pore-distribution and constant pore-morphology and pore-types throughout the porosity ranges studied (Plate 6.6 - 6.11; Appendix 7).

To summarise, there is a high degree of correlation between velocity and porosity (Table 6.3), accounting for at least 43% of the variation in velocity due to linear regression between velocity and porosity (Section 6.3.2) irrespective of pore-type. Pore-structure and pore-type are not important parameters affecting velocity, except under certain conditions, where pore-size, pore-morphology and pore-distribution can significantly reduce the correlation between velocity and porosity as shown in the case of low-porosity micrites, where evenly-distributed, rounded micromolds are dominant.

The high degree of correlation between velocity and porosity suggests that the least-time paths of elastic-wave energy are either confined to the matrix and deviate around the pores, or follow both matrix

and pores, which are assumed to be air-filled. The results of water-saturation on velocity in four sparite cores (Appendix 2; Fig. A2.1) provide some support for the latter observation except where pore-structure and pore-type affect velocity, as in the case of micrites. In the case of sparites (Appendix 2), increasing degree of water-saturation results in increasing velocity, which infers that the least-time paths follow both matrix and pores. This contrasts with the results of previous workers (Wyllie et. al., 1958; Berry, 1959; Sarmiento, 1961), which show that velocity correlates with porosity only in limestones with intergranular porosity. Sarmiento (1961) found that the pores in some Palaeozoic limestones were intergranular below 12% porosity and vuggy above 12% porosity. It was suggested that the intergranular pores were included in the elastic character of the rock, whereas the elastic-wave energy followed a least-time path around the vugs. Where there were vugs, porosity did not correlate with velocity. A similar result was found by Wyllie et. al. (1958), and differences in elastic-wave propagation were explained by differences in pore-size between vugs or fractures and intergranular pores, with a critical pore-size, which was related to the wavelength of elastic-energy. This effect was not observed in the limestone specimens from the Portland Group, possibly because the frequency (150KHz) of elastic-wave energy used (Section 4.3.1) meant that the wavelength varied between 1.25 and 4.34 cms. for the minimum and maximum velocities determined, which is considerably greater than the pore-sizes recorded (Appendix 7). Similarly, no differences in velocity/porosity correlations were observed between limestone specimens with interparticle, intraparticle, intercrystal and moldic porosity (presumably classified as intergranular porosity by previous workers) and those with vuggy porosity. With the exception of micrites, the pore-types, pore-distribution and pore-morphology are constant in the Portland Group limestone-types over a wide porosity-range

(approximately 2% - 40%). This would indicate that the least-time paths of elastic-wave energy, which follow both matrix and pores in low-porosity sparites (Appendix 2), follow the same paths in high-porosity sparites, chalks and microsparites. The effect of pore-structure in micrites which results in the least time-paths being confined to the matrix where porosity is less than 12%, contradicts the results of previous workers.

The limestone-types from the Portland Group thus apparently differ from limestones studied by previous workers in terms of elastic-wave energy-propagation. However, the differences are not absolute, since previous workers did not subdivide the limestones into different types, and the size-limits of intergranular and vuggy pores have not been defined.

No evidence of extensive microfracturing was found, as shown by the results of both reflected-light and Stereoscan analyses (Section 4.6.3). This absence of microfracturing in each limestone-type is illustrated in Plates 6.12 - 6.18, and its significance on the possible relationships between porosity and tectonism has previously been described (Section 5.4.2b), with reference to velocity- and porosity-correlations with lithostratigraphy. A study of Plate 6.13 and Plate 6.18 shows that in the case of chalks and micrites respectively, intercrystal porosity between the microcrystalline calcite, which forms the dominant component of these limestone-types (Section 4.6.1), is present throughout the matrix. This porosity probably forms a small proportion of the total porosity, and cannot appreciably affect velocity/porosity relationships for these limestone-types, as implied by dissimilarities between these two types in terms of correlation coefficients and regression equations (Table 6.3), and by similarities between chalks and sparites in terms of these parameters.

6.4 Conclusions

The four limestone-types studied are characterised by independent inverse velocity/porosity relationships. These relationships can take the form of simple linear, polynomial, exponential, logarithmic or inverse-

velocity functions. However, since only marginal differences occur between correlation coefficients for each function, the simple linear function is adequate to describe the relationship empirically. The correlation coefficients and regression equations differ from those previously published for some Palaeozoic limestones and dolomites (Sarmiento, 1961), but this is probably a result of differences in the data-source.

Extrapolation to the limiting velocity indicates that none of the limestone-types behaves as a quasi-isotropic aggregate of randomly-oriented calcite crystals for elastic-wave propagation.

The least-time paths of elastic-wave energy tend to traverse both matrix and pores in all four limestone-types, except low-porosity micrites, irrespective of pore-type and percentage porosity. This contrasts with the conclusions of previous workers (Wyllie et. al., 1958; Berry, 1959; Sarmiento, 1961), which suggest that, above a critical but unspecified pore-size, the elastic-wave energy follows a least-time path around the pores, as shown by a low correlation coefficient between velocity and porosity. However, the effect of pore-size, pore-morphology and pore-distribution on velocity was not apparently investigated. In the present study, these were important factors in the case of micrites. At low porosities ($\phi < 12\%$), the least-time paths of elastic-wave energy traverse the matrix only, resulting in a low degree of correlation between velocity and porosity. With increasing porosity, they traverse both matrix and pores due to an increase in pore-size and changes in pore-morphology and pore-distribution. In the remaining three limestone-types, pore-structure is not an important factor. Pore-morphology is nearly constant and pore-distribution is random throughout the porosity ranges studied. At least 70% of the velocity-variation is due to linear regression between velocity and percentage-porosity (Section 6.3.2).

A study of pore-orientation shows that 83% of the core-specimens

studied have a random orientation of resultant pore long-axes. Where significant preferred orientations exist these were related to pore-type, in the form of moldic and intercrystal pores. This was apparently a result of the influence of fabric sub-parallel to bedding. Moldic pores are largely derived from shell debris, which sometimes shows a marked preferred orientation, and intercrystal pores are related to calcite, dolomite or quartz, which sometimes exhibit preferred orientation. This is further substantiated by the fact that all significant preferred pore-orientations lie within 10 degrees of true dip. This preferred pore-orientation could, in a few cases, be directly related to velocity-aeolotropy in those lithostratigraphic units from which the core-specimens were derived. Preferred pore-orientation was limited to micrites and microsparites.

It is apparent from this study that factors other than percentage porosity, experimental error in velocity/porosity-determinations, and, in the case of micrites, pore structure, cannot contribute significantly to the velocity-variation observed in limestones from the Portland Group. This is particularly true in the case of sparites and chalks. Velocity-variation in microsparites could also be influenced by mineral content.

A study of velocity/density relationships shows similar but inverse results to those for velocity/porosity relationships, with simple correlation coefficients for each limestone-type differing by less than 7% from those obtained using simple linear regression between velocity and porosity.

It is concluded that velocity can be estimated from porosity, using a simple linear relationship, to within 40% (Table 6.3). Slightly better estimates can be obtained when these limestones are divided into the four basic types.

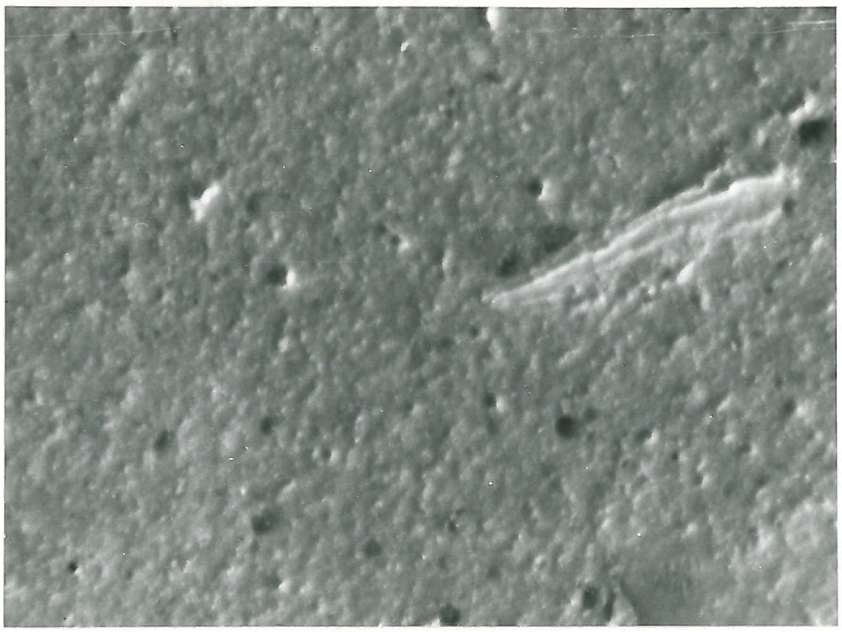
The regression equation derived from the total data for the Portland Group can be applied to porosity-data for other limestones. In the case of

limestones of unknown age but ranging from 0.6% to 23.6% porosity, reported by Koefoed et. al.,(1963), estimated velocities were found to be consistently higher than observed velocities using the regression equation for the Portland Group. However, these velocity differences are within the standard error of the equation. In the case of Solenhofen Limestone, Germany (Peselnick, 1962), velocity-estimates were consistently lower than observed velocities when the appropriate porosities (Flügel et. al., 1968) were used in the regression equation for the Portland Group. Again, these differences in velocity are within the standard error of the equation. The regression equation cannot be applied to sandstones, as shown by a 38% variation between estimated and observed mean velocities, for some core-specimens from the Bunter Sandstone reported by Barker et. al. (1973). The observed mean velocity is less than the estimated mean velocity, and this is probably a result of differences between the velocities of quartz and calcite. A random aggregate of calcite crystals has a velocity of 6800 m/sec. in contrast to 5900 m/sec. for a random aggregate of quartz crystals (Wyllie et. al.,1956).

Photographic plates referred to in Chapter 6

These consist of both photomicrographs using reflected light, and scanning electron micrographs. The core-specimens e.g. WV3Z5 used for these plates, together with the porosity (ϕ) and the limestone-type, are indicated. Core-specimen localities are given in Appendix 5. All scales are given in microns (μ).

Plate 6.1 WV3Z5 (Micrite) ϕ = 9.1%



1000μ

Isolated, evenly-distributed, rounded micromolds. Scattered, elongate molds are also usually present in micrites, being derived from shell-fragments (bioclasts), an example of which is present near right margin of plate.

Photomicrograph (x 46)

Plate 6.2 PLBS3Y2 (Micrite) ϕ = 16.4%

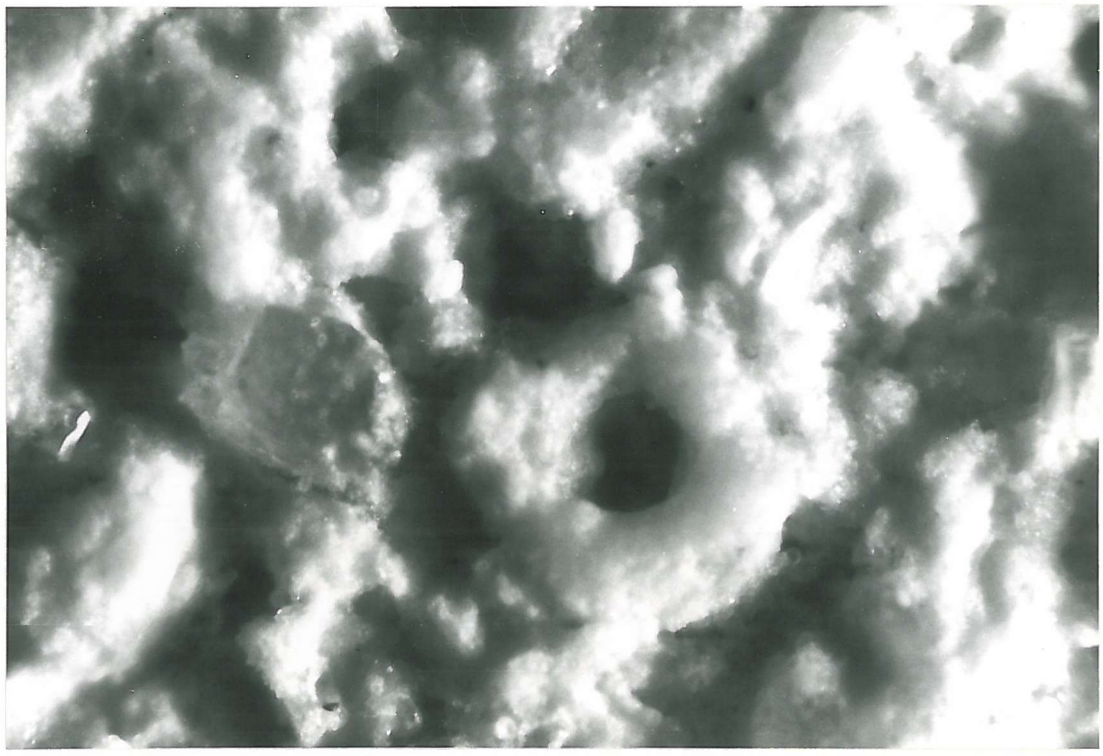


1000μ

Randomly-distributed, irregular-shaped micro-mesomolds, some of which are solution-enlarged. The elongate mold covering entire length of plate is infilled with sparry calcite.

Photomicrograph (x 46)

Plate 6.3 UCL1Z4 (Micrite) ϕ = 26.9%

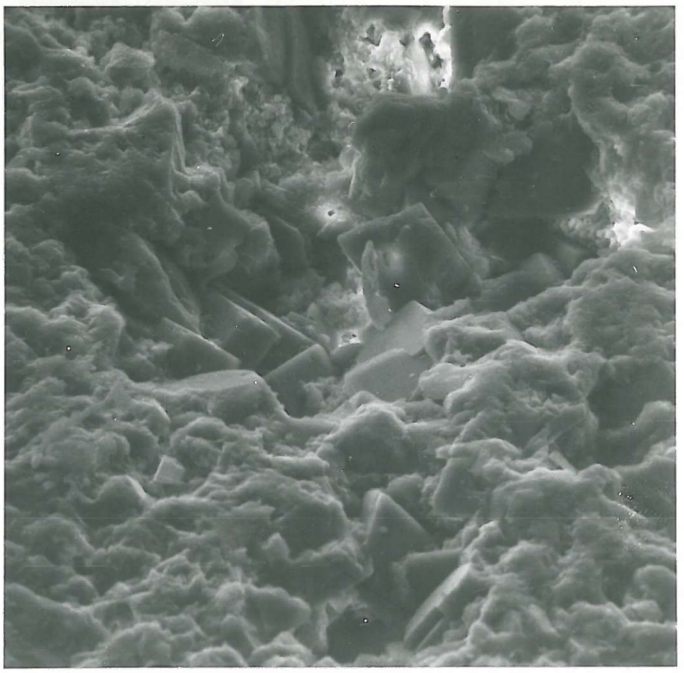


500μ

Randomly-distributed, irregular-shaped, solution-enlarged mesomolds, and mesovugs.

Photomicrograph (x 128)

Plate 6.4 LCA10-1Z2 (Microsparite) ϕ = 6.3%

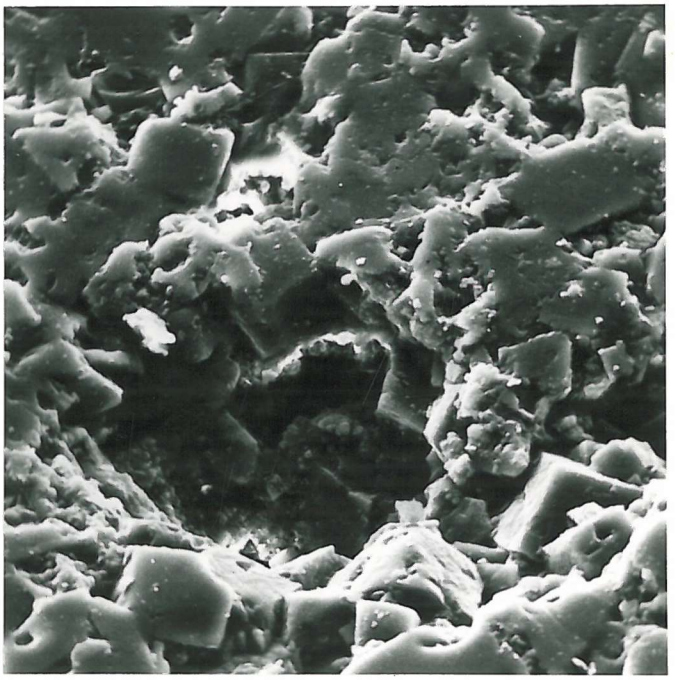


100μ

Intercrystal micro-mesopores grading into micro-mesovugs. Note dolomite rhombohedra.

Scanning Electron Micrograph (x 450)

Plate 6.5 WA28-1X1 (Microsparite) ϕ = 24.7%

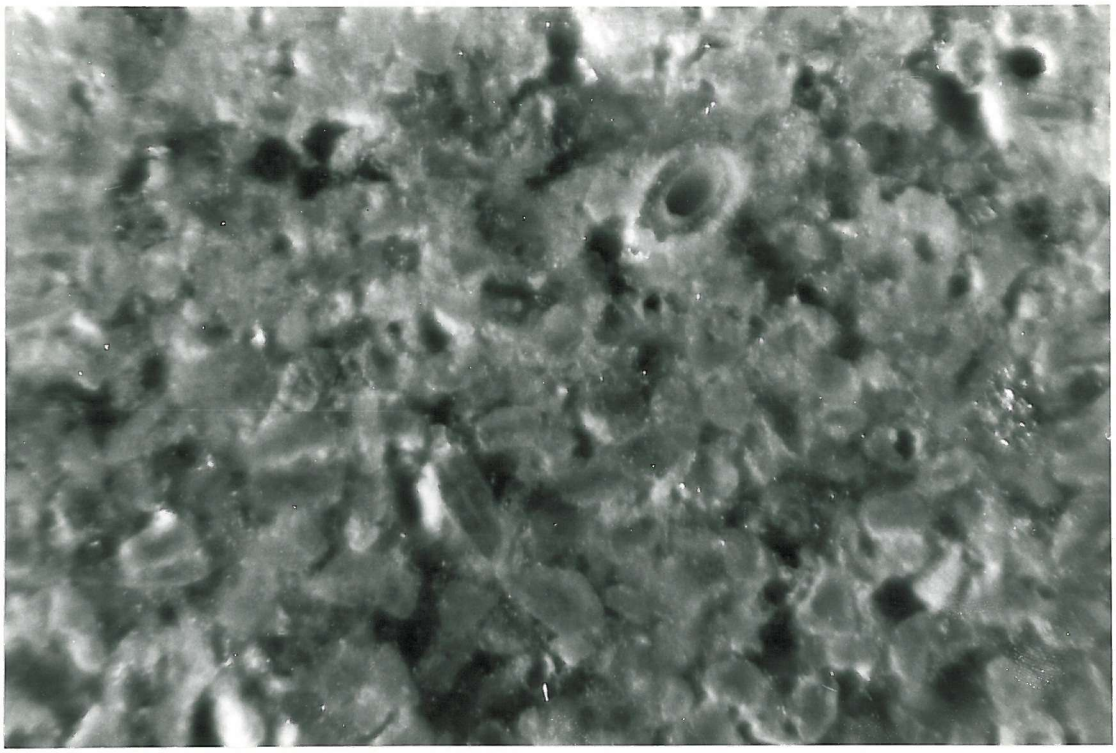


50μ

Intercrystal micro-mesopores, and micro-mesovugs. Note dolomite rhombohedra.

Scanning Electron Micrograph (x 535)

Plate 6.6 WN1Y1 (Sparite) ϕ = 9.6%

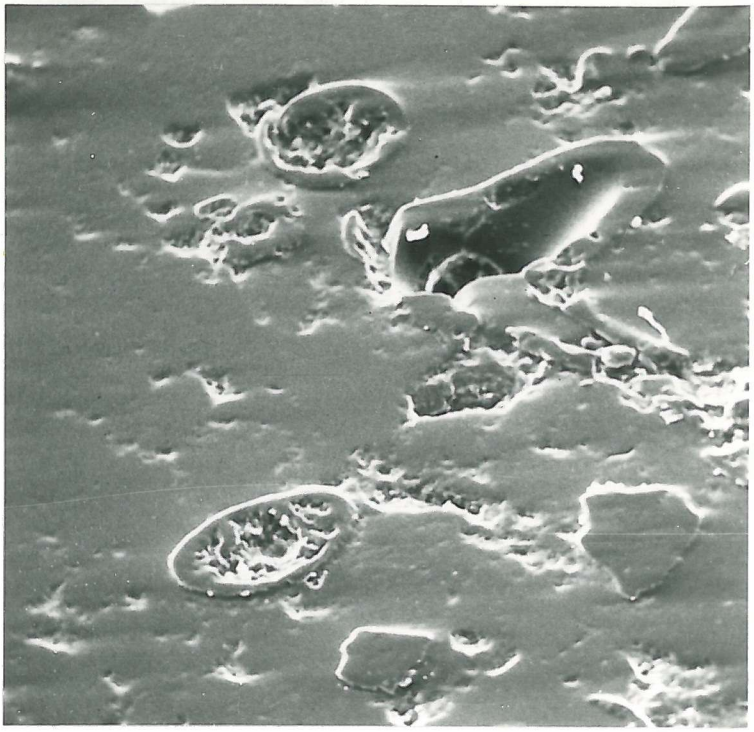


1000μ

Randomly-distributed, interparticle and intraparticle micro-mesopores. "Particles" consist predominantly of ooliths and bioclasts.

Photomicrograph (x 54)

Plate 6.7 WT3Y2 (Sparite) ϕ = 6.7%

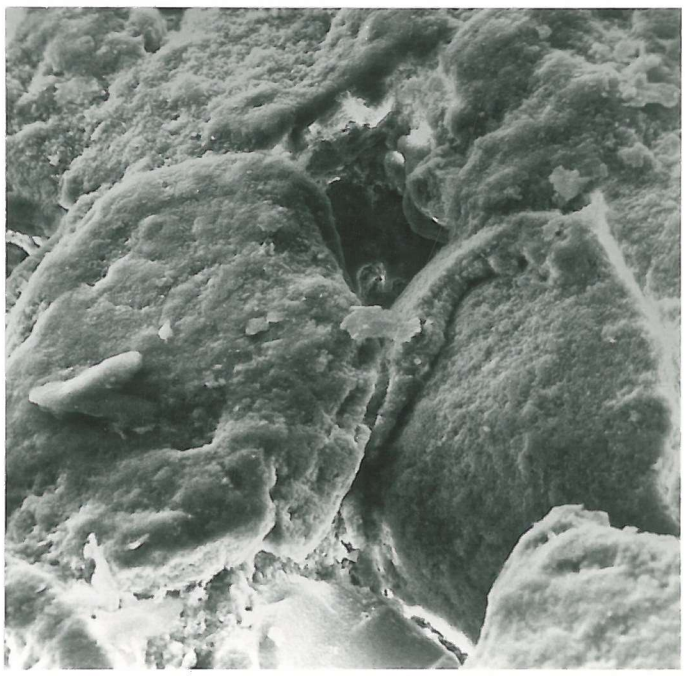


500μ

Randomly-distributed, interparticle and intraparticle micro-mesopores. Note intraparticle pores in sponge (Pachastrella) spicules.

Scanning Electron Micrograph (x 122)

Plate 6.8 UCR2X3 (Sparite) ϕ = 21.1%

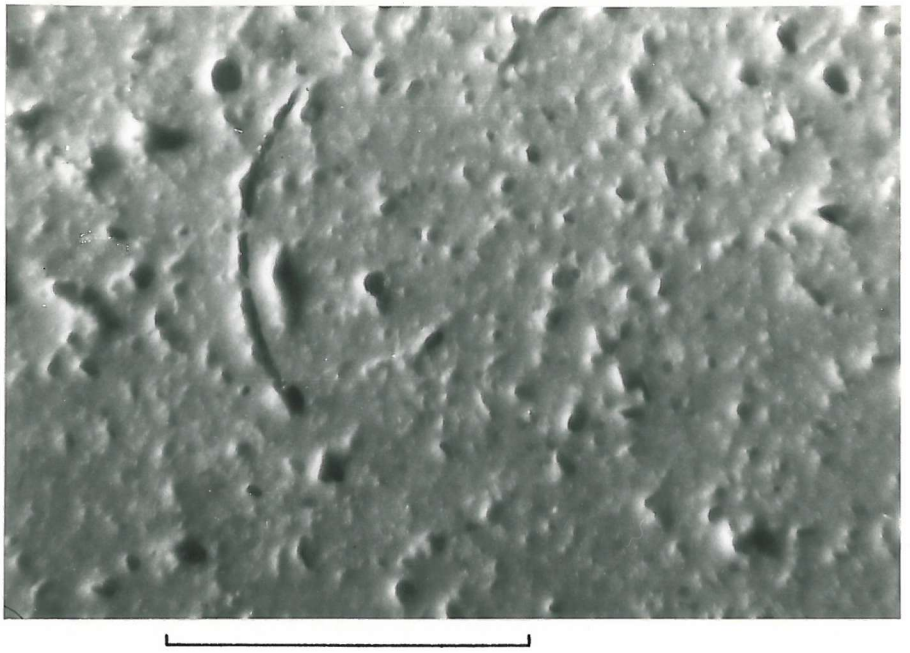


250μ

Interparticle mesopores with ooliths forming the majority of "particles". Note radial structure in outer concentric layers of oolith envelopes.

Scanning Electron Micrograph (x 180)

Plate 6.9 C10-1Y5 (Chalk) ϕ = 7.8%

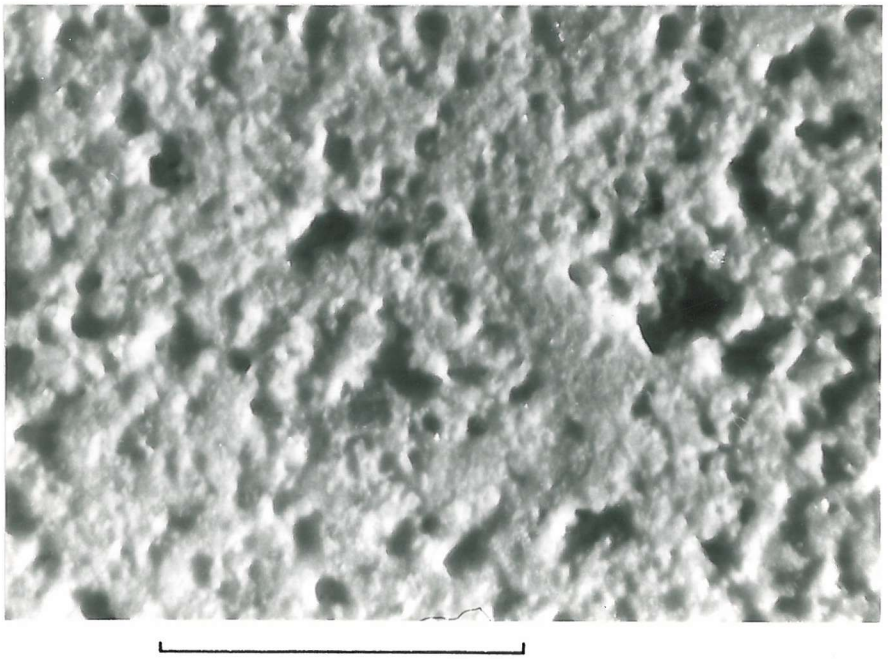


1000μ

Randomly-distributed, regular-shaped micro-mesomolds, some of which are solution-enlarged.

Photomicrograph (x 48)

Plate 6.10 P10-1Y3 (Chalk) ϕ = 16.7%

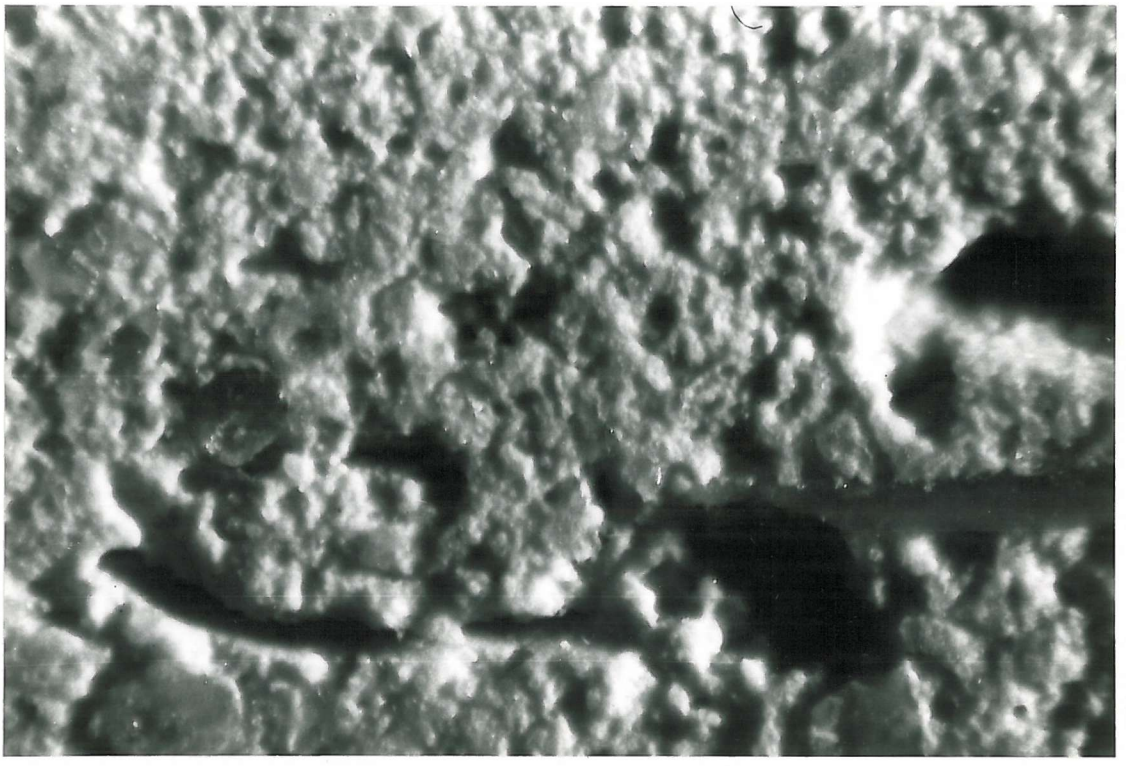


1000μ

Randomly-distributed, regular- and irregular-shaped micro-mesomolds, most of which are solution-enlarged, and grade into mesovugs.

Photomicrograph (x 48)

Plate 6.11 CRC3Y3 (Chalk) ϕ = 32.5%

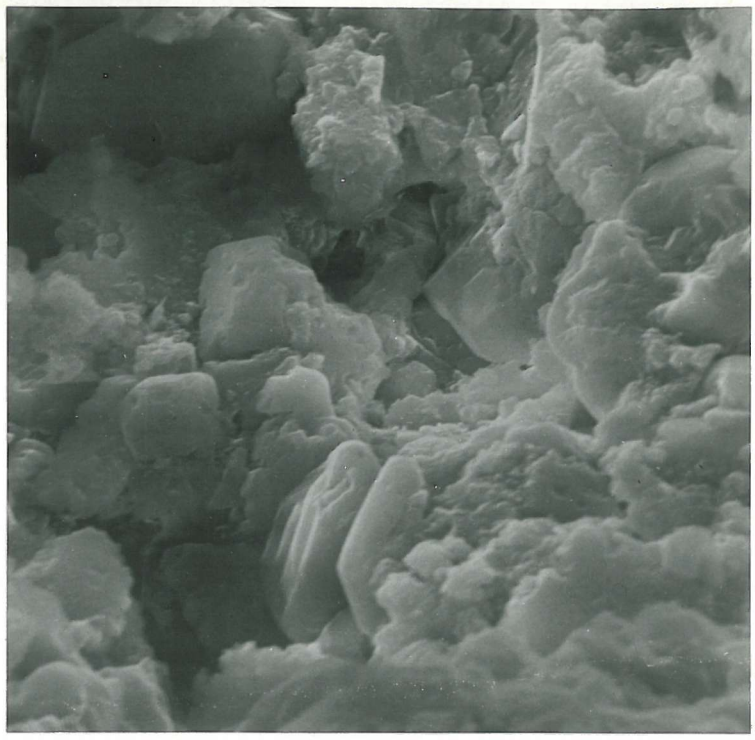


1000μ

Randomly-distributed, irregular-shaped, solution-enlarged micro-mesomolds grading into vugs. A few regular-shaped micro-mesomolds. Note partial infill of elongate mold with sparry calcite in lower right half of plate.

Photomicrograph (x 54)

Plate 6.12 WB1X2 (Microsparite) ϕ = 27.8%

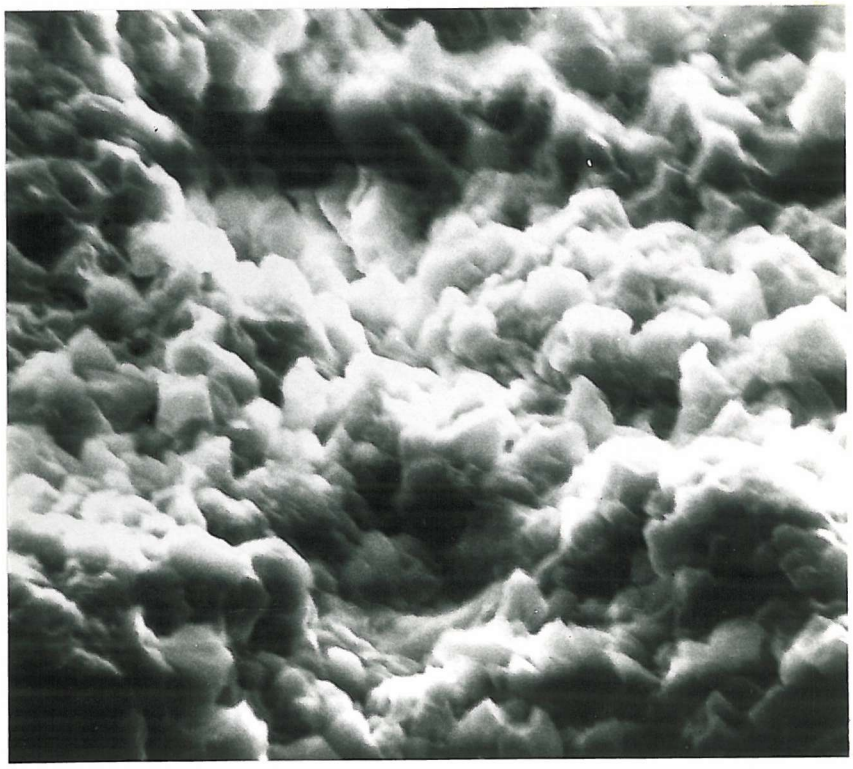


20μ

Intercrystal micro-mesopores grading into vugs. Note euhedral calcite crystals (microspar) and anhedral quartz grains, and an absence of microfractures.

Scanning Electron Micrograph (x 2100)

Plate 6.13 C10-1Y5 (Chalk) ϕ = 7.8%

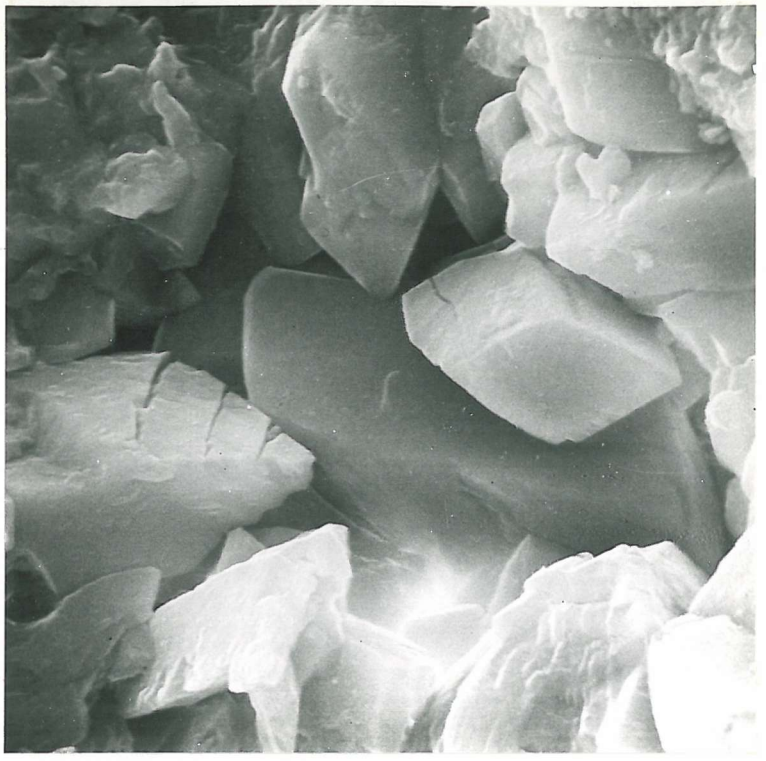


5μ

Intercrystal micropores between microcrystalline calcite (micrite), which forms matrix of specimen. Note absence of microfractures.

Scanning Electron Micrograph (x 5400)

Plate 6.14 UCR2X3 (Sparite) ϕ = 21.1%



20μ

Filled boring mesopore with intercrystal micropores between the infilling sparry calcite crystals (Type III fabrics - Table 4.3). Note localised micro-fractures in calcite crystals, probably formed during sample preparation.

Scanning Electron Micrograph (x 2000)

Plate 6.15 LCV2X4 (Sparite) ϕ = 5.6%

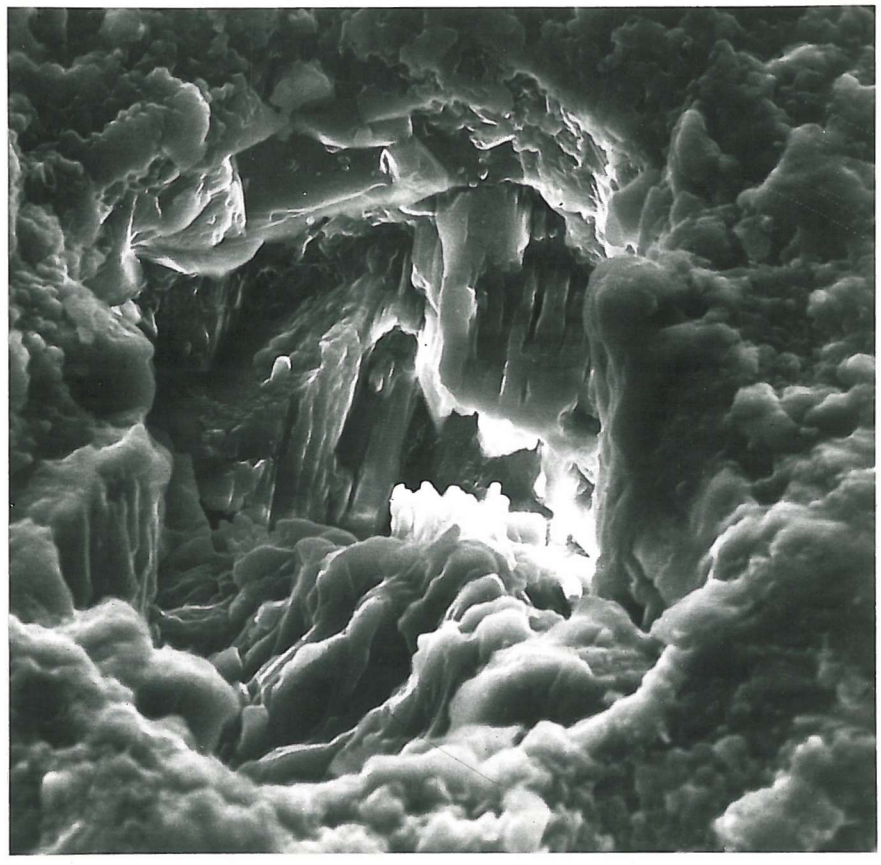


25μ

Sparry calcite crystals (Type III fabrics - Table 4.3) infilling intra-particle mesopore, with intercrystal micro-mesopores between calcite. Note absence of any continuous microfractures.

Scanning Electron Micrograph (x 1710)

Plate 6.16 WV5Y3 (Micrite) ϕ = 9.3%

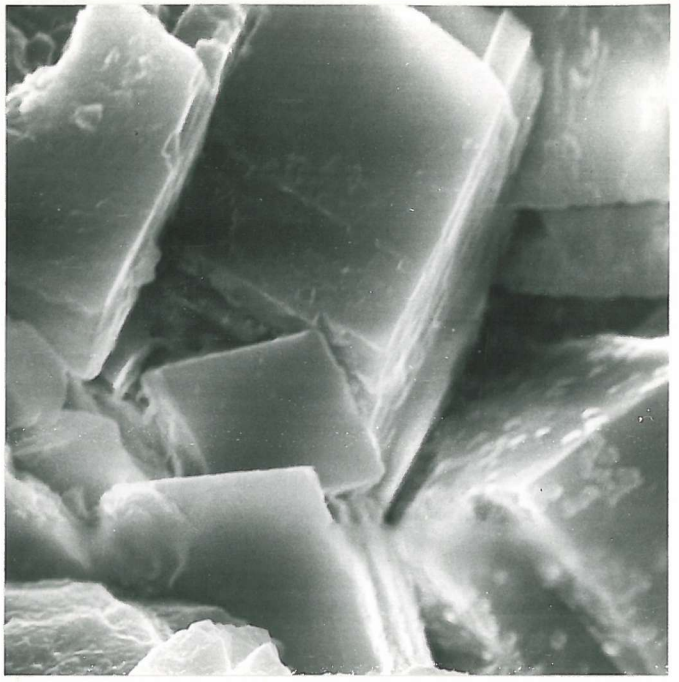


25μ

Reduced microvug, partially infilled with sparry calcite crystals. Note cleaved calcite crystals and absence of microfractures.

Scanning Electron Micrograph (x 1365)

Plate 6.17 CFPS1Z2 (Microsparite) ϕ = 14.8%

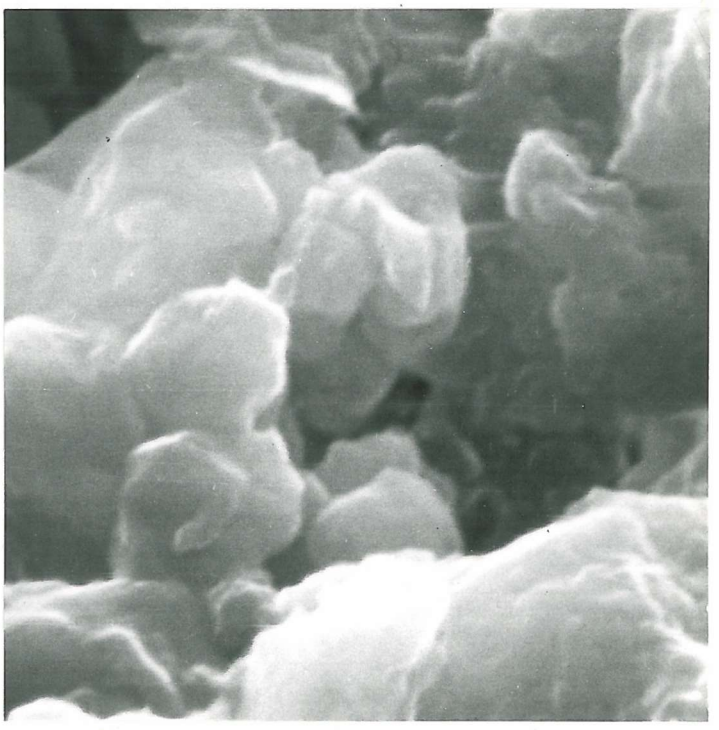


10μ

Dolomite rhombohedra and intercrystal micropores. Note absence of microfractures.

Scanning Electron Micrograph (x 4320)

Plate 6.18 PLBS3Y2 (Micrite) ϕ = 16.4%



2μ

Intercrystal micropores between microcrystalline calcite cement. Note absence of microfractures.

Scanning Electron Micrograph (x 21100)

CHAPTER 7

RELATIONSHIPS BETWEEN VELOCITY, POROSITY AND OTHER PHYSICAL PARAMETERS

7.1 Introduction

The results in the previous chapter indicate that porosity is the most significant velocity-controlling parameter in limestones from the Portland Group. In the case of micrites pore-structure is also important. In chalks and sparites the inverse relationship between velocity and porosity, together with experimental error, accounts for virtually all the velocity-variation. In order to substantiate this conclusion and to investigate other possible causes of velocity-variation in micrites and microsparites, a study was made of the possible relationships between velocity and 22 physical parameters. Data from some 245 core-specimens, representative of the four limestone-types and extended over a wide porosity range (2% - 39%) was analysed. Other than porosity, the physical parameters consisted largely of petrographical factors as defined in Section 4.5.

Multiple-regression analysis of the data, using velocity as the dependent variable and the other physical parameters as the independent variables, was carried out. Equations were computed relating velocity to statistically-significant independent variables. The computation of multiple-correlation coefficients for each equation permitted direct comparisons with the results of simple linear-regression analysis between velocity and porosity (Section 6.3.2).

Additionally, a study was made of simple correlation coefficients in order to determine the degree of dependence of velocity on each of the petrographical factors.

7.2 Methods of Statistical Analysis

Multiple-regression analysis assumes that the dependent variable

can be approximated by a linear function of the independent variables. Since porosity, an independent variable, is linearly related to velocity, the dependent variable (Section 6.3.2), accounting for at least 70% of the variation in velocity in sparites, chalks and microsparites, it was considered that errors due to the above assumption would not significantly affect the results of the analyses for the remaining independent variables. In the case of micrites, where only 43% of the velocity-variation is accounted for, most of the remaining variation is probably attributable to pore-structure (Section 6.3.3c).

The multiple-regression analysis was made on a digital computer using an ICL 1900 series Statistical Analysis System Mark 2 program. The data was initially presented to the program in the form of an observation matrix, which in the case of the four limestone-types, contained several missing values, consisting of certain petrographical parameters. A facility of the Mark 2 program enabled a complete observation matrix to be created, with the missing values replaced by the mean of the appropriate variable. From this a transformed observation matrix was computed, wherein several of the petrographical parameters were combined (these combinations are described in Section 4.5.3). The program next computed a cross-product matrix, which was then used for multiple-regression analysis. Covariance and correlation matrices were also computed, together with the means and standard deviations of each variable in the observation matrices.

The program yields a regression equation of the dependent variable, velocity, on those independent variables which made a significant contribution to the regression. A significance level of 5% was used. The independent variables, which form the final regression equation, are selected by an iterative procedure, whereby every independent variable in the equation has a regression coefficient that is significantly non-zero in the formal t - test sense. Every variable not in the equation has a

regression coefficient that is not significantly non-zero. The regression coefficients of the independent variables are estimated using the method of least-squares. An independent variable is either added or removed from the regression equation at each iteration, depending on whether the Student's t-statistic for that variable, computed from the ratio:

Regression coefficient / Standard error of Regression coefficient,

is significant at the 5% level.

After each iteration, an output of the following parameters is given:

Multiple-regression equation

Standard error of each regression coefficient

Confidence interval

Student's t-statistic for every independent variable

Partial correlation coefficient between each independent variable and the dependent variable, which assumes that the remaining independent variables are held constant

Multiple correlation coefficient between each independent variable and the dependent variable, which takes into account the presence of the other independent variables in the regression equation

Standard error of estimate of the dependent variable

Multiple correlation coefficient between the dependent variable and those independent variables in the equation.

Concluding the analysis, there is an output of the following parameters for each observation of the dependent variable (velocity):

Observed velocity

Estimated velocity, computed using the final equation

Difference between observed and estimated velocities.

Initially, the analysis was made using all independent variables available for each limestone-type. It was then repeated with various combinations of petrographical parameters (Section 4.5.3). In certain cases, independent variables which had either non-significant simple correlation coefficients with velocity, or a predominance of missing values, appeared in the final equation. These were removed from the set of independent variables selected for analysis, and the analysis repeated. Thus several multivariate equations for each limestone-type were computed and the multiple correlation coefficients were used to select the best equation for the prediction of velocity.

7.3 Results

7.3.1 Basic Statistics and Simple Correlation Coefficients

Tables 7.1 - 7.4 show means and their standard errors, maximum and minimum values of each variable, and numbers of missing values for each variable, including combinations of petrographical factors (Section 4.5.3), for the four limestone-types.

The following symbols and units are used in Tables 7.1 - 7.9 for the variables considered, including the combinations of petrographical factors used.

VARIABLE	SYMBOL	UNIT
Velocity	V	metres/sec.
Porosity	ϕ	%
Fabric	F	Planar Elements /cm.
Calcite Cement content	Cc%	%
Oolith content	Ol%	%
Intraclast content	I%	%
Pellet content	P%	%
Bioclast content	B%	%
Dolomite content	D%	%

VARIABLE	SYMBOL	UNIT
Detrital Grains content	Dg%	%
Sponge spicule content	Ss%	%
Calcite Vein content	CV%	%
Silica Replacement content	Sr%	%
Oolith, Intraclast and Pellet content	OIP%	%
Calcite cement and Pellet content	CP%	%
Calcite and Dolomite content	CD%	%
Allochem content	A%	%
Calcite cement mean grain-size	Mcc	microns
Oolith mean size	MO	microns
Intraclast mean size	MI	microns
Pellet mean size	MP	microns
Bioclast mean size	MB	microns
Dolomite mean grain-size	MD	microns
Detrital grains mean size	MDg	microns
Calcite vein mean grain-size	MCv	microns
Silica replacement mean grain-size	MSr	microns
Calcite replacement mean grain-size	MCr	microns
Oolith, Intraclast and Pellet mean size	MOIP	microns
Calcite cement and Pellet mean grain-size	MCP	microns
Calcite and Dolomite mean grain-size	MCD	microns
Allochem mean size	MA	microns

TABLE 7.1

Basic Statistics - Sparites (N = 128)

VARIABLE	No. OF MISSING VALUES	MEAN & S.E.	MAXIMUM VALUE	MINIMUM VALUE
V	0	4592 ± 96	6505	1876
ø	0	14.9 ± 0.9	39.2	1.9
F	0	0.35 ± 0.08	6.93	0.0
Cc%	0	21.0 ± 1.0	66.8	2.5
Ol%	0	36.4 ± 2.2	81.5	0.0
I%	0	8.4 ± 0.8	52.0	0.0
P%	0	4.9 ± 1.0	42.5	0.0
B%	0	22.2 ± 1.1	49.0	1.1
Dg%	0	7.1 ± 1.0	52.4	0.0
Ss%	0	1.5 ± 0.3	15.0	0.0
CV%	0	0.06 ± 0.03	2.5	0.0
Sr%	0	0.4 ± 0.2	25.0	0.0
OIP%	0	50.9 ± 1.5	86.5	17.8
A%	0	71.9 ± 1.5	95.3	18.2
Mcc	0	141 ± 9	481	5
MO	16	244 ± 7	398	69
MI	16	514 ± 15	1038	216
MP	104	80 ± 1	89	63
MB	0	781 ± 39	2667	154
MDg	24	158 ± 4	245	41
MCr	0	27 ± 2	224	2
MSr	108	118 ± 5	209	13
MCv	121	56 ± 2	107	22
MOIP	0	266 ± 9	493	69
MA	0	458 ± 22	1339	80

TABLE 7.2

Basic Statistics - Chalks (N = 31)

VARIABLE	No. OF MISSING VALUES	MEAN & S.E.	MAXIMUM VALUE	MINIMUM VALUE
V	0	3809 ± 148	5717	2770
ø	0	25.8 ± 1.6	38.9	7.8
F	0	0.09 ± 0.04	0.8	0.0
Cc%	0	43.0 ± 2.7	81.6	22.0
I%	0	2.0 ± 0.6	11.0	0.0
P%	0	22.1 ± 2.2	50.2	0.0
B%	0	31.2 ± 2.1	52.0	10.2
Dg%	0	1.1 ± 0.3	5.3	0.0
CV%	0	0.6 ± 0.2	3.2	0.0
Sr%	0	0.1 ± 0.04	1.0	0.0
CP%	0	65.1 ± 2.7	89.8	39.0
A%	0	55.4 ± 2.6	75.5	15.2
Mcc	0	2 ± 0.2	4	1
MI	21	430 ± 9	561	295
MP	3	97 ± 4	134	60
MB	0	490 ± 52	1234	202
MDg	15	81 ± 4	107	35
MCr	0	67 ± 12	273	14
MSr	25	200 ± 37	643	47
MCv	21	32 ± 5	78	4
MCP	0	1 ± 0.2	3	1
MA	0	322 ± 27	760	115

TABLE 7.3

Basic Statistics - Micrites (N = 38)

VARIABLE	No. OF MISSING VALUES	MEAN & S.E.	MAXIMUM VALUE	MINIMUM VALUE
V	0	5248 ± 73	6079	4048
ø	0	9.6 ± 0.7	26.9	1.9
F	0	0.32 ± 0.14	3.59	0.0
Cc%	0	74.0 ± 2.2	96.0	50.6
B%	0	24.3 ± 2.1	49.0	4.0
Dg%	0	1.0 ± 0.4	7.8	0.0
CV%	0	0.8 ± 0.2	5.0	0.0
Sr%	0	0.2 ± 0.06	1.6	0.0
Mcc	0	1 ± 0	1	1
MB	0	585 ± 50	1494	198
MDg	29	114 ± 1.6	148	93
MCr	0	134 ± 12	299	39
MSr	27	115 ± 5	201	35
MCv	22	78 ± 9	350	4

TABLE 7.4

Basic Statistics - Microsparites (N = 48)

VARIABLE	No. OF MISSING VALUES	MEAN & S.E.	MAXIMUM VALUE	MINIMUM VALUE
V	0	4119 ± 114	5426	2755
ϕ	0	16.5 ± 1.1	29.4	5.5
F	0	0.97 ± 0.4	14.71	0.0
Cc%	0	22.7 ± 3.4	73.7	0.0
D%	0	45.8 ± 4.2	86.6	0.0
CV%	0	1.0 ± 0.3	12.5	0.0
Dg%	0	20.7 ± 1.3	35.1	4.4
B%	0	9.7 ± 0.7	22.6	1.2
CD%	0	68.5 ± 1.5	88.7	43.8
Mcc	6	27 ± 1.6	49	15
MD	11	30 ± 0.6	40	23
MCv	33	386 ± 75	1644	17
MDg	0	47 ± 1.3	64	31
MB	0	204 ± 12	349	72
MCD	0	27 ± 1	41	15

The simple correlation coefficients between velocity and the independent variables are shown in Table 7.5.

TABLE 7.5

Simple Correlation Coefficients between Velocity and the Independent Variables

INDEPENDENT VARIABLES	CORRELATION COEFFICIENT (r) BETWEEN VELOCITY AND INDEPENDENT VARIABLES							
	SPARITES		MICRITES		MICROSPARITES		CHALKS	
	r	P+	r	P+	r	P+	r	P+
∅	-0.886	****	-0.547	****	-0.856	****	-0.931	****
F	-0.493	****	-0.584	****	-0.372	***	-0.405	*
Cc%	+0.275	****	+0.057		-0.365	**	+0.533	***
Ol%	-0.514	****	-		-		-	
I%	+0.355	****	-		-		-0.655	****
P%	+0.452	****	-		-		+0.110	
B%	+0.656	****	-0.013		+0.521	****	-0.550	***
D%	-		-		+0.174		-	
Dg%	-0.564	****	-0.331	*	+0.118		-0.651	****
Ss%	+0.193	*	-		-		-	
CV%	+0.201	**	+0.167		+0.024		+0.375	*
Sr%	+0.172	*	-0.113		-		-0.167	
OIP%	-0.297	****	-		-		-	
CP%	-		-		-		+0.613	****
CD%	-		-		-0.345	**	-	
A%	+0.170	*	-		-		-0.512	***
Mcc	+0.402	****	0.0		+0.799	****	-0.694	****
MO	+0.506	****	-		-		-	
MI	-0.431	****	-		-		+0.021	
MP	+0.003		-		-		-0.366	*
MB	+0.522	****	-0.253		-0.618	****	+0.308	
MD	-		-		+0.556	****	-	
MDg	+0.399	****	-0.287		+0.123		-0.211	
MCv	+0.020		+0.033		+0.401	***	+0.271	
MSr	-0.010		+0.318		-		+0.188	
MCr	+0.267	***	-0.371	*	-		+0.567	***
MCIP	+0.294	****	-		-		-	
MCP	-		-		-		-0.675	****
MCD	-		-		+0.789	****	-	
MA	+0.553	****	-		-		+0.135	

+Probability values (P) of r. Only values of P < 5% are indicated since r is considered not significant at P > 5%.

* 5% > p > 2% ** 2% > P > 1% *** 1% > P > 0.1% **** P < 0.1%

A study of Table 7.5 shows the presence of highly-significant correlation coefficients ($P < 0.1\%$) between velocity and several different independent variables, particularly in the case of sparites. The importance of porosity as a highly-significant velocity-controlling parameter is confirmed for all four limestone-types. The percentage-variations in velocity due to regression between velocity and porosity - 78% for sparites, 30% for micrites, 73% for microsparites and 87% for chalks - are similar to those described in Section 6.3.2. This indicates that the limited data used in the multivariate analysis can be considered to be representative of the total data.

The remaining correlation coefficients (Table 7.5), although highly-significant ($P < 0.1\%$) in some cases, are generally considerably lower in magnitude than those between velocity and porosity. Highly-significant negative correlation coefficients ($P < 1\%$) between velocity and fabric for sparites, micrites and microsparites tend to confirm empirically some of the conclusions drawn on velocity/lithostratigraphical relationships and velocity-aeolotropy in Chapter 5. The effect of planar fabric elements (preferred shell-orientation in micrites and sparites, and preferred mineral orientation in microsparites and sparites) apparently produces discontinuities, which impede the propagation of elastic-waves in the core-specimens, thus reducing the velocity. Preferred pore-orientation, which also affects velocity, is apparently related to these planar fabric elements as described in Section 6.3.3b. The absence of any further significant correlation coefficients in the case of micrites suggests the influence of some other factor on velocity; this is probably pore-structure (Section 6.3.3c). The significant correlation coefficients ($P < 2\%$) between velocity and the modal parameters for the remaining limestone-types, are apparently related to the velocity/porosity inverse relationship (Section 6.3.2), which results in corresponding significant

correlation coefficients of opposite sign between porosity and the modal parameters. A study of these modal parameters indicates that in the case of detrital grains, of which quartz is dominant (Section 4.5.3), the significant negative correlations with velocity for sparites and chalks, could also be the result of a random aggregate of quartz having a lower velocity, i.e. 5900 m/sec (Wyllie et al., 1956) than random aggregates of calcite, i.e. 6350 m/sec (Kisslinger, 1953) or dolomite, i.e. 6750 m/sec (Kisslinger, 1953). The significant positive correlation coefficient between porosity and % calcite cement together with a negative though not significant ($P > 5\%$) correlation coefficient between porosity and % dolomite, in microsparites, could be a result of the dolomitisation process. Initial solution of calcite in the form of microcrystalline ooze (Section 4.5.2), followed by precipitation of dolomite, would tend to fill the pore-space (Landes, 1946; Kisslinger, 1953), thus giving the above result. In the case of sparites and chalks, there are significant negative correlations between porosity and % calcite cement, which suggests that increasing calcite cement progressively fills the pore-space.

It is apparent that the significant correlation coefficients ($P < 1\%$) between velocity and mean grain-size of the various petrographical factors (Table 7.5) are again related to the velocity/porosity inverse relationship (Section 6.3.2), as shown by corresponding significant correlation coefficients of opposite sign between porosity and these factors.

7.3.2 Multiple Regression Analysis

a) Sparites

Twenty independent variables were used initially, followed by 16, which included a combination of intraclasts, ooliths and pellets (Section 4.5.3), and finally 14, which included allochems. The results of these analyses are given in Table 7.6. The maximum percentage error to within which velocity can be estimated, computed from the ratio:

$$\frac{\text{Observed Velocity} - \text{Estimated Velocity}}{\text{Estimated Velocity}} \times 100$$

for the observation with the maximum error, is also given.

TABLE 7.6

Results of Linear Multiple-Regression Analysis - Sparites (N = 128)

$N_I = 20$

$V = 5339 - 78\,\phi - 148F + 17\,P\% + 1.5\,MO \pm 453$ ..... Eq. 7.1

$R = 0.912$, $r_{V\phi} = -0.80$, $r_{VF} = -0.25$, $r_{VP\%} = +0.35$, $r_{VMO} = +0.19$

Max. error = 30.9%

$N_I = 16$ (Including OIP% & MOIP); $N_I = 14$ (Including A% & MA).

$V = 6078 - 92\,\phi - 203F - 33\,Ss\% \pm 470$ ..... Eq. 7.2

$R = 0.904$; $r_{V\phi} = -0.87$, $r_{VF} = -0.34$, $r_{VSs\%} = -0.22$

Max. error = 32.9%

INDEX

N_I = Number of Independent Variables R = Multiple correlation coefficient

$r_{V\phi}$ etc. = Partial correlation coefficients between velocity and the independent variables.

Plots of velocity against each independent variable included in the equations, are shown in Figs. 7.1 - 7.5. The simple linear regression equations relating velocity to porosity (as described later) are also illustrated in Fig. 7.1.

A study of the partial correlation coefficients shows porosity to be the major velocity-controlling factor. The minor importance of the remaining independent variables in the equations, is also shown by the partial correlation coefficients. The variable fabric, in the form of both preferred shell- and mineral-orientation, is present in both equations,

Fig. 7.1 Relationships between velocity and porosity

—— Sparites (n = 128)

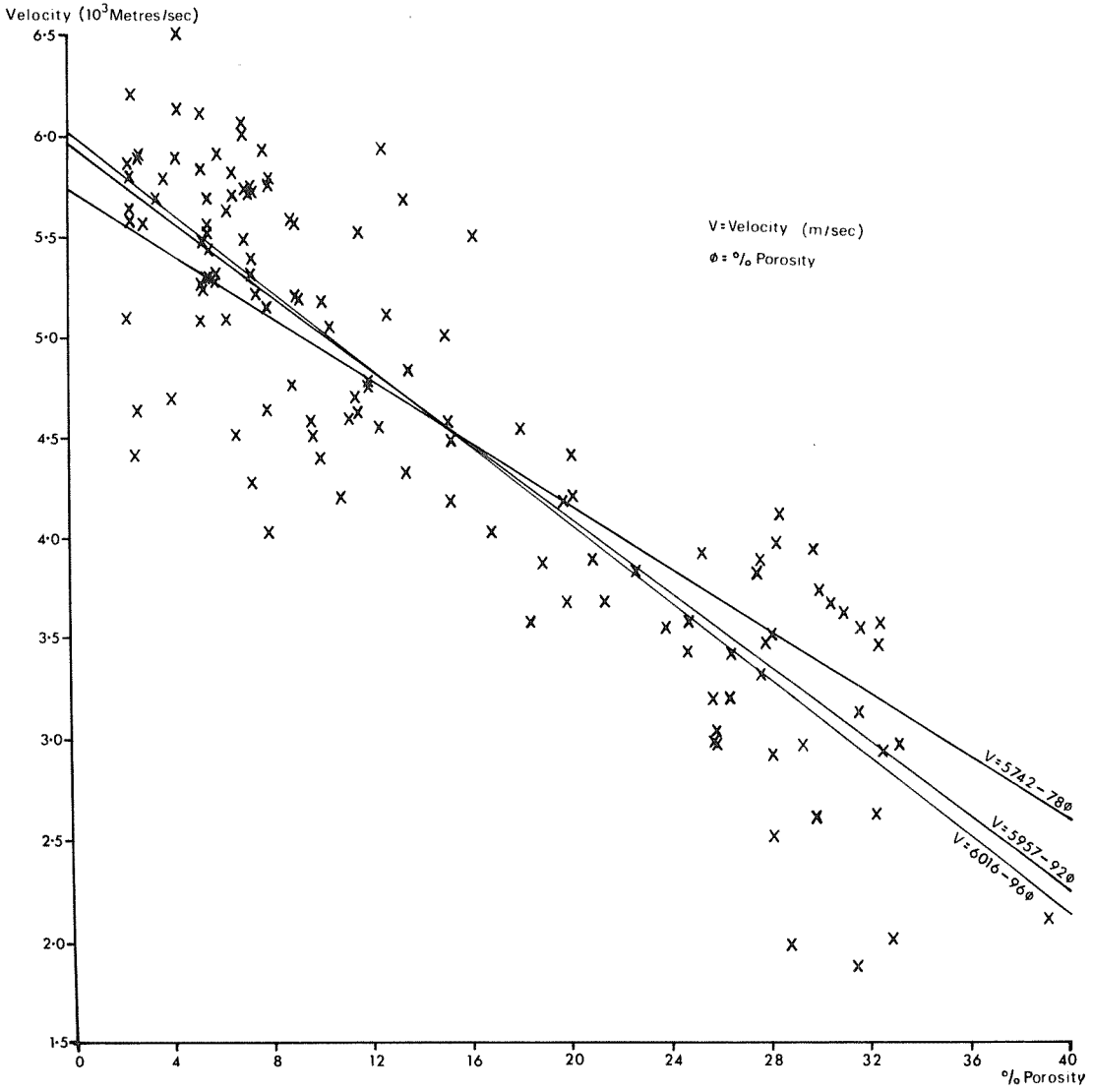


Fig. 7.2 Variation of fabric with velocity
—— Sparites (n = 128)

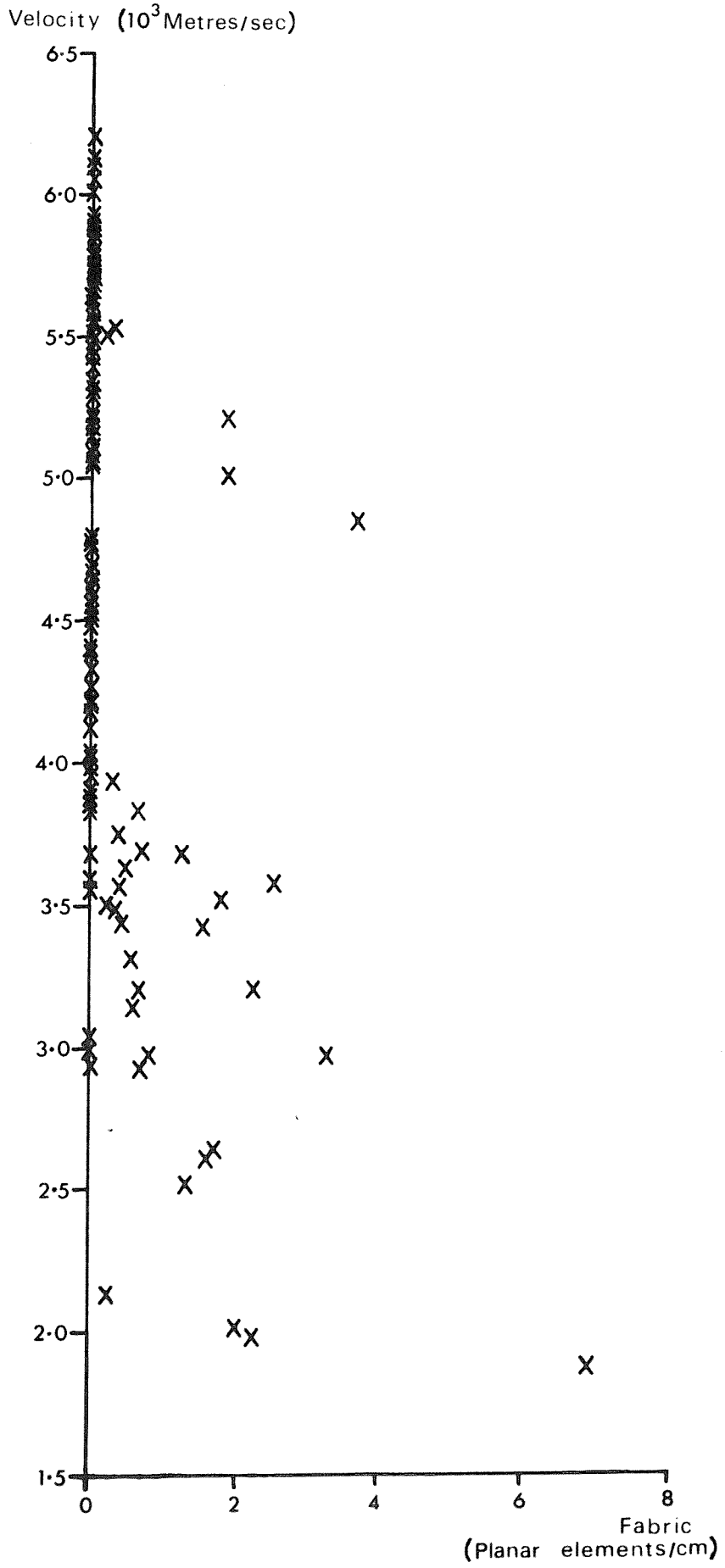


Fig. 7.3 Variation of pellet content with velocity
—— Sparites (n = 128)

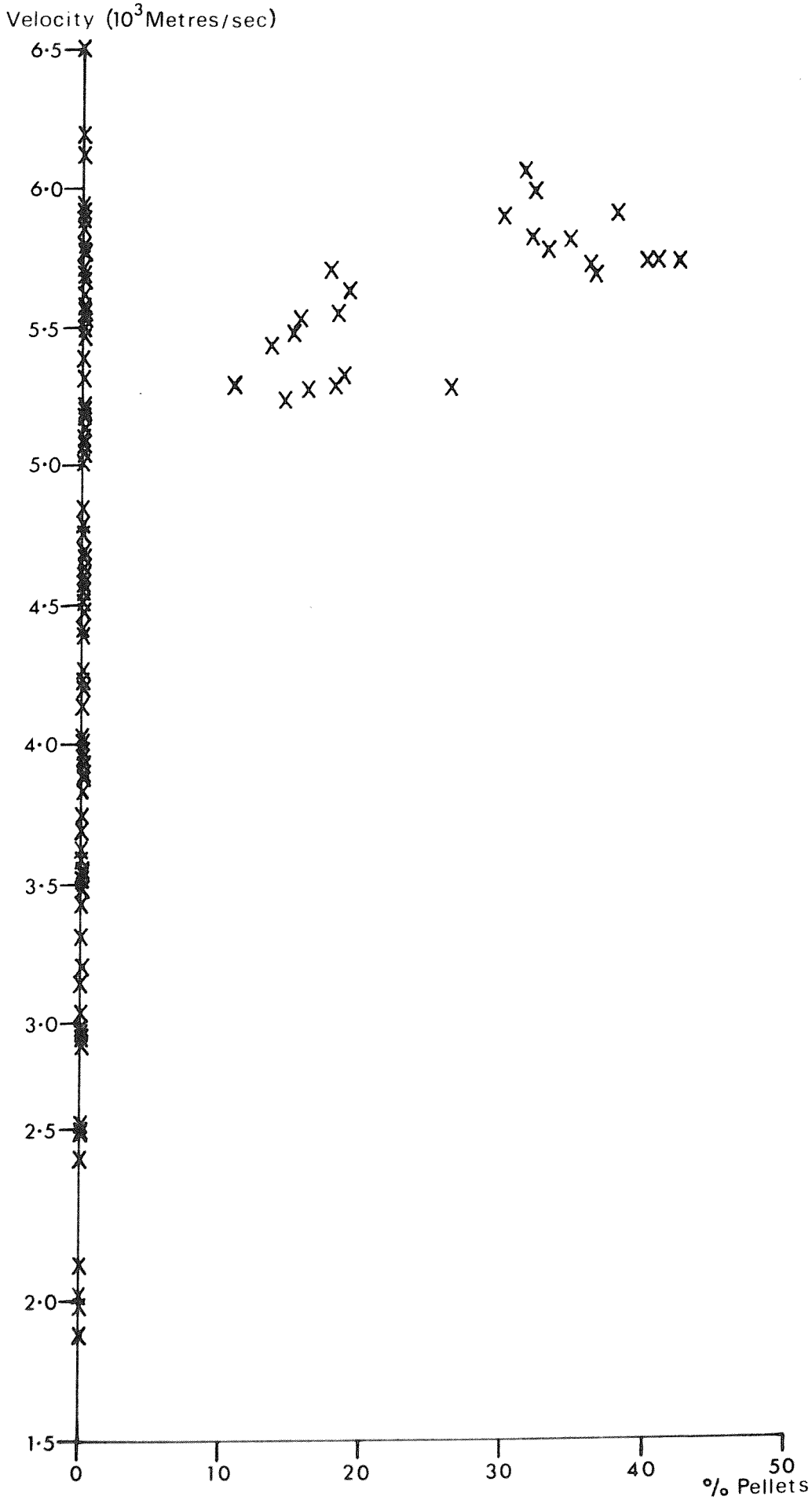


Fig. 7.4 Variation of oolith mean size with velocity
—— Sparites (n = 128)

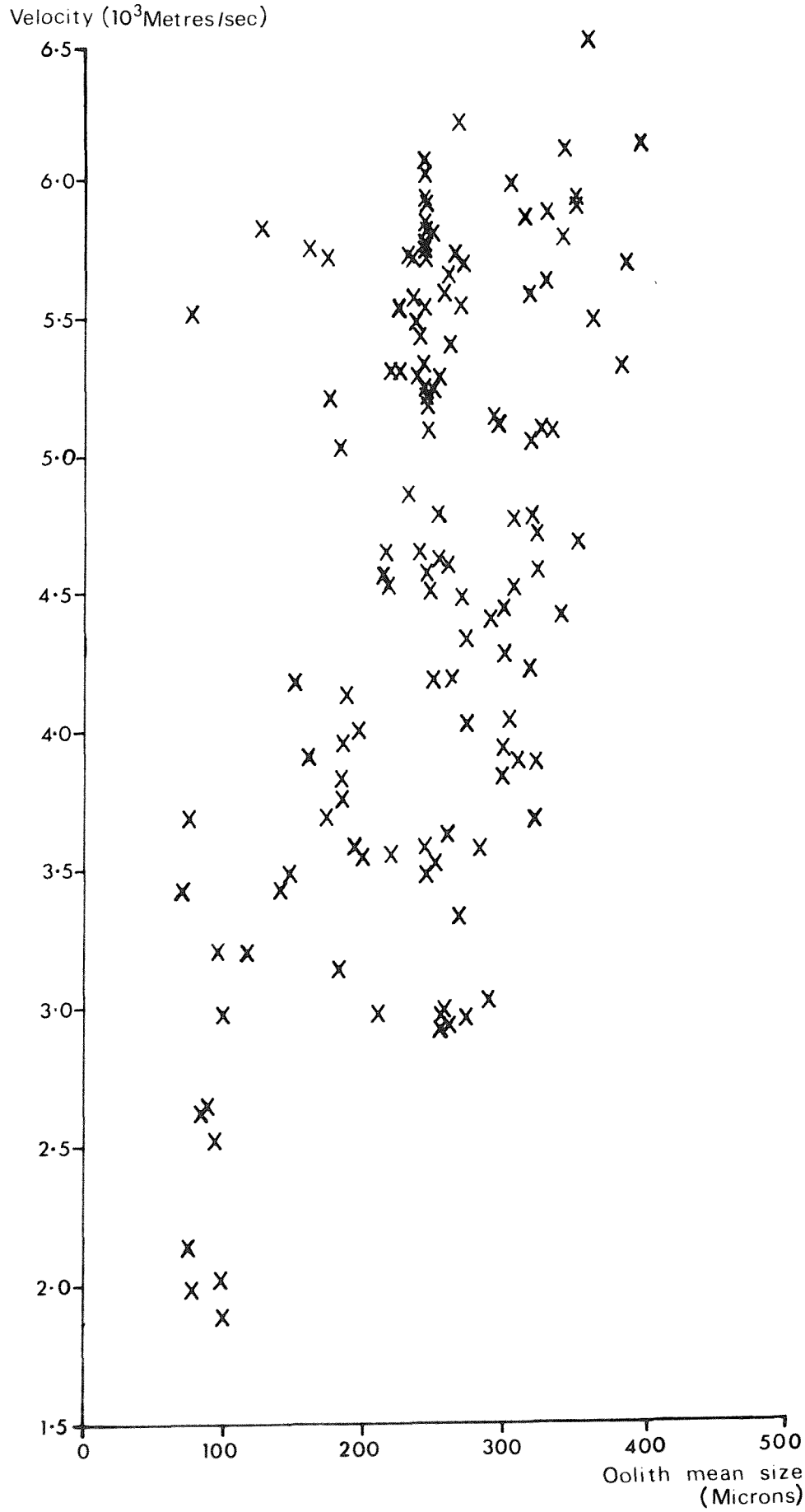
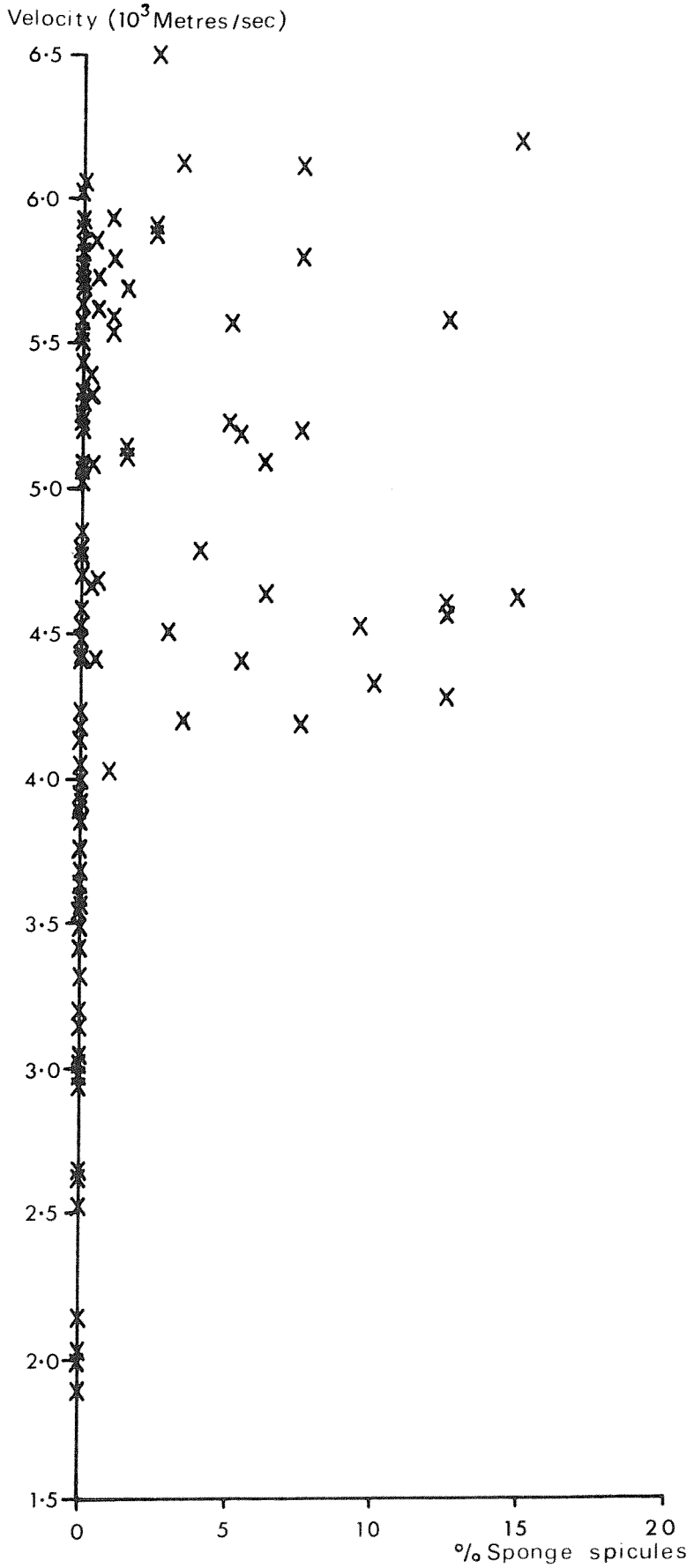


Fig. 7.5 Variation of sponge spicule content with velocity
—— Sparites (n = 128)



forming an inverse relationship with velocity. The importance of this relationship and its effect on velocity/lithostratigraphical relationships described in Chapter 5, has previously been discussed (Section 7.3.1). However, its importance cannot be overemphasised, since 75% of the core-specimens studied do not possess any visible fabric. The inclusion of fabric and other apparently significant independent variables in the regression equations could be due to a reduction in the accuracy of the multiple regression analysis caused by the inclusion of a highly-correlated independent variable, i.e. porosity (Buchan et. al., 1972). However, beyond this explanation it is interesting to speculate as to how the other variables contribute to the velocity-variation. Increase in oolith mean size (MO) results in increasing velocity and it is suggested that this could be related to the radial structure of the oolith, which is defined by a series of calcite fibres formed by inversion from aragonite (Carozzi, 1960), (Plates 4.21; 6.8). The presence of these calcite fibres, which in certain cases extend across the entire diameter of the oolith, might reduce the least-time path of the elastic-waves compared to that in the surrounding material.

In the case of % sponge spicules (Ss%), included in Eq. 7.2, and notwithstanding the fact that only 33% of the core-specimens studied contain sponge spicules, another explanation is possible for the inverse relationship with velocity (Eq. 7.2). As suggested in Section 4.5.3, it is possible that the presence of hollow sponge spicules results in an increase in the porosity that cannot be determined by the liquid-saturation method used in this study (Section 4.4.2), thus causing a lower velocity than that predicted from the observed porosity.

Analysis of the multiple correlation coefficients, standard errors and maximum errors in velocity-estimation (Table 7.6) indicates that Eq. 7.1 gives a marginally more accurate prediction of velocity. Further analyses, with certain independent variables eliminated, resulted

in equations that did not improve the prediction of velocity. Simple linear regression equations between velocity and porosity were formed by substituting the means of the other independent variables in the multiple regression equations. The resulting equations are given below, together with those computed from simple linear regression analysis between velocity and porosity for the 128 core-specimens used in multiple regression analysis and for the 460 core-specimens used in the study of velocity/porosity/density relationships (Chapter 6; Table 6.3).

$V = 5742 - 78\,\phi \pm 453$ ..... Eq. 7.1a (derived from Eq. 7.1)

$r = -0.912$ Max. error = 30.9%

$V = 5957 - 92\,\phi \pm 470$ ..... Eq. 7.2a (derived from Eq. 7.2)

$r = -0.904$ Max. error = 32.9%

$V = 6016 - 96\,\phi \pm 506$ ..... Eq. 7.3 (derived from simple linear regression; N=128)

$r = -0.886$ Max. error = 38.7%

$V = 5816 - 90\,\phi \pm 439$ ..... Eq. 7.4 (derived from simple linear regression; N=460)

$r = -0.890$ Max. error = 37.9%

Equations 7.1a, 7.2a and 7.3 are illustrated in Fig. 7.1 and Eq. 7.4 in Fig. 6.6. Only a small improvement in the prediction of velocity from porosity is apparent by taking into consideration the effects of either fabric, % pellets and oolith mean size or fabric and % sponge spicules. 83% of the velocity-variation is accounted for by regression between velocity and porosity according to the best velocity-prediction equation, i.e. Eq. 7.1a, and 79% according to Eq. 7.4. It is evident from the similarity between Eq. 7.3 and Eq. 7.4 that the sample population used for the multiple regression analysis is fully representative of the entire population used for the simple linear regression analysis (Section 6.3.2).

To conclude, porosity is the dominant velocity-controlling parameter in sparites from the Portland Group, with approximately 80% of

the velocity-variation being due to linear regression between velocity and porosity. Velocity can be predicted to within a maximum possible error of about 38% using porosity alone, and to within about 31% using porosity together with fabric, % pellets and oolith mean size. Further discussion with reference to previous work, is made in Section 7.4.

b) Chalks

Analysis was made initially using 17 independent variables, and then repeated using 15, which included pellets and calcite cement combined, since these parameters show close affinities (Section 4.5.2). Finally, 13 independent variables were used, which included allochems. The three separate analyses resulted in the same multivariate equation, and this, together with the appropriate statistics, is given in Table 7.7.

TABLE 7.7

Results of Linear Multiple-Regression Analysis - Chalks (N = 31)

N_I = 17; N_I = 15 (Including CP% & MCP); N_I = 13 (Including A% & MA)

$V = 5691 - 84\,\phi + 8.5\,MCv \pm 285$ ..... Eq. 7.5

$R = 0.943$; $r_{V\phi} = -0.94$, $r_{VMCv} = +0.41$

Max. error = 12.2%

Plots of velocity against each independent variable present in this multivariate equation (Eq. 7.5) are given in Figs. 7.6 and 7.7.

A study of the partial correlation coefficients indicates that porosity is the dominant velocity-controlling parameter. Calcite vein mean grain-size is relatively unimportant, as shown by the large scatter of data in Fig. 7.7. The effect of increasing calcite vein mean grain-size in producing a velocity increase, may be a result of the sparry calcite in the veins reducing the least-time travel path. There will be a reduction in the number of discontinuities to elastic-wave transmission, with increasing crystal size, thus causing an increase in velocity. However, since only 32% of the core-specimens studied contain calcite

Fig. 7.6 Relationships between velocity and porosity
—— Chalks (n = 31)

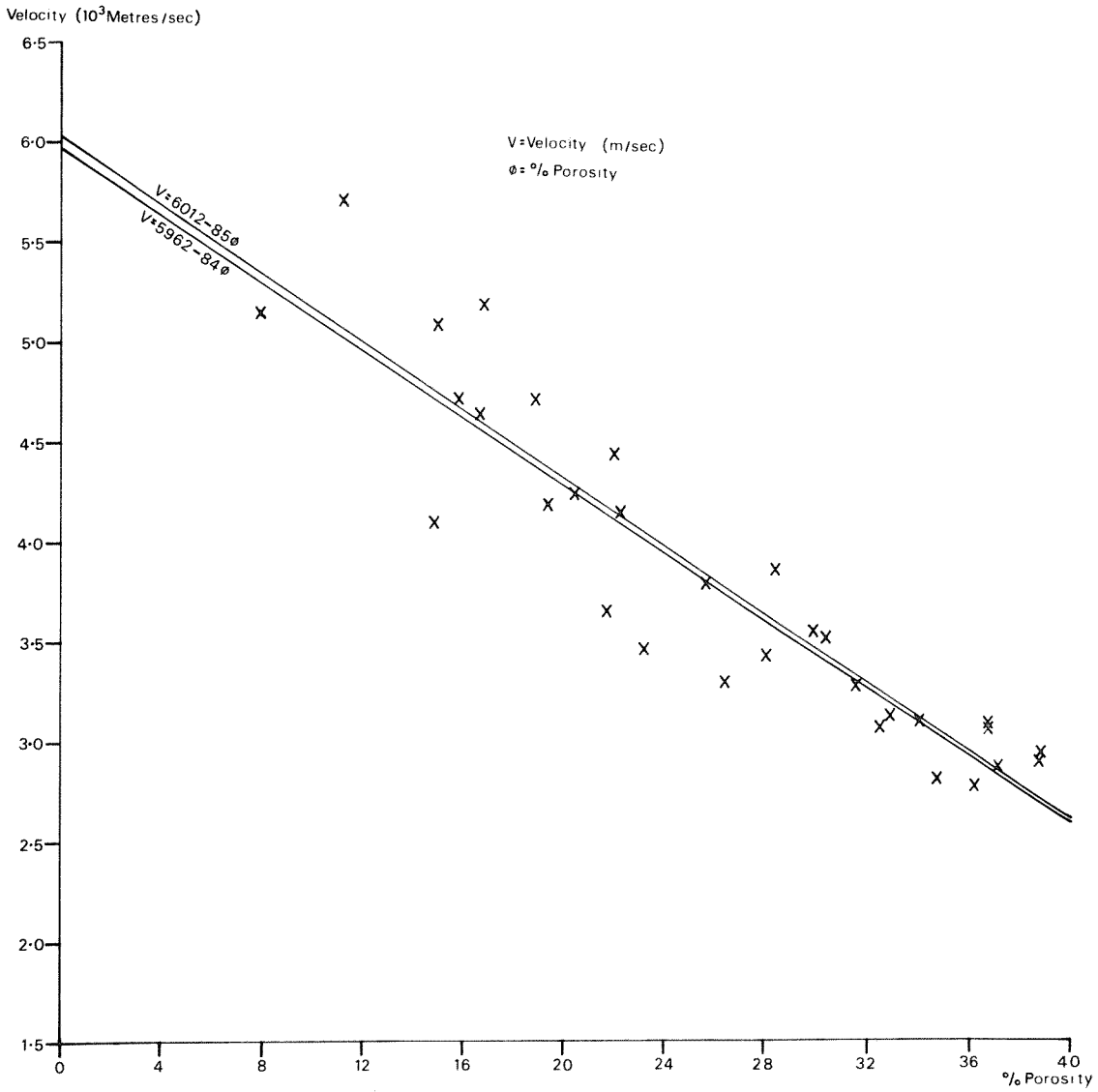
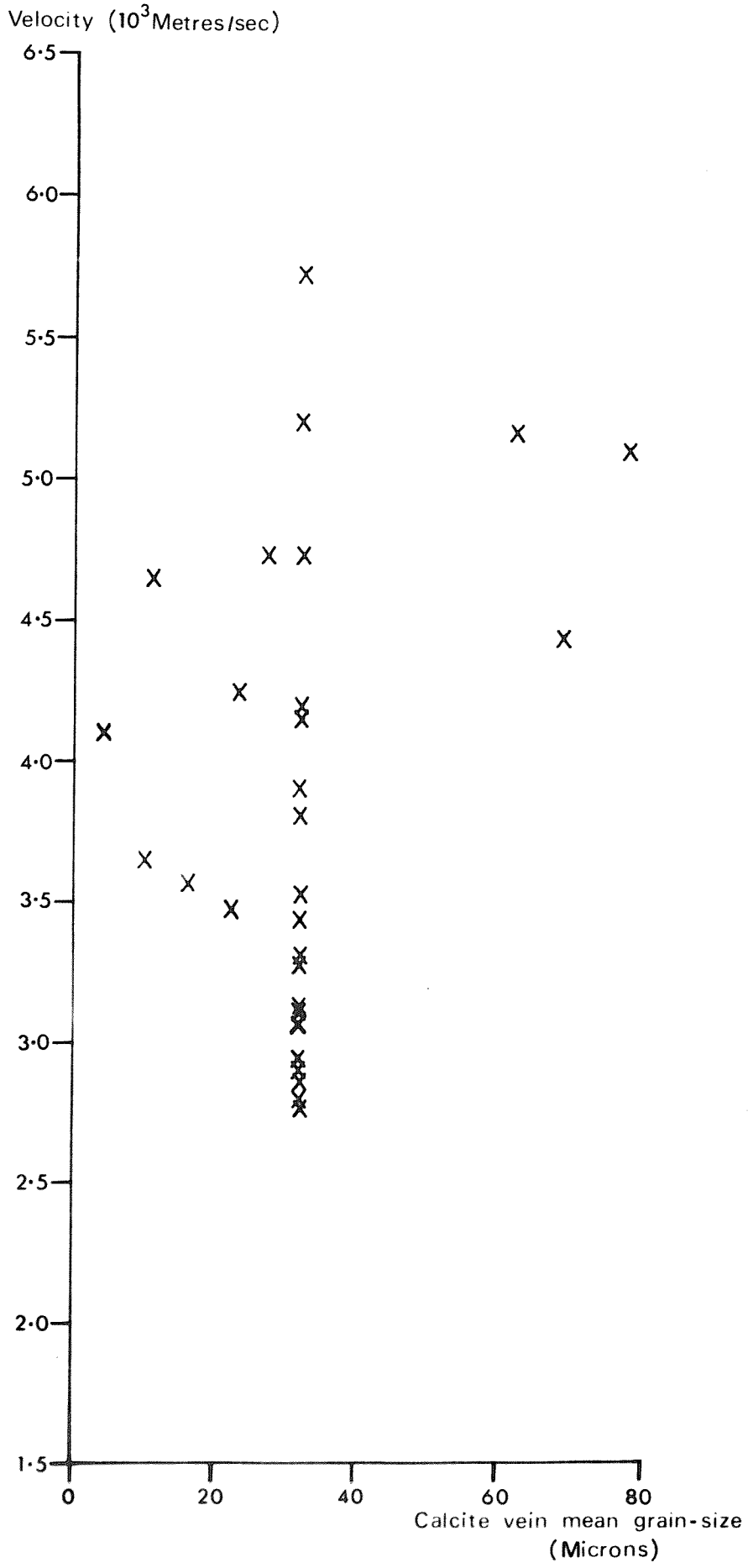


Fig. 7.7 Variation of calcite vein mean grain-size with velocity — Chalks (n = 31)



veins, the inclusion of this variable in the multivariate equation may be an artefact of reduction in accuracy of the multiple regression analysis (Buchan, et. al., 1972).

The multivariate equation (Eq. 7.5) was transformed to a simple linear regression equation (Eq. 7.5a), relating velocity to porosity, by the substitution of the mean of calcite vein mean grain-size. This enabled a direct comparison to be made with the simple linear regression equations. The equations are as follows:

$V = 5962 - 84\,\phi \pm 285$ ..... Eq. 7.5a
(derived from Eq. 7.5)
$r = -0.943$ Max. error = 12.2%

$V = 6012 - 85\,\phi \pm 307$ ..... Eq. 7.6
(derived from simple linear regression; N = 31)
$r = -0.931$ Max. error = 14.0%

$V = 6173 - 92\,\phi \pm 239$ ..... Eq. 7.7
(derived from simple linear regression; N = 162)
$r = -0.919$ Max. error = 17.1%

Equations 7.5a and 7.6 are illustrated in Fig. 7.6 and Equation 7.7 in Fig. 6.7.

A study of the maximum errors in velocity-estimation shows that only a marginal improvement in the prediction of velocity from porosity is obtained by taking into consideration the effect of calcite vein mean grain-size (Eq. 7.5a). Thus, as with sparites, porosity is the dominant velocity-controlling parameter. Velocity can be predicted to within a maximum possible error of 17% using porosity alone, and to within 12% using porosity together with calcite vein mean grain-size. However, this latter prediction is based upon only 31 observations.

c) Micrites

Thirteen independent variables were used initially in the analysis. The resulting multivariate equation (Eq. 7.8) includes the independent variable calcite cement mean grain-size, which has a constant value of approximately one micron (Table 7.3), and a simple correlation

coefficient of 0.0 (Table 7.5). The analysis was therefore repeated, with this variable excluded. The resulting equation (Eq. 7.9) is identical to the initial equation (Eq. 7.8) with the exception of calcite cement mean grain-size, which is replaced by a constant term. Equation 7.9 includes the variable fabric, which is present in only 18% of the core-specimens. A further analysis was made with this variable excluded, and a final equation computed (Eq. 7.10), relating velocity directly to porosity. Plots of velocity against each of the independent variables included in the equations, excluding calcite cement mean grain-size, are shown in Figs. 7.8 - 7.10. The results of the three analyses are given in Table 7.8.

TABLE 7.8

Results of Linear Multiple-Regression Analysis - Micrites (N = 38)

$N_I = 13$

$V = 5115\ Mcc + 10\ B\% - 364F \pm 353$ ..... Eq. 7.8

$R = 0.641$; $r_{VMcc} = +0.99$, $r_{VB\%} = +0.33$, $r_{VF} = -0.64$

Max. error = 17.6%

$N_I = 12$ (Omitting Mcc)

$V = 5115 + 10B\% - 364F \pm 353$ ..... Eq. 7.9

$R = 0.641$; $r_{VB\%} = +0.33$, $r_{VF} = -0.64$

Max. error = 17.6%

$N_I = 11$ (Omitting Mcc and F)

$V = 5789 - 56\ \phi \pm 379$ ..... Eq. 7.10

$R = 0.547$; $r_{V\phi} = -0.55$

Max. error = 14.8%

The occurrence of calcite cement mean grain-size and % bioclasts in the multivariate equations is possibly an artefact produced by the two highly correlated variables, porosity and fabric. There is a simple

correlation coefficient of 0.0 between velocity and calcite cement mean grain-size, whereas % bioclasts has a positive partial correlation coefficient ($r_{VB\%}$ =+0.33) but a negative simple correlation coefficient ($r_{VB\%}$ = -0.013) (Table 7.5) with velocity.

Although fabric, in the form of preferred shell orientation, is present in only 18% of the core-specimens studied, this variable forms a significant velocity-controlling parameter in Equations 7.8 and 7.9, showing an inverse relationship with velocity. Its effect on velocity/lithostratigraphical relationships and velocity-aeolotropy (Chapter 5) has previously been discussed (Section 7.3.1).

The most accurate prediction of velocity is obtained using a simple linear relationship with porosity (Eq. 7.10). However, this equation was derived using the data from 38 core-specimens, and a more reliable equation was obtained using the data from 128 core-specimens in the study of velocity/porosity relationships (Section 6.3.2; Table 6.3). The equations are as follows:

$V = 5789 - 56\,\phi \pm 379$ ... Eq. 7.10
(derived from multiple regression analysis; N=38)
$r = -0.547$ Max. error = 14.8%

$V = 5929 - 68\,\phi \pm 312$ ... Eq. 7.11
(derived from simple linear regression analysis; N = 128)
$r = -0.656$ Max. error = 17.8%

Eq. 7.10 is illustrated in Fig. 7.8 and Eq. 7.11 in Fig. 6.8. Equation 7.11 has a higher correlation coefficient than the three multivariate equations, and enables velocity to be predicted from porosity to within a maximum error of 17.8%. However, the correlation coefficient (-0.656) means that only 43% of the velocity-variation can be attributed to regression between velocity and porosity. It is therefore probable that both % porosity and pore-structure are the major velocity-controlling parameters in micrites (as described in Chapter 6), with fabric having a minor effect.

Fig. 7.8 Relationship between velocity and porosity
—— Micrites (n = 38)

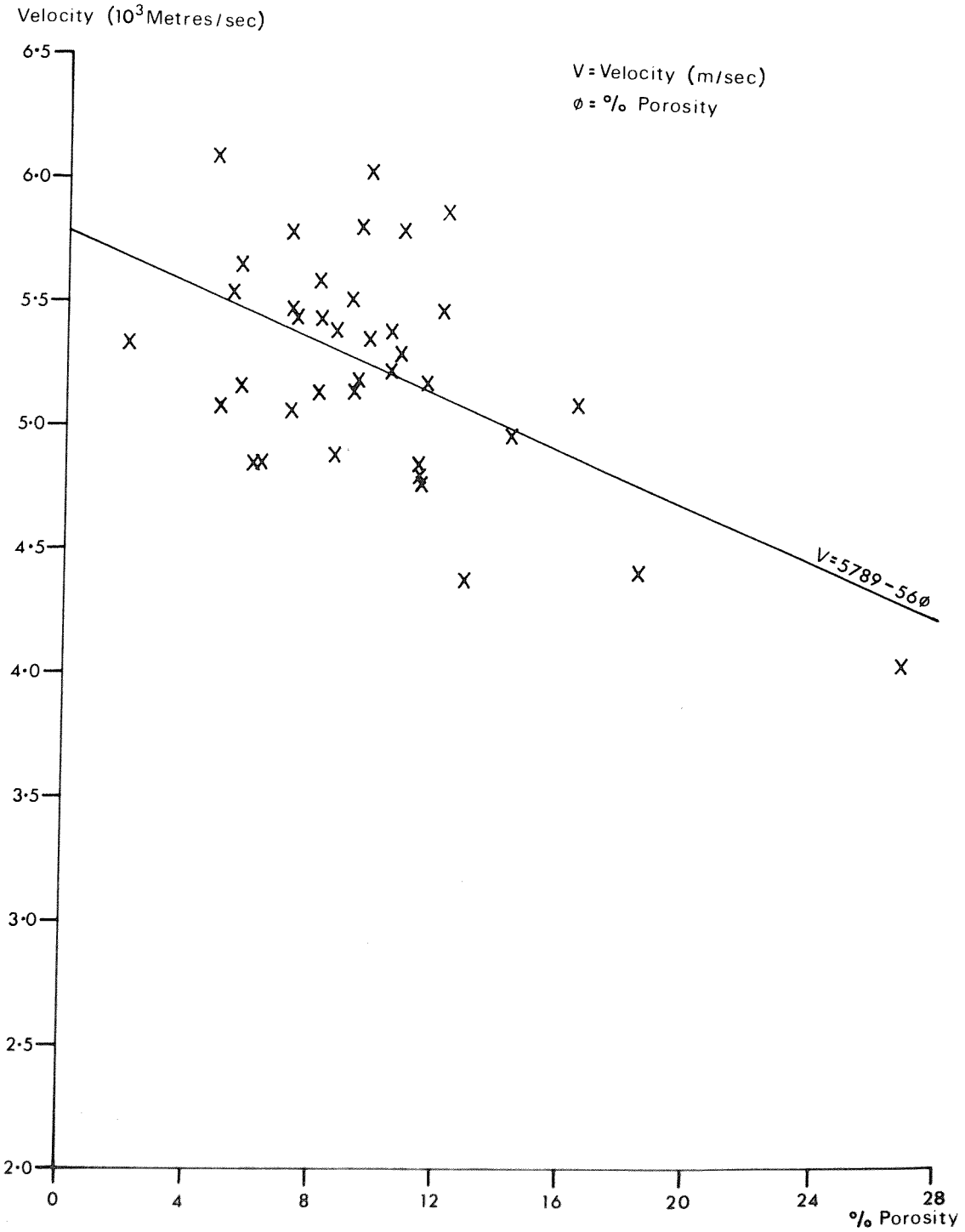


Fig. 7.9 Variation of fabric with velocity
—— Micrites (n = 38)

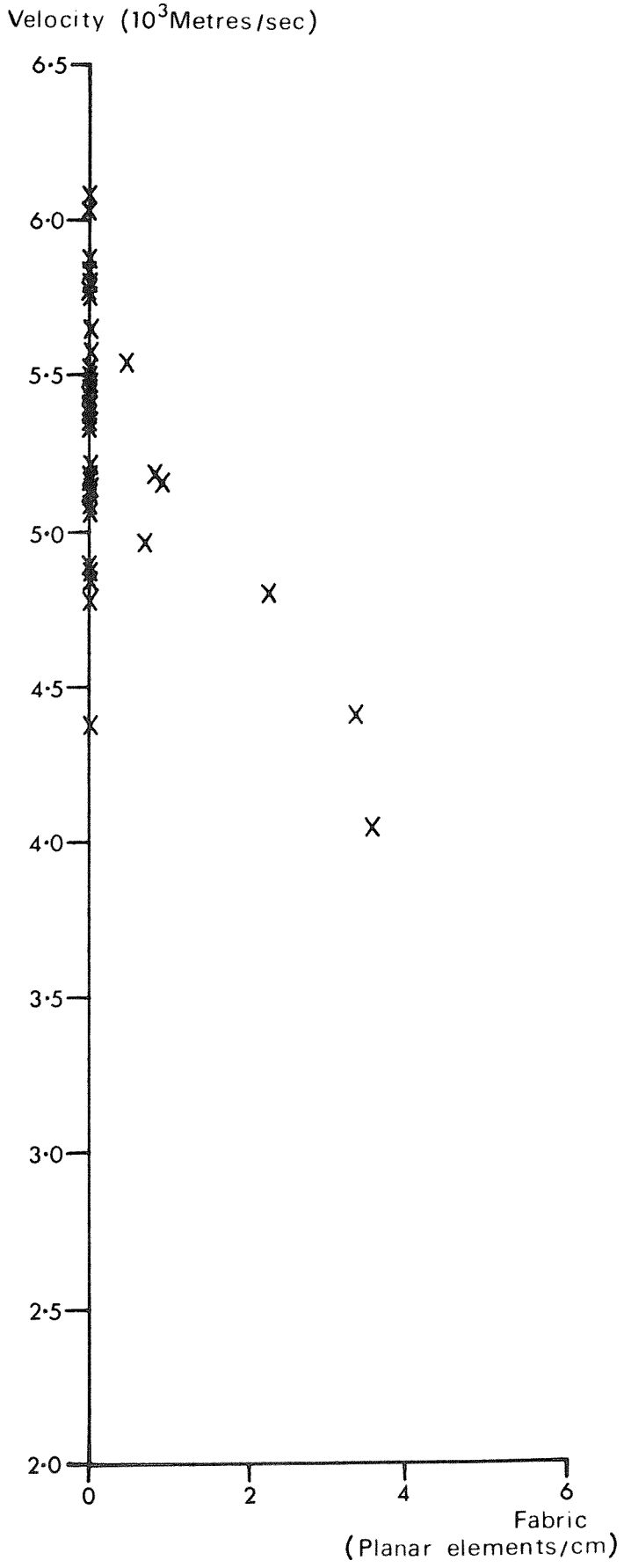
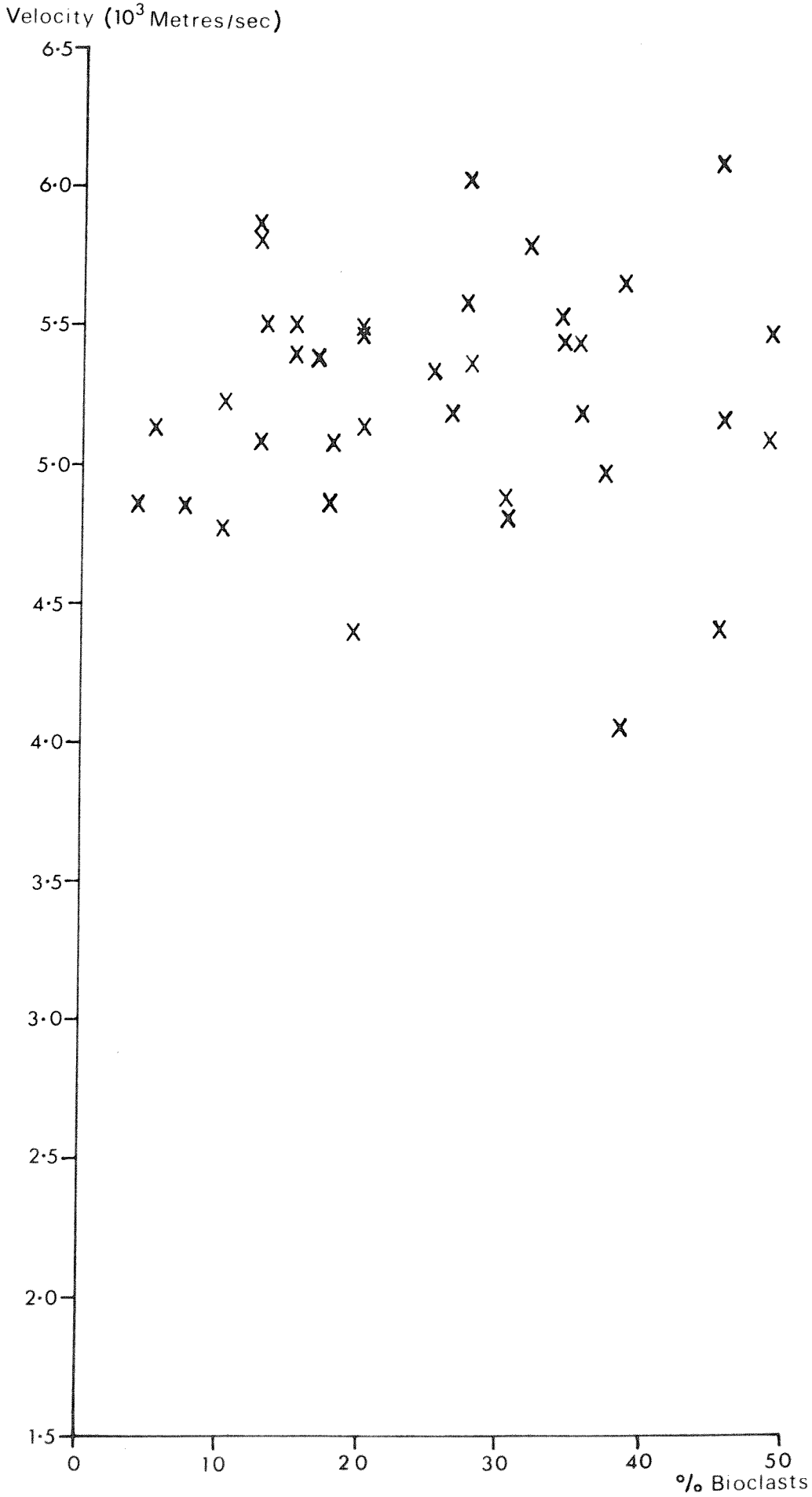


Fig. 7.10 Variation of bioclast content with velocity
—— Micrites (n = 38)



d) Microsparites

The results of the analysis are given in Table 7.9.

TABLE 7.9

Results of Linear Multiple-Regression Analysis - Microsparites (N = 48)

$N_I = 12$

$V = -63F + 5D\% + 46\ CV\% + 37\ B\% + 47\ Mcc + 76\ MD \pm 336$ ..... Eq. 7.12

$R = 0.873$; $r_{VF} = -0.49$, $r_{VD\%} = +0.43$, $r_{VCV\%} = +0.30$, $r_{VB\%} = +0.46$, $r_{VMcc} = +0.79$, $r_{VMD} = +0.88$

Max. error = 24.4%

$N_I = 11$ (Omitting CV%)

$V = -58F + 5\ D\% + 34\ B\% + 47\ Mcc + 79\ MD \pm 348$ ..... Eq. 7.13

$R = 0.843$; $r_{VF} = -0.44$, $r_{VD\%} = +0.37$, $r_{VB\%} = +0.42$, $r_{VMcc} = +0.78$, $r_{VMD} = 0.88$

Max. error = 22.8%

$N_I = 10$ (Including CD% and MCD)

$V = 4776 - 67\ \phi - 67\ F + 22\ B\% - 2\ MB + 16\ MDg \pm 302$ ..... Eq. 7.14

$R = 0.933$; $r_{V\phi} = -0.81$, $r_{VF} = -0.55$, $r_{VB\%} = +0.31$, $r_{VMB} = -0.45$, $r_{VMDg} = +0.41$

Max. error = 28.1%

Twelve independent variables were used initially in the analysis. The resulting multivariate equation (Eq. 7.12) includes the independent variable % calcite veins, and since calcite veins are present in only 31% of the core-specimens studied, and since this variable has a non-significant simple correlation coefficient with velocity (+0.024, Table 7.5), the analysis was repeated with this variable excluded. The effect of combining calcite and dolomite, the carbonate components (Section 4.5.3), was also studied (Eq. 7.14). Each of the independent variables included in the equations (Table 7.9) has been plotted against velocity (Figs. 7.11 - 7.19).

A study of partial correlation coefficients shows that porosity, which is highly-correlated with velocity, is not the sole major velocity-controlling parameter. Calcite and dolomite mean grain-sizes both have highly-significant ($P < 0.1\%$) partial and simple correlation coefficients with velocity, and this could be related to the velocity/porosity inverse relationship (Section 7.3.1). However, since there is a positive relationship between velocity and these parameters, it could also be a result of the reduction in the number of discontinuities to elastic-wave propagation with increasing grain-size.

The variables fabric and % bioclasts are included in all three equations (Table 7.9). Fabric in the form of preferred mineral orientation forms an inverse relationship with velocity for reasons previously described (Section 7.3.1). It is probably directly related to variations in velocity/lithostratigraphical relationships and velocity-aeolotropy (Chapter 5), and preferred pore-orientation (Section 6.3.3b). The importance of % bioclasts as a significant velocity-controlling parameter is probably related to the velocity/porosity inverse relationship, as suggested in the study of simple correlation coefficients (Section 7.3.1).

The inclusion in the equations of % calcite veins and possibly % dolomite, and detrital grains mean size, all having non-significant simple correlations with velocity, are probably artefacts (Buchan et. al., 1972). However, the positive correlation between % dolomite and velocity is in accord with conclusions drawn from velocity/porosity studies (Section 6.3.2). Dolomite, calcite and quartz form the bulk mineralogy of the core-specimens, and since dolomite has a higher velocity than calcite or quartz (Birch, 1942; Kisslinger, 1953; Sarmiento, 1961), increasing % dolomite results in an increase in velocity. However, a study of simple correlation coefficients (Section 7.3.1) indicates that the positive velocity/% dolomite correlation is related to a corresponding negative porosity/% dolomite correlation. The effect of detrital grains

mean size could be similar to that of calcite and dolomite mean grain-sizes described above.

The inverse relationship between velocity and bioclast mean size (Eq. 7.14) is apparently related to a positive correlation between porosity and bioclast mean size (Section 7.3.1).

The effect of variation in mineral content on velocity/porosity relationships, as suggested in Section 6.3.2 and inferred from the results of porosity/density relationships (Section 6.2), is not as pronounced as expected. Only % dolomite forms an independent variable significantly related to velocity (Eq. 7.12; Eq. 7.13), and it is probable that this is a direct result of the velocity/porosity inverse relationship, rather than differences in velocity between dolomite, calcite and quartz.

Comparisons are made between the multivariate equations and the simple linear regression equations derived from both the velocity/porosity data used in the multiple regression analysis and that used in the study of velocity/porosity relationships (Section 6.3.2). These show that the prediction of velocity from porosity is improved by including the parameters present in the multivariate equations. The simple linear equations, together with that derived from Equation 7.14 by the substitution of the means of the independent variables, are as follows:

$V = 5221 - 67\,\phi \pm 302$ ..... Eq. 7.14a
(derived from Eq. 7.14)

$r = -0.933$ Max. error = 28.1%

$V = 5617 - 91\,\phi \pm 414$ ..... Eq. 7.15
(derived from simple linear regression analysis; N = 48)

$r = -0.856$ Max. error = 30.4%

$V = 5613 - 93\,\phi \pm 394$ ..... Eq. 7.16
(derived from simple linear regression analysis; N = 148)

$r = -0.836$ Max. error = 29.6%

Equations 7.14a and 7.15 are illustrated in Fig. 7.11 and Eq. 7.16 in Fig. 6.9. A study of the correlation coefficients indicates that the maximum percentage velocity-variation due to regression between

velocity and porosity is obtained when the effects of fabric, % bioclasts, bioclast mean size and detrital grains mean size are also considered (Eq. 7.14; Eq. 7.14a). This maximum, 87%, contrasts with the maxima for the simple linear regression equations, i.e. 73% (Eq. 7.15) and 70% (Eq. 7.16).

In terms of velocity-estimation, the best equation is Eq. 7.13. However, Eq. 7.14 or Eq. 7.14a have the lowest standard error of velocity estimate and highest correlation coefficient.

7.4 Discussion and Conclusions

The results of both linear multiple-regression analysis and simple correlation coefficients confirm the conclusions of Chapter 6 on velocity/porosity relationships, that porosity is the major velocity-controlling parameter in sparites and chalks, and to a lesser degree in micrites and microsparites. For micrites there is substantiation of the conclusion of Section 6.3.3c, that pore-structure is an important velocity-controlling parameter. The velocity-variation in sparites and chalks can be almost completely accounted for by linear regression between velocity and porosity, since the percentage variation ascribed to the regression is only marginally increased when the effect of physical parameters other than porosity, are considered. In contrast, for microsparites, the analysis clearly shows that several physical parameters in addition to porosity, are important velocity-controlling variables.

A study of the multivariate equations indicates that fabric forms an inverse relationship with velocity in all the limestone-types except chalks. The planar fabric elements probably impede elastic-wave propagation, thus reducing the velocity, in a manner similar to that described by Rinehart et. al. (1961) for critically-oriented open cracks. This empirically confirms the results of velocity/lithostratigraphy (Section 5.4) and velocity-aeolotropy studies (Section 5.3). Planar fabric

elements, lying approximately in the horizontal plane, result in lower vertical velocities and velocity-aeolotropy in certain lithostratigraphic units of the Portland Group where the dip is horizontal. The influence of fabric, for example, preferred mineral-orientation, bedding, preferred-orientation of calcite optic axes, preferred-orientation of planar voids, cleavage and foliation, on velocity-aeolotropy and velocity-anisotropy for a wide range of rock-types, using laboratory methods, has previously been described (Prasada Rao, 1947; Giesel, 1963; Koefoed et. al., 1963; Christensen, 1965; King, 1966; Pros et. al., 1967; Klima et.al., 1968; Thill et. al., 1969). However, empirical relationships between velocity and fabric were not apparently derived by these authors, so that direct comparisons with the results established here cannot be made.

The positive relationships between velocity and % bioclasts in micrites and microsparites, are probably either a result of corresponding inverse relationships between porosity and % bioclasts, or errors due to the inclusion of a highly-correlated independent variable in the analysis (Buchan et. al., 1972). This is substantiated from the study of simple correlation coefficients (Section 7.3.1). However, Buchan et. al., (1972) suggested that an increase in velocity with calcium carbonate content in recent marine sediments, also noted by previous workers (Sutton et. al., 1957; Schreiber, 1968), was related to a corresponding increase in grain-size associated with the influx of bioclasts composed of calcium carbonate. No meaningful comparisons can be made with the Portland Group limestone-types since bioclasts form only a minor component of the calcium carbonate content.

Previous studies on parameters other than porosity, fabric and % bioclasts present in the multivariate equations is limited. It is probable that, as in the case of % bioclasts, the inclusion of these remaining parameters in the equations is a result of either corresponding inverse relationships with porosity, or errors in the multiple regression analysis. For microsparites however, where porosity cannot be related to the total

observed variation in velocity, mean grain-sizes of calcite and dolomite may possibly be directly related to velocity. There is a positive relationship with velocity for both minerals, and this could be a result of the number of grain-contacts decreasing with increasing grain-size. This would decrease the number of discontinuities to elastic-wave transmission and give a velocity-increase. Mineral-composition is also relevant, as shown from Eq. 7.12 and Eq. 7.13 (Table 7.9). An increase of 10 microns in the grain-size of calcite would result in a velocity-increase of 470 metres/sec. whereas a similar increase for dolomite would result in a velocity increase of 790 metres/sec, thus reflecting the velocities in random aggregates of these minerals (Kisslinger, 1953). Positive relationships between grain-size and velocity have previously been described in connection with studies made on recent marine sediments (Sutton et. al., 1957; Hamilton, 1959; Horn et. al., 1968; Schreiber, 1968; Hamilton, 1970; Buchan et. al., 1972). In most instances, empirical relationships between velocity and grain-size have been derived. However, reports of the effect of grain-size on velocity in consolidated rocks are apparently limited to brief statements that velocity is dependent on grain-size distribution and shape (Wyllie et. al., 1956), and on crystallinity in limestones (Press, 1966). Section 6.2 shows that in the case of microsparites, variation in mineral content affects velocity (Section 6.3.2). Random aggregates of the principal minerals, calcite, dolomite and quartz have velocities of 6350 m./sec., 6750 m./sec. (Kisslinger, 1953), and 5900 m./sec. (Wyllie et. al., 1956) respectively. However, only % dolomite is included in the multivariate equations. The positive relationship with velocity is probably not entirely a result of a random aggregate of dolomite having the highest velocity, since there is a corresponding negative correlation between porosity and % dolomite. This could be related to the dolomitisation process reducing the porosity (Section 7.3.1). A similar effect in some Carboniferous limestones and dolomites has been described by Kisslinger (1953). Both

these Carboniferous limestones and dolomites and the Portland Group limestone samples were derived from surface outcrops. However, the effect of mineral variation on velocity is apparently more pronounced at depths in excess of 700 metres (Sarmiento, 1961), possibly as a result of compaction reducing the porosity. Sarmiento (1961) found an inverse relationship between velocity and calcite and quartz content for some Palaeozoic dolomites. In addition to variations in the proportions of calcite, quartz and dolomite, the presence of clays, shales or marls, on both a micro- and macroscale, tends to affect the velocity in both limestones and sandstones (Oliphant, 1950; Schwaetzer, 1958; Berry, 1959; Kuiper et. al., 1959; Nikitin, 1962; Jankowsky, 1970). Also, there is an inverse relationship between velocity and residual material in limestones (Kisslinger, 1953). However, only traces of clays were found in the limestone specimens from the Portland Group (Section 4.5.4.3) so that possible relationships with velocity could not be investigated. The non-carbonate fraction consists mainly of quartz with minor amounts of feldspar and glauconite (Section 4.5.4.3), and results of multiple analysis indicate that the non-carbonate fraction, i.e. % detrital grains, is not a significant velocity-controlling parameter. However, in the case of chalks and sparites, there are highly-significant ($P < 0.1\%$) simple negative correlation coefficients between velocity and % detrital grains.

In conclusion, the results of linear multiple-regression analysis using a maximum of 20 physical parameters including porosity and combinations of petrographical parameters, show that porosity is the most significant and important velocity-controlling variable in sparites and chalks from the Portland Group. In microsparites, several other physical parameters, of which calcite and dolomite mean grain-sizes are most significant, accompany porosity as the velocity-controlling variables. In micrites, factors other than porosity become the major cause of velocity-variation. They are probably pore-structure (Section 6.3.3c)

and to a lesser extent fabric (Section 7.3.2c). Fabric is also a significant velocity-controlling variable in sparites and microsparites, and the inverse relationships between velocity and fabric empirically confirm the conclusions of Chapter 5 on velocity-variation and velocity-aeolotropy within lithostratigraphic units of the Portland Group.

Fig. 7.11 Relationships between velocity and porosity
—— Microsparites (n = 48)

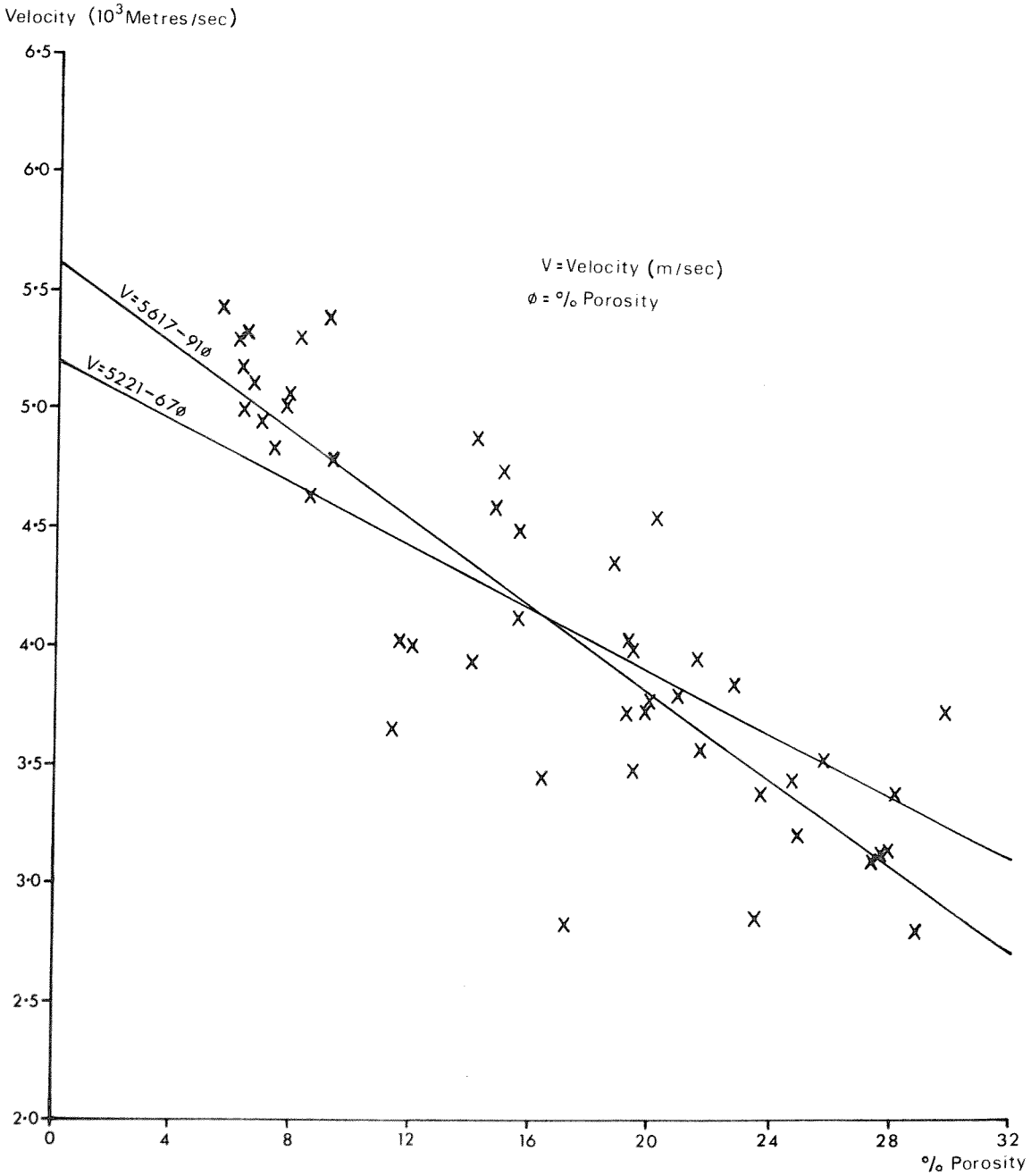


Fig. 7.12 Variation of fabric with velocity
—— Microsparites (n = 48)

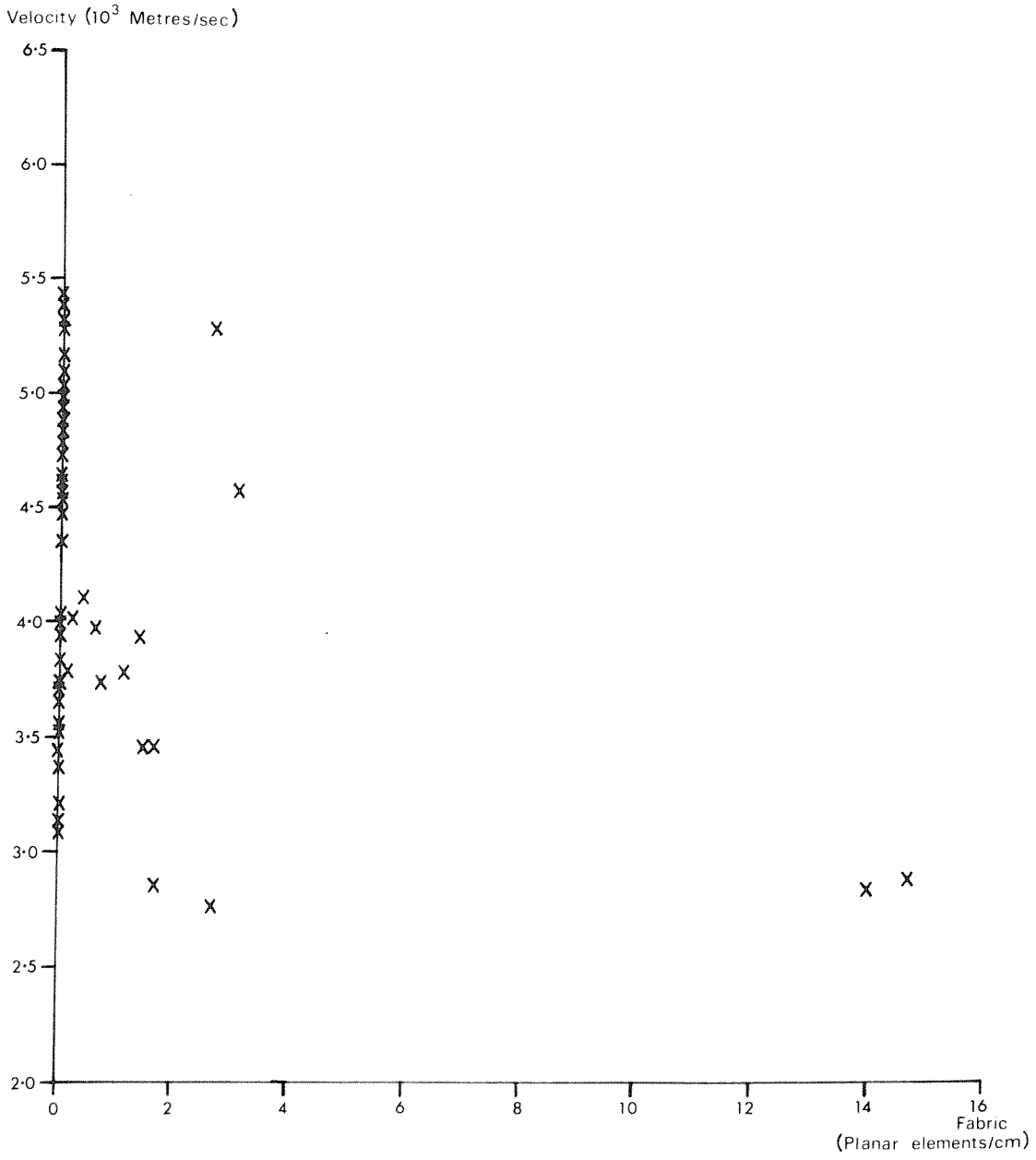


Fig. 7.13 Variation of calcite mean grain-size with velocity
—— Microsparites (n = 48)

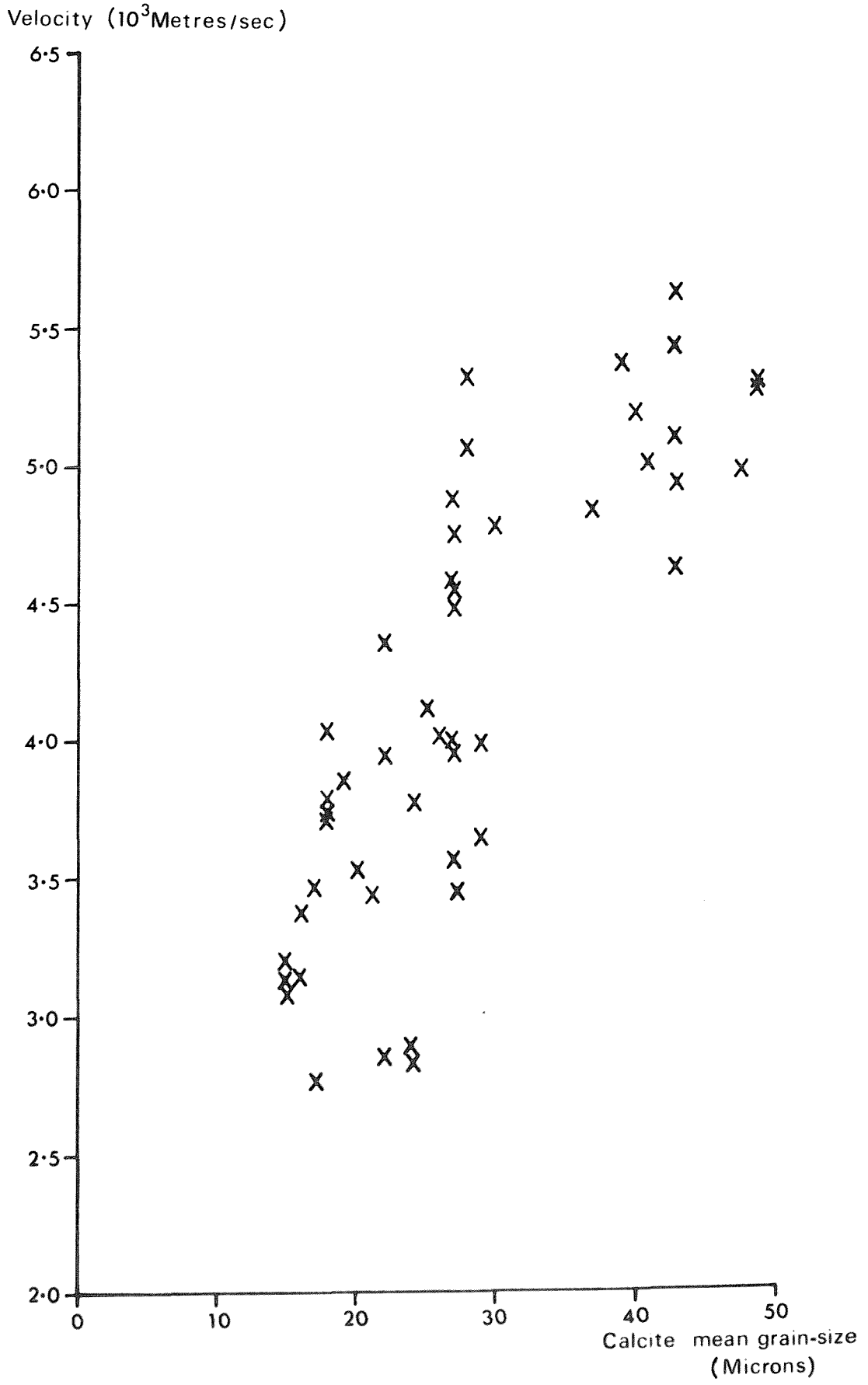


Fig. 7.14 Variation of dolomite mean grain-size with velocity — Microsparites (n = 48)

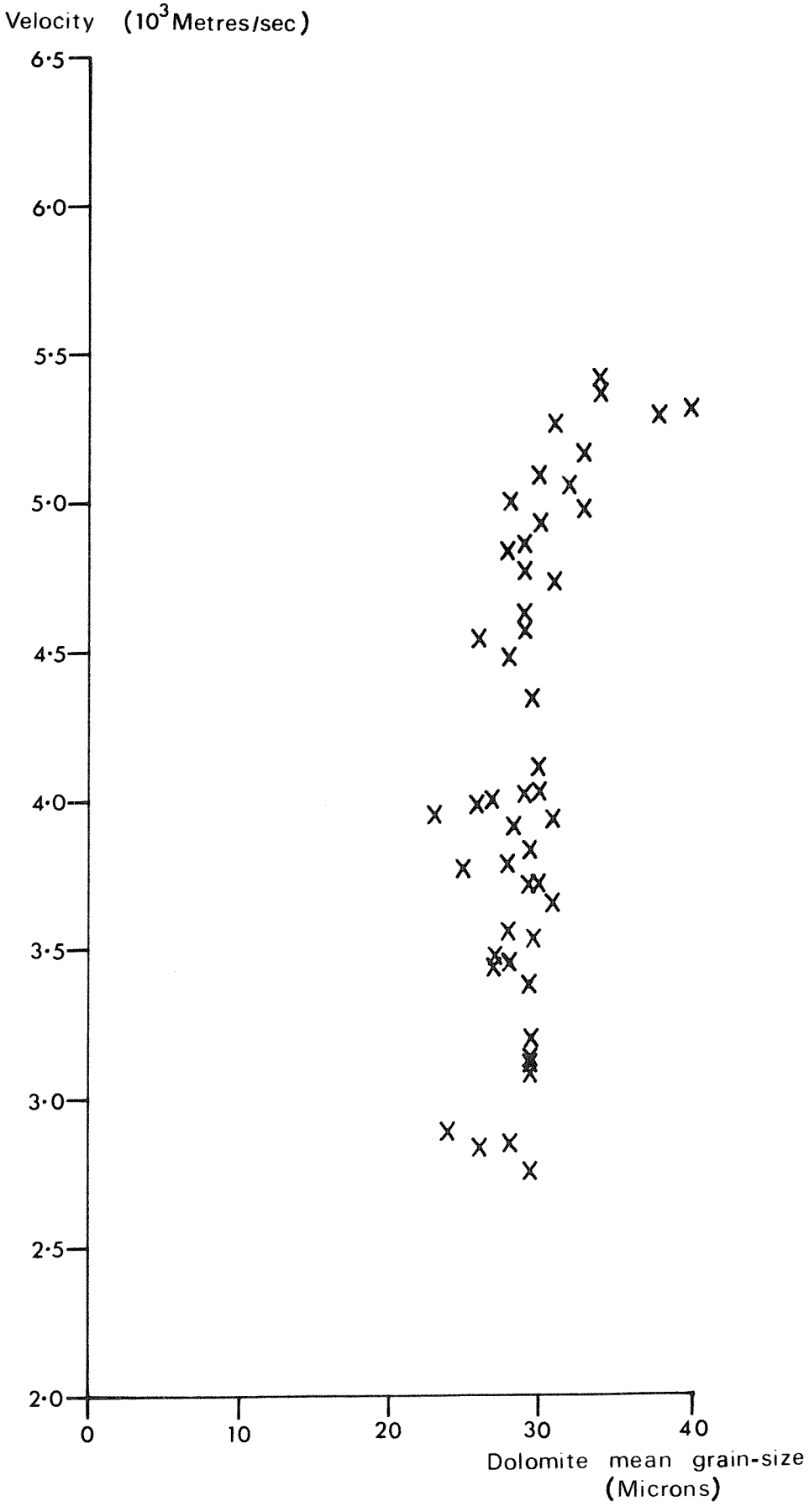


Fig. 7.15 Variation of dolomite content with velocity
—— Microsparites (n = 48)

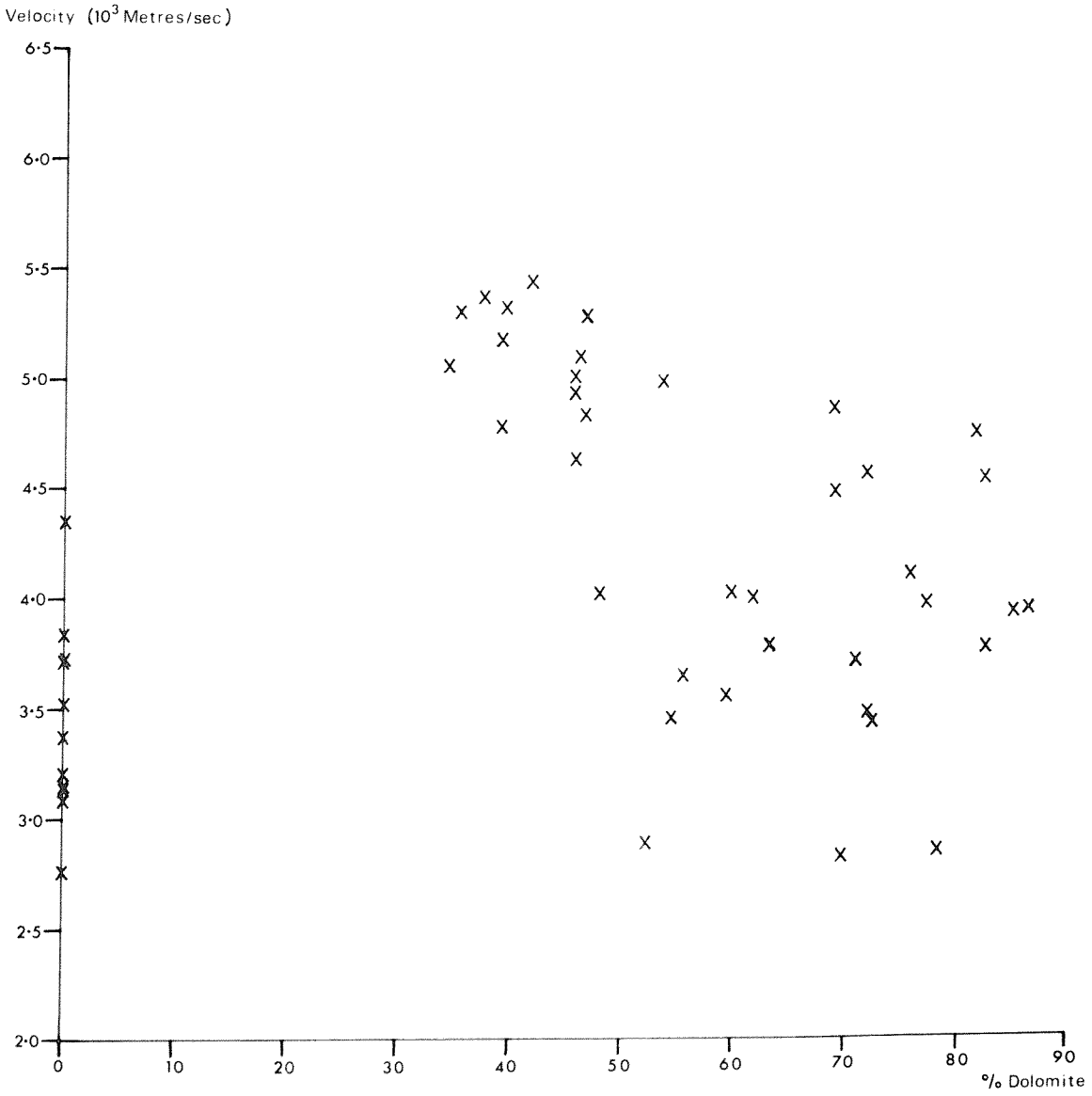


Fig. 7.16 Variation of calcite vein content with velocity
—— Microsparites (n = 48)

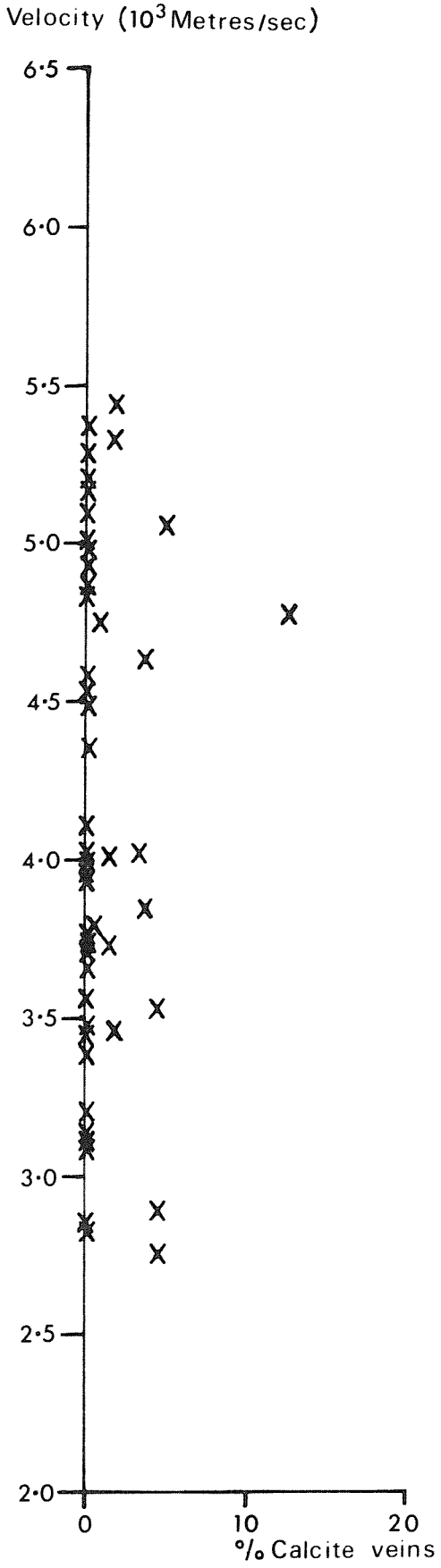


Fig. 7.17 Variation of bioclast content with velocity
—— Microsparites (n = 48)

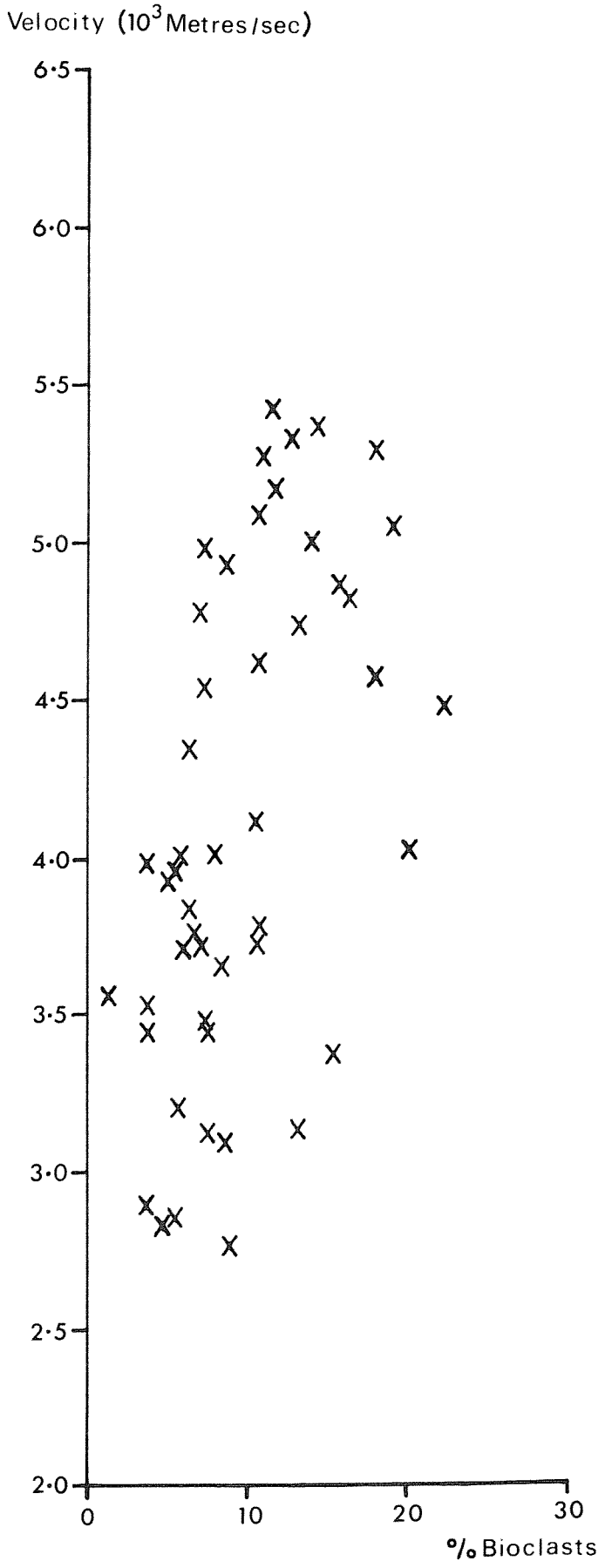


Fig. 7.18 Variation of bioclast mean size with velocity
—— Microsparites (n = 48)

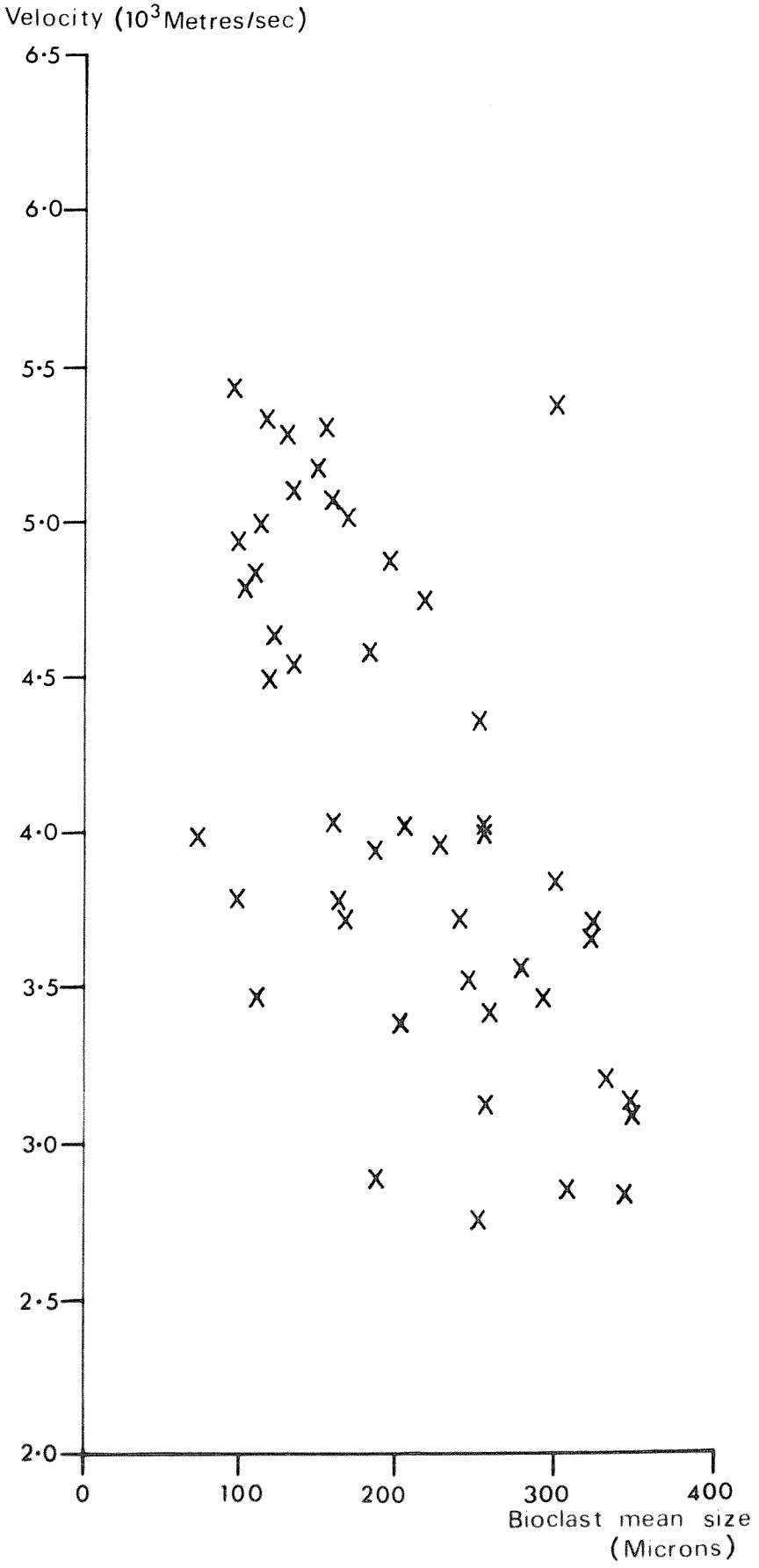
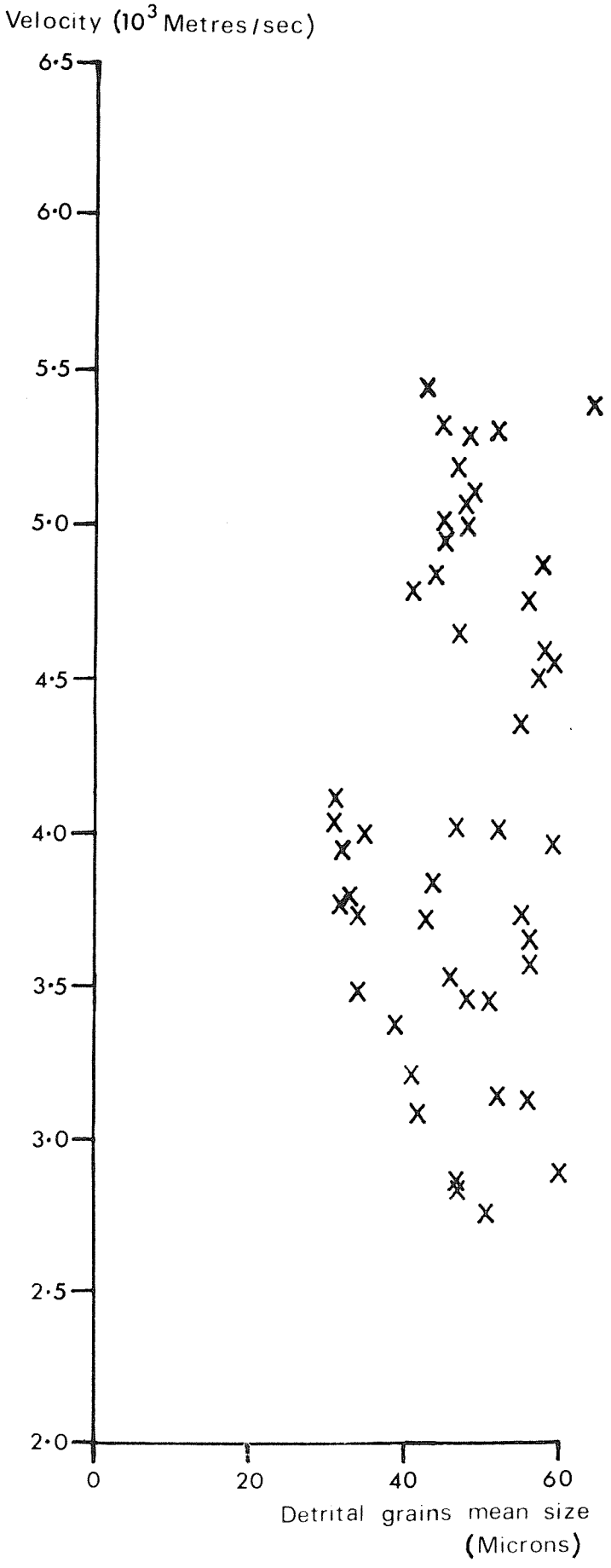


Fig. 7.19 Variation of detrital grains mean size with velocity
—— Microsparites (n = 48)



CHAPTER 8

CONCLUSIONS

The most important conclusion to emerge from the study is the importance of porosity as a major velocity-controlling parameter in limestones from the Portland Group. The relationship between velocity and porosity can take the form of a simple linear function, a polynomial function, an exponential function, a logarithmic function, a linear-logarithmic function and a reciprocal-velocity function. However, for predictions of velocity from porosity, it is recommended that the simple linear function:-

$$V = -88\phi + 5833 \pm 434$$

where V is velocity in metres/sec. and ϕ is % porosity, be used, since only marginal differences exist between the degree of correlation of this and the other functions. This empirical relationship enables velocity to be estimated from porosity to within a maximum error of 40%, in the Portland Group limestones investigated. When these limestones are classified into four basic types, better estimates of velocity can be obtained using the appropriate empirical relationships. Maximum errors in velocity-estimation are thus reduced to a minimum of 17% in the case of chalks and a maximum of 38% in the case of sparites.

Relationships between velocity and density are similar but inverse to those between velocity and porosity. This is as expected from the results of porosity/density studies, which show highly-significant negative correlations between these parameters. However, in the case of microsparites, there is a lower degree of correlation between porosity and density, and this is considered to be a result of variations in the calcite, dolomite and quartz contents.

It is interesting to note the differences observed between the simple correlation coefficients of velocity versus porosity for each limestone-type. In the case of sparites and chalks, and to a lesser extent

microsparites, variation in velocity can be attributed to regression between velocity and porosity, and to experimental error. In the case of micrites, where only 43% of the variation in velocity is due to regression between velocity and porosity, other velocity-controlling factors are probably involved. The results of pore-structure investigations and multiple regression analysis indicate that pore-size, pore-morphology and pore-distribution and, to a lesser extent fabric in the form of preferred shell-orientation, probably have considerable effects on velocity in micrites. These parameters, together with experimental error, may possibly account for the remaining velocity-variation. In the case of microsparites, where 70% of the variation in velocity is due to regression between velocity and porosity, variations in calcite, dolomite and quartz contents may cause some of the remaining velocity-variation.

The results of pore-structure investigations give some indication of possible modes of elastic-wave propagation in the four limestone-types, notwithstanding the limited number of specimens used. Highly-significant correlations between velocity and porosity for the limestone-types suggest that the least-time paths of elastic-wave energy tend to traverse both matrix and pores, with the exception of micrites. In micrites, the regularly-distributed, rounded micromolds, which are dominant at porosities of less than 12%, probably result in the least-time paths being confined to the matrix only. At porosities greater than 12%, the pores become random both in shape and distribution, and there is a general increase in size, resulting in the least-time paths traversing both matrix and pores, as suggested for the other limestone-types. This conclusion has been substantiated by the results of a limited study of the effect of water-saturation on velocity.

The implication that pore-structure does not affect velocity-variation in the other three limestone-types is to be expected, since, unlike

micrites, pore-type, random pore-distribution and pore-morphology are constant throughout the porosity ranges studied.

Multiple regression analysis, using 22 independent variables, confirms that porosity is a dominant velocity-controlling parameter in all four limestone-types. Excepting microsparites, only marginal improvements in degree of correlation can be obtained from the empirical relationships derived from multiple regression analysis, as compared with those derived from simple linear analysis. However, the empirical relationships derived from multiple regression analysis could be subject to some error as described by Buchan et. al. (1972).

Extrapolation of the simple empirical relationships between velocity and porosity to the limiting velocity, i.e. velocity at zero porosity, shows that none of the four limestone-types behaves as a quasi-isotropic aggregate of randomly-oriented calcite crystals in terms of elastic-wave propagation. This conclusion is further substantiated by petrographic analysis.

Correlation studies between velocity and lithostratigraphy in the Portland Group confirm the uncertainties encountered by earlier workers. The wide range of both directional and non-directional velocities in the sequence of lithostratigraphic units studied, together with an absence of velocity-data for several units in these sequences, prevent accurate identification of lithostratigraphic units on a velocity basis.

Results of the limited study of outcrop velocities lead to similar conclusions. Wide ranges of velocity result from differences in the degree of fracturing within lithostratigraphic units. This prevents any meaningful correlation between velocity and these units.

The mean outcrop velocities are considerably less than the mean ultrasonic velocities for the same units. It is concluded that these differences are the result of differences in "sample" size, with outcrop

velocity being the velocity observed for approximately 30 metres of *in situ* fractured limestone, whereas ultrasonic velocity is that in a less than 10 cm. long core-specimen containing no visible fractures. Fracturing is considered to be the most important parameter, which reduces outcrop velocities.

Statistical analysis of velocity-aeolotropy showed that approximately one third of the units studied displayed a definite anisotropy. These units consist of sparite, micrite or microsparite limestone-types. In most cases, this anisotropy is probably caused by horizontally-oriented planar fabric elements. In such units, the mean horizontal velocities exceed the mean vertical velocities, probably as a result of these planar fabric elements increasing the discontinuities to elastic-wave transmission in the vertical direction. This association between planar fabric elements and velocity is confirmed empirically by the results of multiple regression analysis. The presence of preferred pore-orientation, noted in the study of pore-structure, is apparently related to pore-type, i.e. moldic or intercrystal, which in turn is directly related to preferred shell- or mineral-orientation. Pore-orientation has the same effect on velocity as these planar fabric elements.

The study has largely fulfilled the original objectives in that a comprehensive analysis of possible factors affecting velocity in limestones has been achieved. The analysis confirms the importance of porosity as a major velocity-controlling parameter. Additionally, for the first time, the importance of distinguishing between limestone-types is recognised as is the effect of pore-orientation, pore-type, pore-morphology, pore-size and pore-distribution on velocity.

The study clearly demonstrates the need for further research. Although an extremely wide range of porosities is covered, the limitation to four basic limestone-types suggests that further work is needed on other limestone-types, e.g. biolithites, dolomicrites. It would be important also to investigate limestone-types of differing geologic age. Both the pore-structure analysis and the study of velocity/water-saturation relationships showed that both factors controlled velocity and elastic-wave propagation in limestones. However, these studies were limited to small sample populations. Further verification of these observations would be desirable. Such studies should be extended to other limestone-types. It was the intention of the author to study the effect of permeability on velocity, since this is related to both the effective porosity and the diameter of the intercommunicating pores. Because of priority given to other studies, this study was not made, but it is the author's opinion that any future investigations should include a study of permeability. Further studies of pore-size within core-specimens, using methods such as mercury-injection (Pirson, 1958), would probably produce useful results.

Another aspect of the study not extensively investigated is outcrop velocities. The results show the importance of fracturing, and more detailed investigation would be useful. There may be an advantage in detailed studies of limestone blocks of the order of one cubic metre, which would provide material for investigation intermediate between that studied using the hammer seismic method and that studied using the laboratory method.

Any future study must take into consideration the effect of any velocity-anisotropy.

REFERENCES

AMERICAN COMMISSION OF STRATIGRAPHIC NOMENCLATURE, 1961. Code of stratigraphical nomenclature. Bull. Amer. Assoc. Petrol . Geol., 45, 645-665.

ARKELL, W.J., 1933. The Jurassic System in Great Britain. Clarendon Press, Oxford, 681 pp.

ARKELL, W.J., 1935. The Portland Beds of the Dorset Mainland. Proc. Geol. Assoc., 46, 301-347.

ARKELL, W.J., 1938. Three tectonic problems of the Lulworth District: Studies on the Middle Limb of the Purbeck Fold. Quart. Jour. Geol. Soc. Lond., 94, 1-54.

ARKELL, W.J., 1947. The geology of the country around Weymouth, Swanage, Corfe, and Lulworth. Mem. Geol. Surv. U.K., xii + 386 pp.

BARKER, R.D. & WORTHINGTON, P.F., 1973. Some hydrogeophysical properties of the Bunter Sandstone of Northwest England. Geoexploration, 11, 151-170.

BATHURST, R.G.C., 1964. The replacement of aragonite by calcite in the molluscan shell wall. In: J. Imbrie & N.D. Newell (Editors), Approaches to paleoecology. John Wiley and Sons, London, pp. 357-376.

BEERS, R.F., 1940. Velocity stratification as an aid to correlation. Geophysics, 5, 15-21.

BERRY, J.E., 1959. Acoustic velocity in porous media. Am. Inst. Min. Metallurgy Petroleum Trans., 216, 262-270, T.P. 8085.

BIOT, M.A., 1956a. Theory of propagation of elastic waves in a fluid-saturated porous solid. I. Low-frequency range. Jour. Acous. Soc. Amer., 28, 168-178.

BIOT, M.A., 1956b. Theory of propagation of elastic waves in a fluid-saturated porous solid. II. High-frequency range. Jour. Acous. Soc. Amer., 28, 179-191.

BIRCH, F., 1942. Handbook of Physical Constants. Geol. Soc. Amer. Spec. Pap., No. 36.

BIRCH, F., 1960. The velocity of compressional waves in rocks to 10 kilobars, Part 1. Jour. Geophys. Res., 65, 1083-1102.

BIRCH, F., 1961. The velocity of compressional waves in rocks to 10 kilobars, Part 2. Jour. Geophys. Res., 66, 2199-2224.

BIRCH, F. & BANCROFT, D., 1938. Elasticity and internal friction in a long column of granite. Bull. Seismol. Soc. Amer., 28, 243-254.

BLAKE, J.F., 1880. On the Portland rocks of England. Quart. Jour. Geol. Soc. Lond., 36, 189-236.

BORN, W.T. & OWEN, J.E., 1935. Effect of moisture upon velocity of elastic waves in Amherst Sandstone. Bull. Amer. Assoc. Petrol. Geol., 19, 9-18.

BROWN, G., 1961, (Editor). The X-ray identification and crystal structures of clay minerals. Min. Soc. Publ. Lond., 544 pp.

BUCHAN, S., McCANN, D.M. & TAYLOR SMITH, D., 1972. Relations between the acoustic and geotechnical properties of marine sediments. Quart. Jour. Engng. Geol., 5, 265-284.

CAROZZI, A.V., 1960. Microscopic sedimentary petrography. Wiley, New York, N.Y., 485 pp.

CHOQUETTE, P.W. & PRAY, L.C., 1970. Geologic nomenclature and classification of porosity in sedimentary carbonates. Bull. Amer. Assoc. Petrol. Geol., 54, 207-250.

CHRISTENSEN, N.I., 1965. Velocity anisotropy in metamorphic rocks. Trans. Amer. Geophys. Union, 46, 162 (abstract only).

CHRISTENSEN, N.I. & RAMANANANTOANDRO, R., 1971. Elastic moduli and anisotropy of dunite to 10 kilobars. Jour. Geophys. Res., 76, 4003-4010.

COPE, J.C.W., 1969. The Portland Beds. In: H.S. Torrens (Editor), International field symposium on the British Jurassic, Excursion No. 1, Guide for Dorset and South Somerset. Geology Dept., Keele University, U.K., pp. 53-57.

CURRAY, J.R., 1956. The analysis of two-dimensional orientation data. Jour. Geology, 64, 117-129.

DAVIES, G.M., 1956. The Dorset coast: a geological guide. Black, London, 128 pp.

DONATA, R.J., O'BRIEN, P.N.S. & USHER, M.J., 1962. Absorption and dispersion of elastic energy in rocks. Nature, 193, 764-765.

DUNOYER DE SEGONZAC, P. & LAHERRERE, J., 1959. Application of the continuous velocity log to anisotropy measurements in northern Sahara; results and consequences. Geophys. Prosp., 7, 202-217.

EWING, M. & CRARY, A.P., 1935. Propagation of elastic waves in limestone. Trans. Amer. Geophys. Union, 2, 100-103.

FAUST, L.Y., 1951. Seismic velocity as a function of depth and geologic time. Geophysics, 16, 192-206.

FAUST, L.Y., 1953. A velocity function including lithologic variation. Geophysics, 18, 271-288.

FITTON, W.H., 1836. Observations on some of the strata between the Chalk and the Oxford Oolite in the southeast of England. Trans. Geol. Soc., 4, 103-388.

FLUGEL, E., FRANZ, H.E. & OTT, W.F., 1968. Review on electron microscope studies of limestones. In: G. Müller & G.M. Friedman (Editors), Recent developments in carbonate sedimentology in Central Europe. Springer, Berlin, pp. 85-97.

FOLK, R.L., 1959. Practical petrographic classification of limestones. Bull. Amer. Assoc. Petrol. Geol., 43, 1-38.

FOLK, R.L., 1962. Spectral subdivision of limestone types. In: W.E. Ham (Editor), Classification of carbonate rocks. Amer. Assoc. Petrol. Geol. Mem. 1, pp. 62-84.

FOLK, R.L., 1965. Some aspects of recrystallisation in ancient limestones. In: R.C. Murray & L.C. Pray (Editors), Dolomitization and limestone diagenesis. Soc. Econ. Paleontologists Mineralogists Spec. Publ. 13, 14-48.

FRIEDMAN, G.M., 1959. Identification of carbonate minerals by staining methods. Jour. Sediment. Petrol., 29, 87-97.

GARDNER, G.H.F., WYLLIE, M.R.J. & DROSCHAK, D.M., 1965. Hysteresis in the velocity-pressure characteristics of rocks. Geophysics, 30, 111-116.

GASSMANN, F., 1951. Elastic waves through a packing of spheres. Geophysics, 16, 673-685.

GIESEL, W., 1963. Elastische anisotropie in tektonisch verformten sedimentgesteinen. Geophys. Prosp., 11, 423-458.

GOUGH, D.I., 1952. A new instrument for seismic exploration at very short ranges. Geophysics, 17, 311-333.

GRANT, F.S. & WEST, G.F., 1965. Interpretation theory in applied geophysics. McGraw-Hill, New York, p. 8 (584 pp.).

GREELEY, R. & RINEHART, J.S., 1971. Seismic-wave velocity patterns in some pahoehoe basalt flows. Jour. Geophys. Res., 76, 5765-5769.

GRIFFITHS, J.C., 1967. Scientific method in the analysis of sediments. McGraw-Hill, New York, 508 pp.

HAGEDOORN, J.G., 1954. A practical example of an anisotropic velocity-layer. Geophys. Prosp., 2, 52-60.

HAGEDOORN, J.G., 1959. The Plus-minus method of interpreting seismic refraction sections. Geophys. Prosp., 7, 158-182.

HALL, J., 1970. The correlation of seismic velocities with formations in the southwest of Scotland. Geophys. Prosp., 18, 134-148.

HAMILTON, E.L., 1956. Low sound velocities in high-porosity sediments. Jour. Acous. Soc. Amer., 28, 16-19.

HAMILTON, E.L., 1959. Thickness and consolidation of deep-sea sediments. Bull. Geol. Soc. Amer., 70, 1399-1424.

HAMILTON, E.L., 1970. Sound velocity and related properties of marine sediments, North Pacific. Jour. Geophys. Res., 75, 4423-4446.

HASKELL, N.A., 1941. The relation between depth, lithology and seismic wave velocity in Tertiary sandstones and shales. Geophysics, 6, 318-326.

HOEL, P.G., 1947. Introduction to mathematical statistics. Wiley, New York, 427 pp.

HORN, D.R., HORN, B.M. & DELACH, M.N., 1968. Correlation between acoustic and other physical properties of deep-sea cores. Jour. Geophys. Res., 73, 1939-1957.

HOUSE, M.R., 1969a. Portland Stone on Portland. Proc. Dorset Nat. Hist. Archaeol. Soc., 91, 38-39.

HOUSE, M.R., 1969b. The Dorset coast from Poole to Chesil Beach. Geol. Assoc. Guides, No. 22, Benham, Colchester, 32 pp.

HUDDLESTON, W.H., 1883. On the geology of the Vale of Wardour. Proc. Geol. Assoc., 7, 161-185.

HUGHES, D.S. & CROSS, J.H., 1951. Elastic wave velocities in rocks at high pressures and temperatures. Geophysics, 16, 577-593.

HUGHES, D.S. & JONES, H.J., 1951. Elastic wave velocities in sedimentary rocks. Trans. Amer. Geophys. Union, 32, 173-178.

HUGHES, D.S. & KELLY, J.L., 1952. Variation of elastic wave velocity with saturation in sandstone. Geophysics, 17, 739-752.

HURLEY, P.W., 1967, (Editor). Joint report by members of Philips X-ray Spectrometer user groups, Report No. 1. Philips Scientific Equipment, Crawley, U.K. 12 pp.

IDE, J.M., 1937. The velocity of sound in rocks and glasses as a function of temperature. Jour. Geol., 45, 689-716.

JANKOWSKY, W., 1970. Empirical investigation of some factors affecting elastic wave velocities in carbonate rocks. Geophys. Prosp., 18, 103-118.

JODRY, R.L., 1966. Pore geometry of carbonate rocks. Bull. Amer. Assoc. Petrol. Geol., 50, 619 (abstract only).

KING, M.S., 1966. Wave velocities in rocks as a function of changes in overburden pressure and pore fluid saturants. Geophysics, 31, 50-73.

KISSLINGER, C., 1953. The effect of variations in chemical composition on the velocity of seismic waves in carbonate rocks. Geophysics, 18, 104-115.

KLEYN, A.H., 1956. On seismic wave propagation in anisotropic media with applications in the Betun area, South Sumatra. Geophys. Prosp., 4, 56-69.

KLIMA, K. & KULHANEK, O., 1968. Quantitative correlation between preferred orientation of grains and elastic anisotropy of marble. I.E.E.E. Trans. Geosci. Electron., GE - 6 (3), 139-143.

KOEFOED, O., OOSTERVELD, M.M. & ALONS, I.J.G., 1963. A laboratory investigation into the elastic properties of limestones. Geophys. Prosp., 11, 300-312.

KRUMBEIN, W.C., 1951. Some relations among sedimentation, stratigraphy and seismic exploration. Bull. Amer. Assoc. Petrol. Geol., 35, 1505-1522.

KUBOTERA, A., 1954. Determination of elastic wave velocities in rocks by means of ultrasonic impulse transmission. Jour. Physics Earth, 2, 33-38.

KUIPER, J., VAN RYEN, W.M.L. & KOEFOED, O., 1959. Laboratory determinations of elastic properties of some limestones. Geophys. Prosp., 7, 38-44.

LANDES, K.K., 1946. Porosity through dolomitisation. Bull. Amer. Assoc. Petrol. Geol., 30, 305-318.

LAPPIN, M.A., 1971. The petrofabric orientation of olivine and seismic anisotropy of the Mantle. Jour. Geol., 79, 730-740.

LEET, L.D., 1938. Longitudinal velocities in some weathered and unweathered carboniferous rocks. Bull. Seismol. Soc. Amer., 28, 163-168.

McCOLLUM, B. & SNELL, F.A., 1932. Asymmetry of sound velocity in stratified formations. Physics, 2, 174-185.

McLEMORE, E.W., 1963. Probability studies in three variants: Seismic velocity, depth and lithology. Geophysics, 28, 46-86.

MURPHY, W.O., BERG, J.W. & COOK, K.L., 1957. Seismic velocity study of synthetic cores. Geophysics, 22, 813-820.

NAFE, J.E. & DRAKE, C.L., 1957. Variation with depth in shallow and deep water marine sediments of porosity, density and the velocities of compressional and shear waves. Geophysics, 22, 523-552.

NAFE, J.E. & DRAKE, C.L., 1959. Experimental relationship between compressional wave velocity and density. (Fig. 2, p. 1548). In: M. Talwani, G.H. Sutton & J.L. Worzel (Authors), Crustal section across the Puerto Rico Trench. Jour. Geophys. Res., 64, 1545-1555.

NIKITIN, V.N., 1962. Techniques and results of in situ investigations of the elastic properties of limestones by seismic and ultrasonic methods. Bull. Acad. Sci. U.S.S.R., 26, 670-676.

NUR, A. & SIMMONS, G., 1969. The effect of saturation on velocity in low porosity rocks. Earth & Plan. Sci. Lett., 7, 183-193.

OLIPHANT, C.W., 1950. Comparison of field and laboratory measurements of seismic velocities in sedimentary rock. Bull. Geol. Soc. Amer., 61, 759-788.

ONODERA, T.F., 1963. Dynamic investigation of foundation rocks in situ. In: C. Fairhurst (Editor), Rock Mechanics. Pergamon Press, Oxford, pp. 517-533.

PATERSON, N.R., 1956. Seismic wave propagation in porous granular media. Geophysics, 21, 691-714.

PESELNICK, L., 1962. Elastic constants of Solenhofen Limestone and their dependence upon density and saturation. Jour. Geophys. Res., 67, 4441-4448.

PESELNICK, L. & OUTERBRIDGE, W.F., 1961. Internal friction in shear and shear modulus of Solenhofen Limestone over a frequency range of 10^7 cycles per second. Jour. Geophys. Res., 66, 581-588.

PESELNICK, L. & ROBIE, R.A., 1962. Elastic constants of calcite. Jour. Appl. Physics, 33, 2889-2892.

PIRSON, S.J., 1958. Oil reservoir engineering. McGraw-Hill, New York, pp. 30-47.

PRASADA RAO, G.H.S.V., 1947. Anisotropy in the elastic behaviour of rocks. Proc. Indian Acad. Sci., 25, 238-246.

PRESS, F., 1966. Seismic velocities. In: S.P. Clark (Editor), Handbook of physical constants. Mem. Geol. Soc. Amer., 97, 195-218.

PROS, Z. & BABUSKA, V., 1967. A method for investigating the elastic anisotropy on spherical rock samples. Zeit Geophysik, 33, 289-291.

REUSS, A., 1929. Berechnung der Fliessgrenze von Mischkristallen auf Grund der Plastizitätsbedingung fur Einkristalle. Z. angew. Math. U. Mech., 9, 49-58.

RINEHART, J.S., FORTIN, J. & BURGIN, L., 1961. Propagation velocity of longitudinal waves in rocks. Fourth Symp. Rock Mech., Pennsylvania State University, 119-135.

SARMIENTO, R., 1961. Geological factors influencing porosity estimates from velocity logs. Bull. Amer. Assoc. Petrol. Geol., 45, 633-644.

SCHREIBER, B.C., 1968. Sound velocity in deep sea sediments. Jour. Geophys. Res., 73, 1259-1269.

SCHWAETZER, T., 1958. La mesure de la vitesse verticale par le carottage continu (C.V.L.); precision des mesures et discussions de quelques resultats. Geophys. Prosp., 6, 257-284.

SHUMWAY, G., 1958. Sound velocity versus temperature in water-saturated sediments. Geophysics, 23, 494-505.

SHUMWAY, G., 1960. Sound speed and absorption studies of marine sediments by a Resonance Method (Parts I and II). Geophysics, 25, 451-467 & 659-682.

STEINMETZ, R., 1962. Analysis of vectorial data. Jour. Sediment. Petrol., 32, 801-812.

STRAHAN, A., 1898. The geology of the Isle of Purbeck and Weymouth. Mem. Geol. Surv. U.K., xi + 278 pp.

SUTTON, G.H., BERCKHEMER, H. & NAFE, J.E., 1957. Physical analysis of deep-sea sediments. Geophysics, 22, 779-812.

THILL, R.E., WILLARD, R.J. & BUR, T.R., 1969. Correlation of longitudinal velocity variation with rock fabric. Jour. Geophys. Res., 74, 4897-4909.

THOMAS, G.E., 1962. Grouping of carbonate rocks into textural and porosity units for mapping purposes. In: W.E. Ham (Editor), Classification of carbonate rocks. Amer. Assoc. Petrol. Geol. Mem. 1, pp. 193-223.

TIMUR, A. 1968. Velocity of compressional waves in porous media at permafrost temperatures. Geophysics, 33, 584-595.

TIMUR, A., HEMPKINS, W.B. & WEINBRANDT, R.M., 1971. Scanning electron microscope study of pore systems in rock. Jour. Geophys. Res., 76, 4932-4948.

TOCHER, D., 1957. Anisotropy in rocks under simple compression. Trans. Amer. Geophys. Union, 38, 89-94.

TOWNSON, W.G., 1971. Facies analysis of the Portland Group of England and northern France. Unpubl. Ph.D. thesis, Oxford University.

UHRIG, L.F. & VAN MELLE, F.A., 1955. Velocity anisotropy in stratified media. Geophysics, 20, 774-779.

USHER, M.J., 1962. Elastic behaviour of rocks at low frequencies. Geophys. Prosp., 10, 119-127.

VIKSNE, A., BERG, J.W. & COOK, K.L., 1961. Effect of porosity, grain contacts and cement on compressional wave velocity through synthetic sandstones. Geophysics, 26, 77-84.

VOIGT, W., 1928. Lehrbuch der Kristallphysik. B.G. Teubner, Leipzig.

WALDSCHMIDT, W.A., FITZGERALD, P.E. & LUNSFORD, C.L., 1956. Classification of porosity and fractures in reservoir rocks. Bull. Amer. Assoc. Petrol. Geol., 40, 953-974.

WEATHERBY, B.B., BORN, W.T. & HARDING, R.L., 1934. Granite and limestone velocity determinations in Arbuckle Mountains, Oklahoma. Bull. Amer. Assoc. Petrol. Geol., 18, 106-118.

WEATHERBY, B.B. & FAUST, L.Y., 1935. Influence of geological factors on longitudinal seismic velocities. Bull. Amer. Assoc. Petrol. Geol., 19, 1-8.

WEST, S.S., 1950. Dependence of seismic wave velocity upon depth and lithology. Geophysics, 15, 653-662.

WHITE, J.E. & SENGBUSH, R.L., 1953. Velocity measurements in near-surface formations. Geophysics, 18, 54-69.

WILSON, R.C.L., 1966. Silica diagenesis in Upper Jurassic limestones of southern England. Jour. Sediment. Petrol., 36, 1036-1050.

WILSON, R.C.L., 1967. Diagenetic carbonate fabric variations in Jurassic limestones of southern England. Proc. Geol. Assoc., 78, 535-554.

WOEBER, A.F., KATZ, S. & AHRENS, T.J., 1963. Elasticity of selected rocks and minerals. Geophysics, 28, 658-663.

WOODWARD, H.B., 1895. The Jurassic rocks of Britain, Volume 5, The Middle and Upper Oolitic rocks of England (Yorkshire excepted). Mem. Geol. Surv. U.K., xiv + 499 pp.

WYLLIE, M.R.J., GREGORY, A.R. & GARDNER, L.W., 1956. Elastic wave velocities in heterogenous and porous media. Geophysics, 21, 41-70.

WYLLIE, M.R.J., GREGORY, A.R. & GARDNER, G.H.F., 1958. An experimental investigation of factors affecting elastic wave velocities in porous media. Geophysics, 23, 459-493.

APPENDIX 1

OUTCROP VELOCITIES DETERMINED USING A HAMMER-SEISMIC METHOD FOR SOME LITHOSTRATIGRAPHIC UNITS AT SWANWORTH QUARRY

A 1.1 Introduction

The hammer-seismic method, first described by Gough (1952), is well-known as a technique for shallow refraction investigations.

In this study, a total of nine short reversed refraction lines were completed using an R.S.4 multi-channel seismograph as the recording unit, together with a 4.5 Kg. hammer source.

The study was restricted to Swanworth Quarry (Section 3.3.2), since this locality provided suitable continuous exposures at least 50 metres in length, of unweathered rock on the quarry floors (Plate 3.2). Outcrop velocities were determined for those lithostratigraphic units which coincided with working-floor levels within the quarry. This included units from both the Portland Group and overlying Purbeck beds (Section 3.2.1; Table A 1.1).

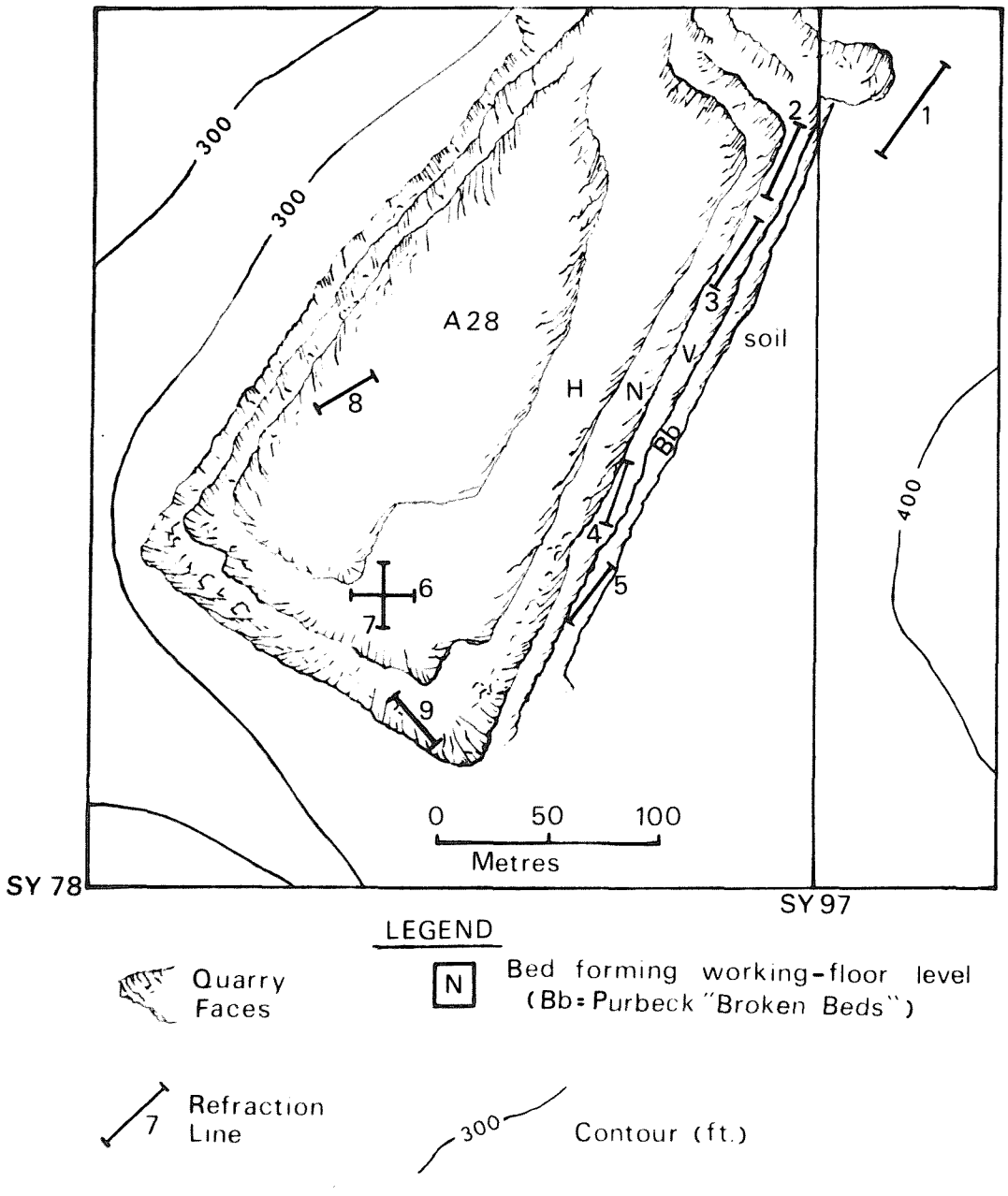
A 1.2 Methods of Velocity-Determination

The relative position of the reversed refraction lines is shown in Fig. A 1.1. The lengths of these lines varied between 30 and 50 metres. Geophones were located at either 3-metre or 5-metre intervals along the lines. R.M.J. geophones with flat bases were used for eight of the lines on the quarry floors, and Electro-tech E.V.S. 2 geophones with spiked bases were used for the remaining line on soil to the east of the quarry (line 1, Fig. A 1.1).

The position of the lines in relation to strike and dip of bedding planes was not considered to be critical, since the maximum dip recorded at Swanworth Quarry was 5° (Section 3.3.2). Thus working levels approximately coincide with bedding planes. In one case (bed H, Table A 1.1), where lines were positioned both approximately parallel and normal to strike, the difference in velocity was only 2%, with the lowest velocity being normal to strike.

Fig. A1.1

Plan of Swanworth Quarry, August, 1971,
showing position of refraction lines



Time-distance graphs were plotted from first-arrival data and best-fitting straight lines were calculated by the method of least-squares. In most cases, these regression lines correspond to direct wave arrivals, with the exception of those lines in which the fit is improved by accepting that the data indicates a shallow refracting interface. The velocity of the surface horizon, i.e. the outcrop velocity, was determined from the direct wave arrivals, and that of the refracting horizon was determined using the minus method of Hagedoorn (1959). The interpretation was extended to allow for calculation of depth to the refracting interface, using Hagedoorn's Plus method (1959). A knowledge of the lithostratigraphic section immediately underlying those refraction lines in which a refracting horizon was indicated, enabled the refracting horizon to be identified. The results are given in Table A 1.1.

In some cases, several velocity-determinations were made on the same lithostratigraphic unit, and a summary of the mean velocities is given in Table A 1.2. Since all velocities are derived from first-arrival travel-times, these velocities are assumed to be longitudinal elastic-wave velocities.

A 1.3 Results

It is clear from the depth-interpretation data (Table A 1.1), that the first-arrival elastic energy is largely confined to near-surface horizons.

The interpreted interfaces between surface and refracting horizons for lines 1 and 5 were found to undulate. An examination of the geological section underlying these lines, indicates that folding of the Purbeck "Broken Beds" (Arkell, 1933, 1947) is a possible explanation in the case of line 1. For line 5, however, the occurrence of a well-developed pattern of master-jointing may also influence the position of this interface. The interface for line 8 is concave in profile. It outcrops apparently at

TABLE A 1.1

Velocities from Reversed Refraction lines at Swanworth Quarry

REFRACTION LINE NUMBER	ORIENTATION & LENGTH OF LINE	SURFACE HORIZON		REFRACTING HORIZON	
		LITHOSTRATIGRAPHIC UNIT*	VELOCITY & S.E. (Metres/sec.)	LITHOSTRATIGRAPHIC UNIT* & MAXIMUM DEPTH TO HORIZON	VELOCITY & S.E. (Metres/sec.)
1	035°—215° 50 m.	Purbeck "Broken Beds" (Rubbly limestone with chert nodules, clays and fractured limestones overlain by soil.)	374 ± 14	Purbeck "Broken Beds" (Folded and fractured laminated limestones forming base of "Broken Beds".) 2·24 m.	925 ± 102
2	025°—205° 35 m.	bed V (Fine-grained limestone)	891 ± 29	None recorded	———
3	030°—210° 35 m.	bed V (Fine-grained limestone)	1001 ± 59	None recorded	———
4	020°—200° 32 m.	bed V (Fine-grained limestone)	922 ± 11	None recorded	———
5	045°—225° 32 m.	Purbeck "Broken Beds" (Folded and fractured laminated limestones)	645 ± 13	Purbeck "Cap" (Fine-grained tufaceous limestone) 1·30 m.	1451 ± 30
6	090°—270° 30 m.	bed H (Shelly oolitic limestone with chert nodules)	899 ± 6	None recorded	———
7 (Perpendicular to centre of Line 6)	000°—180° 30 m.	bed H (Shelly oolitic limestone with chert nodules)	880 ± 10	None recorded	———
8	060°—240° 30 m.	bed A28 (Fractured sandy dolomitic limestone)	802 ± 20	bed A28 (Unfractured sandy dolomitic limestone) 1·92 m.	1448 ± 66
9	140°—320° 30 m.	bed N (Oolitic limestone with chert nodules and stringers)	1207 ± 4	None recorded	———

* Terminology of Purbeck beds after Arkell (1933, 1947)

the surface, 6 metres in from the southwest end of the line, drops rapidly to approximately 2 metres depth and then levels out. An examination of the quarry floor, which was also the lowest working level of the quarry, revealed that the rock was fractured above the position of the interface, probably as a result of quarrying operations. Such operations could also partially account for the anomalous difference of 80% between the direct and refraction velocities observed in the same lithostratigraphic unit (bed A 28).

Both the direct and refraction velocities show a considerable velocity-range. This could be a result of differences in both lithology and degree of fracturing. The fractured and folded limestones (Purbeck "Broken Beds") have the lowest velocities, whereas limestones with chert stringers (bed N), sandy dolomitic limestones (bed A 28), and fine-grained tufaceous limestones (Purbeck "Cap"), have the highest velocities. The results of line 8 indicate the importance of fracturing. Additionally, the 10% difference in velocity found between three lines for the same lithostratigraphic unit (bed V) can probably be attributed to differences in the degree of artificial fracturing and/or jointing.

The velocities determined in this study are considerably less than those determined by previous workers using field-seismic refraction techniques. For example, Weatherby et al. (1934) determined velocities of between 4.0 and 5.5 km/sec. for some Palaeozoic limestones, and Oliphant (1950) determined velocities of between 3.0 and 4.5 km/sec. for some Permian and Carboniferous limestones. These differences could be related to porosity, which usually decreases with increasing geological age as a result of compaction. This would result in pre-Portland Group limestones having a lower porosity and thus a higher velocity. The importance of porosity is supported by the results of Nikitin (1962), which show outcrop velocities of between 2.3 and 4.0 km/sec. for some Upper Cretaceous limestones of less than 4% porosity. Such porosities are considerably less than those determined at Swanworth Quarry (Tables 5.1; 5.14a). Hall (1970) recorded velocities of between 2.0 and

4.0 km./sec. for some Upper Palaeozoic limestones, dolomites and calcareous sandstones using a hammer-seismic refraction method. He suggested that this method gave lower velocities due to seismic attenuation and to the seismic energy being confined to non-saturated surface layers above the water-table. This suggestion is supported by previous workers, e.g. Weatherby et al. (1934); Oliphant (1950), obtaining higher velocities, using explosives as an energy source. An explosive source reduces the attenuation and does not result in the energy being confined to surface layers. It is therefore probable that the exceptionally low velocities determined for limestones from the Portland Group and Purbeck beds, can be attributed to both the method used and to porosity.

A 1.4 Summary and Conclusions

TABLE A 1.2

Mean Velocities for some lithostratigraphic units at Swanworth Quarry using a Hammer-Seismic Method.

LITHOSTRATIGRAPHIC UNIT *	LITHOLOGICAL DESCRIPTION	MEAN VELOCITY AND STANDARD ERROR (Metres/Sec)
Purbeck "Broken Beds"	Folded and fractured laminated limestones	785 ± 198
Purbeck "Cap"	Fine-grained tufaceous limestone	1451 ± 30
bed V	Fine-grained limestone	938 ± 40
bed N	Oolitic limestone with chert stringers and nodules	1207 ± 4
bed H	Shelly oolitic limestone with chert nodules	890 ± 13
bed A 28	Sandy dolomitic limestone:	
	Fractured.	802 ± 20
	Unfractured.	1448 ± 66

* Terminology of Purbeck beds after Arkell (1933, 1947)

Fracturing, either in the form of joints or artificial cracks due to quarrying, is probably the most important parameter affecting *in situ* hammer-seismic velocities at Swanworth Quarry. This is shown in Table A 1.2 by the velocities in bed A 28, and by the low velocity determined in the folded and fractured laminated limestones (Purbeck "Broken Beds"). The importance of fracturing can be shown when comparisons are made with the mean velocities determined in the same lithostratigraphic units, using an ultrasonic method on unfractured core-specimens (Section 4.3). Only three units, bed V, bed N and bed A 28, were studied using both methods. Only mean horizontal velocities from the ultrasonic method (Table 5.1) are used for comparison, since the hammer-seismic method enables only horizontal velocities to be determined, whereas the ultrasonic method is direction-independent. The comparisons, as expected, show considerable differences between the two methods. Mean horizontal velocities using the ultrasonic method are, in all cases greater than the outcrop velocities.

bed	ultrasonic velocity metres/sec.	outcrop velocity metres/sec.
V	5257 ± 45	938 ± 40
N	4456 ± 39	1207 ± 4
A 28	3459 ± 88	1448 ± 66

In this study, the hammer-seismic method determines the velocity of rock *in situ*, including both joints and cracks, over a distance of at least 30 metres, whereas the ultrasonic method determines the velocity in a core-specimen of unfractured rock over a distance of less than 0.1 metres. The differences in the velocities are therefore, probably directly related to the presence of fracturing in the case of the hammer-seismic method. The importance of fracturing, in the form of joints, in reducing field seismic-determined velocities as compared with laboratory-determined velocities, has also been described by several previous workers (Oliphant, 1950; Nikitin,

1962; Onodera, 1963). Attenuation, as discussed by Hall (1970), may also account for some of the observed differences reported here.

The results given in Table A 1.2 also suggest that lithology is probably a velocity-controlling parameter, with fine-grained tufaceous limestones (Purbeck "Cap"), sandy, dolomitic limestones (bed A 28), and limestones with chert stringers (bed N), having the highest velocities. However, identification of lithostratigraphic units from velocity is rendered uncertain by overlapping velocities and limited velocity-data for the lithostratigraphic sequence. This compares closely with the conclusions drawn from the results using the ultrasonic method (Sections 5.2.2a; 5.5), and also confirms previous conclusions drawn from results using field-seismic methods (Leet, 1938; Hall, 1970).

APPENDIX 2

VARIATION IN ULTRASONIC VELOCITY WITH DEGREE OF WATER-SATURATION

A 2.1 Introduction

A limited study was made of the effects of degree of water-saturation on velocity in four core-specimens of the sparite limestone-type and four of the micrite limestone-type. This study was made at an early stage of the main project, and as a result, the core-specimens were restricted to lithostratigraphic units of the Portland Group at Swanworth Quarry (Section 3.3.2) and have porosities not exceeding 12%.

A 2.2 Methods of Analysis

The velocities of the unsaturated cores were first determined, using the method described in Section 4.3. The dry weight of each core was also taken. The cores were oven-dried for 12 hours, and then saturated with distilled water, under vacuum, for 2 and 18 hours respectively. After each saturation, further velocity-determinations and weighings of each core, were made. The weight of water contained in the pores could thus be determined, and this together with the percentage porosity and bulk volume previously determined (Section 4.4.2), enabled the percentage water-saturation of each core to be calculated. This was found to approach 100% after 18 hours saturation, and in order to obtain further data, the cores were then progressively desiccated under atmospheric conditions. Determinations of velocity and weight of each core were made at half-hourly intervals. These determinations were completed after two hours of desiccation and the percentage water-saturation was calculated for all determinations made. The results are listed in Table A 2.1.

The velocity/percentage water-saturation data was analysed statistically using simple linear regression. The correlation coefficients and regression equations for each core-specimen are given in Table A 2.2. The basic data together with the regression lines are plotted in Fig. A 2.1.

A 2.3 Discussion and Conclusions

TABLE A 2.1

Velocity / percentage Water-Saturation Data for some Core-specimens of Micrites and Sparites

STATE OF CORE		CORE-SPECIMEN							
		SPARITES				MICRITES			
		WN1Y5	W01Y3	WQ2Z2	WT3Y2	WV1Z1	WV3Y5	WV4X1	WV5Y3
OVEN-DRIED	VELOCITY	4285	5078	5369	5708	5066	5448	4962	5415
	%SATUR-ATION	0	0	0	0	0	0	0	0
2 HOURS SATUR-ATION	VELOCITY	4480	5557	5739	6349	5194	5516	5088	5502
	%SATUR-ATION	92	85	79	89	85	85	80	89
18HOURS SATUR-ATION	VELOCITY	4536	5650	5845	6387	5222	5554	5126	5532
	% SATUR-ATION	99	94	97	96	97	95	88	92
½ HOUR DESIC-CATION	VELOCITY	4463	5535	5642	6188	5092	5492	5002	5420
	% SATUR-ATION	90	83	68	82	80	79	74	79
1 HOUR DESIC-CATION	VELOCITY	4383	5431	5541	6035	5085	5458	4975	5401
	% SATUR-ATION	68	74	55	68	77	69	68	70
1½HOURS DESIC-CATION	VELOCITY	4300	5318	5340	5750	5062	5438	4949	5420
	% SATUR-ATION	55	36	40	37	52	38	44	44
2 HOURS DESIC-CATION	VELOCITY	4280	5129	5340	5651	5070	5458	4949	5401
	% SATUR-ATION	36	26	31	25	30	27	31	29

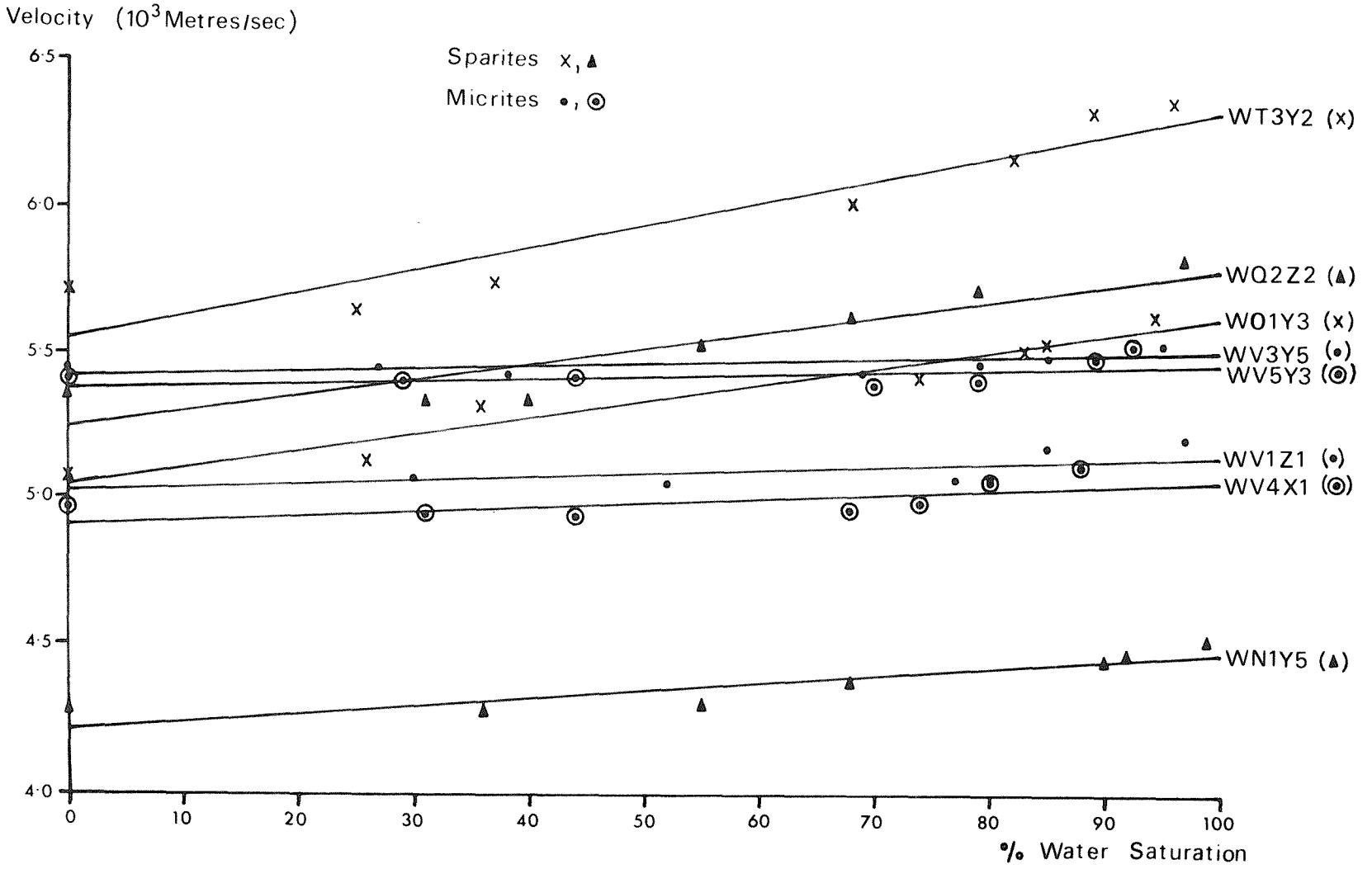
TABLE A 2.2

Results of Simple Linear Regression Analysis on Velocity / percentage Water-Saturation Data for some Core-specimens of Micrites and Sparites.

LIMESTONE TYPE	SPECIMEN NUMBER	% POROSITY	MEAN VELOCITY & S.E. (V)	MEAN SATURATION & S.E. ($\%H_2O$)	CORRELATION COEFFICIENT (r) V-$\%H_2O$	REGRESSION EQUATION & S.E.
SPARITES	WN1Y5	11.8	4389 ± 40	63 ± 13	+0.89***	$V=2.63H_2O + 4224 \pm 51$
	W01Y3	9.1	5385 ± 83	57 ± 14	+0.97****	$V=5.94H_2O+5048 \pm 54$
	WQ2Z2	5.8	5545 ± 77	53 ± 12	+0.91***	$V=5.74H_2O + 5242 \pm 94$
	WT3Y2	6.7	6010 ± 117	57 ± 14	+0.95***	$V=8.06H_2O + 5553 \pm 109$
MICRITES	WV1Z1	10.5	5113 ± 25	60 ± 13	+0.70	$V=1.34H_2O + 5033 \pm 61$
	WV3Y5	9.0	5481 ± 16	56 ± 13	+0.80*	$V=0.97H_2O + 5426 \pm 28$
	WV4X1	11.4	5007 ± 27	55 ± 12	+0.74	$V=1.67H_2O + 4916 \pm 68$
	WV5Y3	9.3	5442 ± 20	58 ± 13	+0.64	$V=0.99H_2O + 5385 \pm 53$

Probability values of r * $P < 0.05$ *** $P < 0.01$ **** $P < 0.001$

Fig. A2.1 Relationships between velocity and degree of water-saturation for some Sparites and Micrites from the Portland Group, Swanworth Quarry



The discussion of results is limited statistically by the size of the populations studied, and no quantitative comparisons are made with previous work.

The most important result is the difference between sparites and micrites, as shown in Table A 2.2 and Fig. A 2.1. For both limestone-types, there is a positive correlation between velocity and percentage water-saturation, but the dependence of velocity on degree of water-saturation is considerably greater for sparites than micrites. There are also differences in correlation coefficients, with those for sparites being significant at the 1% level, but those for micrites being non-significant, with the exception of one core-specimen, marginally significant at the 5% level. These results suggest that the least-time paths of elastic-wave energy in sparites traverse the pores, since velocity in water exceeds that in air, whereas these paths are probably confined to the matrix in micrites. These differences in elastic-wave transmission support some of the conclusions drawn from pore-structure analysis (Section 6.3.3), which indicate that the regularly-scattered, rounded, micromolds in micrites with porosities less than 12%, result in the least-time paths of elastic-wave energy being confined to the matrix. In contrast, sparites have randomly-distributed micro- and mesopores of irregular shape throughout the porosity range studied, including porosities of less than 12%, which result in the least-time paths traversing both matrix and pores, as suggested above.

The results of this limited study agree with previous findings. These show that when velocity determinations in various rock-types, including limestones, are made at frequencies exceeding 500 KHz, there is always a velocity increase with degree of water-saturation (Murphy et. al., 1957; Wyllie et. al., 1958; King, 1966). The converse applies when the frequencies used are less than 40 KHz (Born et. al., 1935; Oliphant, 1950; Usher, 1962; Koefoed et. al., 1963; Section 2.8). Koefoed first suggested

that velocity / water-saturation relationships are frequency-dependent. He suggested that frequency determined the type of system applicable to the rock, with closed systems operating at high frequencies and open systems at low frequencies (Section 2.8). Gassmann (1951) stated that the type of system depended upon frequency, pore-geometry and nature of saturating fluid. When this fluid is air, velocity is independent of frequency (Section 2.3). Biot (1956) predicted that closed systems would result in higher velocities when the fluid was water instead of air, and the opposite in open systems. This would confirm the above conclusions. The present study of Portland Group limestones provides additional evidence indicating that the critical frequency at which there is a transition from open to closed systems lies in the range 40 KHz - 150 KHz (Section 4.3.1).

The importance of pore-structure in influencing velocity/water-saturation relationships has been previously confirmed by Nur et. al. (1969). They showed that in different rocks, using a pulse method of megacycle frequency, velocity increased with water-saturation, when the pores were in the form of microcracks. However, a slight decrease was observed when the pores were in the form of spheroidal holes (Section 2.8). This slight decrease was also observed by Peselnick (1962) using a pulse method at 3MHz, for Solenhofen limestone in which the pores were in the form of spheroidal holes. These results thus agree closely with those for micrites in the present study, with the main pore-types - rounded micromolds - analagous to the spheroidal holes observed by the above workers. However, as shown previously, velocity increases with water-saturation in micrites. This contrasts with previous results and suggests that pore-geometry does not substantially affect the type of system operating, as stated by Gassmann (1951), and implied by these previous results.

APPENDIX 3

LOCATION AND DESCRIPTION OF SAMPLES

A total of 72 samples are listed according to sampling localities (Chapter 3). A lithological description of each sample is given. The site of each sample was measured from the base of the relevant bed, except in cases where the base was not exposed.

LOCALITY: SWANWORTH QUARRY (SY 969784)

SAMPLES:

WV1 : bed V, 3.20m. above base; whitish-grey shelly fine-grained limestone.

WV2 : bed V, 1.86m. above base; greyish-white fine-grained limestone.

WV3 : bed V, 2.84m. above base; whitish-grey shelly fine-grained limestone.

WV4 : bed V, 1.00m. above base; greyish-white fine-grained limestone with isolated shells.

WV5 : bed V, 1.84m. above base; greyish-white fine-grained limestone.

WU1 : bed U, 0.10m. above base; beige shelly oolitic limestone.

WU2 : bed U, 1.55m. above base; beige shelly oolitic limestone.

WU3 : bed U, 1.14m. above base; beige shelly oolitic limestone with several vugs and molds partially infilled with sparry calcite.

WT1 : bed T, 1.79m. above base; beige shelly oolitic limestone.

WT2 : bed T, 0.08m. above base; beige oolitic limestone.

WT3 : bed T, 0.93m. above base; greyish-white oolitic limestone.

WS1 : bed S, 0.30m. above base; whitish-grey fine-grained limestone with greyish-white chert nodules.

WS2 : bed S, 0.30m. above base; whitish-grey fine-grained limestone with greyish-white chert nodules.

WQ1 : bed Q, 2.19m. above base; greyish-white shelly oolitic limestone.

WQ2 : bed Q, 0.84m. above base; greyish-white shelly oolitic limestone.

WQ3 : bed Q, 0.73m. above base; greyish-white oolitic limestone.

WP1 : bed P, 0.15m. above base; beige shelly oolitic limestone.

WP2 : bed P, 0.10m. above base; greyish-white shelly oolitic limestone.

WP3 : bed P, 0.50m. above base; greyish-white shelly oolitic limestone.

WO1 : bed O, 0.43m. above base; greyish-white oolitic limestone.

WO2 : bed O, 0.21m. above base; greyish-white oolitic limestone.

WO3 : bed O, 1.66m. above base; greyish-white shelly oolitic limestone.

WN1 : bed N, 2.73m. above base; beige shelly oolitic limestone with disseminated chert nodules.

WN2 : bed N, 2.84m. above base; whitish-beige oolitic limestone.

WN3 : bed N, 1.95m. above base; beige shelly oolitic limestone with disseminated chert nodules.

WB1 : bed B, 0.49m. above base; dark-grey silty fine-grained limestone.

WB2 : bed B, 0.20m. above base; dark-grey silty fine-grained limestone with chert nodules.

WA28-1 : bed A28, 0.08m. below top; dark-grey silty fine-grained limestone.

WA28-2 : bed A28, 0.10m. below top; dark-grey silty fine-grained limestone.

LOCALITY: EXPOSURE 200m. WEST OF FOSSIL FOREST, LULWORTH COVE (SY 828797)

SAMPLES:

LCV1 : bed V, 1.98m. above base; beige shelly fine-grained limestone with vugs and molds.

LCV2 : bed V, 1.23m. above base; beige shelly limestone.

LOCALITY: DUNGY HEAD, LULWORTH COVE AREA (SY 816799)

SAMPLES:

LCA10-1 : bed A10, 1.11m. below top; black silty fine-grained limestone with calcite veins.

LOCALITY: CHALBURY CAMP (SY 694838)

SAMPLES:

C10-1 : bed 10, 0.72m. above base; white shelly fine-grained limestone.

C10-2 : bed 10, 0.67m. above base; white shelly fine-grained limestone.

C8-1 : bed 8, 1.10m. above base; white chalky fine-grained limestone with isolated shells and chert nodules.

C8-2 : bed 8, 1.63m. above base; whitish-beige fine-grained limestone.

C6-1 : bed 6, 2.78m. above base; white chalky shelly fine-grained limestone.

C6-2 : bed 6, 1.51m. above base; white chalky shelly fine-grained limestone.

C5-1 : bed 5, 0.57m. above base; beige chalky shelly fine-grained limestone.

C5-2 : bed 5, 0.90m. above base; beige chalky shelly fine-grained limestone.

C5-3 : bed 5, 0.55m. above base; white chalky shelly fine-grained limestone.

LOCALITY: CORTON FARM ROAD-CUTTING (SY 636855)

SAMPLES:

CFPS1 : black dolomitic sandstone bed, 1.20m. above base; dark-grey silty fine-grained limestone.

CFPS2 : black dolomitic sandstone bed, 1.05m. above base; dark-grey silty fine-grained limestone.

LOCALITY: PORTESHAM QUARRY (SY 610859)

SAMPLES:

P10-1 : bed 10, 0.50m. above base; white shelly fine-grained limestone.

P8-1 : bed 8, 0.32m. above base; white shelly fine-grained limestone with a few trace fossils.

P6-1 : bed 6, 0.93m. above base; white chalky fine-grained limestone.

LOCALITY: WEST WEARE CLIFFS, ISLE OF PORTLAND (SY 682724)

SAMPLES:

PLPS1 : black dolomitic sandstone bed, 3.30m. above base; dark-grey silty fine-grained limestone with isolated shells.

PLPS2 : black dolomitic sandstone bed, 4.50m. above base; dark-grey silty fine-grained limestone.

PLPS3 : black dolomitic sandstone bed, 3.60m. above base; dark-grey silty fine-grained limestone.

LOCALITY: FRESHWATER BAY, ISLE OF PORTLAND (SY 692702)

SAMPLES:

PLBS1 : Arkell's "Basal Shell Bed" 2.70m. above base; grey shelly fine-grained limestone with a few calcite veins.

PLBS2 : Arkell's "Basal Shell Bed" 2.55m. above base; grey shelly fine-grained limestone with a few calcite veins.

PLBS3 : Arkell's "Basal Shell Bed" 1.18m. above base; grey shelly fine-grained limestone.

LOCALITY: PERRYFIELD QUARRIES, ISLE OF PORTLAND (SY 694712)

SAMPLES:

PLW1 : Whit bed, 1.52m. above base; beige oolitic limestone.

PLW2 : Whit bed, 1.74m. above base; beige oolitic limestone.

PLB1 : Base bed, 0.10m. below top; beige shelly oolitic limestone with cross-bedding discernible.

PLB2 : Base bed, 0.10m. below top; beige oolitic limestone with isolated shells.

LOCALITY: CHILMARK RAVINE (ST 974313)

SAMPLES:

CRU1 : "Upper Building Stones" (Arkell, 1933), 3.27m. above base; beige oolitic limestone with clay lithoclasts and isolated shells.

CRU2 : "Upper Building Stones" (Arkell, 1933), 3.28m. above base; beige oolitic limestone with clay lithoclasts.

CRU3 : "Upper Building Stones" (Arkell, 1933), 0.20m. above base; whitish-beige shelly oolitic limestone.

CRU4 : "Upper Building Stones" (Arkell, 1933), 0.26m. above base; whitish-beige shelly oolitic limestone.

CRC1 : chalky limestone beds, 5.14m. above base; white shelly chalky fine-grained limestone.

CRC2 : chalky limestone beds, 4.82m. above base; white chalky fine-grained limestone.

CRC3 : chalky limestone beds, 5.16m. above base; white shelly chalky fine-grained limestone.

CRR1 : Ragstone beds, 0.51m. above base; beige shelly oolitic limestone.

LOCALITY: UPPER CHICKSGROVE QUARRY (ST 962296)

SAMPLES:

UCL1 : Lamellosus bed, 0.40m. above base; whitish-beige shelly fine-grained limestone.

UCR1 : Ragstone beds, 1.60m. above base; whitish-beige oolitic shelly limestone at base, overlain by whitish-beige shelly fine-grained limestone.

UCR2 : Ragstone beds, 1.32m. above base; beige shelly oolitic limestone.

UCR3 : Ragstone beds, 0.09m. above base; whitish-beige shelly fine-grained limestone with a few calcite veins.

UCM1 : Glauconitic sandy limestone beds, 2.00m. above base; greenish-beige glauconitic sandy oolitic limestone with some cross-lamination.

UCB1 : Basement beds, 5.41m. above base; beige sandy shelly oolitic limestone with some cross-lamination.

UCB2 : Basement beds, 3.90m. above base; beige glauconitic sandy oolitic limestone with some cross-lamination.

UCBS1 : Basal shell beds, 0.10m. below top; grey shelly fine-grained limestone.

APPENDIX 4

CORE-SPECIMEN ORIENTATION

Orientations are listed of cores taken in three orthogonal directions from each sample (Section 4.2). The orientations of cores taken in the "Y" direction coincide with the sample field-orientation.

LOCALITY - SWANWORTH QUARRY [S Y 969784]

SAMPLE No.	FIELD-ORIENTATION	CORE-ORIENTATIONS					
		X		Y		Z	
WV1	178/0	X1	085/0	Y1	178/0	Z1	249/87
		X2	084/0	Y2	178/0	Z2	222/86
WV2	149/0	X1	055/0	Y1	149/0	Z1	294/89
		X2	061/0	Y2	149/0	Z2	227/85
WV3	125/0	X1	220/0	Y1	125/0	Z1	114/87
		X2	214/0	Y2	125/0	Z2	015/82
		X3	215/0	Y3	125/0	Z3	036/83
		X4	216/0	Y4	125/0	Z4	002/86
		X5	216/0	Y5	125/0	Z5	342/85
		X6	219/0	Y6	125/0	Z6	290/87
WV4	039/0	X1	307/0	Y1	039/0	Z1	220/87
WV5	147/0	X1	055/0	Y1	147/0	Z1	284/87
		X2	053/0	Y2	147/0	Z2	083/86
		X3	053/0	Y3	147/0	Z3	092/89
				Y4	147/0		
WU1	249/0	X1	157/0	Y1	249/0	Z1	031/88
		X2	159/0	Y2	249/0	Z2	022/89
		Y3	156/0	Y3	249/0	Z3	VERTICAL
		X4	160/0	Y4	249/0	Z4	032/88
		X5	157/0	Y5	249/0	Z5	VERTICAL
		X6	159/0			Z6	035/89
						Z7	030/89
WU2	127/0	X1	035/0	Y1	127/0	Z1	185/88
		X2	036/0	Y2	127/0	Z2	269/84
		X3	038/0	Y3	127/0	Z3	230/85
WU3	135/0	X1	230/0	Y1	135/0	Z1	064/89
		X2	229/0	Y2	135/0	Z2	VERTICAL
		X3	231/0	Y3	135/0	Z3	321/89
		X4	230/0	Y4	135/0	Z4	282/87

WT1	114/0	X1	204/0	Y1	114/0	Z1	338/86
		X2	202/0	Y2	114/0	Z2	340/86
				Y3	114/0		
WT2	088/0	X1	175/0	Y1	088/0	Z1	010/88
						Z2	334/84
WT3	325/0	X1	235/0	Y1	325/0	Z1	056/88
		X2	232/0	Y2	325/0		
WS1	107/0	X1	019/0	Y1	107/0	Z1	036/83
						Z2	198/89
						Z3	053/88
WS2	124/0	X1	222/0	Y1	124/0	Z1	318/80
		X2	213/0			Z2	339/87
WQ1	125/0	X1	035/0	Y1	125/0	Z1	265/87
		X2	034/0	Y2	125/0	Z2	262/87
		X3	033/0	Y3	125/0	Z3	228/88
		X4	034/0	Y4	125/0	Z4	275/85
		X5	034/0	Y5	125/0	Z5	266/86
						Z6	256/88
WQ2	183/0	X1	271/0	Y1	183/0	Z1	040/85
		X2	278/0	Y2	183/0	Z2	342/87
		X3	277/0	Y3	183/0		
WQ3	294/0	X1	015/0	Y1	294/0	Z1	204/85
		X2	018/0				
WP1	206/0	X1	113/0	Y1	206/0	Z1	328/88
		X2	114/0	Y2	206/0	Z2	332/86
		X3	113/0	Y3	206/0	Z3	295/87
		X4	113/0	Y4	206/0	Z4	301/85
		X5	116/0	Y5	206/0	Z5	314/87
				Y6	206/0	Z6	332/87
WP2	325/0	X1	237/0	Y1	325/0	Z1	074/85

WP3	321/0	X1	230/0	Y1	321/0	Z1	065/86
		X2	227/0	Y2	321/0	Z2	066/85
W01	040/0	X1	304/0	Y1	040/0	Z1	284/88
		X2	310/0	Y2	040/0	Z2	310/88
		X3	309/0	Y3	040/0	Z3	309/89
		X4	309/0	Y4	040/0		
		X5	310/0				
		X6	310/0				
		X7	310/0				
		X8	310/0				
W02	215/0	X1	121/0	Y1	215/0	Z1	110/85
		X2	126/0	Y2	215/0	Z2	056/85
		X3	125/0	Y3	215/0	Z3	073/85
		X4	126/0	Y4	215/0	Z4	040/88
		X5	126/0				
W03	163/0	X1	069/0	Y1	163/0	Z1	212/84
		X2	071/0	Y2	163/0	Z2	069/88
		X3	070/0	Y3	163/0	Z3	287/88
		X4	070/0	Y4	163/0	Z4	285/87
						Z5	254/88
						Z6	287/89
						Z7	285/87
WN1	160/0	X1	253/0	Y1	160/0	Z1	070/83
		X2	254/0	Y2	160/0	Z2	070/83
		X3	251/0	Y3	160/0	Z3	061/83
		X4	253/0	Y4	160/0	Z4	068/84
		X5	251/0	Y5	160/0	Z5	068/84
		X6	253/0	Y6	160/0	Z6	066/83
WN2	165/0	X1	258/0	Y1	165/0	Z1	350/84
		X2	256/0	Y2	165/0	Z2	336/85
		X3	257/0	Y3	165/0	Z3	326/85

WN3	346/0	X1	076/0	Y1	346/0	Z1	258/81
		X2	074/0	Y2	346/0	Z2	258/81
WB1	196/0	X1	105/0	Y1	196/0	Z1	347/86
		X2	105/0	Y2	196/0	Z2	058/86
		X3	105/0	Y3	196/0	Z3	058/86
		X4	103/0	Y4	196/0	Z4	058/86
		X5	104/0	Y5	196/0	Z5	058/86
		X6	105/0				
WB2	031/0	X1	131/0	Y1	031/0	Z1	018/87
		X2	126/0	Y2	031/0	Z2	313/83
		X3	126/0	Y3	031/0	Z3	308/83
		X4	125/0	Y4	031/0	Z4	330/83
WA28-1	328/0	X1	064/0	Y1	328/0	Z1	222/86
				Y2	328/0		
WA28-2	168/0	X1	262/0	Y1	168/0	Z1	090/89
		X2	262/0	Y2	168/0	Z2	028/88
		X3	262/0	Y3	168/0	Z3	342/89
		X4	264/0	Y4	168/0	Z4	065/89
		X5	262/0	Y5	168/0	Z5	VERTICAL
		X6	262/0				

LOCALITY - LULWORTH COVE AREA [S Y 8279]

SAMPLE No	FIELD-ORIENTATION	CORE-ORIENTATIONS					
		X		Y		Z	
LCV1	340/0	X1	064/0	Y1	340/0	Z1	318/83
		X2	065/0	Y2	340/0	Z2	294/84
		X3	064/0	Y3	340/0	Z3	334/83
		X4	064/0	Y4	340/0	Z4	318/83
		X5	065/0	Y5	340/0	Z5	315/80
				Y6	340/0		
LCV2	252/0	X1	160/0	Y1	252/0	Z1	350/88
		X2	155/0	Y2	252/0	Z2	007/83
		X3	152/0	Y3	252/0	Z3	035/85
		X4	153/0			Z4	309/88

LCA10-1	325/0	X1	235/0	Y1	325/0	Z1	230/86
		X2	235/0	Y2	325/0	Z2	230/86
		X3	235/0	Y3	325/0	Z3	230/86
		X4	235/0	Y4	325/0	Z4	230/86
		X5	235/0	Y5	325/0	Z5	230/86
		X6	235/0			Z6	230/86

LOCALITY - CHALBURY CAMP [S Y 694838]

SAMPLE No.	FIELD-ORIENTATION	CORE-ORIENTATIONS					
		X		Y		Z	
C10-1	011/0	X1	105/0	Y1	011/0	Z1	188/81
		X2	105/0	Y2	011/0	Z2	198/80
		X3	104/0	Y3	011/0	Z3	198/81
		X4	102/0	Y4	011/0	Z4	191/82
		X5	102/0	Y5	011/0	Z5	191/82
C10-2	152/0	X1	060/0	Y1	152/0	Z1	184/85
		X2	061/0	Y2	152/0	Z2	209/88
						Z3	263/89
C8-1	356/0	X1	095/0	Y1	356/0	Z1	VERTICAL
		X2	092/0	Y2	356/0	Z2	003/89
		X3	095/0	Y3	356/0	Z3	VERTICAL
		X4	095/0	Y4	356/0	Z4	VERTICAL
		X5	096/0	Y5	356/0		
		X6	096/0	Y6	356/0		
C8-2	155/0	X1	249/0	Y1	155/0	Z1	290/82
		X2	248/0	Y2	155/0	Z2	281/82
		X3	247/0			Z3	281/82
		X4	248/0			Z4	289/83
C6-1	000/0	X1	267/0	Y1	000/0	Z1	135/88
		X2	269/0	Y2	000/0	Z2	135/88
		X3	269/0	Y3	000/0	Z3	123/87
		X4	263/0	Y4	000/0	Z4	023/86
C6-2	094/0	X1	181/0	Y1	094/0	Z1	264/84
		X2	180/0	Y2	094/0	Z2	310/86
		X3	180/0	Y3	094/0	Z3	292/88
		X4	178/0	Y4	094/0	Z4	330/88

C5-1	110/0	X1	193/0	Y1	110/0	Z1	304/82
		X2	191/0	Y2	110/0	Z2	289/81
		X3	190/0	Y3	110/0	Z3	304/82
						Z4	312/83
C5-2	084/0	X1	180/0	Y1	084/0	Z1	047/85
		X2	176/0	Y2	084/0	Z2	033/88
		X3	174/0				
C5-3	014/0	X1	289/0	Y1	014/0	Z1	179/85
		X2	290/0	Y2	014/0	Z2	166/85
		X3	291/0	Y3	014/0		

LOCALITY - CORTON FARM ROAD-CUTTING [S Y 636855]

SAMPLE No.	FIELD-ORIENTATION	CORE-ORIENTATIONS					
		X		Y		Z	
CFPS1	182/0	X1	090/0	Y1	182/0	Z1	228/84
		X2	090/0	Y2	182/0	Z2	128/83
		X3	090/0				
CFPS2	355/0	X1	264/0	Y1	355/0	Z1	060/82
		X2	264/0	Y2	355/0		

LOCALITY - PORTESHAM QUARRY [S Y 610859]

SAMPLE No	FIELD-ORIENTATION	CORE-ORIENTATIONS					
		X		Y		Z	
P6-1	264/0	X1	168/0	Y1	264/0	Z1	142/80
		X2	169/0	Y2	264/0	Z2	149/80
		X3	166/0	Y3	264/0	Z3	194/81
		X4	168/0	Y4	264/0	Z4	194/81
				Y5	264/0		
P8-1	106/0	X1	019/0	Y1	106/0	Z1	276/81
		X2	016/0	Y2	106/0	Z2	276/80
		X3	019/0	Y3	106/0	Z3	275/80
		X4	017/0				

P10-1	300/0	X1	035/0	Y1	300/0	Z1	292/81
		X2	033/0	Y2	300/0	Z2	303/80
				Y3	300/0	Z3	292/81

LOCALITY - WEST WEARE CLIFFS, ISLE OF PORTLAND [S Y 682724]

SAMPLE No	FIELD-ORIENTATION	CORE-ORIENTATIONS					
		X		Y		Z	
PLPS1	210/0	X1	308/0	Y1	210/0	Z1	170/88
		X2	308/0	Y2	210/0	Z2	144/87
		X3	304/0	Y3	210/0	Z3	142/86
		X4	303/0	Y4	210/0	Z4	145/86
		X5	308/0	Y5	210/0	Z5	133/87
		X6	307/0				
PLPS2	220/0	X1	136/0	Y1	220/0	Z1	019/84
		X2	132/0	Y2	220/0	Z2	038/85
		X3	132/0	Y3	220/0	Z3	028/84
				Y4	220/0	Z4	026/86
				Y5	220/0		
				Y6	220/0		
PLPS3	210/0	X1	122/0	Y1	210/0	Z1	043/84
		X2	122/0	Y2	210/0	Z2	024/83
		X3	125/0	Y3	210/0	Z3	052/84
		X4	123/0	Y4	210/0	Z4	045/85
		X5	120/0				
		X6	122/0				

LOCALITY - FRESHWATER BAY, ISLE OF PORTLAND [S Y 692702]

SAMPLE No.	FIELD-ORIENTATION	CORE-ORIENTATIONS					
		X		Y		Z	
PLBS1	320/0	X1	054/0	Y1	320/0	Z1	290/88
		X2	051/0	Y2	320/0	Z2	308/86
		X3	055/0	Y3	320/0	Z3	333/86
		X4	054/0	Y4	320/0	Z4	343/85
		X5	055/0	Y5	320/0	Z5	294/87

PLBS2	320/0	X1	224/0	Y1	320/0	Z1	308/89
		X2	226/0	Y2	320/0	Z2	002/88
		X3	222/0	Y3	320/0	Z3	322/89
		X4	226/0	Y4	320/0	Z4	VERTICAL
		X5	222/0	Y5	320/0	Z5	316/89
PLBS3	040/0	X1	131/0	Y1	040/0	Z1	104/87
		X2	131/0	Y2	040/0	Z2	116/85
		X3	132/0	Y3	040/0	Z3	104/85
		X4	131/0			Z4	105/85
						Z5	083/85
						Z6	130/85

LOCALITY - PERRYFIELD QUARRIES, ISLE OF PORTLAND [S Y 694712]

SAMPLE No.	FIELD-ORIENTATION	CORE-ORIENTATIONS					
		X		Y		Z	
PLW1	125/0	X1	038/0	Y1	125/0	Z1	273/84
		X2	038/0	Y2	125/0	Z2	290/87
		X3	039/0	Y3	125/0	Z3	302/82
		X4	038/0	Y4	125/0	Z4	292/83
		X5	036/0	Y5	125/0	Z5	306/85
PLW2	190/0	X1	090/0	Y1	190/0	Z1	096/83
		X2	090/0	Y2	190/0	Z2	078/84
		X3	096/0	Y3	190/0	Z3	103/85
		X4	096/0	Y4	190/0	Z4	094/82
PLB1	310/0	X1	227/0	Y1	310/0	Z1	127/87
		X2	230/0	Y2	310/0	Z2	112/84
		X3	226/0	Y3	310/0	Z3	150/84
		X4	226/0	Y4	310/0	Z4	150/84
		X5	230/0	Y5	310/0	Z5	144/85
						Z6	149/86
PLB2	300/0	X1	219/0	Y1	300/0	Z1	088/84
		X2	220/0	Y2	300/0	Z2	038/83
		X3	208/0	Y3	300/0	Z3	164/84
		X4	213/0	Y4	300/0	Z4	064/82
		X5	213/0				
		X6	212/0				

LOCALITY - CHILMARK RAVINE [S T 974313]

SAMPLE No.	FIELD-ORIENTATION	CORE-ORIENTATIONS					
		X		Y		Z	
CRU1	080/0	X1	177/0	Y1	080/0	Z1	230/80
		X2	167/0	Y2	080/0	Z2	256/80
				Y3	080/0		
CRU2	187/0	X1	097/0	Y1	187/0	Z1	097/83
		X2	105/0	Y2	187/0	Z2	064/85
		X3	104/0	Y3	187/0	Z3	064/86
		X4	103/0	Y4	187/0	Z4	015/85
		X5	105/0	Y5	187/0	Z5	085/81
		X6	103/0	Y6	187/0	Z6	312/84
		X7	101/0	Y7	187/0	Z7	015/85
		X8	105/0	Y8	187/0	Z8	040/85
		X9	107/0	Y9	187/0	Z9	042/85
				Y10	187/0	Z10	085/83
				Y11	187/0	Z11	035/84
				Y12	187/0	Z12	038/84
CRU3	100/0	X1	007/0	Y1	100/0	Z1	126/80
		X2	007/0	Y2	100/0	Z2	116/81
		X3	007/0	Y3	100/0	Z3	124/80
				Y4	100/0	Z4	124/80
				Y5	100/0		
CRU4	046/0	X1	144/0	Y1	046/0	Z1	026/82
		X2	137/0	Y2	046/0	Z2	092/81
		X3	137/0	Y3	046/0	Z3	086/81
		X4	144/0	Y4	046/0	Z4	087/80
		X5	136/0	Y5	046/0	Z5	086/82
		X6	137/0			Z6	086/82
						Z7	087/80
CRC1	079/0	X1	359/0	Y1	079/0	Z1	180/87
		X2	358/0	Y2	079/0	Z2	185/89

CRC2	120/0	X1	200/0	Y1	120/0	Z1	025/85
		X2	205/0	Y2	120/0	Z2	064/83
		X3	206/0	Y3	120/0	Z3	088/86
				Y4	120/0		
CRC3	034/0	X1	116/0	Y1	034/0	Z1	283/82
		X2	114/0	Y2	034/0	Z2	315/85
		X3	114/0	Y3	034/0	Z3	309/84
		X4	114/0	Y4	034/0	Z4	310/84
		X5	115/0			Z5	309/83
		X6	115/0			Z6	309/84
		X7	116/0				
		X8	116/0				
CRR1	055/0	X1	149/0	Y1	055/0	Z1	013/85

LOCALITY - UPPER CHICKSGROVE QUARRY [S T 962296]

SAMPLE No.	FIELD-ORIENTATION	CORE-ORIENTATIONS					
		X		Y		Z	
UCL1	235/0	X1	155/0	Y1	235/0	Z1	VERTICAL
		X2	152/0	Y2	235/0	Z2	124/89
		X3	155/0	Y3	235/0	Z3	130/88
		X4	154/0			Z4	132/89
UCR1	245/0	X1	158/0	Y1	245/0	Z1	098/88
		X2	156/0	Y2	245/0	Z2	098/88
		X3	158/0	Y3	245/0	Z3	102/87
		X4	156/0	Y4	245/0	Z4	105/87
		X5	158/0	Y5	245/0	Z5	102/88
UCR2	145/0	X1	061/0	Y1	145/0	Z1	312/88
		X2	059/0	Y2	145/0	Z2	326/89
		X3	056/0	Y3	145/0	Z3	326/85
UCR3	144/0	X1	242/0	Y1	144/0	Z1	295/88
		X2	243/0	Y2	144/0	Z2	272/88
UCM1	154/0	X1	074/0	Y1	154/0	Z1	337/87
		X2	074/0	Y2	154/0	Z2	333/87
		X3	068/0	Y3	154/0	Z3	340/88

/contd.over

UCM1 contd.		X4	066/0	Y4	154/0	Z4	331/87
		X5	069/0	Y5	154/0	Z5	334/87
		X6	069/0	Y6	154/0	Z6	325/88
UCB1	320/0	X1	052/0	Y1	320/0	Z1	VERTICAL
		X2	053/0	Y2	320/0	Z2	092/89
		X3	053/0	Y3	320/0	Z3	064/88
		X4	053/0	Y4	320/0	Z4	081/89
		X5	052/0				
UCB2	140/0	X1	221/0	Y1	140/0	Z1	036/89
		X2	221/0	Y2	140/0	Z2	346/88
		X3	220/0	Y3	140/0	Z3	029/86
		X4	224/0	Y4	140/0		
UCBS1	220/0	X1	140/0	Y1	220/0	Z1	038/86
		X2	140/0	Y2	220/0	Z2	038/86
		X3	138/0	Y3	220/0	Z3	028/86
						Z4	032/88

APPENDIX 5

VELOCITY-, POROSITY-, and DENSITY-DETERMINATIONS OF CORE-SPECIMENS

A total of 898 core-specimens are listed, including 84 half-cores derived from transversely bisected core-specimens. Each pair of half-cores is suffixed by the letters 'A' and 'B', with 'A' referring to the upper half-core. The standard deviation of each velocity-determination is given.

LOCALITY - SWANWORTH QUARRY [S Y 969784]

bed V

Core-Specimen	Velocity (m./sec)	Porosity (%)	Density (gm./c.c.)
WV1X1	5156 ± 20	11•2	2•33
WV1X2	5221 ± 25	10•3	2•36
WV1Y1	5379 ± 38	10•3	2•36
WV1Y2	5265 ± 39	11•6	2•33
WV1Z1	5119 ± 23	10•5	2•35
WV1Z2	4358 ± 23	9•2	2•42
WV1Z2A	5795 ± 60	9•3	2•42
WV1Z2B	5143 ± 25	9•2	2•42
WV2X1	4656 ± 39	10•3	2•36
WV2X2	5386 ± 64	8•6	2•42
WV2Y1	4882 ± 29	10•0	2•40
WV2Y2	5864 ± 140	12•1	2•33
WV2Z1	4826 ± 81	10•1	2•37
WV2Z2	5828 ± 21	7•2	2•48
WV2Z2A	4855 ± 41	6•2	2•50
WV2Z2B	5132 ± 88	8•1	2•45
WV3X1	5183 ± 42	9•3	2•38
WV3X2	5365 ± 45	9•6	2•41
WV3X2A	5682 ± 52	7•7	2•46
WV3X2B	5378 ± 38	11•4	2•36
WV3X3	5435 ± 36	7•6	2•45
WV3X3A	5581 ± 74	7•8	2•46
WV3X3B	5559 ± 69	7•4	2•44
WV3X4	5369 ± 21	9•1	2•39
WV3X5	5304 ± 18	9•3	2•40
WV3X5A	5601 ± 74	8•8	2•41
WV3X5B	5378 ± 31	9•8	2•39
WV3X6	5347 ± 21	9•4	2•39
WV3Y1	5161 ± 42	8•5	2•41
WV3Y2	5365 ± 24	4•9	2•52
WV3Y2A	5343 ± 25	1•9	2•58
WV3Y2B	5581 ± 58	7•9	2•45

WV3Y3	5361 ± 21	8·8	2·40
WV3Y3A	5368 ± 52	10·5	2·36
WV3Y3B	5589 ± 34	7·2	2·45
WV3Y4	5502 ± 62	9·0	2·40
WV3Y5	5455 ± 21	9·0	2·40
WV3Y6	5415 ± 26	8·4	2·41
WV3Z1	5229 ± 80	8·6	2·43
WV3Z2	5294 ± 23	9·9	2·38
WV3Z3	5349 ± 18	9·4	2·40
WV3Z4	5503 ± 43	9·3	2·39
WV3Z5	5375 ± 22	9·1	2·39
WV3Z6	5792 ± 85	10·7	2·36
WV4X1	4768 ± 55	11·4	2·34
WV4Y1	4848 ± 16	5·9	2·49
WV4Z1	4846 ± 76	11·3	2·35
WV5X1	5292 ± 43	9·6	2·40
WV5X2	5118 ± 20	7·0	2·45
WV5X2A	5083 ± 40	4·9	2·50
WV5X2B	5505 ± 55	9·1	2·40
WV5X3	5245 ± 65	11·8	2·34
WV5Y1	5465 ± 61	12·0	2·33
WV5Y2	5116 ± 17	7·6	2·44
WV5Y2A	5358 ± 81	7·1	2·45
WV5Y2B	5196 ± 41	8·1	2·43
WV5Y3	5424 ± 16	9·3	2·41
WV5Y4	5113 ± 23	9·5	2·40
WV5Z1	5235 ± 23	8·4	2·43
WV5Z2	5160 ± 27	9·3	2·41
WV5Z3	4935 ± 29	8·1	2·43
WV5Z3A	5116 ± 44	9·0	2·40
WV5Z3B	5060 ± 45	7·1	2·46
bed U			
WU1X1	4985 ± 23	8·8	2·45
WU1X1A	5179 ± 35	7·8	2·47
WU1X1B	5125 ± 61	9·8	2·42
WU1X2	5112 ± 40	7·3	2·45

WU1X3	5688 ± 105	13·5	2·31
WU1X4	5479 ± 109	7·1	2·45
WU1X5	5412 ± 51	12·1	2·34
WU1X6	5081 ± 45	10·6	2·36
WU1Y1	5315 ± 34	7·3	2·44
WU1Y2	5074 ± 23	10·0	2·40
WU1Y3	5021 ± 18	7·7	2·43
WU1Y4	4977 ± 30	9·0	2·44
WU1Y4A	5131 ± 29	8·5	2·45
WU1Y4B	5148 ± 47	9·4	2·42
WU1Y5	4979 ± 28	8·4	2·45
WU1Y5A	5000 ± 33	7·5	2·48
WU1Y5B	5375 ± 58	9·4	2·42
WU1Y6	4927 ± 74	4·7	2·53
WU1Z1	5079 ± 65	5·8	2·49
WU1Z2	4458 ± 33	6·1	2·50
WU1Z3	5017 ± 39	6·7	2·46
WU1Z4	4650 ± 32	5·1	2·55
WU1Z4A	4728 ± 38	6·0	2·51
WU1Z4B	4915 ± 44	4·1	2·58
WU1Z5	4257 ± 22	3·4	2·56
WU1Z5A	4405 ± 41	2·7	2·57
WU1Z5B	4682 ± 57	4·1	2·55
WU1Z6	4882 ± 26	7·0	2·48
WU1Z7	4419 ± 44	11·4	2·36
WU2X1	5457 ± 61	6·4	2·44
WU2X2	5293 ± 24	7·1	2·44
WU2X3	5306 ± 20	5·0	2·48
WU2Y1	5383 ± 30	5·3	2·47
WU2Y2	5395 ± 42	7·4	2·43
WU2Y3	5229 ± 21	5·1	2·46
WU2Y3A	5631 ± 43	4·2	2·53
WU2Y3B	5319 ± 78	6·0	2·38
WU2Z1	4911 ± 36	4·6	2·50
WU2Z2	4650 ± 86	8·0	2·43
WU2Z3	4745 ± 76	6·0	2·48
WU3X1	5117 ± 36	12·8	2·28
WU3X2	5189 ± 144	12·9	2·28

WU3X3	5180 ± 60	6•4	2•45
WU3X4	5935 ± 181	12•5	2•32
WU3Y1	5155 ± 42	5•4	2•50
WU3Y2	4865 ± 19	11•8	2•31
WU3Y3	4596 ± 35	8•7	2•41
WU3Y4	5154 ± 41	10•7	2•36
WU3Z1	5119 ± 19	6•4	2•46
WU3Z2	5039 ± 38	9•5	2•40
WU3Z3	5162 ± 35	5•5	2•49
WU3Z4	5077 ± 18	7•2	2•47
bed T			
WT1X1	5477 ± 20	6•2	2•49
WT1X1A	5676 ± 68	7•0	2•47
WT1X1B	5583 ± 54	5•5	2•51
WT1X2	5581 ± 46	6•2	2•46
WT1Y1	5618 ± 46	6•6	2•45
WT1Y2	5516 ± 33	7•1	2•44
WT1Y3	5597 ± 36	6•4	2•46
WT1Z1	5826 ± 11	3•5	2•54
WT1Z1A	5903 ± 76	2•8	2•55
WT1Z1B	5882 ± 41	4•3	2•54
WT1Z2	5729 ± 26	4•8	2•47
WT2X1	4608 ± 92	11•2	2•31
WT2Y1	4680 ± 55	9•2	2•36
WT2Z1	4326 ± 57	13•5	2•24
WT2Z2	4821 ± 52	11•9	2•30
WT3X1	5774 ± 61	6•9	2•45
WT3X2	6116 ± 64	5•3	2•49
WT3Y1	5594 ± 20	6•8	2•49
WT3Y1A	5568 ± 84	9•1	2•43
WT3Y1B	6111 ± 61	4•4	2•55
WT3Y2	5850 ± 83	6•7	2•44
WT3Z1	6505 ± 36	4•4	2•52
bed S			
WS1X1	5437 ± 41	6•1	2•46

WS1Y1	5334 ± 27	7•2	2•44
WS1Z1	5321 ± 66	7•0	2•44
WS1Z2	5945 ± 74	6•8	2•45
WS1Z3	5614 ± 20	4•9	2•55
WS1Z3A	5579 ± 59	5•0	2•55
WS1Z3B	5797 ± 102	4•9	2•56
WS2X1	5678 ± 97	8•7	2•37
WS2X2	6200 ± 49	1•9	2•55
WS2Y1	5793 ± 70	1•7	2•57
WS2Z1	5526 ± 87	2•9	2•54
WS2Z2	5950 ± 76	2.5	2•55

bed Q

WQ1X1	4508 ± 26	10•7	2•31
WQ1X2	4613 ± 25	2•8	2•51
WQ1X3	4576 ± 14	10•3	2•32
WQ1X4	4532 ± 11	10•7	2•31
WQ1X5	4535 ± 32	10•4	2•32
WQ1Y1	4567 ± 17	11•4	2•29
WQ1Y2	4379 ± 6	11•2	2•30
WQ1Y3	4516 ± 12	10•0	2•32
WQ1Y4	4508 ± 16	10•5	2•31
WQ1Y5	4585 ± 15	11•2	2•31
WQ1Z1	4585 ± 16	9•6	2•32
WQ1Z2	4515 ± 23	9•8	2•32
WQ1Z3	4525 ± 13	11•1	2•29
WQ1Z4	4511 ± 20	9•3	2•32
WQ1Z5	4075 ± 15	10•2	2•32
WQ1Z6	4555 ± 43	12•4	2•27
WQ2X1	5436 ± 83	5•6	2•49
WQ2X2	5854 ± 64	2•4	2•58
WQ2X3	5822 ± 78	4•3	2•52
WQ2Y1	5146 ± 85	7•9	2•45
WQ2Y2	5737 ± 40	2•7	2•58
WQ2Y3	5831 ± 25	3•1	2•56
WQ2Z1	5050 ± 56	6•5	2•47
WQ2Z2	5398 ± 33	5•8	2•49

WQ3X1	5187 ± 36	8·4	2·40
WQ3X2	5084 ± 26	8·4	2·43
WQ3X2A	5226 ± 53	7·5	2·46
WQ3X2B	5204 ± 37	9·2	2·41
WQ3Y1	4929 ± 22	9·7	2·40
WQ3Y1A	5185 ± 57	10·2	2·39
WQ3Y1B	5092 ± 62	9·2	2·41
WQ3Z1	5092 ± 35	10·4	2·35
bed P			
WP1X1	5389 ± 36	3·7	2·53
WP1X2	5672 ± 33	3·4	2·55
WP1X3	5233 ± 41	4·1	2·53
WP1X4	5128 ± 24	7·3	2·44
WP1X5	4932 ± 52	8·0	2·40
WP1Y1	5422 ± 64	4·1	2·51
WP1Y2	5645 ± 27	3·4	2·53
WP1Y3	5539 ± 30	4·8	2·49
WP1Y4	5555 ± 23	4·6	2·52
WP1Y5	5433 ± 34	5·8	2·47
WP1Y6	5590 ± 60	8·9	2·38
WP1Z1	5258 ± 80	4·7	2·50
WP1Z2	5784 ± 84	3·8	2·51
WP1Z3	5546 ± 45	3·0	2·54
WP1Z4	5509 ± 17	9·9	2·50
WP1Z5	5703 ± 39	6·1	2·46
WP1Z6	5704 ± 130	5·1	2·49
WP2X1	5366 ± 22	5·9	2·45
WP2Y1	5091 ± 33	6·4	2·46
WP2Z1	5281 ± 39	6·8	2·44
WP3X1	5677 ± 37	3·6	2·54
WP3X2	5722 ± 37	7·2	2·45
WP3Y1	5712 ± 46	4·8	2·51
WP3Y2	5761 ± 94	5·1	2·49
WP3Z1	5533 ± 88	5·8	2·46
WP3Z2	5613 ± 159	7·7	2·43

bed O

W01X1	4403 ± 26	10·1	2·32
W01X2	4480 ± 7	8·5	2·34
W01X3	4497 ± 22	8·6	2·33
W01X4	4679 ± 24	8·8	2·34
W01X5	4684 ± 77	9·1	2·34
W01X6	4773 ± 34	8·7	2·34
W01X7	4613 ± 16	7·5	2·36
W01X8	4718 ± 27	11·4	2·27
W01Y1	4490 ± 28	7·6	2·39
W01Y2	4505 ± 17	6·6	2·37
W01Y3	4833 ± 59	9·1	2·33
W01Y4	4860 ± 29	7·9	2·37
W01Z1	4605 ± 32	9·2	2·33
W01Z2	4818 ± 33	10·5	2·29
W01Z3	4787 ± 45	11·9	2·25
W02X1	4261 ± 16	11·4	2·30
W02X2	4167 ± 20	10·6	2·31
W02X3	4571 ± 82	9·1	2·35
W02X4	4214 ± 15	10·1	2·32
W02X5	4068 ± 20	10·9	2·29
W02Y1	4195 ± 50	13·7	2·23
W02Y2	4066 ± 13	10·9	2·29
W02Y3	4008 ± 23	11·0	2·29
W02Y4	4024 ± 10	8·0	2·37
W02Z1	4488 ± 15	12·3	2·28
W02Z2	4484 ± 43	11·7	2·30
W02Z3	4435 ± 20	11·2	2·31
W02Z4	4407 ± 8	11·8	2·29
W03X1	5240 ± 46	6·3	2·48
W03X2	5448 ± 57	6·2	2·46
W03X3	5447 ± 23	4·9	2·51
W03X4	5462 ± 19	5·5	2·48
W03Y1	5059 ± 35	7·3	2·43
W03Y2	5364 ± 36	4·9	2·50
W03Y3	5220 ± 28	6·8	2·42
W03Y4	5388 ± 50	3·9	2·52

WO3Z1	4883 ± 33	7·6	2·42
WO3Z2	5051 ± 39	10·5	2·42
WO3Z3	5082 ± 29	5·3	2·44
WO3Z4	4759 ± 31	9·0	2·37
WO3Z5	4724 ± 20	10·4	2·43
WO3Z6	5168 ± 46	8·4	2·39
WO3Z7	4837 ± 29	9·1	2·37

bed N			
WN1X1	4624 ± 30	8·5	2·33
WN1X2	4667 ± 20	8·3	2·33
WN1X3	4696 ± 24	7·5	2·36
WN1X4	4708 ± 26	7·1	2·37
WN1X5	4272 ± 35	7·4	2·37
WN1X6	4606 ± 33	8·1	2·35
WN1Y1	4638 ± 37	9·6	2·31
WN1Y2	4474 ± 17	8·9	2·31
WN1Y3	4491 ± 17	9·2	2·30
WN1Y4	4522 ± 25	8·5	2·33
WN1Y5	4152 ± 18	11·8	2·24
WN1Y6	4382 ± 26	9·9	2·30
WN1Z1	4609 ± 59	12·7	2·31
WN1Z2	4590 ± 32	13·1	2·32
WN1Z3	4429 ± 27	12·7	2·30
WN1Z4	4620 ± 21	12·3	2·31
WN1Z5	4489 ± 13	13·1	2·30
WN1Z6	4692 ± 86	12·3	2·31
WN2X1	4248 ± 28	10·5	2·30
WN2X2	4191 ± 36	19·8	2·07
WN2X3	4491 ± 59	11·6	2·27
WN2Y1	4198 ± 29	10·9	2·30
WN2Y2	4157 ± 22	10·7	2·29
WN2Y3	4377 ± 59	10·0	2·32
WN2Z1	4311 ± 20	9·6	2·32
WN2Z2	4400 ± 28	10·1	2·31
WN2Z3	4398 ± 36	10·7	2·29
WN3X1	4512 ± 28	8·8	2·33
WN3X2	4596 ± 34	11·2	2·25

WN3Y1	4503 ± 20	8·4	2·34
WN3Y2	4523 ± 14	8·7	2·33
WN3Z1	4574 ± 17	9·6	2·31
WN3Z2	4516 ± 33	8·1	2·33
bed B			
WB1X1	3048 ± 18	27·1	1·78
WB1X2	3141 ± 17	27·8	1·83
WB1X3	3074 ± 19	26·2	1·80
WB1X4	3038 ± 12	27·5	1·77
WB1X4A	3119 ± 29	27·6	1·76
WB1X4B	3091 ± 17	27·4	1·78
WB1X5	3053 ± 15	27·0	1·77
WB1X6	3230 ± 26	25·5	1·85
WB1Y1	3030 ± 17	26·6	1·80
WB1Y2	3208 ± 29	24·9	1·82
WB1Y3	3303 ± 10	25·7	1·85
WB1Y3A	3362 ± 38	26·3	1·87
WB1Y3B	3397 ± 13	25·1	1·84
WB1Y4	3373 ± 45	28·1	1·82
WB1Y5	3492 ± 17	23·5	1·89
WB1Z1	2755 ± 14	28·8	1·80
WB1Z2	2803 ± 10	25·4	1·81
WB1Z3	2685 ± 15	26·1	1·79
WB1Z4	2786 ± 15	23·6	1·86
WB1Z5	2789 ± 13	26·2	1·83
WB1Z5A	2962 ± 14	23·7	1·87
WB1Z5B	2759 ± 19	28·8	1·80
WB2X1	4326 ± 61	20·6	1·97
WB2X2	3713 ± 23	29·4	1·92
WB2X3	3739 ± 26	22.0	1·95
WB2X4	3616 ± 18	22·7	1·95
WB2X4A	3844 ± 35	22·7	1·95
WB2X4B	3653 ± 31	22·7	1·94
WB2Y1	4351 ± 14	18·7	1·97
WB2Y2	4190 ± 39	21·5	1·91
WB2Y3	3848 ± 16	22·1	1·94

WB2Y3A	4388 ± 77	19·3	1·98
WB2Y3B	3545 ± 23	24·8	1·89
WB2Y4	3527 ± 23	25·7	1·85
WB2Z1	4025 ± 31	18·8	1·97
WB2Z2	4072 ± 24	18·7	2·00
WB2Z2A	4131 ± 31	17·6	2·02
WB2Z2B	3980 ± 52	19·9	1·98
WB2Z3	3465 ± 23	28·7	1·92
WB2Z4	3720 ± 18	19·1	2·00
bed A28			
WA28-1X1	3445 ± 33	24·7	2·03
WA28-1Y1	3272 ± 33	25·5	2·00
WA28-1Y2	3559 ± 34	21·6	2·10
WA28-1Z1	2891 ± 10	23·6	2·05
WA28-2X1	3761 ± 15	11·7	2·26
WA28-2X1A	3653 ± 23	11·3	2·24
WA28-2X1B	4003 ± 16	12·1	2·28
WA28-2X2	3343 ± 24	15·4	2·19
WA28-2X3	3360 ± 25	16·3	2·18
WA28-2X4	3052 ± 11	20·3	2·08
WA28-2X5	3592 ± 19	15·4	2·19
WA28-2X6	2851 ± 29	23·5	2·00
WA28-2Y1	4051 ± 47	11·6	2·29
WA28-2Y2	3453 ± 32	16·3	2·21
WA28-2Y3	4013 ± 73	11·5	2·22
WA28-2Y4	3304 ± 32	19·5	2·10
WA28-2Y5	3374 ± 19	19·1	2·02
WA28-2Y5A	3569 ± 39	18·0	2·05
WA28-2Y5B	3344 ± 29	20·3	1·99
WA28-2Z1	3279 ± 31	14·6	2·22
WA28-2Z2	2831 ± 16	17·1	2·15
WA28-2Z3	3345 ± 24	15·3	2·19
WA28-2Z4	2899 ± 16	17·9	2·13
WA28-2Z5	3664 ± 21	13·0	2·22
WA28-2Z5A	3435 ± 25	14·8	2·14
WA28-2Z5B	3993 ± 28	11·1	2·29

LOCALITY - LULWORTH COVE AREA [S Y 8279]

bed V

Core-Specimen	Velocity (m./sec.)	Porosity (%)	Density (gm./c.c.)
LCV1X1	5753 ± 27	7·4	2·46
LCV1X2	5757 ± 20	7·3	2·47
LCV1X3	5735 ± 26	6·3	2·47
LCV1X3A	5753 ± 34	7·4	2·45
LCV1X3B	5834 ± 57	5·3	2·48
LCV1X4	5747 ± 10	7·1	2·48
LCV1X5	5822 ± 41	6·6	2·49
LCV1Y1	5739 ± 34	6·9	2·46
LCV1Y1A	5916 ± 44	7·8	2·46
LCV1Y1B	5905 ± 37	6·0	2·46
LCV1Y2	5732 ± 63	6·4	2·49
LCV1Y3	5756 ± 20	8·0	2·45
LCV1Y4	5716 ± 51	6·6	2·49
LCV1Y5	5738 ± 37	5·8	2·45
LCV1Y6	5675 ± 21	7·2	2·47
LCV1Z1	5718 ± 29	7·4	2·47
LCV1Z2	5696 ± 29	5·6	2·47
LCV1Z3	5714 ± 43	6·5	2·46
LCV1Z4	5789 ± 42	8·0	2·46
LCV1Z5	5770 ± 20	7·0	2·46
LCV1Z5A	6060 ± 36	7·0	2·46
LCV1Z5B	6010 ± 61	7·0	2·46
LCV2X1	5238 ± 59	5·4	2·50
LCV2X2	5212 ± 40	5·4	2·50
LCV2X2A	5428 ± 69	5·6	2·49
LCV2X2B	5277 ± 88	5·3	2·50
LCV2X3	5284 ± 26	5·9	2·48
LCV2X4	5295 ± 20	5·6	2·49
LCV2Y1	5298 ± 40	5·5	2·50
LCV2Y2	5558 ± 37	5·6	2·49
LCV2Y3	5322 ± 36	5·9	2·49
LCV2Z1	5494 ± 40	6·0	2·49

LCV2Z1A	5484 ± 105	5•4	2•51
LCV2Z1B	5702 ± 73	6•5	2•47
LCV2Z2	5366 ± 46	6•1	2•48
LCV2Z3	5331 ± 52	5•2	2•51
LCV2Z4	5481 ± 20	6•0	2•48
LCV2Z4A	5526 ± 67	5•6	2•50
LCV2Z4B	5637 ± 57	6•4	2•46
bed A10			
LCA10-1X1	5007 ± 52	7•7	2•38
LCA10-1X2	5012 ± 30	8•0	2•37
LCA10-1X2A	5098 ± 49	6•6	2•38
LCA10-1X2B	4991 ± 59	6•3	2•38
LCA10-1X3	4899 ± 35	8•4	2•37
LCA10-1X4	5080 ± 33	7•5	2•39
LCA10-1X5	4784 ± 33	11•2	2•34
LCA10-1X6	4675 ± 22	9•2	2•34
LCA10-1X6A	4837 ± 18	7•3	2•36
LCA10-1X6B	4628 ± 33	8•5	2•31
LCA10-1Y1	5069 ± 34	7•3	2•37
LCA10-1Y1A	5281 ± 31	6•1	2•37
LCA10-1Y1B	4929 ± 62	6•9	2•37
LCA10-1Y2	5374 ± 63	9•1	2•36
LCA10-1Y3	5055 ± 54	7•8	2•39
LCA10-1Y4	5307 ± 64	7•0	2•41
LCA10-1Y5	4780 ± 42	9•3	2•38
LCA10-1Z1	5296 ± 36	8•2	2•37
LCA10-1Z2	5319 ± 34	6•3	2•39
LCA10-1Z3	5324 ± 14	7•0	2•38
LCA10-1Z3A	5439 ± 77	6•2	2•38
LCA10-1Z3B	5433 ± 46	6•3	2•37
LCA10-1Z4	5212 ± 46	7•5	2•37
LCA10-1Z4A	5166 ± 51	6•2	2•37
LCA10-1Z4B	5426 ± 82	5•5	2•37
LCA10-1Z5	5339 ± 28	6•9	2•40
LCA10-1Z6	5101 ± 52	6•0	2•41

LOCALITY - CHALBURY CAMP [S Y 694838]

bed 10

Core-Specimen	Velocity (m./sec.)	Porosity (%)	Density (gm./c.c.)
C10-1X1	4151 ± 22	24.3	2.02
C10-1X2	4180 ± 28	23.2	2.05
C10-1X3	4054 ± 12	22.9	2.06
C10-1X4	4250 ± 17	21.5	2.10
C10-1X5	4284 ± 51	22.5	2.07
C10-1Y1	4443 ± 24	21.9	2.09
C10-1Y2	4656 ± 105	18.1	2.19
C10-1Y3	4254 ± 23	24.1	2.03
C10-1Y4	4268 ± 85	20.2	2.13
C10-1Y5	5158 ± 75	7.8	2.47
C10-1Z1	4002 ± 20	26.3	1.97
C10-1Z2	4127 ± 20	22.5	2.07
C10-1Z3	3961 ± 22	26.2	1.97
C10-1Z4	3870 ± 14	23.9	2.03
C10-1Z5	3876 ± 25	24.6	2.01
C10-2X1	4346 ± 18	22.1	2.08
C10-2X2	4403 ± 22	20.4	2.13
C10-2Y1	4421 ± 58	21.0	2.11
C10-2Y2	4448 ± 36	22.6	2.07
C10-2Z1	4131 ± 26	22.6	2.07
C10-2Z2	4025 ± 32	22.9	2.06
C10-2Z3	4727 ± 37	15.7	2.25
bed 8			
C8-1X1	4061 ± 28	24.5	2.01
C8-1X2	3819 ± 27	25.2	1.99
C8-1X3	3818 ± 23	25.4	1.99
C8-1X4	3809 ± 36	26.1	1.97
C8-1X5	3992 ± 29	25.9	1.98
C8-1X6	3901 ± 44	26.1	1.97
C8-1Y1	3949 ± 28	25.3	1.99
C8-1Y2	3908 ± 43	26.3	1.96

C8-1Y3	3679 ± 22	27°1	1°94
C8-1Y4	3898 ± 26	25.1	2.00
C8-1Y5	3749 ± 28	27.2	1.94
C8-1Y6	3759 ± 32	23.2	2.05
C8-1Z1	4191 ± 22	19.3	2.16
C8-1Z2	4072 ± 25	24.0	2.03
C8-1Z3	4217 ± 17	19.6	2.14
C8-1Z4	4201 ± 19	21.5	2.09
C8-2X1	5108 ± 39	14.9	2.26
C8-2X2	4873 ± 34	16.7	2.21
C8-2X3	4607 ± 34	20.0	2.14
C8-2X4	4357 ± 30	18.6	2.17
C8-2Y1	4727 ± 63	17.2	2.20
C8-2Y2	4741 ± 37	18.5	2.16
C8-2Z1	4441 ± 26	20.6	2.12
C8-2Z2	4652 ± 62	16.6	2.23
C8-2Z3	4667 ± 64	20.2	2.13
C8-2X4	4552 ± 34	21.3	2.10

bed 6

C6-1X1	3181 ± 19	32.8	1.79
C6-1X2	3357 ± 20	32.1	1.81
C6-1X3	3311 ± 35	31.9	1.82
C6-1X4	3629 ± 26	28.4	1.91
C6-1Y1	3778 ± 46	25.3	1.99
C6-1Y2	3729 ± 26	27.0	1.94
C6-1Y3	3475 ± 39	28.7	1.90
C6-1Y4	3291 ± 18	31.5	1.82
C6-1Z1	3464 ± 19	31.0	1.84
C6-1Z2	3483 ± 18	30.0	1.86
C6-1Z3	3537 ± 20	30.3	1.86
C6-1Z4	3537 ± 54	31.0	1.84
C6-2X1	3493 ± 38	27.0	1.94
C6-2X2	3336 ± 13	28.4	1.91
C6-2X3	3463 ± 55	27.3	1.93
C6-2X4	3283 ± 29	27.8	1.92
C6-2Y1	3372 ± 35	27.8	1.92

C6-2Y2	3359 ± 25	27.1	1.94
C6-2Y3	3392 ± 31	25.6	1.98
C6-2Y4	3304 ± 18	26.3	1.96
C6-2Z1	3369 ± 22	27.5	1.93
C6-2Z2	3325 ± 20	26.4	1.95
C6-2Z3	3370 ± 13	27.0	1.94
C6-2Z4	3379 ± 30	25.9	1.97
bed 5			
C5-1X1	4149 ± 45	22.1	2.08
C5-1X2	3463 ± 27	24.4	2.02
C5-1X3	3477 ± 30	23.1	2.05
C5-1Y1	3554 ± 78	29.8	1.87
C5-1Y2	3515 ± 65	27.5	1.93
C5-1Y3	3573 ± 40	27.7	1.93
C5-1Z1	3650 ± 46	21.7	2.09
C5-1Z2	3635 ± 36	21.6	2.09
C5-1Z3	3308 ± 20	25.8	1.98
C5-1Z4	3307 ± 33	23.8	2.04
C5-2X1	3667 ± 40	28.0	1.92
C5-2X2	3859 ± 48	28.3	1.91
C5-2X3	3755 ± 44	26.9	1.95
C5-2Y1	3545 ± 26	29.5	1.88
C5-2Y2	3657 ± 32	29.3	1.89
C5-2Z1	3638 ± 31	28.1	1.92
C5-2Z2	3486 ± 27	29.1	1.89
C5-3X1	4726 ± 111	14.7	2.28
C5-3X2	4157 ± 45	20.0	2.13
C5-3X3	4461 ± 33	18.1	2.19
C5-3Y1	3326 ± 69	31.3	1.83
C5-3Y2	3713 ± 39	24.5	2.01
C5-3Y3	4246 ± 44	20.3	2.13
C5-3Z1	4108 ± 23	14.8	2.27
C5-3Z2	3776 ± 23	20.5	2.12

LOCALITY - CORTON FARM ROAD-CUTTING [S Y 636855]

black dolomitic sandstone bed

Core-Specimen	Velocity (m./sec.)	Porosity (%)	Density (gm./c.c.)
CFPS1X1	4739 ± 71	15.2	2.35
CFPS1X2	4865 ± 52	14.0	2.38
CFPS1X3	4700 ± 76	14.8	2.36
CFPS1Y1	4488 ± 15	15.6	2.36
CFPS1Y2	4526 ± 35	15.0	2.35
CFPS1Z1	4566 ± 43	14.9	2.36
CFPS1Z2	4575 ± 46	14.8	2.36
CFPS2X1	4745 ± 60	15.1	2.35
CFPS2X2	4848 ± 83	14.6	2.37
CFPS2Y1	4547 ± 79	20.1	2.22
CFPS2Y2	4572 ± 33	16.1	2.32
CFPS2Z1	3948 ± 20	21.5	2.19

LOCALITY - PORTESHAM QUARRY [S Y 610859]

bed 10

Core-Specimen	Velocity (m./sec.)	Porosity (%)	Density (gm./c.c.)
P10-1X1	4001 ± 71	26.9	1.95
P10-1X2	3881 ± 35	27.0	1.95
P10-1Y1	4451 ± 49	24.5	2.02
P10-1Y2	3838 ± 26	26.3	1.97
P10-1Y3	5204 ± 88	16.7	2.23
P10-1Z1	4093 ± 35	24.7	2.02
P10-1Z2	5717 ± 70	11.1	2.34
P10-1Z3	5541 ± 101	12.3	2.34

bed 8

P8-1X1	4192 ± 51	19·9	2·14
P8-1X2	3764 ± 27	26·3	1·97
P8-1X3	4003 ± 60	25.3	2·00
P8-1X4	4081 ± 107	27·6	1·92
P8-1Y1	4041 ± 40	21·9	2·07
P8-1Y2	3989 ± 19	24·3	2·02
P8-1Y3	4068 ± 30	24·8	2·01
P8-1Z1	3913 ± 26	24·9	2·00
P8-1Z2	4077 ± 51	25·4	1·99
P8-1Z3	3797 ± 14	25·6	1·99

bed 6

P6-1X1	3828 ± 61	28·3	1·92
P6-1X2	3899 ± 47	27.3	1·94
P6-1X3	3767 ± 63	27.8	1·93
P6-1X4	3657 ± 27	27·4	1·94
P6-1Y1	3738 ± 31	28·0	1·93
P6-1Y2	3793 ± 20	25·4	2·00
P6-1Y3	3441 ± 31	27·9	1·93
P6-1Y4	3836 ± 86	27·5	1·93
P6-1Y5	3509 ± 32	29·0	1·90
P6-1Z1	3533 ± 15	29·6	1·88
P6-1Z2	3686 ± 29	28·2	1·92
P6-1Z3	3670 ± 17	27·4	1·94
P6-1Z4	3446 ± 18	28·4	1·91

LOCALITY - WEST WEARE CLIFFS, ISLE OF PORTLAND [S Y 682724]

black dolomitic sandstone bed

Core-Specimen	Velocity (m./sec.)	Porosity (%)	Density (gm./c.c.)
PLPS1X1	4023 ± 12	19·2	2·24
PLPS1X2	4093 ± 18	17·9	2·27
PLPS1X3	4019 ± 22	19·4	2·23
PLPS1X4	4147 ± 10	18·0	2·27

PLPS1X5	4139 ± 23	18•2	2•27
PLPS1X6	4219 ± 24	17•9	2•28
PLPS1Y1	3527 ± 13	25•0	2•07
PLPS1Y2	3779 ± 21	22•4	2•14
PLPS1Y3	3809 ± 15	20•8	2•18
PLPS1Y4	3787 ± 21	20•9	2•18
PLPS1Y5	3810 ± 11	21•7	2•16
PLPS1Z1	4209 ± 29	14•8	2•36
PLPS1Z2	4017 ± 23	17•4	2•29
PLPS1Z3	3969 ± 24	19•6	2•22
PLPS1Z4	3772 ± 15	19•9	2•22
PLPS1Z5	3751 ± 20	18•9	2•25
PLPS2X1	4495 ± 39	15•4	2•34
PLPS2X2	4385 ± 20	14•7	2•36
PLPS2X3	4133 ± 18	13•0	2•39
PLPS2Y1	4114 ± 18	16•6	2•31
PLPS2Y2	4085 ± 9	14•6	2•35
PLPS2Y3	4111 ± 22	15•5	2•32
PLPS2Y4	4173 ± 18	14•9	2•38
PLPS2Y5	4207 ± 14	12•1	2•43
PLPS2Y6	4333 ± 26	12•1	2•42
PLPS2Z1	3943 ± 25	14•0	2•36
PLPS2Z2	3969 ± 21	13•5	2•36
PLPS2Z3	3999 ± 7	15•7	2•33
PLPS2Z4	4081 ± 36	14•6	2•34
PLPS3X1	3997 ± 67	20•7	2•17
PLPS3X2	3992 ± 20	18•5	2•23
PLPS3X3	3942 ± 18	19•2	2•21
PLPS3X4	3914 ± 25	19•7	2•21
PLPS3X5	3969 ± 19	20•0	2•20
PLPS3X6	3990 ± 33	19•4	2•20
PLPS3Y1	4002 ± 28	20•4	2•17
PLPS3Y2	3722 ± 16	19•8	2•21
PLPS3Y3	3916 ± 7	20•1	2•20
PLPS3Y4	3793 ± 19	19•8	2•21
PLPS3Z1	3448 ± 20	19•8	2•20
PLPS3Z2	3547 ± 14	18•2	2•23
PLPS3Z3	3474 ± 15	19•4	2•20
PLPS3Z4	3499 ± 31	20•6	2•16

LOCALITY - FRESHWATER BAY, ISLE OF PORTLAND [S Y 692702]

Arkell's "Basal Shell Bed"

Core-Specimen	Velocity (m./sec.)	Porosity (%)	Density (gm./c.c.)
PLBS1X1	5366 ± 60	16.8	2.20
PLBS1X2	5639 ± 123	15.4	2.23
PLBS1X3	6079 ± 51	4.7	2.50
PLBS1X4	5804 ± 32	4.3	2.52
PLBS1X5	5772 ± 62	5.0	2.50
PLBS1Y1	5616 ± 34	4.6	2.51
PLBS1Y2	5636 ± 39	4.3	2.52
PLBS1Y3	5832 ± 39	4.7	2.50
PLBS1Y4	5651 ± 22	5.5	2.49
PLBS1Y5	5735 ± 44	5.5	2.50
PLBS1Z1	5644 ± 20	6.4	2.46
PLBS1Z2	5746 ± 123	7.4	2.45
PLBS1Z3	5550 ± 28	6.4	2.47
PLBS1Z4	5435 ± 52	8.1	2.43
PLBS1Z5	5620 ± 37	4.6	2.49
PLBS2X1	5715 ± 65	5.5	2.48
PLBS2X2	5521 ± 34	5.5	2.49
PLBS2X3	5528 ± 41	5.2	2.49
PLBS2X4	5629 ± 31	5.5	2.49
PLBS2X5	5509 ± 15	6.0	2.48
PLBS2Y1	5470 ± 33	7.1	2.47
PLBS2Y2	5752 ± 62	7.9	2.43
PLBS2Y3	5488 ± 13	6.3	2.47
PLBS2Y4	5570 ± 41	5.7	2.47
PLBS2Y5	5578 ± 56	6.8	2.44
PLBS2Z1	5217 ± 26	5.4	2.52
PLBS2Z2	5219 ± 38	7.2	2.48
PLBS2Z3	5096 ± 29	7.0	2.47
PLBS2Z4	5157 ± 23	5.5	2.49
PLBS2Z5	5217 ± 19	7.7	2.44
PLBS3X1	5777 ± 120	9.2	2.43
PLBS3X2	5855 ± 67	4.7	2.54
PLBS3X3	6020 ± 54	5.5	2.52

PLBS3X4	5774 ± 89	7·1	2·50
PLBS3Y1	5516 ± 137	16·8	2·22
PLBS3Y2	5096 ± 54	16·4	2·24
PLBS3Y3	4843 ± 116	16·5	2·24
PLBS3Z1	5176 ± 52	11·5	2·36
PLBS3Z2	5069 ± 47	12·2	2·35
PLBS3Z3	5292 ± 69	12·1	2·35
PLBS3Z4	5414 ± 67	10·5	2·40
PLBS3Z5	5697 ± 69	8·4	2·42
PLBS3Z6	5575 ± 34	9·4	2·43

LOCALITY - PERRYFIELD QUARRIES, ISLE OF PORTLAND

[S Y 694712]

Whit bed

Core-Specimen	Velocity (m.sec.)	Porosity (%)	Density (gm./c.c.)
PLW1X1	3980 ± 23	18·0	2·19
PLW1X2	4215 ± 48	20·2	2·14
PLW1X3	4319 ± 42	18·4	2·18
PLW1X4	3975 ± 18	20·8	2·12
PLW1X5	3985 ± 35	20·7	2·12
PLW1Y1	3878 ± 40	22·2	2·08
PLW1Y2	4180 ± 44	19·7	2·15
PLW1Y3	3957 ± 41	20·2	2·14
PLW1Y4	3896 ± 19	20·9	2·12
PLW1Y5	4010 ± 29	20·6	2·13
PLW1Z1	4349 ± 27	19·1	2·15
PLW1Z2	4417 ± 13	20·0	2·14
PLW1Z3	4440 ± 32	18·2	2·19
PLW1Z4	4378 ± 15	19·1	2·16
PLW1Z5	4685 ± 33	17·0	2·22
PLW2X1	3844 ± 11	22·7	2·07
PLW2X2	3828 ± 9	21·3	2·10
PLW2X3	3909 ± 21	21·0	2·11
PLW2X4	3805 ± 15	22·2	2·08
PLW2Y1	3916 ± 34	19·1	2·17
PLW2Y2	3885 ± 13	18·9	2·17

PLW2Y3	3869 ± 10	17·1	2·22
PLW2Y4	3921 ± 20	17·5	2·21
PLW2Z1	4511 ± 8	18·2	2·19
PLW2Z2	4557 ± 18	18·8	2·17
PLW2Z3	4531 ± 23	17·7	2·20
PLW2Z4	4556 ± 34	17·4	2·21
Base bed			
PLB1X1	4516 ± 32	18.0	2.26
PLB1X2	4450 ± 31	15·5	2·26
PLB1X3	4428 ± 34	14·8	2·27
PLB1X4	4389 ± 19	16·8	2·23
PLB1X5	4525 ± 65	13·6	2·32
PLB1Y1	4241 ± 49	15·7	2·26
PLB1Y2	4039 ± 25	17·0	2·23
PLB1Y3	4321 ± 47	12·5	2·32
PLB1Y4	4201 ± 25	16·3	2·25
PLB1Y5	4192 ± 26	15·3	2·27
PLB1Z1	4209 ± 42	14·8	2·29
PLB1Z2	4628 ± 64	12·0	2·35
PLB1Z3	4485 ± 44	16·9	2.21
PLB1Z4	4412 ± 41	17·4	2.21
PLB1Z5	4483 ± 27	15·3	2.26
PLB1Z6	4421 ± 39	14·8	2·29
PLB2X1	4703 ± 60	11·5	2·38
PLB2X2	4614 ± 19	14·7	2·29
PLB2X3	4729 ± 40	12·6	2·33
PLB2X4	4379 ± 64	14·0	2·31
PLB2X5	4703 ± 46	14·3	2·30
PLB2X6	4455 ± 92	13·1	2·34
PLB2Y1	4592 ± 31	15·2	2·28
PLB2Y2	4714 ± 29	13·4	2·33
PLB2Y3	4661 ± 26	13·9	2·31
PLB2Y4	4641 ± 23	12·9	2·34
PLB2Z1	4776 ± 19	12·0	2·36
PLB2Z2	4728 ± 28	14·2	2·30
PLB2Z3	4739 ± 17	13·3	2·33
PLB2Z4	4781 ± 23	12·3	2·36

LOCALITY - CHILMARK RAVINE [S T 974313]

"Upper Building Stones" (Arkell, 1933)

Core-Specimen	Velocity (m./sec.)	Porosity (%)	Density (gm./c.c.)
CRU1X1	2940 ± 13	30.8	1.74
CRU1X2	2792 ± 27	31.7	1.82
CRU1Y1	2690 ± 7	33.6	1.76
CRU1Y2	2927 ± 19	28.2	1.82
CRU1Y3	2975 ± 19	26.2	1.87
CRU1Z1	3518 ± 23	28.1	1.81
CRU1Z2	3493 ± 17	32.4	1.80
CRU2X1	2982 ± 20	33.2	1.78
CRU2X2	2972 ± 26	29.4	1.76
CRU2X3	3002 ± 19	31.7	1.82
CRU2X4	3034 ± 27	25.9	1.83
CRU2X5	3028 ± 22	28.9	1.79
CRU2X6	3075 ± 18	32.6	1.79
CRU2X7	3025 ± 15	33.3	1.77
CRU2X8	2994 ± 16	33.7	1.76
CRU2X9	3112 ± 16	29.8	1.74
CRU2Y1	2939 ± 39	32.6	1.80
CRU2Y2	3019 ± 21	26.3	1.85
CRU2Y3	3063 ± 13	29.1	1.78
CRU2Y4	2986 ± 12	25.8	1.88
CRU2Y5	2997 ± 25	27.6	1.83
CRU2Y6	3117 ± 23	29.1	1.78
CRU2Y7	2928 ± 28	32.7	1.80
CRU2Y8	2914 ± 25	30.0	1.78
CRU2Y9	2884 ± 32	29.3	1.79
CRU2Y10	3055 ± 26	28.1	1.82
CRU2Y11	2908 ± 26	34.4	1.75
CRU2Y12	3028 ± 40	27.0	1.84
CRU2Z1	3458 ± 22	33.4	1.77
CRU2Z2	3631 ± 36	31.0	1.84
CRU2Z3	3618 ± 10	30.6	1.87
CRU2Z4	3633 ± 34	30.2	1.86
CRU2Z5	3674 ± 49	30.0	1.86

CRU2Z6	3658 ± 38	30·4	1·85
CRU2Z7	3585 ± 56	26·4	1·87
CRU2Z8	3587 ± 42	24·8	1·89
CRU2Z9	3456 ± 42	31·2	1·83
CRU2Z10	3573 ± 34	27·7	1·83
CRU2Z11	3486 ± 27	26·9	1·84
CRU2Z12	3446 ± 44	26·9	1·83
CRU3X1	3947 ± 63	28·9	1·89
CRU3X2	3990 ± 73	28·3	1·90
CRU3X3	3824 ± 41	27·1	1·94
CRU3Y1	3899 ± 95	27·7	1·93
CRU3Y2	3966 ± 73	26·2	1·94
CRU3Y3	3981 ± 53	29·2	1·89
CRU3Y4	3587 ± 58	33·5	1·76
CRU3Y5	3585 ± 45	32·5	1·79
CRU3Z1	3750 ± 28	30.1	1·87
CRU3Z2	3826 ± 34	28·1	1·91
CRU3Z3	3495 ± 27	31·4	1·83
CRU3Z4	3830 ± 29	27·6	1·93
CRU4X1	3729 ± 33	29·8	1·87
CRU4X2	4157 ± 56	26·4	1·95
CRU4X3	3684 ± 28	30·5	1·85
CRU4X4	3344 ± 51	32·3	1·80
CRU4X5	4008 ± 46	26·2	1·96
CRU4X6	4135 ± 52	28·4	1·91
CRU4Y1	3451 ± 21	31·0	1·83
CRU4Y2	3885 ± 27	29·3	1·88
CRU4Y3	4021 ± 55	26·9	1·94
CRU4Y4	3758 ± 57	32·3	1·81
CRU4Y5	3953 ± 52	29·8	1·87
CRU4Z1	3476 ± 36	30·5	1·85
CRU4Z2	3558 ± 45	31·7	1·81
CRU4Z3	3210 ± 25	28·5	1·90
CRU4Z4	3259 ± 34	29·2	1·90
CRU4Z5	3412 ± 20	31·0	1·84
CRU4Z6	3147 ± 21	31·6	1·82
CRU4Z7	3626 ± 49	27·4	1·93

chalky limestone beds

CRC1X1	3064 ± 36	33.3	1.78
CRC1X2	2805 ± 19	34.7	1.75
CRC1Y1	2926 ± 42	31.7	1.82
CRC1Y2	2792 ± 17	36.5	1.69
CRC1Z1	3108 ± 27	34.0	1.76
CRC1Z2	3111 ± 13	34.2	1.76
CRC2X1	2850 ± 35	32.7	1.79
CRC2X2	2770 ± 24	36.2	1.70
CRC2X3	2773 ± 21	33.6	1.77
CRC2Y1	2607 ± 17	36.6	1.68
CRC2Y2	3075 ± 69	36.7	1.68
CRC2Y3	2598 ± 15	35.2	1.72
CRC2Y4	2612 ± 17	34.4	1.74
CRC2Z1	2963 ± 9	34.3	1.63
CRC2Z2	2946 ± 7	38.9	1.63
CRC2Z3	2984 ± 43	37.2	1.67
CRC3X1	2866 ± 31	37.2	1.67
CRC3X2	3122 ± 43	32.5	1.80
CRC3X3	3130 ± 10	32.9	1.78
CRC3X4	3067 ± 14	35.3	1.72
CRC3X5	2968 ± 10	34.9	1.73
CRC3X6	2816 ± 12	36.9	1.68
CRC3X7	2995 ± 35	36.0	1.70
CRC3X8	2718 ± 23	36.7	1.68
CRC3Y1	3128 ± 45	34.8	1.73
CRC3Y2	2985 ± 19	33.2	1.79
CRC3Y3	3075 ± 29	32.5	1.79
CRC3Y4	2815 ± 36	37.6	1.69
CRC3Z1	2896 ± 7	38.8	1.62
CRC3Z2	2916 ± 10	38.2	1.64
CRC3Z3	3002 ± 16	37.3	1.67
CRC3Z4	2988 ± 16	35.3	1.72
CRC3Z5	3039 ± 7	33.5	1.77
CRC3Z6	3074 ± 17	36.8	1.68

Ragstone beds

CRR1X1	3686 ± 36	21·5	2·09
CRR1Y1	3926 ± 41	25·4	1·99
CRR1Z1	3319 ± 25	27·7	1·79

LOCALITY - UPPER CHICKSGROVE QUARRY [S T 962296]

Lamellosus bed

Core-Specimen	Velocity (m./sec.)	Porosity (%)	Density (gm./c.c.)
UCL1X1	5353 ± 42	9·6	2·39
UCL1X2	5394 ± 20	11·1	2·33
UCL1X3	5030 ± 25	12·9	2·33
UCL1X4	5528 ± 35	11·6	2·37
UCL1Y1	5339 ± 20	10·0	2·36
UCL1Y2	6025 ± 167	9·6	2·41
UCL1Y3	4989 ± 28	12·4	2·34
UCL1Z1	4407 ± 16	18·4	2·19
UCL1Z2	4005 ± 16	22·6	2·07
UCL1Z3	3452 ± 35	30.2	1·87
UCL1Z4	4048 ± 70	26·9	1·95

Ragstone beds

UCR1X1	4839 ± 68	16·9	2·19
UCR1X2	4799 ± 27	11·3	2·37
UCR1X3	5202 ± 35	9·1	2·43
UCR1X4	4959 ± 80	14·2	2·29
UCR1X5	5269 ± 55	9·7	2·41
UCR1Y1	5394 ± 22	8·8	2·41
UCR1Y2	5329 ± 15	6·2	2·47
UCR1Y3	5440 ± 84	7·3	2·43
UCR1Y4	5447 ± 47	6·6	2·46
UCR1Y5	5240 ± 50	12·2	2·34
UCR1Z1	4868 ± 99	13·6	2·31
UCR1Z2	4822 ± 43	16·7	2·23

UCR1Z3	4400 ± 32	13·7	2·30
UCR1Z4	4988 ± 65	14·2	2·29
UCR1Z5	5013 ± 26	15·1	2·28
UCR2X1	3553 ± 32	23·9	2·02
UCR2X2	3498 ± 5	27·1	1·95
UCR2X3	3565 ± 22	21·1	2·11
UCR2Y1	3452 ± 14	21·4	2·10
UCR2Y2	3484 ± 14	24·0	2·03
UCR2Y3	3539 ± 20	24·7	2·01
UCR2Z1	3495 ± 24	27·9	1·91
UCR2Z2	3431 ± 18	24·7	2·01
UCR2Z3	3360 ± 17	27·7	1·92
UCR3X1	4607 ± 31	13·5	2·31
UCR3X2	4893 ± 96	8·6	2·43
UCR3Y1	4776 ± 99	11·0	2·37
UCR3Y2	4850 ± 35	12·4	2·33
UCR3Z1	4422 ± 27	13·2	2·31
UCR3Z2	4382 ± 28	12·8	2·33
Glauconitic sandy limestone beds			
UCM1X1	2510 ± 18	30·6	1·84
UCM1X2	2807 ± 18	26·3	1·96
UCM1X3	2617 ± 30	28·4	1·90
UCM1X4	2976 ± 33	25·9	1·97
UCM1X5	2544 ± 17	30·1	1·86
UCM1X6	3201 ± 40	25·8	1·97
UCM1Y1	2010 ± 18	32·9	1·78
UCM1Y2	2222 ± 36	32·8	1·79
UCM1Y3	2226 ± 20	32·3	1·80
UCM1Y4	2405 ± 24	28·2	1·91
UCM1Y5	2611 ± 28	29·7	1·87
UCM1Y6	2791 ± 29	25·2	1·97
UCM1Z1	2379 ± 22	27·7	1·91
UCM1Z2	2382 ± 15	26·9	1·94
UCM1Z3	2453 ± 23	26·6	1·95
UCM1Z4	2401 ± 25	26·9	1·93
UCM1Z5	2124 ± 23	28·6	1·88
UCM1Z6	1876 ± 23	31·5	1·81

Basement beds

UCB1X1	3422 ± 32	26•5	1•94
UCB1X2	2616 ± 14	33•0	1•76
UCB1X3	3738 ± 65	27•8	1•91
UCB1X4	3685 ± 68	20•0	2•11
UCB1X5	2930 ± 8	28•7	1•87
UCB1Y1	3663 ± 30	21•8	2•05
UCB1Y2	3241 ± 24	28•2	1•88
UCB1Y3	2676 ± 19	30•9	1•82
UCB1Y4	2511 ± 19	28•2	1•88
UCB1Z1	2638 ± 13	32•3	1•78
UCB1Z2	2816 ± 9	29•7	1•85
UCB1Z3	2439 ± 16	30•3	1•83
UCBLZ4	2818 ± 6	27•7	1•90
UCB2X1	2259 ± 29	35•1	1•69
UCB2X2	2144 ± 23	39•2	1•60
UCB2X3	4265 ± 14	15•4	2•25
UCB2X4	5505 ± 23	16•2	2•21
UCB2Y1	3693 ± 38	23•5	2•00
UCB2Y2	3203 ± 23	26•4	1•93
UCB2Y3	3766 ± 46	27•2	1•90
UCB2Y4	3926 ± 37	24•7	1•95
UCB2Z1	3776 ± 16	28•3	1•87
UCB2Z2	2033 ± 12	32•7	1•76
UCB2Z3	1992 ± 18	28•9	1•69

Basal shell beds

UCBS1X1	4278 ± 58	17•0	2•22
UCBS1X2	4541 ± 71	14•7	2•28
UCBS1X3	4587 ± 52	9•7	2•48
UCBS1Y1	4564 ± 65	9•7	2•40
UCBS1Y2	4401 ± 30	14•3	2•29
UCBS1Y3	4642 ± 43	10•3	2•38
UCBS1Z1	3594 ± 36	18•5	2•17
UCBS1Z2	3453 ± 26	18•6	2•18
UCBS1Z3	3500 ± 35	14•6	2•28
UCBS1Z4	3515 ± 36	16•9	2•22

APPENDIX 6

LIMESTONE CLASSIFICATION OF CORE-SPECIMENS

The limestone classification is that of Folk (1959, 1962); (see Fig.4.1). 245 core-specimens that were thin-sectioned, are listed. The limestone-type, as defined in Section 4.6.1, is also indicated.

LOCALITY - SWANWORTH QUARRY [S Y 969784]

bed V

Core-Specimen	Limestone Classification	Limestone-Type
WV1X2	Sparse Biomicrite	
WV1Y1	Sparse Biomicrite	
WV1Z2A	Sparse Biomicrite	
WV1Z2B	Fossiliferous Micrite	
WV2X2	Sparse Biomicrite	
WV2Y2	Sparse Biomicrite	
WV2Z2A	Sparse Biomicrite	
WV2Z2B	Sparse Biomicrite	
WV3X1	Sparse Biomicrite	
WV3Y2A	Sparse Biomicrite	All Micrites
WV3Y2B	Sparse Biomicrudite	
WV3Y4	Sparse Biomicrite	
WV3Z6	Sparse Biomicrudite	
WV4X1	Fossiliferous Micrite	
WV4Y1	Fossiliferous Micrite	
WV4Z1	Fossiliferous Micrite	
WV5X2A	Sparse Biomicrite	
WV5X2B	Sparse Biomicrite	
WV5Y1	Sparse Biomicrite	
WV5Z3B	Sparse Biomicrite	

bed U

WU1X3	Unsorted Fossiliferous Intraclastic Oosparite	
WU1X4	Unsorted Fossiliferous Oosparite	
WU1Y1	Unsorted Fossiliferous Intraclastic Oosparite	
WU1Z5A	Unsorted Fossiliferous Oosparite	
WU1Z5B	Unsorted Fossiliferous Intraclastic Oosparite	All Sparites

WU2Y2	Unsorted Fossiliferous Oolitic Intrasparite	
WU2Z2	Unsorted Fossiliferous Oolitic Intrasparite	
WU3X1	Unsorted Fossiliferous Intraclastic Oosparite	
WU3X4	Unsorted Oolitic Biosparite	
bed T		
WT1Y1	Unsorted Fossiliferous Intraclastic Oosparite	All Sparites
WT1Z1A	Unsorted Fossiliferous Oosparite	
WT1Z1B	Unsorted Fossiliferous Oosparite	
WT2Z1	Unsorted Fossiliferous Intraclastic Oosparite	
WT3X2	Unsorted Fossiliferous Oosparite	
WT3Y1A	Unsorted Fossiliferous Oosparite	
WT3Y1B	Unsorted Fossiliferous Oosparite	
WT3Z1	Unsorted Fossiliferous Oosparite	
bed S		
WS1Z3A	Unsorted Fossiliferous Intraclastic Oosparite	All Sparites
WS1Z3B	Unsorted Fossiliferous Intraclastic Oosparite	
WS2X2	Sandy Unsorted Fossiliferous Intraclastic Oosparite	
bed Q		
WQ1X2	Unsorted Fossiliferous Intraclastic Oosparite	
WQ1Z2	Unsorted Fossiliferous Intraclastic Oosparite	

WQ1Z6	Unsorted Fossiliferous Oolitic Intrasparite	All Sparites
WQ2X2	Unsorted Oolitic Biosparudite	
WQ2Y1	Unsorted Fossiliferous Oosparite	
WQ3X2A	Sandy Unsorted Fossiliferous Intrasparite	
WQ3X2B	Unsorted Fossiliferous Intrasparite	
WQ3Y1A	Sandy Unsorted Fossiliferous Intrasparite	
WQ3Y1B	Unsorted Fossiliferous Intrasparite	
bed P		
WP1Y6	Unsorted Fossiliferous Oosparite	All Sparites
WP1Z2	Unsorted Fossiliferous Oosparite	
WP1Z3	Unsorted Fossiliferous Intraclastic Oosparite	
WP2Y1	Unsorted Fossiliferous Oosparite	
WP3X1	Unsorted Fossiliferous Oosparite	
WP3X2	Unsorted Fossiliferous Oosparite	
bed O		
WO1Y2	Unsorted Fossiliferous Oosparite	All Sparites
WO1Z3	Unsorted Fossiliferous Intraclastic Oosparite	
WO2Y4	Unsorted Fossiliferous Oosparite	
WO3Z2	Unsorted Fossiliferous Oosparite	
WO3Z3	Unsorted Fossiliferous Oosparite	
WO3Z4	Unsorted Fossiliferous Oosparite	

bed N

WN1X5	Unsorted Fossiliferous Oosparite	All Sparites
WN1Y1	Unsorted Fossiliferous Oosparite	
WN2X2	Unsorted Fossiliferous Intraclastic Oosparite	
WN2Y1	Unsorted Fossiliferous Intraclastic Oosparite	
WN2Z2	Unsorted Fossiliferous Oosparite	
WN3X2	Unsorted Fossiliferous Intraclastic Oosparite	

bed B

WB1X2	Silty Sparse Biomicrosparite	All Microsparites
WB1X4A	Silty Fossiliferous Microsparite	
WB1X4B	Silty Sparse Biomicrosparite	
WB1Y2	Silty Fossiliferous Microsparite	
WB1Y4	Silty Sparse Biomicrosparite	
WB1Z1	Silty Sparse Biomicrosparite	
WB2X2	Silty Fossiliferous Microsparite	
WB2X4A	Silty Fossiliferous Microsparite	
WB2Y1	Silty Fossiliferous Microsparite	
WB2Y4	Silty Fossiliferous Microsparite	
WB2Z4	Silty Sparse Biomicrosparite	

bed A28

WA28-1X1	Silty Dolomitised Fossiliferous Micro-sparite

WA28-1Y2	Silty Dolomitised Fossiliferous Microsparite	
WA28-1Z1	Silty Dolomitised Fossiliferous Microsparite	
WA28-2X1A	Silty Dolomitised Sparse Biomicrosparite	
WA28-2X1B	Silty Dolomitised Fossiliferous Microsparite	All Microsparites
WA28-2X6	Silty Dolomitised Fossiliferous Microsparite	
WA28-2Y2	Silty Dolomitised Sparse Biomicrosparite	
WA28-2Y3	Silty Dolomitised Sparse Biomicrosparite	
WA28-2Z2	Silty Dolomitised Fossiliferous Microsparite	

LOCALITY - LULWORTH COVE AREA [S Y 8279]

bed V

Core-Specimen	Limestone Classification	Limestone-Type
LCV1X3A	Unsorted Intraclastic Biopelsparite	
LCV1X3B	Unsorted Intraclastic Biopelsparite	
LCV1X4	Unsorted Intraclastic Biopelsparite	
LCV1X5	Unsorted Intraclastic Biopelsparite	
LCV1Y1A	Unsorted Intraclastic Biopelsparite	
LCV1Y1B	Unsorted Biopelsparite	
LCV1Y3	Unsorted Biopelsparite	
LCV1Z1	Unsorted Biopelsparite	
LCV1Z2	Unsorted Intraclastic Biopelsparite	
LCV1Z4	Unsorted Intraclastic Biopelsparite	
LCV1Z5A	Unsorted Biopelsparite	
LCV1Z5B	Unsorted Intraclastic Biopelsparite	All Sparites
LCV2X1	Unsorted Fossiliferous Oolitic Pelletiferous Intrasparite	
LCV2X2A	Unsorted Fossiliferous Pelletiferous Intrasparite	
LCV2X2B	Unsorted Intraclastic Biopelsparite	
LCV2X3	Unsorted Fossiliferous Oolitic Pelletiferous Intrasparite	
LCV2X4	Unsorted Fossiliferous Pelletiferous Intrasparite	
LCV2Y1	Unsorted Intraclastic Biopelsparite	
LCV2Y2	Unsorted Fossiliferous Pelletiferous Intrasparite	
LCV2Y3	Unsorted Intraclastic Biopelsparite	

LCV2Z1A	Unsorted Intraclastic Biopelsparite
LCV2Z1B	Unsorted Fossiliferous Pelletiferous Intrasparite
LCV2Z4A	Unsorted Intraclastic Biopelsparite
LCV2Z4B	Unsorted Fossiliferous Pelletiferous Intrasparite

bed A10

LCA10-1X1	Silty Dolomitised Sparse Biomicrosparite	All Microsparites
LCA10-1X2A	Silty Dolomitised Sparse Biomicrosparite	
LCA10-1X2B	Silty Dolomitised Fossiliferous Microsparite	
LCA10-1X6A	Silty Dolomitised Sparse Biomicrosparite	
LCA10-1X6B	Silty Dolomitised Sparse Biomicrosparite	
LCA10-1Y1A	Silty Dolomitised Sparse Biomicrosparite	
LCA10-1Y1B	Silty Dolomitised Sparse Biomicrosparite	
LCA10-1Y2	Sandy Dolomitised Sparse Biomicrosparite	
LCA10-1Y3	Silty Dolomitised Sparse Biomicrosparite	
LCA10-1Y5	Silty Dolomitised Sparse Biomicrosparite	
LCA10-1Z1	Silty Dolomitised Sparse Biomicrosparite	
LCA10-1Z2	Silty Dolomitised Sparse Biomicrosparite	
LCA10-1Z4A	Silty Dolomitised Sparse Biomicrosparite	
LCA10-1Z4B	Silty Dolomitised Sparse Biomicrosparite	

LOCALITY - CHALBURY CAMP [S Y 694838]

Core-Specimen	Limestone Classification	Limestone-Type
bed 10		
C10-1Y1	Packed Biopelmicrite	All Chalks
C10-1Y5	Sparse Biopelmicrite	
C10-2Z3	Packed Biopelmicrite	
bed 8		
C8-1Z1	Sparse Biomicrite	All Chalks
C8-2X1	Sparse Biomicrite	
C8-2Z2	Sparse Biomicrite	
bed 6		
C6-1Y4	Packed Biopelmicrite	All Chalks
C6-1Z3	Sparse Biopelmicrite	
C6-2Y4	Sparse Biopelmicrite	
bed 5		
C5-1X1	Sparse Biopelmicrite	All Chalks
C5-1X3	Sparse Biopelmicrite	
C5-1Y1	Packed Biopelmicrite	
C5-1Z1	Packed Biopelmicrite	
C5-2X2	Packed Biopelmicrite	
C5-3X1	Packed Biopelmicrite	
C5-3Y3	Packed Biopelmicrite	
C5-3Z1	Packed Biopelmicrite	

LOCALITY - CORTON FARM ROAD-CUTTING [S Y 636855]

black dolomitic sandstone bed		
Core-Specimen	Limestone Classification	Limestone-Type
CFPS1X2	Silty Dolomitised Sparse Biomicrite	All Microsparites
CFPS1Y1	Dolomitised Sparse Biomicrite	
CFPS1Z2	Dolomitised Sparse Biomicrite	
CFPS2X1	Dolomitised Sparse Biomicrite	
CFPS2Y1	Dolomitised Fossiliferous Micrite	
CFPS2Z1	Dolomitised Fossiliferous Micrite	

LOCALITY - PORTESHAM QUARRY [S Y 610859]

bed 10		
Core-Specimen	Limestone Classification	Limestone-Type
P10-1Y3	Packed Biopelmicrite	Chalk
P10-1Z2	Packed Biopelmicrite	Chalk
bed 8		
P8-1Z3	Packed Biopelmicrite	Chalk
bed 6		
P6-1Y3	Packed Fossiliferous Pelmicrite	Chalk

LOCALITY - WEST WEARE CLIFFS, ISLE OF PORTLAND [S Y 682724]

black dolomitic sandstone bed

Core-Specimen	Limestone Classification	Limestone-Type
PLPS1X1	Dolomitised Sparse Biomicrosparite	All Microsparites
PLPS1Y4	Silty Dolomitised Sparse Biomicrosparite	
PLPS1Z4	Dolomitised Fossiliferous Microsparite	
PLPS2Y3	Dolomitised Sparse Biomicrosparite	
PLPS2Z1	Dolomitised Fossiliferous Microsparite	
PLPS3X6	Silty Dolomitised Fossiliferous Microsparite	
PLPS3Y2	Silty Dolomitised Fossiliferous Microsparite	
PLPS3Z3	Silty Dolomitised Fossiliferous Microsparite	

LOCALITY - FRESHWATER BAY, ISLE OF PORTLAND [S Y 692702]

Arkell's "Basal Shell Bed"

Core-Specimen	Limestone Classification	Limestone-Type
PLBS1X3	Sparse Biomicrite	All Micrites
PLBS1Y4	Sparse Biomicrite	
PLBS1Z4	Sparse Biomicrite	
PLBS2X3	Sparse Biomicrite	
PLBS2Y1	Sparse Biomicrite	
PLBS2Z4	Sparse Biomicrite	
PLBS3X4	Sparse Biomicrite	
PLBS3Y2	Sparse Biomicrite	
PLBS3Z1	Sparse Biomicrite	

LOCALITY - PERRYFIELD QUARRIES, ISLE OF PORTLAND [S Y 694712]

Core-Specimen	Limestone Classification	Limestone-Type
Whit bed		
PLW1X2	Sorted Fossiliferous Oosparite	All Sparites
PLW1Y4	Sorted Fossiliferous Oosparite	
PLW1Z2	Sorted Fossiliferous Oosparite	
PLW2X1	Sorted Fossiliferous Oosparite	
PLW2Y2	Sorted Fossiliferous Oosparite	
PLW2Z1	Sorted Fossiliferous Intraclastic Oosparite	
Base bed		
PLB1Y2	Unsorted Fossiliferous Oosparite	All Sparites
PLB1Y5	Unsorted Fossiliferous Oosparite	
PLB1Z5	Unsorted Fossiliferous Oosparite	
PLB2X1	Unsorted Fossiliferous Oosparite	
PLB2Y1	Unsorted Fossiliferous Oosparite	
PLB2Z1	Unsorted Fossiliferous Oosparite	

LOCALITY - CHILMARK RAVINE [S T 974313]

"Upper Building Stones" (Arkell, 1933)

Core-Specimen	Limestone Classification	Limestone-Type
CRU1Y2	Sorted Oosparite	All Sparites
CRU1Z1	Sorted Oosparite	
CRU1Z2	Sorted Oosparite	
CRU2X1	Sorted Oosparite	
CRU2X2	Sorted Oosparite	
CRU2X4	Sorted Oosparite	
CRU2Y1	Sorted Oosparite	
CRU2Y4	Sorted Fossiliferous Intraclastic Oosparite	
CRU2Z2	Sorted Fossiliferous Oosparite	
CRU2Z8	Sorted Oosparite	
CRU3X2	Sorted Oosparite	
CRU3Y1	Sorted Fossiliferous Intraclastic Oosparite	
CRU3Y5	Sorted Fossiliferous Oosparite	
CRU3Z1	Sorted Fossiliferous Oosparite	
CRU3Z4	Sorted Fossiliferous Oosparite	
CRU4X3	Sorted Fossiliferous Oosparite	
CRU4X6	Sorted Fossiliferous Intraclastic Oosparite	
CRU4Y5	Sorted Fossiliferous Oosparite	
CRU4Z2	Sorted Fossiliferous Oosparite	
CRU4Z6	Sorted Fossiliferous Oosparite	
chalky limestone beds		
CRC1X2	Packed Pelletiferous Biomicrite	
CRC1Z1	Packed Biopelmicrite	

CRC2X2	Packed Biopelmicrite	All Chalks
CRC2Y2	Packed Intraclastic Pelletiferous Biomicrite	
CRC2Z2	Packed Intraclastic Pelletiferous Biomicrite	
CRC3X1	Packed Pelletiferous Biomicrite	
CRC3X3	Packed Pelletiferous Biomicrite	
CRC3Y3	Packed Biopelmicrite	
CRC3Z1	Packed Biopelmicrite	
CRC3Z6	Packed Biopelmicrite	

Ragstone beds

CRR1X1	Unsorted Fossiliferous Oosparite	All Sparites
CRR1Y1	Unsorted Fossiliferous Oosparite	
CRR1Z1	Unsorted Oosparite	

LOCALITY - UPPER CHICKSGROVE QUARRY [S T 962296]

Lamellosus bed

Core-Specimen	Limestone Classification	Limestone-Type
UCL1X1	Sparse Biomicrite	Micrite
UCL1X4	Poorly Washed Biosparite	Sparite
UCL1Y2	Sparse Biomicrite	Micrite
UCL1Z1	Sparse Biomicrite	Micrite
UCL1Z4	Sparse Biomicrudite	Micrite

Ragstone beds

UCR1X2	Sparse Biomicrite	Micrite
UCR1X3	Unsorted Fossiliferous Intraclastic Oosparite	Sparite

UCR1X4	Sparse Biomicrite	Micrite
UCR1Y3	Sparse Biomicrite	Micrite
UCR1Z1	Unsorted Fossiliferous Intraclastic Oosparite	Sparite
UCR1Z5	Unsorted Fossiliferous Oosparite	Sparite
UCR2X1	Sandy Unsorted Fossiliferous Oosparite	Sparite
UCR2Z1	Sandy Unsorted Fossiliferous Oosparite	Sparite
UCR2Z2	Sandy Unsorted Fossiliferous Oosparite	Sparite
UCR3X2	Sparse Biomicrite	Micrite
UCR3Z2	Sparse Biomicrudite	Micrite
Glauconitic sandy limestone beds		
UCM1X4	Sandy Sorted Fossiliferous Oosparite	
UCM1X6	Sandy Sorted Fossiliferous Oosparite	
UCM1Y1	Sandy Sorted Fossiliferous Oosparite	All Sparites
UCM1Y5	Sandy Sorted Fossiliferous Oosparite	
UCM1Z6	Sandy Sorted Fossiliferous Oosparite	
Basement beds		
UCB1X1	Sandy Sorted Fossiliferous Oosparite	
UCB1X4	Sandy Sorted Fossiliferous Oosparite	
UCB1Y4	Silty Sorted Fossiliferous Oosparite	
UCB1Z1	Sandy Sorted Fossiliferous Oosparite	All Sparites
UCB2X2	Sandy Sorted Oosparite	
UCB2X4	Sandy Sorted Oosparite	

UCB2Y2	Coarse Calcareous Siltstone	
UCB2Z3	Sandy Sorted Fossiliferous Oosparite	
Basal shell beds		
UCBS1X3	Poorly Washed Biosparite	Sparite
UCBS1Z1	Silty Poorly Washed Biosparite	Sparite

APPENDIX 7

PORE CLASSIFICATION, -DIMENSIONS AND -ORIENTATION OF SOME 36 CORE-SPECIMENS

36 core-specimens, representative of the four limestone-types recognised, are listed. The pore-classification is that of Choquette and Pray (1970) (see Fig.4.2). Pore-orientation is defined in terms of the azimuth and magnitude of the resultant vector of pore long-axes (Section 6.3.3b). The vector magnitudes were tested using a Rayleigh test of significance (Curray, 1956), and probabilities are listed of the vector magnitudes being obtained by chance sampling of a random population. At probabilities less than 0.05, the vector magnitudes are considered to be significantly different from randomness.

LIMESTONE-TYPE - SPARITE

Core-Specimen	% Porosity	Pore-Dimensions				Pore-Orientation				Porosity Classification
		No. of readings	Mean & S.D. (microns) Long-Axis (L)	Mean & S.D. (microns) Short-Axis (S)	L/S	No. of readings	Azimuth of Resultant Vector (degrees)	Magnitude of Resultant Vector (%)	Probability (p)	
WU3X1	12·8	50	304 ± 586	134 ± 204	1.99	42	025.4	7.1	p > 0.80	Interparticle and intraparticle micro-mesopores dominant. A few reduced and filled small megamolds.
WP1Z3	3·0	50	124 ± 82	62 ± 39	2.07	45	339.9	4·9	p > 0.80	Interparticle and intraparticle micro-mesopores dominant. Several filled meso-megamolds. A few micro-borings in ooliths.
WN1Y1	9·6	50	138 ± 96	71 ± 53	2.15	47	023.5	13.3	p > 0.40	Interparticle and intraparticle micro-mesopores dominant. A few micro-mesomolds.
LCV2X4+	5.6	50	154 ± 181	60 ± 35	2·47	43	297.0	7.9	p > 0.70	Intraparticle micro-mesovugs dominant. Interparticle and intraparticle micro-mesopores also present.
PLW2X1+	11·5	50	279 ± 212	90 ± 53	3·55	46	070·1	13·0	p > 0.40	Interparticle mesopores dominant. Several micro-mesointraparticle pores, and a few microborings in ooliths.
PLB1Y2	17·0	50	190 ± 140	78 ± 48	2·62	43	083.3	15.3	p > 0.30	Interparticle mesopores and intraparticle micropores dominant.
CRR1Y1	25·4	50	203 ± 203	75 ± 53	2·91	46	068.2	10.2	p > 0·60	Interparticle and intraparticle micro-mesopores dominant. A few microborings in ooliths.
UCB1X4	20·0	50	255 ± 212	88 ± 50	3·05	48	044.6	17.6	p > 0.20	Intercrystal and inter-particle micro-mesopores dominant. A few intra-particle micro-mesopores.
UCB1Y4	28·2	50	347 ± 247	127 ± 60	2·78	48	044·6	17·0	p > 0·20	Intercrystal and inter-particle micro-mesopores dominant. A few intra-particle micropores.

UCB1Z1	32·3	50	243 ± 158	96 ± 65	2·68	48	288.5	2.4	p > 0.95	Intercrystal and inter-particle micro-mesopores dominant. A few intra-particle micro-mesopores.

LIMESTONE-TYPE - MICRITE

Core-Specimen	% Porosity	Pore-Dimensions				Pore-Orientation				Porosity Classification
		No.of readings	Mean & S.D.(microns) Long-Axis (L)	Mean & S.D.(microns) Short-Axis (S)	L/S	No. of Readings	Azimuth of Resultant Vector (degrees)	Magnitude of Resultant Vector (%)	Probability (p)	
WV4X1	11·4	50	114 ± 197	64 ± 93	1·70	35	354·6	43·7*	p < 0.01	Micro-mesomolds dominant. A few reduced molds.
WV4Y1+	5·9	50	101 ± 83	55 ± 29	1·74	37	349.3	33.2*	p < 0.02	Micro-mesomolds dominant.
WV4Z1	11·3	50	65 ± 38	43 ± 14	1·50	37	081.3	29.8*	p < 0.04	Micro-mesomolds dominant.
WV5X2A	4·9	50	128 ± 185	69 ± 67	1·96	33	302·3	20·7	p > 0·20	Micro-mesomolds dominant.
PLBS3X4	7·1	50	105 ± 121	52 ± 39	1·99	33	005·7	18·3	p > 0·30	Micromolds dominant. A few mesomolds and solution-enlarged mesomolds.
PLBS3Y2+	16·4	50	129 ± 109	69 ± 43	1·97	36	351·2	8·4	p > 0·70	Mesomolds, solution-enlarged mesomolds, and mesovugs dominant. A few micromolds.
PLBS3Z1	11·5	50	147 ± 171	66 ± 40	2·21	37	284·4	1·6	p > 0.99	Micro-mesomolds dominant. Some molds are solution-enlarged. A few of these pores are reduced or filled.
UCL1Z1+	18·4	50	292 ± 313	98 ± 63	3·32	41	275·3	23·7	p > 0·05	Micro-mesomolds, solution-enlarged mesomolds, and mesovugs dominant. Some of these pores are reduced or filled.
UCL1Z4	26·9	50	307 ± 253	132 ± 71	2·41	42	275·8	28.6*	p < 0.04	Micro-mesomolds, solution-enlarged mesomolds, and mesovugs dominant. Some of these pores are reduced.
UCR3Z2+	12·8	50	485 ± 2305	92 ± 71	18·2	38	352·8	21·8	p > 0.10	Mesomolds and solution-enlarged mesomolds dominant. A few micromolds and micro-fractures.

LIMESTONE-TYPE - CHALK

Core-Specimen	% Porosity	Pore-Dimensions				Pore-Orientation				Porosity Classification
		No. of readings	Mean & S.D. (microns) Long-Axis (L)	Mean & S.D. (microns) Short-Axis (S)	L/S	No. of Readings	Azimuth of Resultant Vector (degrees)	Magnitude of Resultant Vector (%)	Probability (p)	
C10-1Y5+	7.8	50	120 ± 103	60 ± 41	2·10	38	271·9	12·9	p > 0·50	Micro-mesomolds dominant. A few solution-enlarged mesomolds.
C5-1X3	23·1	50	123 ± 112	60 ± 38	1·97	42	012·2	4·7	p > 0·90	Micro-mesomolds, solution-enlarged mesomolds, and mesovugs dominant.
C5-1Y1	29·8	50	126 ± 124	57 ± 29	2·13	38	051·8	4·4	p > 0·90	Micro-mesomolds, solution-enlarged mesomolds, and mesovugs dominant.
C5-1Z1+	21·7	50	167 ± 144	63 ± 32	2·70	42	083·3	20·8	p > 0·10	Micro-mesomolds and solution-enlarged mesomolds dominant. Some mesovugs also present.
P10-1Y3	16·7	50	136 ± 105	67 ± 30	2·10	39	055·4	9·8	p > 0·60	Micro-mesomolds, solution-enlarged mesomolds, and mesovugs dominant.
P10-1Z2	11·1	50	112 ± 61	65 ± 36	1·89	41	278·9	23·6	p > 0·05	Micro-mesomolds dominant. Some solution-enlarged mesomolds also present.
CRC2Z2	38·9	50	253 ± 260	87 ± 49	2·76	41	351·6	24·1	p > 0·05	Micro-mesomolds, solution-enlarged mesomolds, and mesovugs dominant.
CRC3Y3	32·5	50	311 ± 387	126 ± 88	2·20	38	085·1	16·1	p > 0·30	Micro-mesomolds, solution-enlarged mesomolds, and mesovugs dominant. Some of these pores are reduced or filled.

LIMESTONE TYPE - MICROSPARITE

Core-Specimen	% Porosity	Pore-Dimensions				Pore-Orientation				Porosity Classification
		No.of readings	Mean & S.D. (microns) Long-Axis (L)	Mean & S.D. (microns) Short-Axis (S)	L/S	No.of Readings	Azimuth of Resultant Vector (degrees)	Magnitude of Resultant Vector (%)	Probability (p)	
WB1X2+	27·8	50	101 ± 93	44 ± 32	2·34	48	295·4	9·4	p > 0·60	Intercrystal micro-mesopores, solution-enlarged intercrystal mesopores, and mesovugs dominant. A few micro-mesomolds and solution-enlarged mesomolds.
WA28-1X1+	24·7	50	66 ± 43	37 ± 24	1·87	46	000·0	4·5	p > 0·90	Intercrystal micro-mesopores, solution-enlarged intercrystal mesopores, and mesovugs dominant.
WA28-2X1B	12·1	50	63 ± 39	33 ± 15	1·87	49	039·6	3·0	p > 0·95	Intercrystal micro-mesopores dominant. Some solution-enlarged intercrystal mesopores, and mesovugs. A few intraparticle mesopores.
WA28-2Y3+	11·5	50	83 ± 70	41 ± 28	2·08	48	323.9	7.7	p > 0·70	Intercrystal micro-mesopores dominant. Some solution-enlarged intercrystal mesopores, and mesovugs. A few micro-mesomolds.
WA28-2Z2	17·1	50	76 ± 57	39 ± 37	2·12	46	074·7	29·6*	p < 0·02	Intercrystal micro-mesopores dominant. Some solution-enlarged intercrystal mesopores, and mesovugs. A few mesomolds.
LCA10-1Z2+	6·3	50	67 ± 52	32 ± 21	2·02	48	311·0	10·1	p > 0·60	Intercrystal micro-mesopores dominant. Some solution-enlarged intercrystal mesopores. A few micro-mesomolds, solution-enlarged mesomolds, and mesovugs.
CFPS1Z2+	14·8	50	107 ± 206	42 ± 46	2·10	48	063·4	15·7	p > 0·30	Intercrystal micro-mesopores, solution-enlarged intercrystal mesopores, and mesovugs dominant. A few intraparticle micro-mesopores, mesomolds and solution-enlarged mesomolds.

PLPS1Z4	19·9	50	94 ± 83	40 ± 27	2·34	50	087·7	24·8*	$p < 0.05$	Intercrystal micro-mesopores, solution-enlarged intercrystal mesopores, and mesovugs dominant. A few mesomolds and solution-enlarged mesomolds.

\+ Indicates that specimens were analysed using a Scanning Electron Microscope (Section 4.6.3) in addition to a reflecting-light microscope.

* Indicates that vector magnitudes are significantly different from randomness.